รายงานการวิจัย

เรื่อง

การพัฒนาพอลิเมอร์นำไฟฟ้าเพื่อประยุกต์เป็นเซนเซอร์ แอคชูเอเตอร์ และการปลดปล่อยยา

โดย

ศ.ดร.อนุวัฒน์ ศิริวัฒน์

หน่วยงาน

วิทยาลัยปิโตรเลียมละปิโตรเคมี

จุฬาลงกรณ์มหาวิทยาลัย

สนับสนุนโดย

งบประมาณแผ่นดิน ประจำปี 2556

1 ตุลาคม 2555 – 30 กันยายน 2556

รายงานการวิจัยเรื่อง

การพัฒนาพอลิเมอร์นำไฟฟ้าเพื่อประยุกต์เป็นเซนเซอร์ แอคชูเอเตอร์ และการปลดปล่อยยา

หน่วยงาน: วิทยาลัยปิโตรเลียมและปิโตรเคมี จุฬาลงกรณ์มหาวิทยาลัย

ระยะเวลา: 1 ตุลาคม 2555 – 30 กันยายน 2556

ผู้วิจัย: ศ. ดร. อนุวัฒน์ ศิริวัฒน์

รายงานการวิจัยเรื่อง
การพัฒนาพอลิเมอร์นำไฟฟ้าเพื่อประยุกต์เป็นเซ็นเซอร์แอคชูเอเตอร์ และการปลดปล่อยยา

ส่วนที่ 1

ผลกระทบของอัตราส่วนของซิลิกาต่ออลูมินาในซีโอไลต์ซีเอสเอ็มไฟต์ที่มีผลต่อความว่องไวในการตอบสนองต่อก๊าซคาร์บอนมอนอกไซด์ของคอมโพสิตโพลีเอทิลีนไดออกซีไทโอฟีนและซีโอไลต์ซีเอสเอ็มไฟต์ (Interaction of carbon monoxide with PEDOT-PSS/zeolite composite:effect of Si/Al ratio of ZSM-5 zeolite)

ส่วนที่ 2

การศึกษาสมบัติไฟฟ้าเชิงกลของเจลเซลลูโลสเชื่อมขวางทางกายภาพกับสารผลึกเหลว 1-บิวทิล-3-เมททิลอิมมิดาโซเลียมคลอไรด์ (Physically cross-linked cellulosic gel via 1-butyl-3-methylimidazolium chloride ionic liquid and its electromechanical responses)

ส่วนที่ 3

การศึกษาคุณสมบัติเชิงกลทางไฟฟ้าของเจลลาติน (Ala-Gly-Pro-Arg-Gly-Glu-4Hyp-Gly-Pro-) จากผลกระทบของอุณหภูมิและสนามไฟฟ้า (Bio-compatible gelatins (Ala-Gly-Pro-Arg-Gly-Glu-4Hyp-Gly-Pro-) and electromechanical properties: effects of temperature and electric field)

ส่วนที่ 4

ผลกระทบของปริมาณสารเชื่อมโยง, ลักษณะของยา, และปริมาณของกระแสไฟฟ้าต่อการควบคุมการปลดปล่อยยาภายใต้สนามไฟฟ้าจากแผ่นอัลจิเนตไฮโดรเจล (Effects of crosslinking ratio, model drugs, and electric field strength on electrically controlled release for alginate-based hydrogel)

หน่วยงาน: วิทยาลัยปิโตรเลียมและปิโตรเคมี จุฬาลงกรณ์มหาวิทยาลัย

ผู้วิจัย: ศ. ดร. อนุวัฒน์ ศิริวัฒน์

กิตติกรรมประกาศ

คณะผู้วิจัยขอขอบคุณ ทุนอุดหนุนการวิจัยจากเงินงบประมาณแผ่นดิน ประจำปีงบประมาณ 2556

บทคัดย่อภาษาไทย

ส่วนที่ 1 ผลกระทบของอัตราส่วนของซิลิกาต่ออลูมินาในซีโอไลต์ซีเอสเอ็มไฟต์ที่มีผลต่อความว่องไวในการตอบสนองต่อก๊าซคาร์บอนมอนอกไซด์ของคอมโพสิตโพลีเอทิลีนไดออกซีไทโอฟีนและซีโอไลต์ซีเอสเอ็มไฟต์

โพลิเมอร์นำไฟฟ้าโพลีเอทิลีนไดออกซีไทโอฟีนซึ่งผ่านการเติมสารเจือเพื่อให้มีค่าการนำไฟฟ้ามากขึ้น ด้วยโพลีนสไตรีนซัลโฟนิก ถูกใช้เพื่อเป็นเมตริกซ์ของคอมสิทระหว่างโพลีเอทิลีนไดออกซีไทโอฟีนกับซีโอไลต์ที่อัตราส่วนของซิลิกาต่ออลูมินาที่แปรเปลี่ยนอยู่ในช่วง 23-280 โดยสารทั้งสองผสมกันด้วยอัตราส่วนร้อยละ 20 โดยปริมาตร เพื่อศึกษาผลของอัตราส่วนของซิลิกาต่อ อลูมินาของซีโอไลต์ที่มีต่อค่าการนำไฟฟ้าของคอมโพสิทที่มีต่ออันตรกิริยาต่อก๊าซคาร์บอนมอนอกไซด์ พบว่าค่าการนำไฟฟ้าของสารคอมโพสิทจะแปรเปลี่ยนตามพื้นที่ผิวสำหรับดูดซับโมเลกุลก๊าซคาร์บอนมอนอกไซด์ โดยค่าความไวของการนำไฟฟ้าของคอมโพสิทที่มีต่อก๊าซคาร์บอนมอนอกไซด์จะมีค่าเพิ่มขึ้น เมื่ออัตราส่วนของซิลิกาต่ออลูมินาของซีโอไลต์ซีเอสเอมไฟว์ลดลง และพบว่าการผสมซีโอไลต์ซีเอสเอมไฟว์กับโพลิเมอร์นำไฟฟ้าโพลีเอทิลีนไดออกซีไทโอฟีน จะช่วยให้ความไวของการนำไฟฟ้าของคอมโพสิทมีค่าเพิ่มขึ้น เมื่อเปรียบเทียบกับโพลิเมอร์นำไฟฟ้าโพลีเอทิลีนไดออกซีไทโอฟีนตอนเริ่มต้น โดยซีโอไลต์ซีเอสเอมไฟว์มีส่วนช่วยเพิ่มอันตรกิริยาระหว่างก๊าซคาร์บอนมอนอกไซด์กับโพลิเมอร์นำไฟฟ้าโพลีเอทิลีนไดออกซีไทโอฟีน และคอมโพสิทของโพลิเมอร์นำไฟฟ้าโพลีเอทิลีนไดออกซีไทโอฟีน-โพลีนสไตรีนซัลโฟนิกและซีโอไลต์ซึ่งมีอัตราส่วนของซิลิกาต่ออลูมินาเท่ากับ 23 นั้น มีค่าความไวต่อการนำไฟฟ้าที่มีต่อก๊าซคาร์บอนมอนอกไซด์สูงสุด

ส่วนที่ 2 การศึกษาสมบัติไฟฟ้าเชิงกลของเจลเซลลูโลสเชื่อมขวางทางกายภาพกับสารผลึกเหลว 1-บิวทิล-3-เมทธิลอิมมิดาโซเลียมคลอไรด์

เซลลูโลสสามารถถูกใช้งานเป็นวัสดุฉลาดได้เพราะมีสมบัติเพียโซอิเล็กทริก ซึ่งถูกใช้งานอย่างกว้างขวางในซื่อ เซลลูโลสที่ตอบสนองต่อไฟฟ้า ในขณะที่สารผลึกเหลวชนิด1-บิวทิล-3-เมทธิลอิมมิดาโซเลียมคลอไรด์เป็นตัวทำละลายอิเล็กโตรไลท์ที่น่าสนใจในงานด้านแอคชูเอเตอร์เนื่องจากมีความเสถียรสูง มีความมีขั้วที่เหมาะสม นำไฟฟ้าดี เจลเซลลูโลสเชื่อมขวางทางกายภาพกับสารผลึกเหลวชนิดดังกล่าวจึงถูกเตรียมและทดสอบคุณลักษณะเพื่อการใช้งานด้านแอคชูเอเตอร์ จากการทดสอบการเฉือนภายใต้สนามไฟฟ้ากระแสตรง ที่อุณหภูมิ 303 เคลวิน ค่ามอดูลัสเพิ่มขึ้นเมื่อ

สนามไฟฟ้าเป็น 1 กิโลโวลต์ต่อมิลลิเมตร และลดลงเมื่อสนามไฟฟ้าเป็น 0 กิโลโวลต์ต่อมิลลิเมตร สลับกันไปจนเข้าสู่สภาวะนิ่ง เนื่องจากสนามไฟฟ้าทำให้เกิดการโพลาไรซ์ของไอออนบวกของสารผลึกเหลว การโพลาไรซ์ของหมู่ไฮดรอกซิลบนเซลลูโลส และการจัดเรียงตัวภายใต้แรงเฉือนขณะทดสอบ สอดคล้องกับค่าคงที่ไดอิเล็กทริก การทดสอบการเอียงภายใต้สนามไฟฟ้ากระแสตรงชี้ให้เห็นว่าการเคลื่อนที่ของไอออนบวกของสารผลึกเหลวส่งผลโดยตรงต่อมุมการเอียงที่มากขึ้น และปรากฏการแกว่งกลับไปกลับมาของชิ้นงานเมื่อค่าความเข้มสนามไฟฟ้ามีค่าระหว่าง 525 ถึง 550 โวลต์ต่อมิลลิเมตร

ส่วนที่ 3 การศึกษาคุณสมบัติเชิงกลทางไฟฟ้าของเจลลาติน (Ala-Gly-Pro-Arg-Gly-Glu-4Hyp-Gly-Pro-) จากผลกระทบของอุณหภูมิและสนามไฟฟ้า

เจลาติน (Ala-Gly-Pro-Arg-Gly-Glu-Gly-4Hyp-Pro-) เป็นโปรตีนที่ผลิตโดยการย่อยบางส่วนจาก คอลลาเจนที่สกัดจากกระดูกเนื้อเยื่อเกี่ยวพันอวัยวะ และบางส่วนของลำไส้สัตว์ ในงานวิจัยนี้ฟิล์มเจลาตินถูกเตรียมขึ้นโดยวิธีการหล่อฟิล์มในสารละลายที่ใช้น้ำเป็นตัวทำละลาย คุณสมบัติด้านเชิงกลไฟฟ้า สมบัติด้านความร้อนและความสามารถในการบวมตัวได้ถูกศึกษาภายใต้อิทธิพลของอัตราส่วนการเชื่อมขวางสายโซ่เจลาติน ระดับความแข็งแรงของเจล อุณหภูมิ ความถี่ และความเข้มของสนามไฟฟ้า จากผลการทดสอบแสดงให้เห็นว่าเจลลาตินบริสุทธิ์ที่มีความแข็งแรงของเจลระดับสูง กลาง ต่ำ รวมทั้ง เจลลาตินที่มีการเชื่อมขวางร้อยละ3 ของเจลที่มีความแข็งแรงระดับสูง มีค่าการตอบสนองด้านการเพิ่มความแข็งแรงภายใต้สนามไฟฟ้า เท่ากับ 2.30 2.16 1.26 และ 0.49 ตามลำดับ ซึ่งพบว่าค่าเหล่านี้จะมากกว่าเมื่อเปรียบเทียบกับวัสดุที่มีความสามารถตอบสนองทางไฟฟ้าอื่นๆเช่นเดียวกัน

ส่วนที่ 4 ผลกระทบของปริมาณสารเชื่อมโยง, ลักษณะของยา, และปริมาณของกระแสไฟฟ้าต่อการควบคุมการปลดปล่อยยาภายใต้สนามไฟฟ้าจากแผ่นอัลจิเนตไฮโดรเจล

การศึกษาลักษณะการควบคุมการปลดปล่อยยาภายใต้สนามไฟฟ้าของแผ่นอัลจิเนตไฮโดรเจลที่เตรียมขึ้นจากเทคนิคการหล่อสารละลายของอัลจิเนตซึ่งถูกเชื่อมโยงสายโซ่ด้วยเกลือแคลเซียมคลอไรด์ การศึกษาลักษณะการแพร่และการปลดปล่อยยาจากแผ่นอัลจิเนตไฮโดรเจลประกอบด้วยยาที่มีประจุลบ คือ กรดเบนโซอิคและกรดแทนนิค และยาที่มีประจุบวก คือ กรดโฟลิค ซึ่งจะศึกษาด้วยอุปกรณ์ที่เรียกว่า modified Franz Diffusion cell โดยในอุปกรณ์นี้จะประกอบด้วยสารละลายบัฟเฟอร์ พีเอช 5.5 ที่อุณหภูมิ 37 องศาเซลเซียส และทำการศึกษาเป็นระยะเวลา 48 ชั่วโมง ภายใต้อิทธิพลของอัตราส่วน

ของสารเชื่อมโยงสายโซ่ (อัตราส่วนระหว่างปริมาณของสารเชื่อมโยงสายโซ่ต่อปริมาณอัลจิเนต), ขนาดของรูในแผ่นไฮโดรเจล, ขนาดและประจุของยา และปริมาณของกระแสไฟฟ้าและชนิดของขั้วไฟฟ้าที่ใช้ในการกระตุ้นการปลดปล่อยยาจากแผ่นไฮโดรเจล จากการศึกษาพบว่าปริมาณการแพร่ของยาลดลงเมื่ออัตราส่วนของสารเชื่อมโยงสายโซ่และขนาดของยาเพิ่มขึ้น สำหรับการควบคุมการแพร่ของยาภายใต้สนามไฟฟ้าพบว่า การแพร่ของยาขึ้นอยู่กับชนิดของขั้วไฟฟ้าและประจุของยาในแต่ละระบบ

บทคัดย่อภาษาอังกฤษ

ส่วนที่ 1 Interaction of carbon monoxide with PEDOT-PSS/zeolite composite:effect of Si/Al ratio of ZSM-5 zeolite

Composites with poly(3,4-ethylenedioxythiophene) doped with poly(styrene sulfonic acid), PEDOT-PSS, as the matrix containing ZSM-5 zeolites of various Si/Al ratios in the range of 23-280 at 20% (v/v) were fabricated to investigate the effect of Si/Al ratios on electrical conductivity sensitivity responses towards carbon monoxide (CO). The electrical conductivity responses of PEDOTPSS/ZSM-5 composites were altered due to the available adsorption sites for CO molecules. The electrical conductivity sensitivity to CO increases with decreasing Si/Al ratios. The composites produce irreversible responses when replacing CO with nitrogen. The addition of ZSM-5 zeolites to the pristine PEDOT-PSS improves the electrical conductivity sensitivity of the composites by enhancing the interaction between PEDOT-PSS and CO gas. The composite of ZSM-5 zeolites with a Si/Al ratio equal to 23 gives the highest electrical conductivity sensitivity toward CO.

ส่วนที่ 2 Physically cross-linked cellulosic gel via 1-butyl-3-methylimidazolium chloride ionic liquid and its electromechanical responses

Cellulose shows promising piezoelectric properties widely used in electroactive papers (EAPaps), however its solubility still remains a challenging problem. 1-Butyl-3-methylimidazolium Chloride (BMIM+Cl−), a well-known room temperature ionic liquid (RTIL), is utilized here to dissolve a microcrystalline cellulose. The BMIM+Cl− – cellulose gels are prepared by the solvent casting method. The electromechanical properties of the cellulose gels are investigated under the oscillatory shear mode at electric field strengths between 0 and 1 kV/mm and as functions of temperature. The storage modulus (G′) increases linearly with temperature up to 333 K at 1 rad/s in the absence of electric field strength. The storage moduli (G′) also increase linearly with temperature up to 313 K at 1 rad/s in the presence of 1 kV/mm of electric field strength and decreases above 313 K, consistent with the behavior of dielectric permittivity (ε′). The elastic–plastic–viscous transition is observed in the presence of 1 kV/mm. It is shown that the conditions imposed by electric field strength and temperature alter the transition temperature, and lower the dielectric constant, the storage modulus, and the actuation performance. In the deflection experiments, under applied DC electric field,

the deflection distances of the gels linearly increase with increasing electric field strength along with the dielectrophoresis forces above the electrical yield strength of 100 V/mm. The back and forth swinging occurs under the constant electric field strength between 525 and 550 V/mm due to the competition between the anion and cation movements within the ionic liquid. Electrostatic force microscope (EFM) is then employed to investigate the gel topology and the cationic channel and aggregation that control the actuation behavior. The Phy gel is shown here to be promising for actuator applications over other existing dielectric elastomers studied at a room temperature in terms of the electrical yield strength, the bending angle, the generated dielectrophoresis force, the energy density, the force density, the mechanical power, the power density, G′at 1 rad/s at 0.25% strain, and the relatively high ε'_r,20 Hz.

ส่วนที่ 3 Bio-compatible gelatins (Ala-Gly-Pro-Arg-Gly-Glu-4Hyp-Gly-Pro-) and electromechanical properties: effects of temperature and electric field

Gelatin (Ala-Gly-Pro-Arg-Gly-Glu-4Hyp-Gly-Pro-) is a protein produced by the partial hydrolysis of a collagen extracted from bones, connective tissues, organs, and some intestines of animals. In this work, gelatin films were prepared by the film casting method in an aqueous solvent. The electromechanical properties, thermal properties, and the degree of swelling were investigated as a function of gelatin crosslinking ratio or the gel strength, temperature, frequency, and electric field strength. The high, medium, low, and the 3% crosslinked high-gel-strength gelatin films possess the storage modulus sensitivity values of 2.30, 2.16, 1.26, and 0.49, respectively; these values are much greater than those of other electroactive materials, suggesting the gelatins studied as a potential artificial muscle or actuator.

ส่วนที่ 4 Effects of crosslinking ratio, model drugs, and electric field strength on electrically controlled release for alginate-based hydrogel

The drug release characteristics of calcium alginate hydrogels, (Ca-Alg), under an electric field assisted transdermal drug delivery system were systematically investigated. The Ca-Alg hydrogels were prepared by the solution-casting using CaCl2 as a crosslinking agent. The diffusion coefficients and the release mechanism of the anionic model drugs, benzoic acid and tannic acid, and a cationic model drug, folic acid on the Ca-Alg hydrogels were determined and investigated using a modified Franz-Diffusion cell in an MES buffer solution of pH 5.5, at a temperature of 37_C, for 48 h. The influences of the crosslinking ratio, —the mole of the crosslinking agent to the mole of the alginate monomer—mesh size, model drug size, drug charge, electric field strength, and electrode polarity were systematically studied. The drug diffusion coefficient decreased with an increasing crosslinking ratio and drug size for all of the model drugs. The drug diffusion coefficient is precisely controlled by an applied electric field and the electrode polarity depending on the drug charge, suitable for a tailor-made transdermal drug delivery system.

สารบัญเรื่อง

เรื่อง	หน้า
กิตติกรรมประกาศ	3
บทคัดย่อภาษาไทย	
ส่วนที่ 1	4
ส่วนที่ 2	4
ส่วนที่ 3	5
ส่วนที่ 4	5
บทคัดย่อภาษาอังกฤษ	
ส่วนที่ 1	6
ส่วนที่ 2	6
ส่วนที่ 3	7
ส่วนที่ 4	7
บทนำ	
ส่วนที่ 1	10
ส่วนที่ 2	10
ส่วนที่ 3	11
ส่วนที่ 4	12
เนื่องเรื่อง (วิธีดำเนินการวิจัย)	
ส่วนที่ 1	12
ส่วนที่ 2	13
ส่วนที่ 3	14
ส่วนที่ 4	15
อภิปรายและวิจารณ์ผลการทดลอง	
ส่วนที่ 1	16
ส่วนที่ 2	19
ส่วนที่ 3	23
ส่วนที่ 4	25

เรื่อง	หน้า
สรุปและเสนอแนะเกี่ยวกับการวิจัยในขั้นต่อไป	
ส่วนที่ 1	27
ส่วนที่ 2	28
ส่วนที่ 3	28
ส่วนที่ 4	29
บรรณานุกรม	30
ภาคผนวก	
ส่วนที่ 1	35
ส่วนที่ 2	45
ส่วนที่ 3	67
ส่วนที่ 4	85
ประวัตินักวิจัยและคณะ	108

๑. บทนำ

<u>ส่วนที่ 1</u>

ก๊าซพิษคาร์บอนมอนอไซด์ถูกปล่อยออกมาจากยานพาหนะต่างๆ โรงงานอุตสาหกรรมและห้องปฏิบัติการต่างๆ วัสดุหลากหลายชนิดถูกนำมาใช้พัฒนาเป็นตัวตรวจวัดก๊าซคาร์บอนมอนอกไซด์ โดยตัวตรวจวัดก๊าซคาร์บอนมอนอกไซด์ใช้กันอยู่ในปัจจุบันนั้นทำมาจากวัสดุประเภทโลหะออกไซด์กึ่งตัวนำซึ่งมีความว่องไวในการตรวจวัดสูง แต่การตรวจวัดก๊าซจะต้องทำที่อุณหภูมิสูง ซึ่งทำให้เพิ่มค่าใช้จ่ายในการใช้งานและยังมีข้อจำกัดในการใช้งานที่อุณหภูมิห้อง เนื่องจากคุณสมบัติเฉพาะในการเกิดออกซิไดซ์ของวัสดุประเภทโพลิเมอร์ วัสดุโพลิเมอร์หลายชนิดจึงได้รับความสนใจในการนำมาพัฒนาเพื่อใช้เป็นตัวตัวตรวจวัดก๊าซคาร์บอนมอนอกไซด์ แต่เนื่องด้วยวัสดุโพลิเมอร์ยังมีความจำเพาะเจาะจงกับก๊าซชนิดต่างๆ ไม่มากเพียงพอ จึงได้มีความพยายามพัฒนาแก้ไขปัญหานี้ เพื่อให้ได้วัสดุตรวจวัดก๊าซที่มีความแม่นยำ มีความจำเพาะเจาะจง ว่องไวในการตอบสนองต่อก๊าซ วัสุดนั้นมีความคงทนใช้งานได้นานและมีราคาที่เหมาะสม

ซีโอไลซ์นั้นได้รับความสนใจที่จะนำมาใช้พัฒนาวัสดุตรวจวัดก๊าซเช่นกัน การที่ผู้วิจัยเลือกใช้ซีโอไลซ์มาผสมกับวัสดุโพลิเมอร์นำไฟฟ้าเพื่อนำมาพัฒนาวัสดุตรวจวัดก๊าซที่มีความเฉพาะตัว เนื่องจากซีโอไลซ์นั้น มีโครงสร้างที่เหมาะสม มีรูพรุนสามารถแยกขนาดของก๊าซที่แพร่มาได้ นอกจากนี้ไอออนบวกภายในรูพรุนของมันยังช่วยในการดูดซับโมเลกุลของก๊าซ การนำวัสดุโพลิเมอร์ไฟฟ้ามาผสมกับซีโอไลซ์ นั้นเป็นการรวมคุณสมบัติของสารสองชนิดที่ต่างกันให้ได้วัสดุใหม่ที่มีความเฉพาะตัวและเหมาะสมต่อการใช้งานเป็นวัสดุตรวจวัดก๊าซ งานวิจัยนี้ได้นำวัสดุโพลิเมอร์นำไฟฟ้าพอลิเอทิลีนไดออกซีไทโอฟีนมาผสมซีโอไลต์ซีเอสเอ็มไฟต์เพื่อพัฒนาเป็นวัสดุตรวจวัดก๊าซคาร์บอนมอนอกไซด์ โดยศึกษาผลของค่าอัตราส่วนของซิลิกาต่ออลูมินาที่มีผลต่อค่าการนำไฟฟ้าที่ตอบสนองต่อคาร์บอนมอนอกไซด์ เพื่อจะได้เลือกใช้ชนิดของซีโอไลต์ที่เหมาะสมในการพัฒนางานวิจัยต่อไป

<u>ส่วนที่ 2</u>

เซลลูโลสมีสมบัติเพียโซอิเล็กทริกซึ่งถูกใช้งานอย่างกว้างขวางในซื่อ เซลลูโลสที่ตอบสนองต่อไฟฟ้า อย่างไรก็ตามความสามรถในการละลายเซลลูโลสยังคงต้องการการพัฒนาต่อไป เนื่องจากแรงยึดเหนี่ยวระหว่างโมเลกุลของหมู่ฟังก์ชันไฮดรอกซิลที่สูง สารผลึกเหลวชนิด

1-บิวทิล-3-เมททิลอิมมิดาโซเลียมคลอไรด์เป็นตัวทำละลายอิเล็กโตรไลท์ที่น่าสนใจ เนื่องจากมีความสามารถในการกลายเป็นไอต่ำ มีความเสถียรสูง มีความมีขั้วที่เหมาะสม นำไฟฟ้าดี และสามารถนำกลับมาใช้ใหม่ได้ ในงานวิจัยนี้ทำการศึกษาสมบัติไฟฟ้าเชิงกลที่จำเป็นต่อการใช้งานด้านแอคชูเอเตอร์ของเจลเซลลูโลสเชื่อมขวางทางกายภาพกับสารผลึกเหลว 1-บิวทิล-3-เมททิลอิมมิดาโซเลียมคลอไรด์ โดยมุ่งเน้นศึกษาปัจจัยความเข้มสนามไฟฟ้ากระแสตรง อุณหภูมิ และค่าไดอิเล็กทริก

ส่วนที่ 3

การศึกษาเกี่ยวกับพลังงานทางไฟฟ้าและแรงเชิงกลมีมานานนับ 10 ปี โดยพอลิเมอร์ที่ตอบสนองต่อสนามไฟฟ้า (Electroactive polymers; EAPs) เป็นวัสดุที่เหมาะสมต่อการศึกษา เนื่องจากมีน้ำหนักเบา มีพลังงานสูง มีความยืดหยุ่นสูง ซึ่งสามารถนำไปใช้ประยุกต์กับงานกล้ามเนื้อเทียมได้ เจลาตินเป็นวัสดุชนิดหนึ่งที่สามารถตอบสนองต่อสนามไฟฟ้า เจลาตินคือโปรตีนที่เปลี่ยนรูปมาจากคอลลาเจน ซึ่งแปรรูปมาจากโปรตีนในร่างกายของสัตว์เช่น ผิวหนัง เส้นเอ็น กระดูกอ่อน และ กระดูก เป็นต้น เจลาตินประกอบด้วยโครงสร้างของไกลซีน โพรลีน และ 4-ไฮดรอกซีโพรลีน โดยโครงสร้างของเจลาตินจะจัดเรียงตัวเป็น อลานีน ไกลซีน โพรลีน อาจีนีน ไกลซีน กลูตามีน 4ไฮดรอกซีโพรลีน ไกลซีน โพรลีน ตามลำดับ โดยในโครงสร้างจะประกอบด้วย14% 4ไฮดรอกซีโพรลีน 16% โพรลีน 26% ไกลซีน มีเพียงผลิตภัณฑ์ที่มาจากสัตว์เท่านั้นที่ประกอบด้วยไฮดรอกซีโพรลีน ที่ทำให้เกิดความยืดหยุ่นและมีเพียงปริมาณเล็กน้อย เจลาตินสามารถขึ้นรูปเป็นฟิล์มได้ดี ทั้งนี้ยังมีความเข้ากันได้ทางชีวภาพ เป็นวัสดุที่ย่อยสลายได้ หาซื้อได้ง่าย และราคาถูก โดยปกติแล้ว เจลาตินจะถูกนำมาใช้ในงานทางเภสัชกรรมและทางการแพทย์ เช่น หลอดเลือดเทียม เป็นตัวจ่ายยา วัสดุรักษาแผล และกล้ามเนื้อเทียม อย่างไรก็ตามเจลาตินจะมีคุณสมบัติเชิงกลที่ต่ำ ซึ่งเป็นข้อจำกัดในการใช้งาน การปรับปรุงคุณสมบัติเชิงกลของเจลาตินอาจทำได้โดยดึงยืดเจลาตินให้เกิดการจัดเรียงตัวที่มากขึ้น วิธีการเชื่อมขวางทางสายโซ่จากวิธีทางกายภาพและทางเคมี โดยทางกายภาพวิธีที่นิยมใช้คือรังสีอุลตาไวโอเล็ต แต่วิธีนี้ยังคงมีประสิทธิภาพที่ต่ำ ส่วนกระบวนการทางเคมีนิยมใช้สารจำพวกฟอมอลดีไฮด์ เช่น กลูตารัลดีไฮด์ คาโบดีไมด์ และ เดกทราน ไดอัลดีไฮด์ โดยที่สารกลูตารัลดีไฮด์เป็นสารเคมีที่นิยมใช้กันมากที่สุดเนื่องจาก มีประสิทธิภาพสูงในการทำปฏิกิริยา ทั้งนี้ข้อดีของสารกลูตารัลดีไฮด์ คือ หาง่าย ราคาถูก และ ประสิทธิภาพในการทำปฏิกิริยาสูง ในงานของเราจึงมุ่งเน้นไปที่การพัฒนาเจลาตินให้มีคุณสมบัติที่เหมาะสมต่อการเป็นวัสดุที่ตอบสนองต่อสนามไฟฟ้า โดยมีการศึกษาในคุณสมบัติของการตอบสนองเชิงกลทางไฟฟ้า คุณสมบัติทางความ

ร้อน ผลของการบวม โดยศึกษาจากผลกระทบของ ปริมาณการเชื่อมขวางของสายโซ่ อุณหภูมิ ความถี่ และสนามไฟฟ้า

ส่วนที่ 4

ระบบนำส่งยาเข้าสู่ร่างกายมีวัตถุประสงค์เพื่อป้องกันไม่ให้ยาสลายตัวระหว่างการส่งผ่านภายในร่างกายก่อนที่ยาจะไปถึงอวัยวะหรือส่วนที่เป็นเป้าหมายในการรักษา เพื่อให้การรักษาเกิดประสิทธิภาพสูงสุด ปัจจุบันระบบการนำส่งยามีหลายวิธี ซึ่งการนำส่งยาผ่านผิวหนังเป็นวิธีหนึ่งที่ได้รับความสนใจ เนื่องจากไม่ก่อให้เกิดความเจ็บปวดต่อผู้ป่วย หลีกเลี่ยงการถูกทำลายของยาที่ทางเดินอาหารและตับ สามารถควบคุมการปลดปล่อยยาได้ง่าย เช่น เมื่อต้องการหยุดยา สามารถดึงแผ่นแปะออกจากผิวหนัง แต่เนื่องจากข้อจำกัดของการซึมผ่านของผิวหนังที่ไม่ยอมให้สารอื่นสารหรือสิ่งแปลกปลอมเข้าสู่ร่างได้ง่าย ทำประสิทธิภาพในการรักษาลดลง ดังนั้นจึงต้องอาศัยตัวช่วยจากภายนอกกระตุ้นการซึมผ่านของยาผ่านผิวหนัง ซึ่งการใช้กระแสไฟฟ้าเป็นวิธีหนึ่งที่ช่วยควบคุมการซึมผ่านของยาผ่านผิวหนังภายใต้การเปลี่ยนแปลงกระแส (Current) หรือแรงดันไฟฟ้า (voltage) ทำให้เกิดความต่างศักย์ที่ขั้วไฟฟ้า ส่งผลให้มีการเคลื่อนที่ของไอออนต่างๆรวมทั้งยาในระบบ ไฮโดรเจลเป็นวัสดุชนิดหนึ่งที่นิยมใช้ในการควบคุมการปลดปล่อยยา เนื่องจากไฮโดรเจลเป็นวัสดุที่สามารถบวมตัวได้ในสารละลายต่างๆ เช่น น้ำ หรือ สารละลายบัฟเฟอร์ และสามารถตอบสนองต่อสิ่งกระตุ้นต่างๆ เช่น ไฟฟ้า ดังนั้นไฮโดรเจลจึงนำกลไกการบวมตัวนี้มาใช้ในการควบคุมการปลดปล่อยยา

2. เนื้อเรื่อง (วิธีดำเนินการวิจัย)

ส่วนที่ 1

2.1 ศึกษาค้นคว้าและรวบรวมข้อมูลเกี่ยวกับงานวิจัย รวมทั้งสั่งซื้อเครื่องแก้วและสารเคมี

2.2 เตรียมตัวอย่างคอมโพสิตระหว่างโพลีเอทิลีนไดออกซีไทโอฟีนและซีโอไลต์ซีเอสเอ็มไฟต์เพื่อวิเคราะห์คุณลักษณะเฉพาะโดยเครื่องมือวิเคราะห์ทางวิทยาศาสตร์

สังเคราะห์พอลิเอทิลีนไดออกซีไทโอฟีน โดยวิธีการสังเคราะห์แบบออกซิเดทีฟเคมิเคิลพอลิเมอไรเซชั่น ในสารละลายของโพลีซัลโฟนิกและโซเดียมเปอร์ซัลเฟต และเตรียมคอมโพสิทของพอลิเอทิลีนไดออกซีไทโอฟีนกับซีโอไลต์ซีโอไลต์ซีเอสเอ็มไฟต์

พิสูจน์โครงสร้างทางเคมีด้วยเทคนิค Fourier Transform Infrared Spectrophotometry (FTIR), วิเคราะห์มอร์ฟอลอจีโดยการใช้เทคนิคกล้องจุลทรรศน์อิเลคตรอนทั้งแบบส่องกราด (SEM) คุณสมบัติความเสถียรทางความร้อนด้วย Thermogravimetric Analysis (TGA) ลักษณะความเป็นผลึกของสารผสมด้วย X-ray diffractometer (XRD) พื้นที่ผิวและขนาดรูพรุนของซีโอไลต์ด้วยเครื่อง autosorb นอกจากนี้ได้ทำการศึกษาความสามารถในการนำไฟฟ้า ความเสถียร การตอบสนองต่อก๊าซพิษของพอลิพอลิเอทิลีนไดออกซีไทโอฟีน, ซีโอไลต์และคอมโพสิต โดยใช้เครื่อง custom build two-point probe, ใช้ special construct gas cell ในการเก็บก๊าซพิษและศึกษาปฏิกิริยาที่เกิดขึ้นระหว่างก๊าซพิษกับสารผสมด้วยเครื่อง Temperature program desorption (TPD)

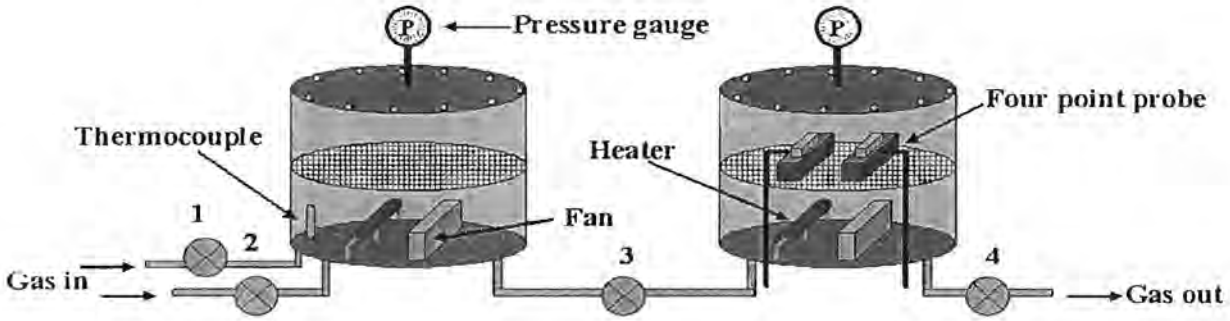

รูปที่ 1 เครื่องมือตรวจวัดการตอบสนองทางไฟฟ้าภายใต้สภาวะก๊าซ

ส่วนที่ 2

2.3 ศึกษาค้นคว้าและรวบรวมข้อมูลเกี่ยวกับงานวิจัย รวมทั้งสั่งซื้อเครื่องแก้วและสารเคมี

2.4 เตรียมตัวอย่างเจลเซลลูโลสเชื่อมขวางทางกายภาพกับสารผลึกเหลว 1-บิวทิล-3-เมททิลอิมมิดาโซเลียมคลอไรด์เพื่อวิเคราะห์คุณลักษณะเฉพาะโดยเครื่องมือวิเคราะห์ทางวิทยาศาสตร์

ในขั้นตอนการเตรียมเจลเซลลูโลสเชื่อมขวางทางกายภาพกับสารผลึกเหลว 1-บิวทิล-3-เมททิลอิมมิดาโซเลียมคลอไรด์ เซลลูโลสถูกละลายในสัดส่วน13เปอร์เซ็นต์ด้วยอุณหภูมิ 100 องศาเซลเซียสเป็นเวลา 15 นาที ซึ่งเทียบเท่ากับ 6.19 เท่าโดยโมลของอัตราส่วนระหว่างโมลของสารผลึกเหลวต่อโมลของหน่วยกลูโคส จากการผสมจะได้ของเหลวหนืดซึ่งจะถูกลดความหนืดด้วยพลาสติไซเซอร์ 1.5 มิลลิลิตรเป็นเวลา 60 นาทีซนิดไดเมทิลอะเซททามายด์โดยแสดงสมบัติเป็นตัวทำละลายร่วมด้วย สารละลายผ่านกระบวนการลดก๊าซและขึ้นรูปเป็นตัวอย่างโดยวิธีการหล่อในแม่พิมพ์เส้นผ่านศูนย์กลางขนาด 25 มิลลิเมตร ความหนา 1 มิลลิเมตร และถูกเก็บไว้ในสภาวะสูญญากาศเป็น

เวลา 12 ชั่วโมงและสภาวะห้องเป็นเวลา 24 ชั่วโมง ตัวอย่างที่ผ่านการขึ้นรูปจะถูกนำไปวิเคราะห์คุณสมบัติด้านไฟฟ้าเชิงกล ไดอิเล็กทริก สภาพพื้นผิวและแรงทางไฟฟ้าสถิตย์ในขั้นต่อไป

การวิเคราะห์คุณสมบัติด้านไฟฟ้าเชิงกลอาศัยการทดสอบด้วยเครื่องรีโอมิเตอร์ที่วัดมอดูลัสแรงเฉือนภายใต้ความเข้มสนามไฟฟ้ากระแสตรง โดยชิ้นงานตัวอย่างถูกประกบด้วยชั้นฉนวนพอลิอิมิด การวัดเริ่มด้วยการหาช่วงวิสโคอิลาสติกด้วยโหมดกวาดความเครียดซึ่งให้ค่าที่เหมาะสมในช่วง 0.25% ความเครียด จากนั้นทดสอบการตอบสนองด้านไฟฟ้าเชิงกลชั่วคราวภายใต้สนามไฟฟ้า 0 และ 1 กิโลโวลต์ต่อมิลลิเมตร ที่อุณหภูมิ 303 และ 333 เคลวิน

การวัดค่าไดอิเล็กทริกถูกวัดด้วยเครื่อง LCRที่ต่อกับเครื่องรีโอมิเตอร์ ที่อุณหภูมิ 303 และ 333 เคลวิน ในช่วงความถี่ 20 ถึง 1 เมกกะเฮิรตซ์ โดยค่าคงที่ไดอิเล็กทริกคือค่าไดอิเล็กทริกที่ความถี่ 20 เฮิรตซ์หารด้วยค่าไดอิเล็กทริกของสุญญากาศที่มีค่า 8.85 พิคโคฟารัดต่อเมตร 20 ถึง 1 เมกกะเฮิรตซ์

การทดสอบการเอียงภายใต้สนามไฟฟ้าไม่เกิน 550 โวลต์ต่อมิลลิเมตร ถูกทดสอบด้วยการวางชิ้นงานในแนวตั้ง ชิ้นงานถูกแขวนลอยในซิลิโคน ซึ่งชิ้นงานอยู่ระหว่างอิเล็กโทรดทองแดงที่ห่างกัน 30 มิลลิเมตร

กล้องตรวจสอบสภาพพื้นผิวและแรงทางไฟฟ้าสถิตถูกใช้ทดสอบด้วยแอมพลิจูด 5 โวลต์ โดยอาศัยหัวทดสอบซิลิคอนเคลือบด้วยชั้นตัวนำไฟฟ้า รัศมีหัวทดสอบ 40 นาโนเมตร โดยการสแกนครั้งแรกเพื่อการตรวจสอบสภาพพื้นผิวโดยการตรวจสอบความสูงของแต่ละตำแหน่งในชิ้นงาน รอบที่สองสแกนที่ความสูง 10 นาโนเมตรเทียบกับความสูงที่วัดได้จากการสแกนครั้งแรกเพื่อตรวจสอบหาแรงทางไฟฟ้าสถิตย์

<u>ส่วนที่ 3</u>

2.5 ศึกษาค้นคว้าและรวบรวมข้อมูลเกี่ยวกับงานวิจัย รวมทั้งสั่งซื้อเครื่องแก้วและสารเคมี

2.6 เตรียมตัวอย่างเจลาตินฟิล์มและเจลาตินที่ใช้สารรกลูตารัลดีไฮด์เป็นตัวเชื่อมขวางเพื่อวิเคราะห์คุณลักษณะเฉพาะโดยเครื่องมือวิเคราะห์ทางวิทยาศาสตร์ พิสูจน์คุณสมบัติทางความร้อนด้วยเครื่อง Thermal gravimetric analyzer (DuPont, model TGA 2950) และ Differential scanning calorimetry (Instruments DSC METTLER 822, วิเคราะห์คุณสมบัติเชิงกลทางไฟฟ้าและทางความร้อนด้วยเครื่อง Melt rheometer (Rheometric Scientific, ARES), ศึกษาการเบี่ยงเบนของวัสดุโดยใช้ตัวบันทึกภาพวีดีโอ

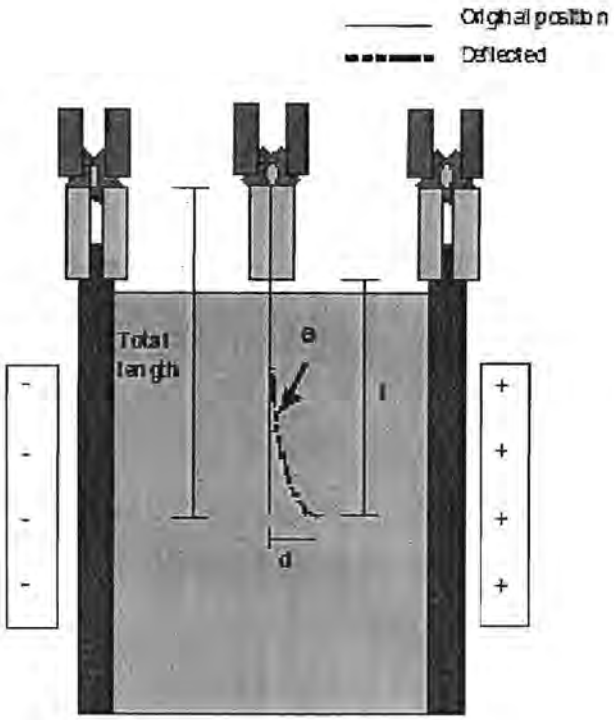

รูปที่ 2 รูปภาพการเบี่ยงเบนของวัสดุเมื่ออยู่ภายใต้สนามไฟฟ้า

ส่วนที่ 4

2.7 ศึกษาค้นคว้าและรวบรวมข้อมูลเกี่ยวกับงานวิจัย รวมทั้งสั่งซื้อเครื่องแก้วและสารเคมี

2.8 เตรียมแผ่นอัลจิเนตไฮโดรเจลเพื่อศึกษาลักษณะการบวมน้ำของแผ่นไฮโดรเจล

แผ่นอัลจิเนตไฮโดรเจลเตรียมขึ้นด้วยวิธีการหล่อ (Casting) โดยการผสมสารละลายอัลจิเนตกับสารละสารแคลเซียมคลอไรด์ซึ่งเป็นสารเชื่อมโยงในอัตราส่วนต่างๆ จากนั้นเทสารละลายผสมลงในจานแก้วเพื่อขึ้นขึ้นรูปเจล

ลักษณะการบวมตัวและขนาดของรูพรุ่นภายในแผ่นอัลจิเนตไฮโดรเจล ถูกศึกษาด้วยเทคนิคกล้องจุลทรรศน์อิเลคตรอนทั้งแบบส่องกราด (SEM) หลังจากแผ่นไฮโดรเจลถูกทำให้บวมตัวในน้ำ นอกจากนี้ได้ทำการศึกษาลักษณะการบวมตัวและขนาดรูพรุ่นภายในแผ่นไฮโดรเจลจากการคำนวณค่าต่างๆ ที่ได้จากชั่งน้ำหนักเจลก่อนและหลังการบวมตัวในสารละลายบัฟเฟอร์ พีเอช 5.5

2.9 เตรียมผสมยาลงในแผ่นอัลจิเนตไฮโดรเจลเพื่อศึกษาการปลดปล่อยยาจากแผ่นอัลจิเนตไฮโดรเจล

ยาถูกนำใส่ในแผ่นอัลจิเนตไฮโดรเจลโดยการผสมสารละลายอัลจิเนตกับยา จากนั้นใส่สารละสารแคลเซียมคลอไรด์ซึ่งเป็นสารเชื่อมโยงในอัตราส่วนต่างๆ เทสารละลายผสมลงในจานแก้วเพื่อ

ขึ้นขึ้นรูปเจล ลักษณะการปลดปล่อยยาจากแผ่นอัลจิเนตไฮโดรเจลถูกศึกษาด้วยอุปกรณ์ "Modified Franz Diffusion cell" ดังรูป

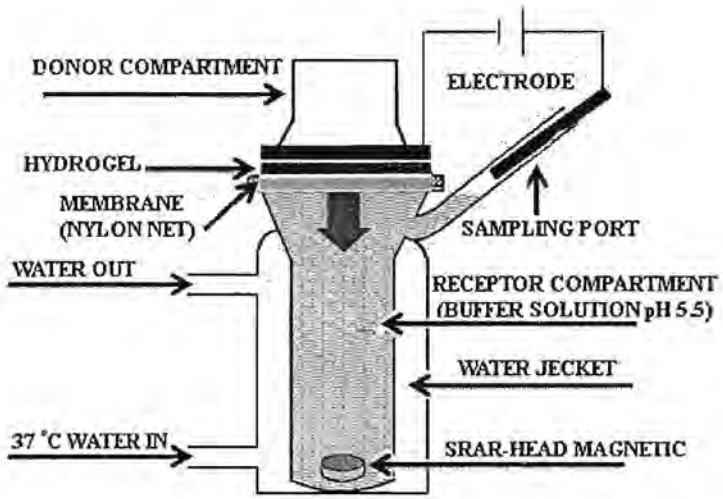

รูปที่ 3 อุปกรณ์ทดสอบการปลดปล่อยยา

3. อภิปรายและวิจารณ์ผลการทดลอง

ส่วนที่1

3.1 ผลการทดสอบค่าการนำไฟฟ้าและการว่องไวในการตอบสนองทางไฟฟ้าภายใต้สภาวะก๊าซของคอมโพสิตระหว่างโพลีเอทิลีนไดออกซีไทโอฟีนและซีโอไลต์ซีเอสเอ็มไฟต์

3.1.1 ผลกระทบของอัตราส่วนของมอนอเมอร์เอทิลีนไดออกซีไทโอฟีนต่อโพลีซัลโฟนิกที่มีต่อค่าการนำไฟฟ้าของโพลีเอทิลีนไดออกซีไทโอฟีน

ผลจากการสังเคราะห์พอลิเอทิลีนไดออกซีไทโอฟีน โดยวิธีการสังเคราะห์แบบออกซิเดทีฟเคมิเคิลพอลิเมอไรเซชั่น ในสารละลายของโพลีซัลโฟนิกและโซเดียมเปอร์ซัลเฟต โดยใช้อัตราส่วนของมอนอเมอร์เอทิลีนไดออกซีไทโอฟีนต่อโพลีซัลโฟนิกในช่วง 1:1 – 1:10 พบว่า พอลิเอทิลีนไดออกซีไทโอฟีนที่สังเคราะห์จากการเตรียมอัตราส่วนของมอนอเมอร์เอทิลีนไดออกซีไทโอฟีนต่อโพลีซัลโฟนิกเท่ากับ 1:1 นั้นให้ค่าการนำไฟฟ้าสูงที่สุด ผู้ทำวิจัยจึงนำพอลิเอทิลีนไดออกซีไทโอฟีนที่สังเคราะห์ได้จากอัตราส่วนดังกล่าวมาเตรียมคอมโพสิตระหว่างโพลีเอทิลีนไดออกซีไทโอฟีนและซีโอไลต์ซีเอสเอ็มไฟต์ เพื่อนำไปวัดความว่องไวในการตอบสนองทางไฟฟ้าภายใต้สภาวะก๊าซในขั้นตอนต่อไป

3.1.2 ผลกระทบของปริมาณซีโอไลต์ซีเอสเอ็มไฟต์ที่มีต่อค่าการนำไฟฟ้าและการว่องไวในการตอบสนองทางไฟฟ้าภายใต้สภาวะก๊าซ

จากการทดลองเพื่อศึกษาความสัมพันธ์ระหว่างความว่องไวในการตอบสนองการตอบสนองต่อก๊าซคาร์บอนมอนอกไซด์ของคอมโพสิตระหว่างโพลีเอทิลีนไดออกซีไทโอฟีนและซีโอไลต์ซีเอสเอ็มไฟต์ โดยเลือกใช้ปริมาณของซีโอไลต์ซีเอสเอ็มไฟต์ในเมทริกต์ของโพลิเมอร์ที่อัตราส่วนโดยปริมาตรร้อยละ 0, 10, 20, 30, 40 และ 50 ที่อุณหภูมิ 27 องศาเซลเซียสและความดัน 1 บรรยากาศ พบว่าความว่องไวในการตอบสนองทางไฟฟ้าภายใต้สภาวะก๊าซคาร์บอนมอนอกไซด์ของคอมโพสิตระหว่างโพลีเอทิลีนไดออกซีไทโอฟีนและซีโอไลต์ซีเอสเอ็มไฟต์ มีค่าความว่องไวในการตอบสนองทางไฟฟ้าเพิ่มขึ้นเมื่อปริมาณซีโอไลต์เพิ่มขึ้น และมีความว่องไวในการตอบสนองทางไฟฟ้าสูงสุดเมื่ออัตราส่วนของซีโอไลต์ซีเอสเอ็มไฟต์ในเมทริกต์ของโพลิเมอร์มีค่าเท่ากับร้อยละ 20 โดยปริมาตร และเมื่อเพิ่มปริมาณของซีโอไลต์ซีเอสเอ็มไฟต์ ในเมทริกต์ของโพลิเมอร์ให้มากกว่าร้อยละ 20 โดยปริมาตร พบว่าคอมโพสิตจะมีค่าความว่องไวในการตอบสนองทางไฟฟ้าลดลง ผู้ทำวิจัยจึงเลือกใช้อัตราส่วนดังกล่าวมาเตรียมคอมโพสิตระหว่างโพลีเอทิลีนไดออกซีไทโอฟีนและซีโอไลต์ซีเอสเอ็มไฟต์ เพื่อนำไปวัดความว่องไวในการตอบสนองทางไฟฟ้าภายใต้สภาวะก๊าซในขั้นตอนต่อไป

3.1.3 ผลกระทบของอัตราส่วนของซิลิกาต่ออลูมินาในซีโอไลต์ซีเอสเอ็มไฟต์ที่มีผลต่อความว่องไวในการตอบสนองต่อก๊าซคาร์บอนมอนอกไซด์ของคอมโพสิตระหว่างโพลีเอทิลีนไดออกซีไทโอฟีนและซีโอไลต์ซีเอสเอ็มไฟต์

จากการทดลองเพื่อศึกษาความสัมพันธ์ระหว่างความว่องไวในการตอบสนองการตอบสนองต่อก๊าซคาร์บอนมอนอกไซด์ของคอมโพสิตระหว่างโพลีเอทิลีนไดออกซีไทโอฟีนและซีโอไลต์ซีเอสเอ็มไฟต์ โดยเลือกใช้อัตราส่วนของซิลิกาต่ออลูมินาในซีโอไลต์ซีเอสเอ็มไฟต์ในเมทริกต์ของโพลิเมอร์ที่อัตราส่วน 23, 50, 80 และ 280 ที่อุณหภูมิ 27 องศาเซลเซียสและความดัน 1 บรรยากาศ จากผลการทดลองพบว่า อัตราส่วนของซิลิกาต่ออลูมินาของซีโอไลต์ซีเอสเอ็มไฟต์ของคอมโพสิตระหว่างโพลีเอทิลีนไดออกซีไทโอฟีนและซีโอไลต์ซีเอสเอ็มไฟต์ มีผลต่อความว่องไวในการตอบสนองทางไฟฟ้าภายใต้สภาวะก๊าซคาร์บอนมอกไซด์ อันเนื่องมาจากอัตราส่วนของซิลิกาต่ออลูมินาของซีโอไลต์ซีเอสเอ็มไฟต์ดังกล่าวมีผลทำให้คุณสมบัติในการดูดซับก๊าซคาร์บอนมอกไซด์ของซีโอไลต์ซีเอสเอ็มไฟต์เปลี่ยนแปลง

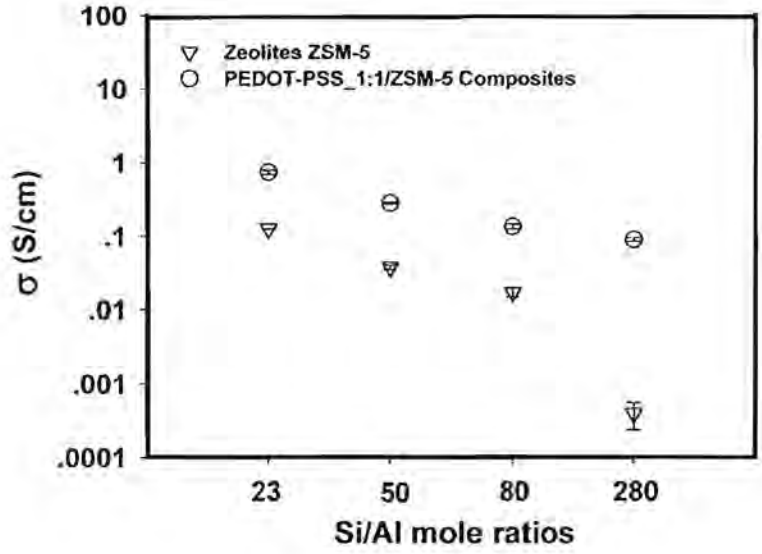

รูปที่ 4 กราฟแสดงความสัมพันธ์ระหว่างค่าการนำไฟฟ้าของซีโอไลต์ซีเอสเอ็มไฟต์และคอมโพสิต ระหว่างโพลีเอทิลีนไดออกซีไทโอฟีนและซีโอไลต์ซีเอสเอ็มไฟต์ที่มีอัตราส่วนของซิลิกาต่ออลูมินา ตั้งแต่ 23 - 280 โดยปริมาณของซีโอไลต์ซีเอสเอ็มไฟต์ในเมทริกต์ของโพลิเมอร์มีอัตราส่วนโดย ปริมาตรร้อยละ 20 ที่อุณหภูมิ 27 องศาเซลเซียสและความดัน 1 บรรยากาศ

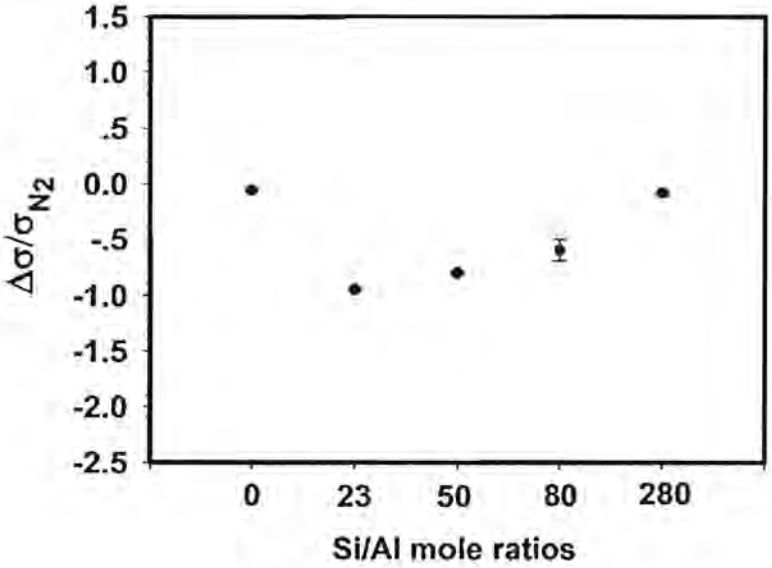

รูปที่ 5 กราฟแสดงความสัมพันธ์ระหว่างความว่องไวในการตอบสนองต่อก๊าซคาร์บอนมอนอกไซด์ ของโพลีเอทิลีนไดออกซีไทโอฟีนและคอมโพสิตระหว่างโพลีเอทิลีนไดออกซีไทโอฟีนและซีโอไลต์ซี เอสเอ็มไฟต์กับอัตราส่วนของซิลิกาต่ออลูมินาของซีโอไลต์ซีเอสเอ็มไฟต์เมทริกต์ของโพลิเมอร์ที่ อัตราส่วนโดยปริมาตรร้อยละ 20 ที่อุณหภูมิ 27 องศาเซลเซียสและความดัน 1 บรรยากาศ

โดยมีความสัมพันธ์กับอัตราส่วนของซิลิกาต่ออลูมินาในซีโอไลต์ซีเอสเอ็มไฟต์ดังนี้ เมื่ออัตราส่วนของซิลิกาต่ออลูมินาในซีโอไลต์ซีเอสเอ็มไฟต์มีค่าลดลงจาก 280 เป็น 23 ความว่องไวในการตอบสนองทางไฟฟ้าภายใต้สภาวะก๊าซของคอมโพสิต จะมีค่าเพิ่มขึ้น เนื่องมาจากคอมโพสิตที่อัตราส่วนของซิลิกาต่ออลูมินาในซีโอไลต์ซีเอสเอ็มไอออนมีค่าลดลง มีผลทำให้ซีโอไลต์มีตำแหน่งภายในโพรงของซีโอไลต์ที่สามารถให้โมเลกุลของก๊าซมาเกาะได้มากขึ้น ทำให้เพิ่มความสารมารถในการดูดซับก๊าซของคอมโพสิต ซึ่งเป็นการเพิ่มโอกาสให้โมเลกุลของก๊าซมาจับกับโพลิเมอร์โพลีเอทิลีนไดออกซีไทโอฟีนได้ดีมากยิ่งขึ้น จึงเหนี่ยวนำก๊าซคาร์บอนมอนอกไซด์ได้ดียิ่งขึ้น ทำให้ความว่องไวในการตอบสนองทางไฟฟ้าภายใต้สภาวะก๊าซของคอมโพสิตมีค่าเพิ่มขึ้น

ส่วนที่ 2

3.2 ผลการทดสอบคุณสมบัติเชิงกลทางไฟฟ้าของเจลเซลลูโลสเชื่อมขวางทางกายภาพกับสารผลึกเหลว 1-บิวทิล-3-เมททิลอิมมิดาโซเลียมคลอไรด์

3.2.1 ผลการทดสอบการตอบสนองด้านไฟฟ้าเชิงกลชั่วคราวภายใต้สนามไฟฟ้า 0 และ 1 กิโลโวลต์ต่อมิลลิเมตร ที่อุณหภูมิ 303 และ 333 เคลวิน

จากแผนภาพที่1 ค่ามอดูลัสเพิ่มขึ้นเมื่อสนามไฟฟ้าเป็น1 กิโลโวลต์ต่อมิลลิเมตร และลดลงเมื่อสนามไฟฟ้าเป็น 0 กิโลโวลต์ต่อมิลลิเมตรสลับกันไปจนเข้าสู่สภาวะนิ่ง เนื่องจากสนามไฟฟ้าทำให้เกิดการโพลาไรซ์ของไอออนบวกของสารผลึกเหลว การโพลาไรซ์ของหมู่ไฮดรอกซิลบนเซลลูโลส และการจัดเรียงตัวภายใต้แรงเฉือนขณะทดสอบ เมื่อลดสนามไฟฟ้าเป็น 0 กิโลโวลต์ต่อมิลลิเมตรจะไม่กลับไปสู่ค่าเริ่มต้นเนื่องจากไดโพลโมเมนต์ที่ค้างอยู่ในชิ้นงานและจะเข้าสู่สภาวะนิ่งในวินาทีที่ 1800 ที่อุณหภูมิ 333 เคลวิน ค่ามอดูลัสภายใต้สนามไฟฟ้าเป็น 0 กิโลโวลต์ต่อมิลลิเมตรสูงกว่าภายใต้สนามไฟฟ้าเป็น 1 กิโลโวลต์ต่อมิลลิเมตรเพราะอุณหภูมิส่งเสริมการโพลาไรซ์ของไอออนบวกของสารผลึกเหลว การโพลาไรซ์ของหมู่ไฮดรอกซิลบนเซลลูโลส และการจัดเรียงตัวภายใต้แรงเฉือนขณะทดสอบให้มากขึ้น แต่เมื่ออยู่ภายใต้สนามไฟฟ้าเป็น1 กิโลโวลต์ต่อมิลลิเมตร ค่ามอดูลัสเพิ่มขึ้นน้อยกว่ากรณีภายใต้สนามไฟฟ้าเป็น 0 กิโลโวลต์ต่อมิลลิเมตรเนื่องจากการรวมตัวกลับของสารผลึกเหลว การผ่อนคลายภายใต้สนามไฟฟ้าของเซลลูโลสที่มากขึ้น

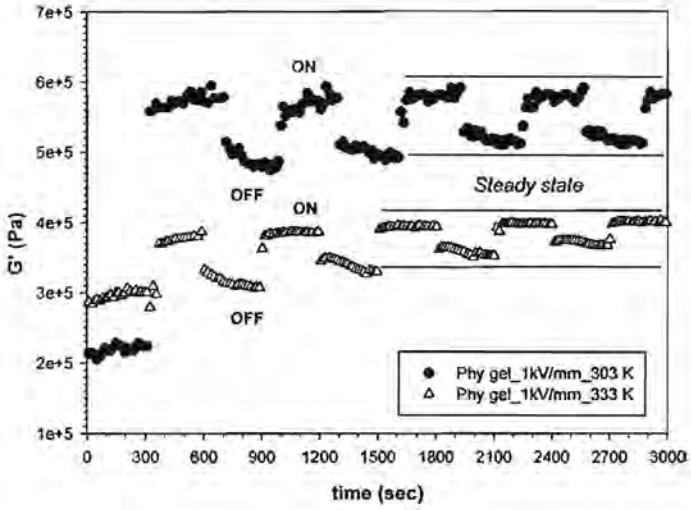

รูปที่ 6 การตอบสนองด้านไฟฟ้าเชิงกลชั่วคราวภายใต้สนามไฟฟ้า 0 และ 1 กิโลโวลต์ต่อมิลลิเมตร ที่อุณหภูมิ 303 และ 333 เคลวิน 0.25เปอร์เซ็นต์ความเครียดและความถี่1เรเดียนต่อวินาที

3.2.2 <u>ผลการทดสอบค่าไดอิเล็กทริกที่ความถี่ระหว่าง20ถึง1เมกกะเฮิรตซ์ ที่อุณหภูมิ303 และ 333 เคลวิน</u>

ค่าไดอิเล็กทริกที่ความถี่ระหว่าง 20 ถึง 1เมกกะเฮิรตซ์ ที่อุณหภูมิ 303 และ 333 เคลวินถูกรายงานในรูปที่ 7 ซึ่งแสดงให้เห็นว่าเจลตัวอย่างประกอบด้วยคุณลักษณะหลักของไดอิเล็กทริกชนิดไอออนซึ่งเพิ่มขึ้นเมื่อความถี่เพิ่มขึ้น โดยค่าคงที่ไดอิเล็กทริกเพิ่มขึ้นสูงสุดที่อุณหภูมิเท่ากับ313เคลวินเนื่องจากอุณหภูมิส่งเสริมการเคลื่อนที่ของไอออนบวกของสารผลึกเหลวซึ่งเหนี่ยวนำให้เกิดค่าไดโพลโมเมนต์ที่มากขึ้นแต่หากอุณหภูมิสูงเกิน313เคลวิน ค่าคงที่ไดอิเล็กทริกจะลดลงเนื่องจากการการรวมตัวกลับของสารผลึกเหลวเช่นกัน

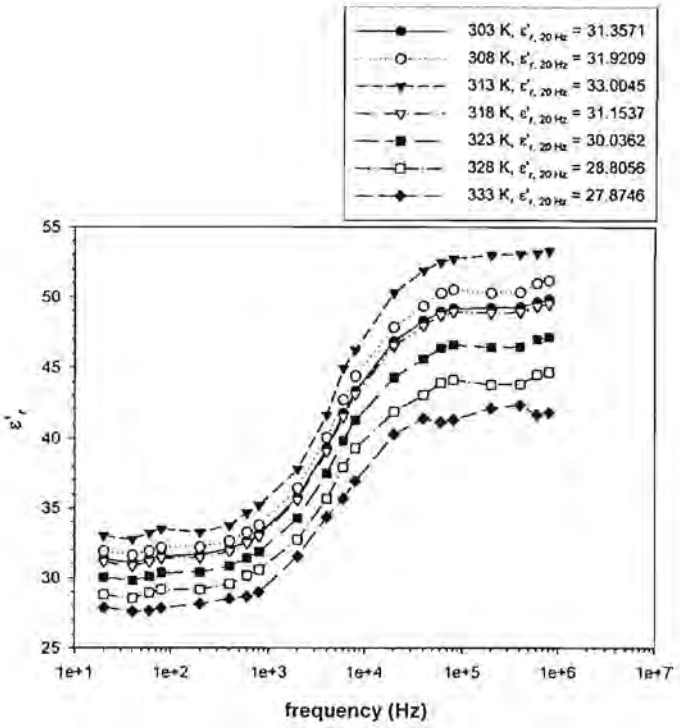

รูปที่ 7 ค่าไดอิเล็กทริกในช่วงความถี่ 20 ถึง 1 เมกกะเฮิรตซ์ ที่อุณหภูมิ 303 และ 333 เคลวิน

3.2.3 <u>ผลการทดสอบการเอียงของชิ้นงานภายใต้สนามไฟฟ้าไม่เกิน 550 โวลต์ต่อมิลลิเมตร ที่อุณหภูมิ 303 เคลวิน</u>

การทดสอบการเอียงของชิ้นงานภายใต้สนามไฟฟ้าไม่เกิน 550 โวลต์ต่อมิลลิเมตร ถูกแสดงในรูปที่ 8 พบว่าเมื่อสนามไฟฟ้ามีค่าเท่ากับ 500 โวลต์ต่อมิลลิเมตร ชิ้นงานเอียงไปด้านขวาที่เป็นด้านอิเล็กโทรดแอโนดที่มีศักย์ไฟฟ้าสูงกว่าด้านตรงข้าม เนื่องด้วยการเคลื่อนที่หลักของไอออนบวกของสารผลึกเหลวเข้าหาด้านแคโทดด้วยแรงทางไฟฟ้าสถิตย์แล้วทำให้เกิดไอออนิกโพลาไรเซชั่นและแรงดึงภายในชิ้นงานเนื่องจากปริมาตรสุทธิที่แตกต่างระหว่างสองด้านของชิ้นงาน ร่วมกับอิเล็กทรอนิกโพลาไรเซชั่นของหมู่ไฮดรอกซิลของเซลลูโลส ดังที่ทราบกันดีว่าเซลลูโลสที่ตอบสนองต่อไฟฟ้าอาศัยการทำงานบนพื้นฐานโพลาไรเซชั่นทั้งส่วนของไอออนและอิเล็กทรอนิกส์ ที่น่าสนใจคือการปรากฏการแกว่งกลับไปกลับมาของชิ้นงานเมื่อค่าความเข้มสนามไฟฟ้ามีค่าระหว่าง 525 ถึง 550 โวลต์ต่อมิลลิเมตร โดยมุมการแกว่งมีค่ามากขึ้นเมื่อความเข้มสนามไฟฟ้าสูงขึ้น ปรากฏการณ์นี้ถูกคาดว่ามีสาเหตุมาจากการเคลื่อนที่แข่งขันกันระหว่างไอออนบวกและลบของสารผลึกเหลวด้วยแรงทางไฟฟ้าสถิตย์

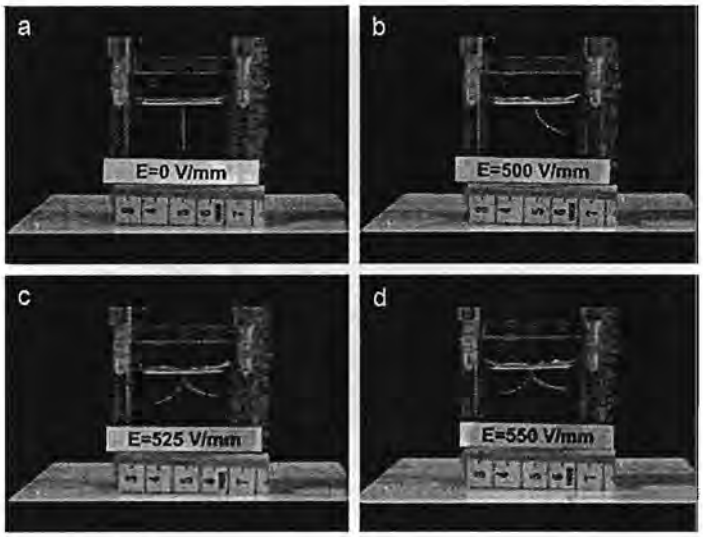

รูปที่ 8 การทดสอบการเอียงของชิ้นงานภายใต้สนามไฟฟ้าเท่ากับ 0 500 525 และ 550 โวลต์ต่อมิลลิเมตร ที่อุณหภูมิ 303 เคลวิน โดยอิเล็กโทรดแคโทรดและแอโนดอยู่ด้านซ้ายและขวาของแผนภาพตามลำดับ

3.2.4 ผลการทดสอบสภาพพื้นผิวและแรงทางไฟฟ้าสถิตย์ที่อุณหภูมิ 303 เคลวิน

สภาพพื้นผิวและแรงทางไฟฟ้าสถิตถูกตรวจสอบดังแสดงในรูปที่ 9 ปรากฏสภาพพื้นผิวที่ไม่เรียบในระดับนาโนเมตรและกลุ่มไอออนที่ชอบน้ำดังแสดงในส่วนที่สว่าง ซึ่งกลุ่มไอออนดังกล่าวมีลักษณะเป็นท่อทอดยาวเพื่อสะดวกต่อการเคลื่อนที่ของไอออนและโปรตรอนภายในเจล

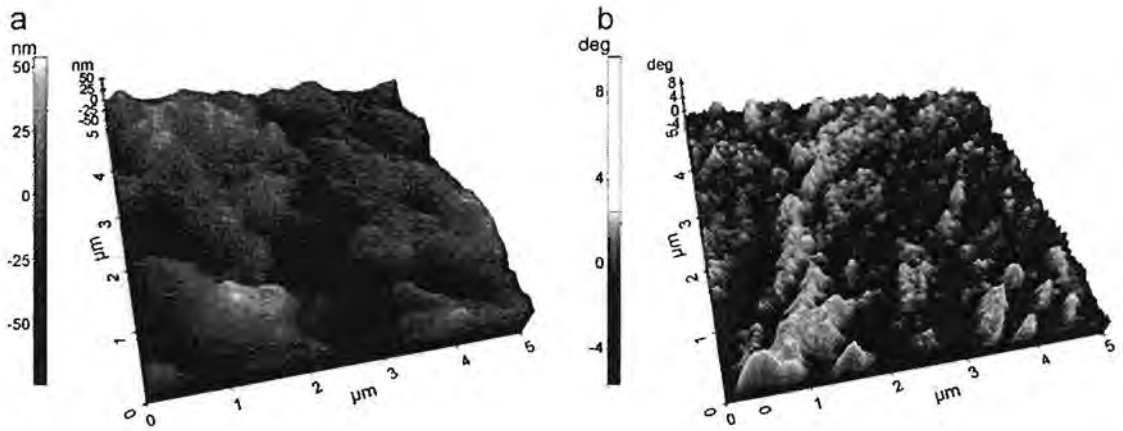

รูปที่ 9 สภาพพื้นผิวและแรงทางไฟฟ้าสถิตที่อุณหภูมิ 303 เคลวิน

ส่วนที่ 3

3.3 ผลการทดสอบคุณสมบัติเชิงกลทางไฟฟ้าของเจลาตินในแต่ละความแข็งแรงของเจลและเจลาตินที่มีสารเชื่อมขวางที่ในผลกระทบของสนามไฟฟ้าและอุณหภูมิ

3.3.1 ผลกระทบของสนามไฟฟ้า

ผลของสนามไฟฟ้าต่อคุณสมบัติเชิงกลของเจลาตินความแข็งระดับสูง กลาง ต่ำ และ 3% ของเจลาตินที่มีสารเชื่อมขวางโดยความเข้มของสนามไฟฟ้า 0-1 kV/mm รูปที่ 10 พบว่าการตอบสนองต่อความแข็งแรงของวัสดุจพเพิ่มขึ้นเมื่อความเข้มสนามไฟฟ้ามากขึ้น โดยที่ความว่องไวของการตอบสนองของวัสดุเท่ากับ 2.30, 2.16, 1.26, และ 0.49 สำหรับเจลาตินความแข็งระดับสูง กลาง ต่ำ และ 3% ของเจลาตินที่มีสารเชื่อมขวางตามลำดับ เมื่อมีการให้สานมไฟฟ้าจะเกิดไดโพลโมเมนต์ในโครงสร้างของเจลาตินซึ่งส่งผลต่อการการจัดเรียงตัวของโครสร้าง จึงส่งผลให้การตอบสนองทางเชิงกลของวัสดุมีค่าเพิ่มขึ้น

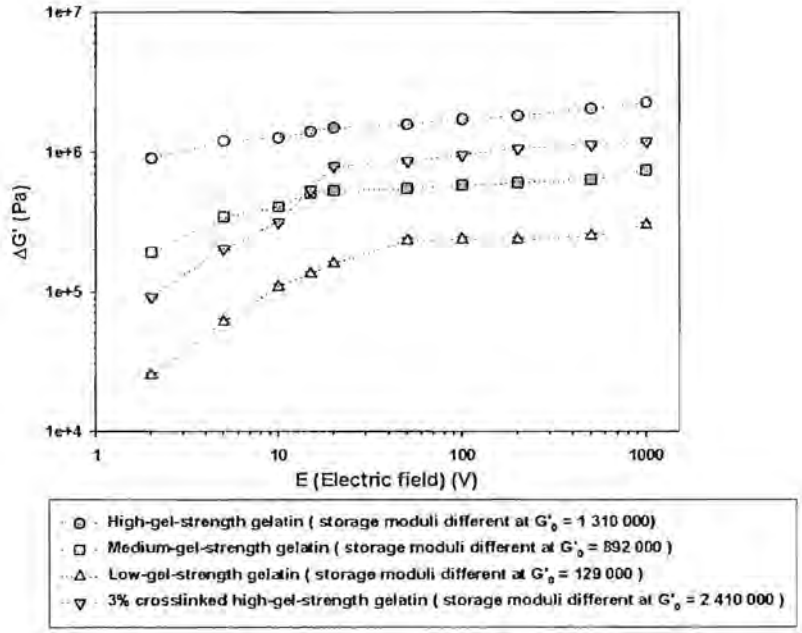

รูปที่ 10 การตอบสนองของความแข็งแรงของฟิล์มเจลาตินชนิดความแข็งแรงสูง กลาง ต่ำ และ 3% ของเจลาตินที่มีสารเชื่อมขวาง

3.3.2 ผลกระทบของอุณหภูมิ

จากการทดลองเพื่อศึกษาคุณสมบัติเชิงกลทางไฟฟ้าของเจลาตินความแข็งระดับสูง กลาง ต่ำ และ 3% ของเจลาตินที่มีสารเชื่อมขวางในผลของอุณหภูมิ จากรูปที่ 11 พบว่าความแข็งแรงของวัสดุลดลงเมื่ออุณหภูมิเพิ่มขึ้น เนื่องจากผลของอุณหภูมิส่งผลต่อการเคลื่อนไหวของโมเลกุลได้มากขึ้น โดยพบว่าความแข็งแรงของวัสดุมีอยู่ในสนามไฟฟ้าจะมีความแข็งแรงสูงกว่าวัสดุอื่นๆที่ปราศจากสนามไฟฟ้าที่อุณหภูมิใดใด เป็นผลมาจากไดโพลโมเมนต์ในโครงสร้างวัสดุที่เกิดขึ้นจากสนามไฟฟ้า ทั้งนี้ยังพบว่าความว่องไวต่อการตอบสนองความแข็งแรงของวัสดุเพิ่มขึ้นเมื่ออุณหภูมิเพิ่มขึ้น

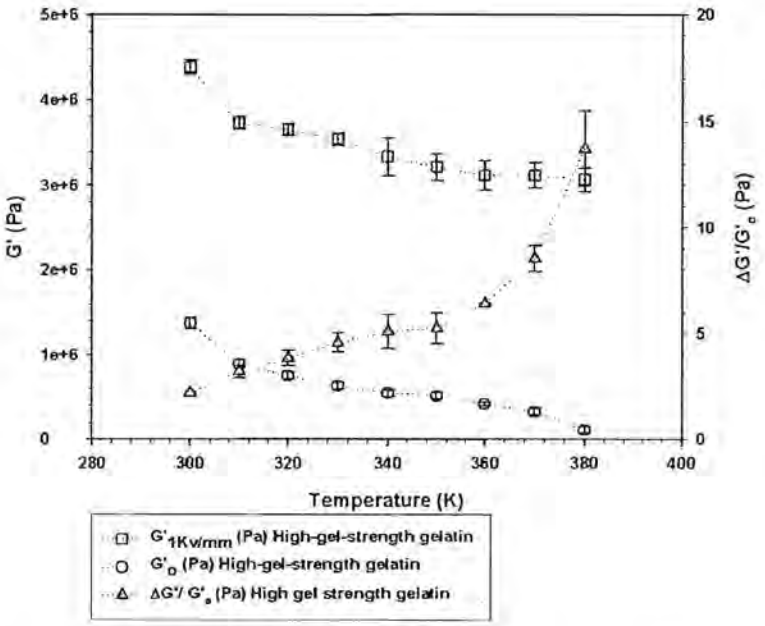

รูปที่ 11 การตอบสนองของความแข็งแรงของฟิล์มเจลาตินในผลของอุณหภูมิ

3.3.3 การตอบสนองการเบี่ยงเบนของฟิล์มเจลาติน

จากการทดลองเพื่อศึกษาการตอบสนองด้วยการเบี่ยงเบนของฟิล์มเจลาตินภายใต้สนามไฟฟ้า พบว่าฟิล์มเจลาตินจะตอบสนองด้วยการเบนไปทางขั้วบวกซึ่งหมายความว่าเจลาตินแสดงความเป็นขั้วลบเมื่ออยู่ภายใต้สนามไฟฟ้า เนื่องมาจากผลของไดโพลโมมนต์ของหมู่คาโบนิลในโครงสร้างเจลาติน ดังแสดงในรูปที่ 12 ทั้งนี้พบว่าเจลาตินความแข็งแรงต่ำจะเบี่ยงเบนได้มากกว่าเจลาตินความแข็งแรงสูง โดยฟิล์มจะเริ่มเบี่ยงเบนที่สนามไฟฟ้า 600 V/mm

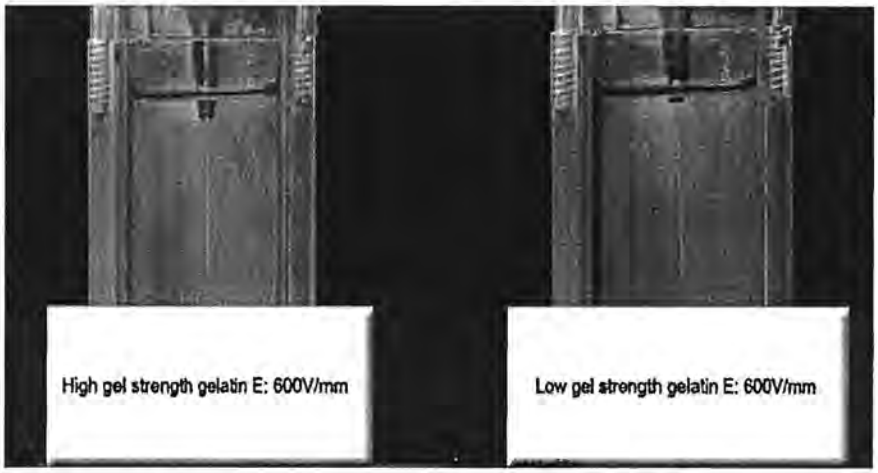

รูปที่ 12 การเบี่ยงเบนของฟิล์มเจลาตินภายใต้สนามไฟฟ้าความเข้ม 600 V/mm

ส่วนที่ 4

3.4 ผลการศึกษาการปลดปล่อยยาจากแผ่นอัลจิเนตไฮโดรเจล

3.4.1 อิทธิพลของปริมาณสารเชื่อมโยงต่อการปลดปล่อยยาจากแผ่นอัลจิเนตไฮโดรเจล

จากการศึกษาการปลดปล่อยยาชนิดเบนโซอิกแอซิดจากแผ่นอัลจิเนตไฮโดรเจล ภายใต้อิทธิพลของปริมาณสารเชื่อมโยง พบว่าปริมาณการแพร่ผ่านของยาผ่านแผ่นไฮโดรเจลลดลง เมื่อมีการเพิ่มปริมาณสารเชื่อมโยง เนื่องจากปริมาณสารเชื่อมโยงที่เพิ่มขึ้นส่งผลให้ความสามารถในการบวมน้ำของเจลลดลง และรูพรุนภายในเจลมีขนาดเล็ก ดังนั้นปริมาณยาแพร่ผ่านไฮโดรเจลออกมาจึงลดลงด้วย

3.4.2 อิทธิพลของชนิดของยาต่อการปลดปล่อยยาจากแผ่นอัลจิเนตไฮโดรเจล

ในงานวิจัยเลือกใช้ยา 3 ชนิด ที่มีขนาดโมเลกุลและความสามารถในการแตกตัวเป็นไอออนต่างกัน คือ เบนโซอิกแอซิดขนาดโมเลกุล 5.58 อังสตรอม โฟลิกแอซิดขนาดโมเลกุล 8.31 อังสตรอม และแทนนิกแอซิดขนาดโมเลกุล 36.84 อังสตรอม สำหรับความสามารถในการแตกตัวที่ค่าพีเอช 5.5 เบนโซอิกแอซิดและแทนนิกแอซิดสามารถแตกตัวเป็นไอออนลบ โฟลิกแอซิดสามารถแตกตัวเป็นไอออนบวก ผลการศึกษาพบว่าการปริมาณการแพร่ผ่านของเบนโซอิกแอซิดมากที่สุด เนื่องจากขนาดโมเลกุลของเบนโซอิกแอซิดเล็กที่สุด ต่อมาเป็นโฟลิกแอซิดและแทนนิกแอซิดตามลำดับ นอกจากนี้ยังพบว่าผลของการแตกตัวเป็นไอออนบวกกับลบยังมีผลต่อการแพร่ผ่านของยาคือ ยาที่มีความสามารถในการแตกตัวเป็นลบ นั่นคือ เบนโซอิกแอซิดและแทนนิกแอซิด สามารถ

แพร่ผ่านได้ดีกว่ายาที่เป็นบวก คือ โฟลิกแอซิด เนื่องจากยาที่เป็นบวกจะสร้างแรงดึงดูดระหว่างประจุบวกของยากับประจุลบของคาร์บอกซีเลท (COO^-) บนสายโซ่ของอัลจิเนต ซึ่งส่งผลให้การแพร่ผ่านของยาลดลง เมื่อเปรียบเทียบกับยาที่แตกตัวเป็นลบซึ่งจะสร้างแรงผลักสำหรับช่วยผลักยาออกมาจากระบบแทน

3.4.3 อิทธิพลของกระแสไฟฟ้าต่อการปลดปล่อยยาจากแผ่นอัลจิเนตไฮโดรเจล

การศึกษาการปลดปล่อยยาจากแผ่นอัลจิเนตไฮโดรเจลโดยการใช้แผ่นอิเล็กโทรดชนิดแคโทรดวางบนแผ่นเจล ผลการศึกษาพบว่ายาชนิดเบนโซอิกแอซิดและแทนนิกแอซิด ถูกปลดปล่อยออกมาจากแผ่นเจลมากขึ้นเมื่อมีการใช้กระแสไฟฟ้ามากขึ้น (V = 0.5-5 โวลล์) ในขณะที่การปลดปล่อยโฟลิกแอซิดลดลงเมื่อมีใช้กระแสไฟฟ้ามากขึ้น เนื่องจากประจุบนอิเล็กโทรดชนิดแคโทรดเป็นลบซึ่งดึงดูดกับโฟลิกแอซิดที่เป็นประจุบวกไว้มากขึ้น ทำให้การปลดลปล่อยโฟลิกแอซิดน้อยลง

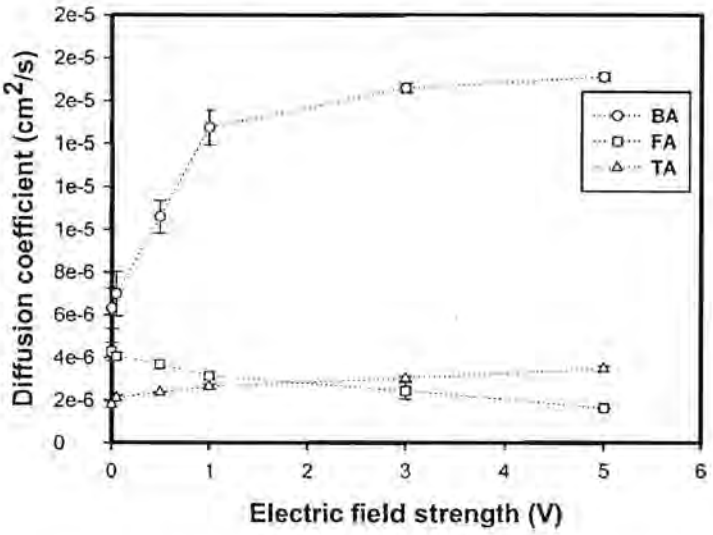

รูปที่ 13 กราฟแสดงความสัมพันธ์ระหว่างความสามารถในการแพร่ของยาแต่ละชนิดต่อปริมาณของกระแสไฟฟ้า

3.4.4 อิทธิพลของชนิดของขั้วอิเล็คโทรดต่อการปลดปล่อยยาจากแผ่นอัลจิเนตไฮโดรเจล

การศึกษาผลของชนิดของขั้วอิเล็กโทรดโดยวางแผ่นอิเล็กโทรดชนิดแคโทรด หรือชนิดแอโนดลงบนแผ่นไฮโดรเจลเปรียบเทียบกับกรณีไม่ใช้กระแสไฟฟ้าในการปลดปล่อยยาชนิดเบนโซอิกแอซิด ผลการศึกษาพบว่าปริมาณการแพร่ผ่านของยามากที่สุดเมื่อใช้ขั้วอิเล็กโทรดชนิดแคโทรดวางบนแผ่นเจล เนื่องจากมีการสร้างแรงผลักระหว่างประจุลบของยากับขั้วอิเล็กโทรดดันยา

ออกจากระบบ ขณะที่ปริมาณการแพร่ผ่านของยาน้อยที่สุดเมื่อใช้ขั้วอิเล็กโทรดชนิดแอโนดวางบนแผ่นเจล เนื่องจากมีการสร้างแรงดึงดูดระหว่างประจุลบของยากับประจุบวกของขั้วอิเล็กโทรดดึงดูดยาไว้ในระบบ

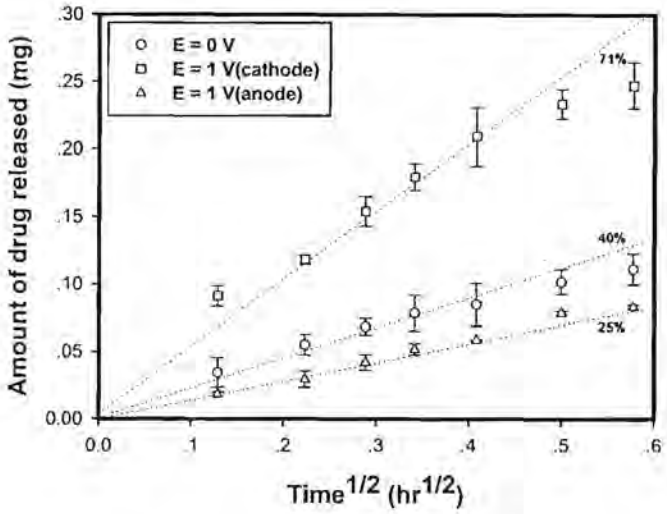

รูปที่ 14 กราฟแสดงความสัมพันธ์ระหว่างปริมาณยาที่ปลดปล่อยออกแผ่นอัลจิเนตไฮโดรเจลกับเวลาที่เปลี่ยนไป

4. สรุปและเสนอแนะเกี่ยวกับการวิจัยในขั้นต่อไป

ส่วนที่ 1

จากการศึกษาข้างต้น ทำให้ทางผู้วิจัยสามารถสรุปได้ว่า การเติมซีโอไลต์ซีเอสเอ็มไฟต์ลงไปในเมทริกต์ของโพลิเมอร์นำไฟฟ้าโพลีเอทิลีนไดออกซีไทโอฟีน จะช่วยเพิ่มความว่องไวในการตอบสนองทางไฟฟ้าภายใต้สภาวะก๊าซคาร์บอนมอนอกไซด์ของคอมโพสิต โดยปริมาณของซีโอไลต์ที่เหมาะสมที่สุดที่ควรใช่เตรียมคอมโพสิตคือร้อยละ 20 โดยปริมาตร และอัตราส่วนของซิลิกาต่ออลูมินาในซีโอไลต์ซีเอสเอ็มไฟต์สามารถส่งผลต่อความว่องไวในการตอบสนองทางไฟฟ้าภายใต้สภาวะก๊าซ อันเนื่องมาจากความสามารถในการดูดซับก๊าซเปลี่ยนแปลงไปตามอัตราส่วนของซิลิกาต่ออลูมินาในซีโอไลต์ซีเอสเอ็มไฟต์ โดยคอมโพสิตที่มีอัตราส่วนของซิลิกาต่ออลูมินาในซีโอไลต์ซีเอสเอ็มไฟต์เท่ากับ 23 มีความว่องไวในการตอบสนองทางไฟฟ้าภายใต้สภาวะก๊าซสูงสุด

ส่วนที่ 2

จากการศึกษาข้างต้นทำให้ทางผู้วิจัยสามารถสรุปได้ว่า จากการทดสอบการเฉือนภายใต้สนามไฟฟ้ากระแสตรง ที่อุณหภูมิ 303 เคลวิน ค่ามอดูลัสเพิ่มขึ้นเมื่อสนามไฟฟ้าเป็น 1 กิโลโวลต์ต่อมิลลิเมตร และลดลงเมื่อสนามไฟฟ้าเป็น 0 กิโลโวลต์ต่อมิลลิเมตรสลับกันไปจนเข้าสู่สภาวะนิ่ง เนื่องจากสนามไฟฟ้าทำให้เกิดการโพลาไรซ์ของไอออนบวกของสารผลึกเหลว การโพลาไรซ์ของหมู่ไฮดรอกซิลบนเซลลูโลส และการจัดเรียงตัวภายใต้แรงเฉือนขณะทดสอบ แต่เมื่อเพิ่มอุณหภูมิเป็น 333 เคลวิน ค่ามอดูลัสเพิ่มขึ้นน้อยลงเนื่องจากการรวมตัวกลับของสารผลึกเหลวและการผ่อนคลายภายใต้สนามไฟฟ้าของเซลลูโลสที่มากขึ้น สอดคล้องกับค่าคงที่ไดอิเล็กทริกที่เพิ่มขึ้นสูงสุดที่อุณหภูมิเท่ากับ 313 เคลวินและลดลงเมื่ออุณหภูมิสูงเกิน 313 เคลวิน การทดสอบการเอียงภายใต้สนามไฟฟ้ากระแสตรงชี้ให้เห็นว่าการเคลื่อนที่ของไอออนบวกของสารผลึกเหลวส่งผลโดยตรงต่อมุมการเอียงที่มากขึ้น และปรากฏการแกว่งกลับไปกลับมาของชิ้นงานเมื่อค่าความเข้มสนามไฟฟ้ามีค่าระหว่าง 525 ถึง 550 โวลต์ต่อมิลลิเมตร ซึ่งคาดว่ามีสาเหตุมาจากการเคลื่อนที่แข่งขันกันระหว่างไอออนบวกและลบของสารผลึกเหลวด้วยแรงทางไฟฟ้าสถิตย์

ส่วนที่ 3

คุณสมบัติเชิงกลทางไฟฟ้าของฟิล์มเจลาตินถูกศึกษาในผลของสนามไฟฟ้าและอุณหภูมิ จากการศึกษาพบว่า ความแข็งแรงของวัสดุจะเพิ่มขึ้นเมื่อความแข็งแรงของเจลเพิ่มขึ้นภายใต้อิทธิพลของสนามไฟฟ้า ในผลของอุณหภูมิพบว่าความแข็งแรงของวัสดุลดลงเมื่อเพิ่มอุณหภูมิ โดยที่ฟิล์มเจลาตินที่ปราศจากสารเชื่อมขวางจะมีการตอบสนองต่อความแข็งแรงและความไวต่อการตอบสนองสูงกว่าฟิล์มเจลาตินที่มีสารเชื่อมขวาง ในส่วนของการศึกษาการเบี่ยงเบนของฟิล์มเจลาตินภายใต้สนามไฟฟ้า พบว่าระยะการเบี่ยงเบนของฟิล์มเจลาตินจะเพิ่มขึ้นเมื่อเพิ่มความเข้มของสนามไฟฟ้า

ส่วนที่ 4

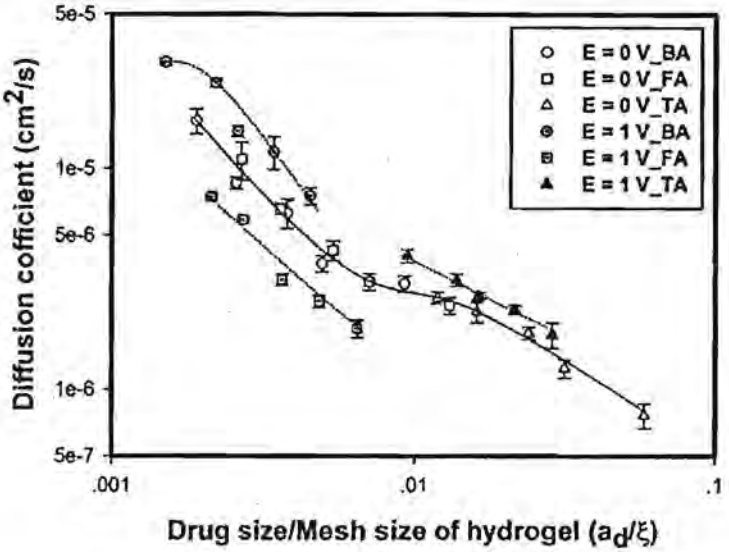

รูปที่ 15 กราฟแสดงความสัมพันธ์ระหว่างความสามารถในการแพร่ของยาแต่ละชนิดต่อค่าอัตราส่วนของขนาดโมเลกุลยาต่อขนาดรูพรุนของแผ่นอัลจิเนตไฮโดรเจล

จากการศึกษาข้างต้นสามารถสรุปผลการศึกษาดังนี้ ปริมาณการแพร่ผ่านของยาขึ้นอยู่กับอัตราส่วนระหว่างขนาดของยากับขนาดของรูภายในแผ่นอัลจิเนตไฮโดรเจล ซึ่งปริมาณการแพร่ผ่านของยามากขึ้นเมื่ออัตราส่วนระหว่างระหว่างขนาดของยากับขนาดของรูภายในแผ่นอัลจิเนตไฮโดรเจลลดลง โดยอัตราส่วนระหว่างขนาดของยากับขนาดของรูภายในแผ่นอัลจิเนตไฮโดรเจลลดลงเมื่อโมเลกุลของยามีขนาดเล็ก หรือรูภายในแผ่นเจลมีขนาดใหญ่เมื่อมีการใช้ปริมาณสารเชื่อมโยงลดลง นอกจากนี้ปริมาณการแพร่ผ่านของยายังขึ้นอยู่กับแรงผลักหรือแรงดึงดูดระหว่างยากับขั้วอิเล็กโทรดเมื่อมีการให้กระแสไฟฟ้า ส่งผลให้สามารถควบคุมปริมาณการปลดปล่อยยาให้มากหรือน้อยได้ตามต้องการ ดังนั้นแผ่นอัลจิเนตไฮโดรจึงวัสดุอีกชนิดหนึ่งที่มาสามารถนำมาใช้ในการควบคุมการปลดปล่อยยาภายใต้กระแสไฟฟ้าได้

บรรณานุกรม

ส่วนที่ 1

[1] Adhikari, B.; Majumdar, S.; *Prog. Polym. Sci.* **2004**, 29, 699.
[2] Lange, U.; Roznyatovskaya, N.V.; Mirsky V.M.; *Anal. Chim. Acta.* **2008**, 614, 1.
[3] Bhambare, K.S.; Gupta, S.; Mench, M.M.; Ray, A.; *Sens. Actuator B-Chem.* 2008, **134**, 803.
[4] Fang, Y.K.; Lee, J.J.; *Thin Solid Films* **1989**, 169, 51.
[5] Dixit, V.; Misra, S.C.K.; Sharma, B.S.; *Sens. Actuator B-Chem.* **2005**, 104, 90.
[6] Mathur, S.C.K.; Mathur, P.; Srivastava, B.K.; *Sens. Actuator A-Phys.* **2004**,114, 30.
[7] Watcharaphalakorn, S.; Ruangchuay, L.; Chotpattananont, D.; Sirivat, A;, Schwank, J.; *Polym. Int.* **2005**, 54, 1126.
[8] Densakulprasert, N.; Wannatong, L.; Chotpattananont, D.; Hiamtup, P.; Sirivat, A.; Schwank, J.; *Mater. Sci. Eng. B* **2005**, 117, 276.
[9] Saxena, V.; Malhotra, B.D.; *Curr. Appl. Phys.* **2003**, 3, 293.
[10] Ram, M.K.; Yavuz, O.; Aldissi, M.; *Synth. Met.* **2005**, 151, 77.
[11] Ram, M.K.; Yavuz, O.; Lahsangah, V.; Aldissi, M.; *Sens. Actuator B-Chem.* **2005**, 106, 750.
[12] Guernion, N.; de Lacy Costello B.P.J.; Ratcliffe, N.M.; *Synth. Met.* **2002**, 128, 139.
[13] Bavastrelloa, V.; Erokhina, V.; Carraraa, S.; Sbranab, F.; Riccib, D.; Nicolini, C.; *Thin Solid Films* **2004**, 468, 17.
[14] Chen, Y.; Li, Y.; Wang, H.; Yang, M.; *Carbon* **2007**, 45, 357.
[15] Hosseini, S.H.; Entezami, A.A.; *J. Appl. Polym. Sci* .**2003**, 90, 49.
[16] Bai, H.; Shi, G.; *Sensors* **2007**, 7, 267.
[17] Prissanaroon, W.; Ruangchuay, L.; Sirivat, A.; Schwank, J.; *Synth. Met.* **2000**, 114, 65.
[18] Groenendaal, L.; Jonas, F.; Freitag, D.; Pielartzik, H.; Rynolds, J.R.; *Adv. Mat.* **2000**, 12, 482.
[19] Louwet, F.; Groenendaal, L.; Dhaen, J.; Manca, J. Van Luppen, J.; Verdonck, E.; Leenders, L.; *Synth. Met.* **2003**, 135-136, 115.
[20] Chuapradit, C.; Wannatong, L.R.; Chotpattananont, D.; Hiamtup, P.; Sirivat, A.; Schwank, J.; *Polymer* **2005**, 46, 947.
[21] Thuwachaowsoan, K.; Chotpattananont, D.; Sirivat, A.; Rujiravanit, R.; Schwank, J.W.; *Mater. Sci. Eng. B* **2007**, 140, 23.
[22] Soontornworajit, B.; Wannatong, L.; Hiamtup, P.; Niamlang, S.; Chotpattananont, D.; Sirivat, A.; Schwank, J.; *Mater. Sci. Eng. B* **2007**, 136, 78.
[23] Han, D.; Yang, G.; Song, J.; Niu, L.; Ivaska, A.; *J. Electroanal Chem.* **2007**, 602, 24.
[24] Garreau, S.; Louarn, G.; Buisson, J.P.; Froyer, G.; Lefrant, S.; *Macromolecules* **1999**, 32, 6807.
[25] Chun, L.; Imae, T.; *Macromolecules*, **2004**, 37, 2411.
[26] Martin, B.D.; Nikolov, N.; Pollack, S.K.; Saprigin, A.; Shashidhar, R. Zhang, F.; Heiney, P.A.; *Synth. Met.* **2004**, 142, 187.
[27] Kiebooms, R.; Aleshin, A.; Hutchison, K.; Wudl, F.; Heeger, A.; *Synth. Met.* **1999**, 101, 436.
[28] Wichiansee, W.; Sirivat, A.; *Mater. Sci. Eng. C* **2009**, 29, 78.

[29] Jönsson, S.K.M.; Birgerson, J.; Crispin, X.; Greczynski, G.; Osikowicz, W.; van der Gon A.W.D.; Salaneck, W.R.; Fahlman, M.; *Synth. Met.* **2003**, 139, 1.
[30] Vacca, P.; Petrosino, M.; Miscioscia, R.; Nenna, G.; Minarini, C.; Sala, D.D.; Rubino, A.; *Thin Solid Films* **2008**, 516, 4232.
[31] Álvaro, M.; Cabeza, J.F.; Fabuel, D.; García, H.; Guijarro, E.; de Juan, J.L.M.; *Chem. Mater.* **2006**, 18, 26.
[32] Kooser, A.; Gunter, R.L.; Delinger, W.D.; Porter, T.L; Eastman, M.P; *Sens. Actuator B-Chem.* **2004**, 99, 474.
[33] Yang, Y.; Jiang, Y.; Jianhua, X.; Junsheng, Y.; *Polymer* **2007**, 48, 4459.
[34] Auerbach, S.M.; Carrado, K.A.; Dutta, P.K. *Handbook of Zeoite Science and Technology*, Marcel Dekker Inc., New York, **2001**.
[35] Costa, C.; Dzikh, I.P.; Lopes, J.M.; Lemos, F.; *J. Mol. Catal. A-Chem.* **2000**, 154, 193.

ส่วนที่ 2

[1] Kuhn, W. *Experientia.* **1949**, 5, 318-9.
[2] Kuhn, W.; Hargitay, B.; Katchalsky, A.; Eisenberg. H. *Nature* **1950**, 165, 514-6.
[3] Katchalsky, A. *Experientia.* **1949**, 5, 319-320.
[4] Sadeghipour, K.; Salomon, R.; Neogi, S. *Smart Mater. Struct.* **1992**, 1, 172-9.
[5] Oguro, K. Actuator element.U.S.Patent 5, **1993**, 268,082.
[6] Shahinpoor, M.; Bar-Cohen, Y.; Simpson, J.; Smith, J. *Smart Mater. Struct.* **1998**, 7, R15-30.
[7] Mallavarapu, K.; Leo, D.J. *J Intel Mat Syst Str.* **2001**, 12, 143-55.
[8] Kothera, C.S.; Leo, D.J. *J Intel Mat Syst Str.* **2005**, 16, 3-13.
[9] Bar-Cohen, Y.; Leary, S.; Shahinpoor, M.; Harrison, J.; Smith, J. *SPIE.* **1999**, 3669, 51-6.
[10] Bar-Cohen, Y.; Leary, S.; Shahinpoor, M.; Harrison, J.O.; Smith, J. *SPIE.* **1999**, 3669, 57-63.
[11] Bennett, M.D.; Leo, D.J.; Wilkes, G.L.; Beyer, F.L.; Pechar, T.W. *Polymer* **2006** 47, 6782-6796.
[12] Bennett, M.D.; Leo, D.J. *Sensor Actuat A-Phys.* **2004**, 115, 79-90.
[13] Green, M.D.; Long, T.E. *Polymer Reviews* **2009**, 49, 291-314.
[14] Mahadeva, S.K.; Kim, J. *J. Phys. Chem. C.* **2009**, 113, 12523–12529.
[15] Kadokawa, J.; Murakami, M.; Kaneko, Y. *Carbohydres Res.* **2008**, 343, 769–772.
[16] Kunchornsup, W.; Sirivat, A. *J Sol-Gel Sci Technol.* **2010**, 56, 19–26.
[17] Niamlang, S.; Sirivat, A. *Macromol. Symp.* **2007**, 264, 176-183.
[18] Niamlang, S.; Sirivat, A. *Smart Mater. Struct.* **2008**, 17, art. no. 035036.
[19] Kim, J.; Kang, K.; Yun, S. *Sens. Actuators A-Phys.* **2007**, 133, 401-406.
[20] Kim, J.; Jung, W.; Kim, H.S. *Sensor Actuat A-Phys.* **2007**, 140, 225–231.
[21] Timoshenko, S.P.; Gere, J.M. Mechanics of Materials, third ed., Chapman & Hall, New York, USA, **1990**.
[22] Smith, T.S.; Seugling, R.M. *Precis. Eng.* **2006**, 30, 245-264.
[23] Jung, Y.; Park, H.; Jo, N.; Jeong, H. *Sens. Actuators A-Phys.* **2007**, 136, 367-373.
[24] Pelrine, R.E.; Kornbluh, R.D.; Joseph, J.D. *Sens. Actuators A-Phys.* **1998**, 64, 77-85.
[25] Diaconu, I.; Dorohoi, D.O.; Topoliceanu, F. *IEEE Sensors J.* **2006**, 6, 876-880.

[26] Watanabe, M.; Hirai, T. *J. Polym. Sci. Part B* **2004**, 42, 523-531.
[27] Hiamtup, P.; Sirivat, A.; Jamieson, A.M. *Mater. Sci. Eng. Part C* 2007, 28, 1044-1051.
[28] Mukai, K.; Asaka, K.; Kiyohara, K.; Sugino, T.; Takeuchi, I.; Fukushima, T.; Aida, T. *Electrochim Acta.* **2008**, 53, 5555–5562.
[29] Terasawa, N.; Takeuchi, I.; Matsumoto, H. *Sensor Actuat B-Chem.* **2009**, 139, 624–630.
[30] Terasawa, N.; Takeuchi, I.; Matsumoto, H.; Mukai, K.; Asaka, K. *Sensor Actuat B-Chem.* **2011**, 156, 539– 545.
[31] Yun , G.Y.; Kim, H.S.; Kim, J.; Kim, K.; Yang, C. Sens. *Actuators A-Phys.* **2008**, 141, 530–535.
[32] Liu, W.; Cheng, L.; Zhang, Y.; Wang, H.; Yu, M. *J Mol Liq.* **2008**, 140, 68–72.
[33] Domańska, U.; Bogel-Łukasik, E. *Fluid Phase Equilibr.* **2004**, 218, 123-129.
[34] Kim, J.; Yun, S.; Ounaies, Z. *Macromolecules* **2006**, 39, 4202-4206.
[35] Kim, J.; Ampofo, J.; Craft, W.; Kim, H.S. Mech Mater. **2008**, 40, 1001–1011.
[36] Ludeelerd, P.; Niamlang, S.; Kunaruksapong, R.; Sirivat, A. *J Phys Chem solids* **2010**, 71, 1243–1250.
[37] Kunanuruksapong, R.; Sirivat, A. *Mat Sci Eng A-Struct.* **2007**, 454–455, 453–460.
[38] Kunanuruksapong, R.; Sirivat, A. *Appl. Phys. A* **2008**, 92, 313–320.
[39] Thipdech, P.; Kunanuruksapong, R.; Sirivat, A. *eXPRESS Polymer Letters* **2008**, 12, 866–877.
[40] Kittel, C. Introduction to Solid State Physics, eighth ed., John Wiley & Sons, Inc., **2005**.
[41] Raju, G.G. Dielectrics in Electric Fields, Marcel Dekker, New York, **2003**.
[42] Riad, A.J.; Korayem, M.T.; Abdul Malik, T.G. *Physica B.* **1999**, 270, 140.
[43] Kunanuruksapong, R.; Sirivat, A. *Current Applied Physics* **2011**, 11, 393-401.
[44] Sato, T.; Watanabe, H.; Osaki, K. *Macromolecules* **1996**, 29, 6231-6239.
[45] Rubinstein, M.; Colby, R.H. Polymer Physics, first ed., Oxford, **2003**.
[46] Mahadeva, S.K.; Yi, C.; Kim, J. *Macromol Res.* **2009**, 17, 116-120.
[47] Bazhenow, V.A. *Consultants Bureau.* **1961**.
[48] Liu, Y.; Liu, S.; Lin, J.; Wang, D.; Jain, V.; Montazami, R.; Heflin, J.R.; Li, J.; Madsen, L.; Zhang, Q.M. *Appl Phys Lett.* **2010**, 96, 223503.
[49] Yi, S.; Zhang, F.; Li, W.; Huang, C.; Zhang H.; Pan, M. *J Membrane Sci.* **2011**, 366, 349–355.

ส่วนที่ 3

[1] Krause, S.; Bohon. K. *Macromolecules* **2001**, 34, 7179.
[2] Zhang, Y.Z.; Venugopal, J.; Huang, Z.-M.; Lim, C.T.; Ramakrishna, S. *Polymer* **2006**, 47, 2911-2917.
[3] Yang, X.J.; Zheng, P.J.; Cui, Z.D.; Zhao, N.Q.; Wang, Y.F.; Yao. K.D. *Polym. Int.* **1997**, 44, 448–452.
[4] Marois, Y.; Chakfe, N.; Deng, X.; Marois, M.; How, T.; King, M. *Biomaterials* **1995**, 16, 1131–1139.
[5] Bigi, A.; Cojazzi, G.; Panzavolta, S.; Rubini, K.; Roveri, N. *Biomaterial* **2001**, 22, 763-768.
[6] Bottoms, E.; Cater, C.W.; Shuster, S. *Nature* 1966, 211, 97-8.

[7] Draye J.P.; Delaey, B.; Van de Voorde, A.; Van Den Bulcke, A.; De Reu B.; Schacht, E. *Biomaterials* **1998**, 19, 1677-1687.
[8] Schach, E.; Van Den Bulcke, A.; Bogdanov, B.; Draye, J.P.; Delaey, B. *Polym. Mater. Sci. Eng.* **1998**, 79, 222-223.
[9] Fujimori. E. *Biopolymers* **1965**, 3, 115-9
[10] Khor, E. *Biomaterials* 1997, 18, 95-105
[11] Abrusci, C.; Martin-Gonzalez, A.; Amo, A.D.; Corrales, T.; Catalina, F. *Polym. Degrad. Stabil.* **2004**, 86, 283-291.
[12] Flory, P.J.; Rehner. J.J. *Chem. Phys.* **1943**, 11, 521-526.
[13] Apostolov, A.A.; Boneva, D.; Vassileva, E.; Mark, J.E.; Fakirov, S. *J. Appl. Polym. Sci.* **2000**, 76, 2041-2048.
[14] Martucci, J.F.; Ruseckaite, R.A.; Vazquez, A. *Mat. Sci. Eng. A* **2006**, 435-436, 681-686.
[15] Fraga, A.N.; Williams, R.J.J. *Polymer* 1985, 26, 113-118.
[16] Li, M.; Guo, Y.; Wei, Y.; Macdiamid, A.G.; Lelkes, P.I. *Biomaterials* **2005**, 27, 2705-2715.
[17] Chotpattananont, D.; Sirivat, A.; Jamieson, A.M. *Colloid Polym. Sci.* **2004**, 282, 357-365.
[18] Perline, R.E.; Kornbluh, R.D.; Joseph, J.P. *Sensor Actuat.Phys. A* **1998**, 64, 77-85.
[19] Liu, B.; Shaw, T.M. *J. Rheol.* **2001**, 45, 641-657.
[20] Shiga. T. *Advances in Polymer Science* **1997**, 134/20, Springer-Verlag, Berlin.
[21] Pelrin, R.; Kornbluh, R.; Joseph, J.; Heydt, R.; Pei, Q.; Chiba, S. *Mat. Sci. Eng. C* **2000**, 11, 89-100.
[22] Kunanuruksapong, R.; Sirivat, A. *Mat. Sci. Eng. A* **2007**, 454-455, 453-460.
[23] Thongsak, K.; Kunanuruksapong, R.; Sirivat, A.; Lerdwijitjarud, W. *Mat. Sci. Eng. A* **2010**, 527, 2504-2509
[24] Tangboriboon, N.; Sirivat, A.; Kunanuruksapong, R.; Wongkasemjit, S. *Mat. Sci. Eng. C* 2009, 29, 1913-1918.
[25] Hiamtup, P.; Sirivat, A.; Jamieson, A.M. *Mat. Sci. Eng. C* **2008**, 28, 1044-1051.
[26] Wichiansee, W.; Sirivat, A. *Mat. Sci. Eng. C* 2009, 29, 78-84.
[27] Puvanatvattana, T.; Chotpattananont, D.; Hiamtup, P.; Niamlang, S.; Sirivat, A.; Jamieson. A.M. *React. Funct. Polym.* **2006**, 66, 1575-1588.
[28] Shiga, T.; Okada, A.; Kurauchi, T. *Macromolecules* **1993**, 26, 6958-6963.
[29] Shiga, T.; Okada, A.; Kurauchi, T. *J. Mater. Sci. Lett.* **1995**, 14, 514-515.
[30] Sato, T.; Watanabe, H.; Osaki, K. *Macromolecules* **1996**, 29, 6231-6239.
[31] Timoshenko, S.P.; Goodier, J.N. Theory of elasticity, 3rd ed. McGraw-Hill, Auckland, **1970**.
[32] Gere, J.M. Mechanics of Materials, 3rd ed. Chapman & Hall, **1972**.
[33] Alici, G.; Mui, B.; Cook, C. *Sensor Actuat.Phys. A* **2006**, 126, 396.
[34] Dai, C.A.; Kao, A.; Chang, C.; Tsai, W.; Chen, W.; Liu, W.; Shih, W.; Ma, C.C. *Sensor Actuat. A-Phy.* **2009**, 155, 152-162.
[35] Kunanuruksapong, R.; Sirivat, A. *Curr. Appl. Phys.* **2010**, 1-10.

ส่วนที่ 4

[1] Gupta, P.; Vermani, K.; Grarg, S. *Drug Discov. Today* **2002**,7, 569-579.
[2] Kshirsagar, N.A. *Indian. J. Pharmacol.* **2000**, 32, S54-S61.

[3] Stott, P.W.; Williams, A.C.; Barry, B.W. *J. Control. Release* **1998**,50, 297-308.
[4] Riviere, J.E.; Papich, M.G.; *Adv. Drug Delivery Rev.* **2001**, 50, 175–203.
[5] Chien, Y.W.; Lelawong, P.; Siddiqui, O.; Sun, Y.; Shi, W.M. *J. Control. Release* **1990**, 13, 263-278.
[6] Juntanon, K.; Niamlang, S.; Rujriravanit, R.; Sirivat, A. *Int. J. Pharm.* **2008**, 356, 1-11.
[7] Kim, J.S.; Yoon, G.S.; Lee, M.S.; Lee, H.J.; Kim, S. *Sensor Actuator* **2003**, B96, 1-5.
[8] Qiu, Y.; Park, K. *Adv. Drug Delivery Rev.* **2001**, 53, 321-339.
[9] Pasparakis, G.; Bouropoulos, N. *Int. J. Pharm.* **2006**, 3323, 34-42.
[10] Badwan, A.A.; Abumalooh, A.; Sallam, E.; Abukalaf, A.; Jawan, O. *Drug Dev. Ind. Pharm.* **1985**, 11, 239-256.
[11] Aslani, P.; Kennedy, A.R. *J. Control. Release* **1996**, 42, 75-82.
[12] Al-Musa, S.; Fara, A.D.; Badwan, A.A. *J. Control. Release* **1999**, 57, 223-232.
[13] Gonzalez-Rodriguez, M.L.; Holgado, M.A.; Sanchez-Lafuenete, C.; Rabasco, A.M.; Fini, A. *Int. J. Pharm.* **2002**, 232, 225–234.
[14] Mohan, N.; Nair, P.D. *Trends Biomater. Artif. Organs* **2005**, 18.
[15] Pathak, T.S.; Kim, J.S.; Lee, S.J.; Baek, D.J.; Paeng, K.J. *J. Polym. Environ.* **2008**, 16, 198-204.
[16] Peppas. N.A.; Wright, S.L. *Eur. J. Pharm. Biopharm.* **1998**, 46, 15-29.
[17] Wells, L.A.; Sheardown, H. *Eur. J. Pharm. Biopharm.* **2011**.
[18] Peppas, N.A; Canal, T. *J. Biomed. Mater. Res.* **1989**, 23, 1183-1193.
[19] Chan, A.W; Neufeld, R.J. *Biomaterials* **2009**, 30, 6119-6129.
[20] Peppas, N.A.; Wright, S.L. *Macromolecules* **1996**, 29, 8798-8804.
[21] Korsmeyer, R.W.; Gurny, R.; Doelker, E.; Buri, P.; Peppas, N.A. *Int. J. Pharm.* **1983**, 15:25-35.
[22] Pradhan, R.; Budhathoki, U.; Thapa, P. *KUSET.* **2008**, 1, 55-67.
[23] Higuchi, T. *J. Pharm. Sci.* **1963**, 2, 1145-1149.
[24] Reichling, J.; Landvatter, U.; Wagner, H.; Kostka, K.H.; Schaefer, U.F. *Eur. J. Pharm. Biopharm.* **2006**, 64, 222–228.
[25] Mahmoodi, M.; Khosroshahi, M.E.; Atyabi, F. *International Journal of Biology and Biomedical Engineering* **2010**, 4, 35-42.
[26] Prajapati, R.; Mahajan, H.; Surana, S. *IJNDD* **2011**, 3, 9-16.
[27] Basak, S.C.; Kumar, K.S.; Ramalingam, M. *J. Pharm. Sci.* **2008**, 44, 477-483.
[28] Stockwell, A.F.; Davis, S.S.; Walker, S.E. *J. Control. Release* **1986**, 3, 167-175.
[29] Niamlang, S.; Sirivat, A. *Int. J. Pharm.* **2009**, 371, 126-133.
[30] Chansai, P.; Sirivat, A.; Niamlang, S.; Chotpattananont, D.; Viravaidya-Pasuwat, K. *Int. J. Pharm.* **2009**, 381, 25-33.
[31] Veronika, K.; Eugenia, K.; Marc, L.M.; Svetlana, A.S. *Chem. Mater.* **2006**, 18, 328-336.
[32] Shilpa, K.; Gareth, D.R.; Jayne, L. *J. Control. Release* **1999**, 60, 355-365.
[33] Sudaxshina M. *J. Control. Release* 2003, 92, 1-17.
[34] Kikuchi, A.; Kawabuchi, M.; Watanabe, A.; Sugihara, M.; Sakurai, Y.; Okano, T. *J. Control. Release* **1999**, 58, 21-28.

ภาคผนวก

ส่วนที่ 1

Interaction of carbon monoxide with PEDOT-PSS/Zeolite composite: Effect of Si/Al ratio of ZSM-5 zeolite

Pojjawan Chanthaanont, Anuvat Sirivat *
*Conductive and Electroactive Polymer Research Unit, The Petroleum and Petrochemical College, Chulalongkorn University, Bangkok, 10330,Thailand; Fax: 662 611 7221; email: anuvat.s@chula.ac.th

Abstract: Composites with Poly(3,4-ethylenedioxythiophene) doped with poly(styrene sulfonic acid), PEDOT-PSS, as the matrix containing ZSM-5 zeolites of various Si/Al ratios in the range of 23-280 at 20% (v/v) were fabricated to investigate the effect of Si/Al ratios on electrical conductivity sensitivity responses towards carbon monoxide (CO). The electrical conductivity responses of PEDOT-PSS/ZSM-5 composites were altered due to the available adsorption sites for CO molecules. The electrical conductivity sensitivity to CO increases with decreasing Si/Al ratios. The composites produce irreversible responses when replacing CO with nitrogen. The addition of ZSM-5 zeolites to the pristine PEDOT-PSS improves the electrical conductivity sensitivity of the composites by enhancing the interaction between PEDOT-PSS and CO gas. The composite of ZSM-5 zeolites with a Si/Al ratio equal to 23 gives the highest electrical conductivity sensitivity toward CO.

Introduction

For environmental and safety concerns, the development of sensors to detect the presence and the concentration of toxic or otherwise dangerous gases from spills and industrial leaks is needed. The fabrication of stable sensors with high sensitivity and very good selectivity towards the substance to be detected has been pursued.

CO is a very dangerous gas emitted from automobiles and industrial plants. Various materials have been employed in detecting CO at intermediate and low levels. Commercial CO gas sensors, typically based on semiconducting metal oxide sensors (e.g. tin oxide) and operating on the basis of catalytic reactions between the semiconductor and contact gases, produces a change in semiconductor conductance [1]. The metal oxide sensor provides rapid response, but it needs to operate at high temperature [2-4]. Various polymeric materials have been investigated as CO gas sensing materials due to their acid-base or oxidizing characteristics. The unique doping process of a conductive polymer makes it favorable towards the sensing characteristics, but the conductive polymer still has poor selectivity towards gaseous analyzes [5-8]. The ultimate desired characteristics of gas sensors are: accuracy, reliability, selectivity, sensitivity, rapid responsibility, miniaturization capability, stability and low cost.

Currently, research on new gas sensing materials to be used as matrices on the sensor device is still being pursued. Conductive polymers have received increasing attention in the field of gas sensing materials [9]. The combination of conductive polymers with

other materials such as metals or metaloxide nanoparticles [10-12], carbon nanotubes [13-14], and insulating polymers [15] have been developed and studied.
Conductive polymers offer various advantages in sensor applications over their metallic counterparts: they are relatively low cost, their fabrication techniques are simple, they can be deposited on various types of substrates, they offer a wide choice of chemical structures, and their sensors can operate at near room temperature [16,17]. Poly(3,4-ethylenedioxythiophene), or PEDOT, possesses excellent properties: ease of synthesis, excellent stability, and wet processability when doped with poly(styrene sulfonic acid) (PSS) [18,19]. Becuase of these properties, PEDOT-PSS or PSS-doped PEDOT are potential candidates as new and unique sensory materials.

Recently, zeolites have been used in gas sensor applications in combination with conductive polymers [8, 20-22]. Because of the well-defined structure of a zeolite, it can separate the desired gas molecule from others and the presence of a cation in the cavity also facilitates gas interactions. The main reason for mixing a conductive polymer with a zeolite is to combine the advantages of the two materials. In our work, we propose to combine a conductive polymer, PEDOT, with ZSM-5 zeolites to investigate the potential of the composites for use as CO sensing materials. The effect of Si/Al ratios of the zeolite on electrical sensitivity responses of the composites are investigated and reported here.

Results and discussion

Characterization of Poly(3,4-ethylenedioxythiophene)

PEDOT-PSS was synthesized by the polymerization of 3,4-ethylenedioxythiophene (EDOT) in an aqueous solution of PSS using $S_2O_8^{2-}$ as the oxidant. From the FTIR spectrum of the PEDOT-PSS, the peaks at 1520 and 1339 cm^{-1} can be assigned to the C=C and the C-C stretchings in the thiophene ring [23,24] and the peaks at 929 cm^{-1} and 834 cm^{-1} correspond to the symmetric vibration of C-S bond in the thiophene ring [23-25]. The peaks at 1127 and 1039 cm^{-1} are assigned to the stretching mode of the ethylenedioxy group [23,24], and the peaks at 1198 and 929 cm^{-1} correspond to the -SO_3^- and the S-OH stretchings of the PSS molecule [23,26]. The vibration of the bending mode of the C-H bond in EDOT monomer (~892 cm^{-1}) is not present [23]. This result confirms the formation of PEDOT molecular chains. The absorption peak at 1645 cm^{-1} can be assigned to the oxidation state of PEDOT which indicates the successful doping of the PEDOT polymer with PSS. In summary, the FTIR spectrum data indicate the successful formation of PEDOT molecular chains doped with PSS counterion. Four transitions were observed in the PEDOT-PSS thermograms: 30-110 °C, 160-380 °C, 380-550 °C, and 560-900 °C; they can be referred to as the loss of water, the side chain degradation, and the polymer backbone degradations of PSS and PEDOT, respectively [27,28]. From the XRD patterns of the PEDOT-PSS, there is no characteristic peak observed by X-ray diffraction, the broad scattering background indicates the amorphous nature of the materials [27,28]. The mean particle diameter of PEDOT-PSS_1:1 was determined to be approximately 34 ± 0.22 μm. The micrograph in Figure 1 of PEDOT-PSS particles shows rough surfaces and irregular shapes; they are moderately dispersed. The density of PEDOT-PSS_1:1 is 1.4750 ± 0.0003 g/cm^3.

Characterization of Zeolite ZSM-5 and Composites

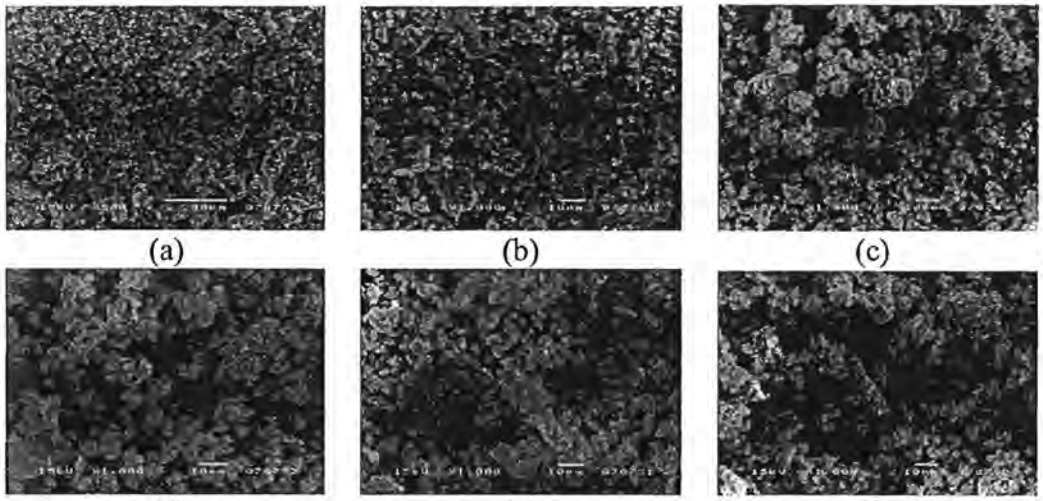

Fig. 1. Morphology of PEDOT-PSS_1:1 particles, ZSM-5 powders, and PEDOT-PSS_1:1/zeolite composites: a) PEDOT-PSS_1:1 at 500x; b) PEDOT-PSS_1:1 at 1000x; c) PEDOT-PSS_1:1/ ZSM-5(23) at 1000x; d) PEDOT-PSS_1:1/ ZSM-5(50) at 1000x; e) PEDOT-PSS_1:1/ ZSM-5(80) at 1000x; and f) PEDOT-PSS_1:1/ ZSM-5(280) at 1000x.

Tab. 1. Specific surface areas, pore width, the pore volume, crystal size, and specific conductivity of ZSM-5 (Si/Al = 23, 50, 80 and 280)

Sample	Si/Al ratio	Surface area (m^2/g)	Pore width (Å)	Pore volume (cm^3/g)	Crystal size μm	Specific Conductivity (S/cm)
ZSM-5(23)	23	329 ± 4.7	5.85 ± 0.013	0.39 ± 0.015	5.61 ± 0.04	$(1.257 \pm 0.028) \times 10^{-1}$
ZSM-5(50)	50	336 ± 5.1	5.91 ± 0.021	0.35 ± 0.013	5.69 ± 0.21	$(3.726 \pm 0.283) \times 10^{-2}$
ZSM-5(80)	80	347 ± 8.6	6.08 ± 0.017	0.28 ± 0.011	5.78 ± 0.04	$(1.690 \pm 0.223) \times 10^{-2}$
ZSM-5(280)	280	355 ± 2.8	6.21 ± 0.048	0.27 ± 0.023	5.94 ± 0.19	$(3.957 \pm 1.592) \times 10^{-4}$

The mean particle diameters of ZSM-5 with Si/Al mole ratios of 23, 50, 80, and 280 are 5.61 ± 0.04, 5.69 ± 0.21, 5.78 ± 0.04 and 5.94 ± 0.19 μm, respectively. The morphology of the zeolites and the composites is shown in Figure 1. Zeolite ZSM-5 particles possess irregular crystal shapes and appear to be inhomogeneously dispersed in the conductive polymer matrix of the composites. The specific surface areas, pore width, and pore volume of ZSM-5 (Si/Al = 23, 50, 80 and 280) of the H-form are tabulated in Table 1. The pore size of zeolites ZSM-5 (Si/Al = 23, 50, 80, and 280) are 5.85 ± 0.013, 5.91 ± 0.021, 6.08 ± 0.017, and 6.21 ± 0.048 Å, respectively. The corresponding surface areas are 329 ± 4.7, 336 ± 5.1, 347 ± 8.6 and 355 ± 2.8, m^2/g, respectively. Zeolites ZSM-5 (Si/Al = 23, 50, 80 and 280) have comparable surface areas and pore sizes but zeolites ZSM-5 (23) has a greater pore free volume, and more cations are contained within the pores.

Electrical Conductivity under Air and Nitrogen Exposure

The specific electrical conductivity measurements of PEDOT-PSS, zeolite ZSM-5, and composites under air were carried out at 27 ± 1 °C at 1 atm. The specific electrical conductivity of the PEDOT-PSS at various EDOT:PSS mole ratios under air exposure is shown in Figure 2. It varies from (1.169 ± 0.003) x 10^{1} S/cm to (1.802 ± 0.612) x 10^{-3} S/cm as the EDOT:PSS mole ratio is varied from 1:1 to 1:10. The specific electrical conductivity of the PEDOT-PSS increases with EDOT:PSS mole ratio due to the reduction of the insulating PSS shell surrounding the conducting PEDOT-PSS grains, which improves the pathways for charge transport [29,30]. Concerning the influence of the framework Si/Al ratio, we studied a series of zeolites having in common the same structure and charge-balancing cation, but differing in the framework Si/Al ratio in the range of 23-280 .The specific electrical conductivity of the zeolites ZSM-5 (Figure 2) decreases with increasing Si/Al mole ratio. It varies from (1.257 ± 0.028) x 10^{-1} S/cm to (3.957 ± 1.592) x 10^{-4} S/cm as the Si/Al mole ratio is varied from 23 to 280. This is due to the increase in the number of cations present with decreasing Si/Al ratio. Therefore, the ion migration increases which enhances the apparent electrical conductivity [31]. For the composites of PEDOT-PSS_1:1 with zeolite ZSM-5, the same result occurs for the specific electrical conductivity (Figure 2); it varies from (7.415 ± 0.466) x 10^{-1} S/cm to (8.853 ± 0.509) x 10^{-2} S/cm as Si/Al mole ratio is varied from 23 to 280. The specific electrical conductivity values of the composites are lower than the pure PEDOT-PSS_1:1, but are higher than those of the pure zeolites. The electrical conductivity measurement of PEDOT-PSS_1:1 under air exposure is greater than the electrical conductivity value under N_2 exposure; this can be related to the interaction of oxygen and moisture in the air with the active sites [20].

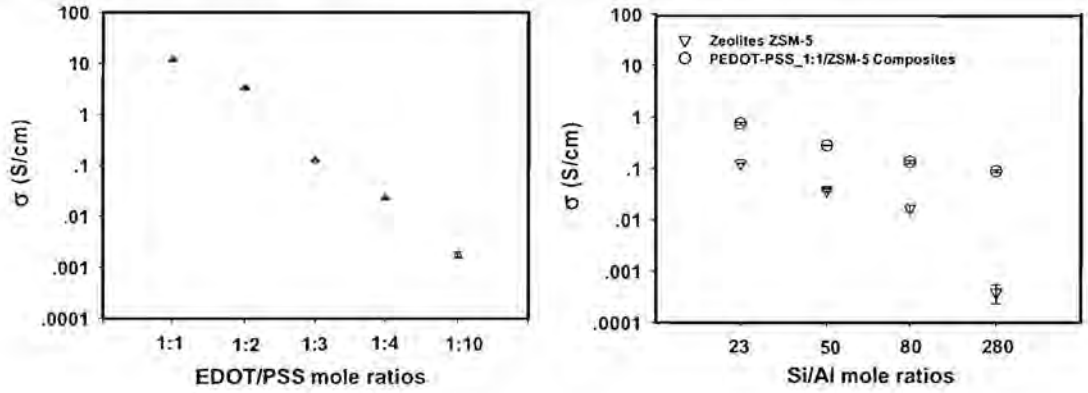

(a) (b)

Fig. 2. Specific electrical conductivity (S/cm) of: (a) PEDOT-PSS and (b) ZSM-5 and PEDOT-PSS_1:1/ZSM-5 when exposed to air at temperature (T_c) of 27 ± 1 °C.

Electrical Conductivity Response to Carbon monoxide

The effect of Si/Al ratios of zeolite on the electrical sensitivity responses of the composites was investigated. PEDOT-PSS, with EDOT:PSS mole ratios of 1:1, was chosen and blended with ZSM-5 zeolites (Si/Al = 23, 50, 80 and 280) to form PEDOT-PSS_1:1/ZSM-5 at a zeolite amount of 20% (v/v). The electrical conductivity response $(\Delta\sigma=\sigma_{CO}-\sigma_{N_2})$ is identified as the difference in the steady state electrical conductivity

value when exposed to the target gas (CO) and the steady state electrical conductivity value when exposed to N_2 at the same pressure and temperature, namely 1 atm at 27 ± 1 °C. Due to the differences in initial electrical conductivity values of the various composites, the interaction between the target gas and the sensing materials can be compared through the electrical conductivity sensitivity ($\Delta\sigma/\sigma_{N_2}$), which is defined as the ratio of the electrical conductivity response and the electrical conductivity value under pure N_2 exposure at the same pressure and temperature.

Tab. 2. Electrical sensitivity of PEDOT-PSS_1:1 and its composites when exposed to CO under chamber temperature (T_c) of 27 ± 1 °C, at 1 atm; K = correction factor = 3.625×10^{-4} (probe no. 1) and 7.759×10^{-4} (probe no. 2)

Samples	σ_{air} (S/cm)	$\Delta\sigma$ (S/cm)	$\Delta\sigma/\sigma_{N2int}$	$\Delta\sigma_r$ (S/cm)
PEDOT-PSS_1-1	$(1.169 \pm 0.003) \times 10^{1}$	$(-6.41 \pm 1.55) \times 10^{-1}$	$(-5.72 \pm 0.14) \times 10^{-2}$	$(-7.22 \pm 1.39) \times 10^{0}$
EDOT-PSS_1:1/ZSM-5 (23)	$(7.415 \pm 0.466) \times 10^{-1}$	$(-5.92 \pm 4.05) \times 10^{-3}$	$(-9.47 \pm 0.10) \times 10^{-1}$	$(-1.04 \pm 0.81) \times 10^{-4}$
EDOT-PSS_1:1/ZSM-5 (50)	$(2.794 \pm 0.085) \times 10^{-1}$	$(-4.24 \pm 2.83) \times 10^{-3}$	$(-8.03 \pm 0.12) \times 10^{-1}$	$(-4.34 \pm 1.13) \times 10^{-4}$
EDOT-PSS_1:1/ZSM-5 (80)	$(1.333 \pm 0.105) \times 10^{-1}$	$(-1.24 \pm 0.35) \times 10^{-3}$	$(-5.98 \pm 0.96) \times 10^{-1}$	$(-4.56 \pm 0.26) \times 10^{-4}$
DOT-PSS_1:1/ZSM-5 (280)	$(8.853 \pm 0.509) \times 10^{-2}$	$(-4.69 \pm 0.16) \times 10^{-4}$	$(-8.45 \pm 1.71) \times 10^{-2}$	$(-3.71 \pm 0.72) \times 10^{-5}$

The electrical sensitivity values of PEDOT-PSS_1:1 and its composites with zeolites when exposed to air, N_2, and CO were measured under a chamber temperature (T_c) of 27 ± 1 °C at 1 atm (Figure 3). The electrical conductivity sensitivity of PEDOT-PSS_1:1/zeolite ZSM-5 composites toward CO negatively increases with decreasing the Si/Al mole ratio of the ZSM-5 zeolites. PEDOT-PSS_1:1/ZSM-5(Si/Al = 23) has the highest electrical conductivity sensitivity value, $(-9.47 \pm 0.10) \times 10^{-1}$ S/cm. For PEDOT-PSS_1:1/ZSM-5(Si/Al = 50), PEDOT-PSS_1:1/ZSM-5(Si/Al = 80), PEDOT-PSS_1:1/ZSM-5(Si/Al = 280), and PEDOT-PSS_1:1, the sensitivity values are $(-8.03 \pm 0.12) \times 10^{-1}$ S/cm, $(-5.98 \pm 0.14) \times 10^{-1}$ S/cm, $(-8.45 \pm 0.14) \times 10^{-2}$ S/cm, and $(-5.72 \pm 0.14) \times 10^{-2}$ S/cm, respectively. This result can be related to fact that the amount of cations increases with decreasing Si/Al ratio. ZSM-5(Si/Al = 23) has the highest aluminum content and thus the highest cation content in its zeolite framework; this leads to a higher number and strength of active sites available on the surface for the target gas molecules to diffuse deeper into the composites, and this enhances the interaction between the conductive polymer and the target gas; and the sensitivity increases. Further evidence is that we find that the recoverable response of PEDOT-PSS_1:1/ZSM-5(Si/Al = 23) is $(-1.04 \pm 0.81) \times 10^{-4}$ whereas the initial response is $(-5.92 \pm 4.05) \times 10^{-3}$; thus a great difference in response is observed. This suggests that the electrical conductivity response is irreversible when CO is replaced by N_2. The irreversibility of conductive polymers has been reported in some literature. However, the irreversibility mechanism is still not clear. In a previous work, the researchers used a Ni-containing polymer, poly(ethylene oxide), as the active sensing material to detect the presence of carbon monoxide gas. In small concentrations, the sensor was fully recoverable; however, for very large concentrations, irreversible chemical changes in the polymeric sensing material occurred [32].

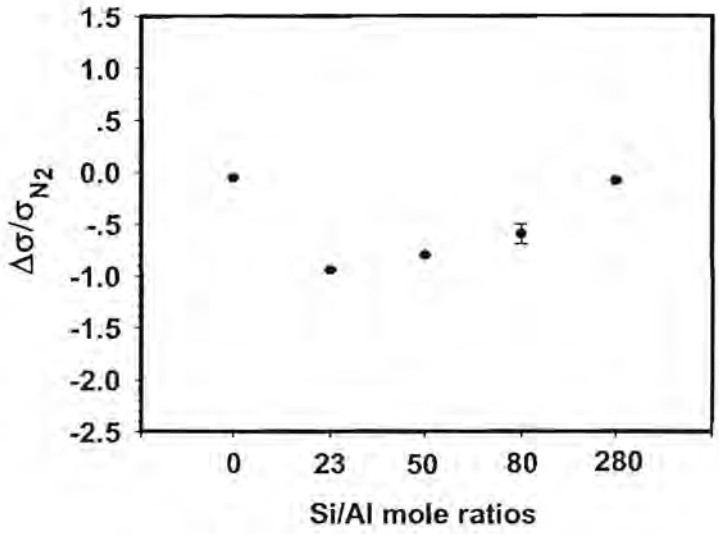

Fig. 3. Electrical conductivity sensitivity values of PEDOT-PSS_1:1 (0) and PEDOT-PSS_1:1/ZSM-5 composites when exposed to CO (1000 ppm) at temperature (T_c) of 27 ± 1 °C at 1 atm.

The temporal response time (t_r) is the time required for the electrical conductivity value to rise from its initial value in N_2 towards the equilibrium value when exposed to CO. The temporal response times of PEDOT-PSS_1:1, PEDOT-PSS_1:1/ZSM-5(Si/Al = 23), PEDOT-PSS_1:1/ZSM-5(Si/Al = 50), PEDOT-PSS_1:1/ZSM-5(Si/Al = 80), and PEDOT-PSS_1:1/ZSM-5(Si/Al = 280) are 37, 87, 60, 52, and 46 minutes, respectively. By adding ZSM-5, a longer response time is observed, and the response time increases with decreasing Si/Al mole ratios of the ZSM-5. The response time of PEDOT-PSS_1:1/ZSM-5(Si/Al = 23) is longer than PEDOT-PSS_1:1 and that of the other composites, corresponding to the higher density of the adsorption sites available for CO molecules. The addition of ZSM-5 zeolites can thus enhance the interaction between PEDOT-PSS_1:1 and CO molecules; thus the zeolites can improve the sensitivity of the pristine PEDOT-PSS_1:1, but at the expense of a longer response time.

Investigation of Interactions of Adsorbed CO

The interaction of CO and PEDOT-PSS was further investigated via FTIR spectroscopy under 1 atm at 27 ± 1 °C. The FTIR spectra of PEDOT-PSS before, during, and after the CO exposure are shown in Figure 5. The adsorption peak that indicates the doping level of the polymer at 1645 cm^{-1} shifts to a lower wave-number position (1635 cm^{-1}) after exposing to CO gas. This result is evidently related to the observed decrease in electrical conductivity of PEDOT-PSS when exposed to CO [33]. When the PEDOT-PSS is exposed to CO, the negative charge at the carbon atom of $^{-}C{\equiv}O^{+}$ is incorporated into the polymer backbone of the PEDOT (Figure 4). The positive charge of the polymer backbone becomes neutral and the transport of charge carriers is hindered, thus accounting for the decrease in electrical conductivity of the PEDOT-PSS under CO exposure. When CO is removed, the adsorption peak at 1635 cm^{-1} remains observable. This indicates that the interaction between CO and PEDOT-PSS is irreversible,

corresponding to the irreversible conductivity response observed when replacing CO by N_2.

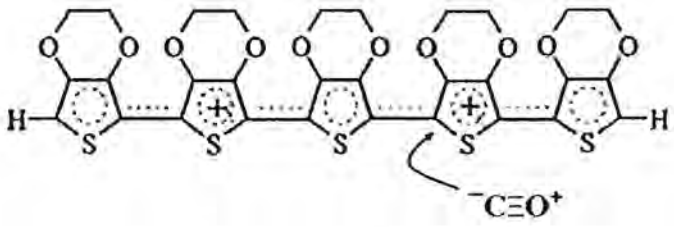

Fig. 4. Proposed mechanism of CO-PEDOT interaction.

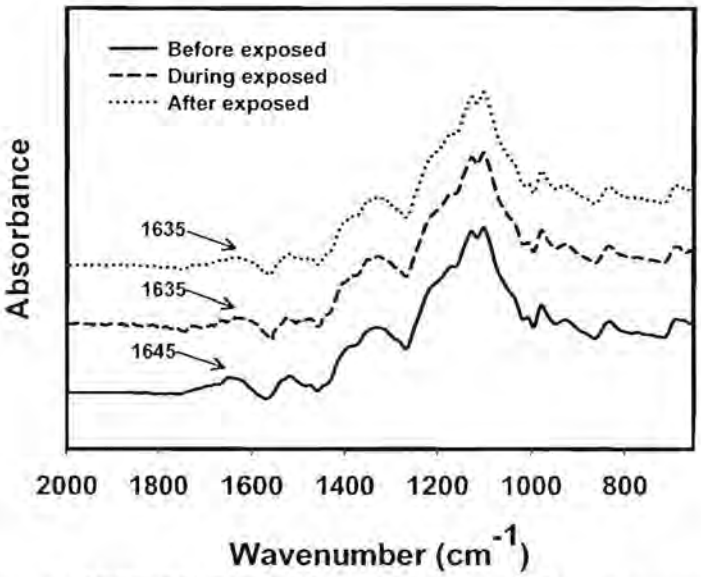

Fig. 5. FTIR spectra of PEDOT-PSS before, during, and after exposure to CO.

The temperature programmed desorption experiment (TPD) was carried out, after the saturatation of adsorption of CO and flushing with He. TPD thermograms of ZSM-5 zeolites of various Si/Al ratios are shown in Figure 6. Adsorbed CO was desorbed during TPD starting from about 27 °C and ending at about 600 °C. This suggests that the adsorbed CO on HZSM-5 is also present as the chemisorbed species (or irreversibly adsorbed), with the exception of HZSM-5 with Si/Al= 280 where no CO desorption can be detected during the TPD experiment. This observation indicates that chemisorption of CO on ZSM-5(280) does not occur. Thus, the TPD thermograms are consistent with the results obtained from FTIR and electrical conductivity sensitivity responses; this is due to the weak base properties of the CO molecule. The TPD thermograms suggest a weak chemical interaction between H^+ and CO. The TPD thermograms of ZSM-5 show two desorption peaks: the low-temperature peak and the high-temperature peak; this result can be related to the weak active site and the strong active site, respectively. The thermogram peak of HZSM-5(23) is greater than the others, which indicates that more

active sites are available for CO adsorption relative to the other HZSM-5 samples [34,35].

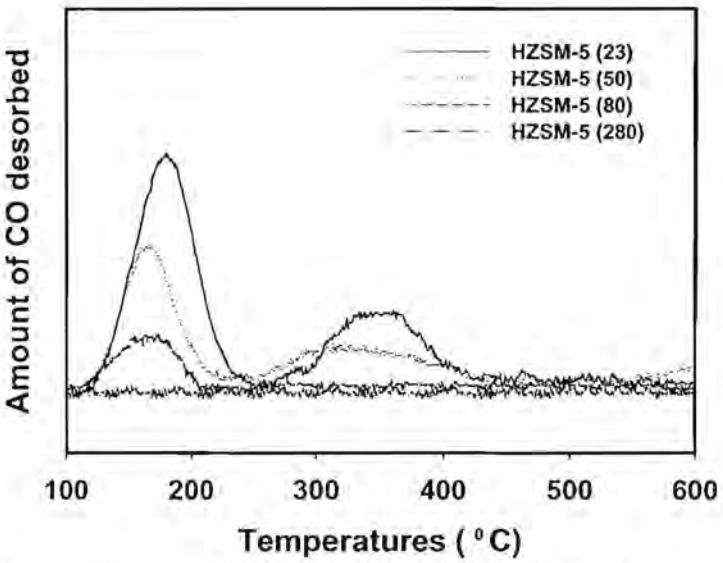

Fig. 6. CO-TPD thermograms of HZSM-5 of various Si/Al ratios.

Conclusions

Poly(3,4-ethylenedioxythiophene) doped with poly(styrene sulfonic acid), PEDOT-PSS, was successfully synthesized via oxidative polymerization at various EDOT to PSS mole ratios. The composites with PEDOT-PSS as the matrix containing ZSM-5 zeolites of various Si/Al ratios at 20% (v/v) were used to investigate the electrical conductivity sensitivity responses towards CO. The specific electrical conductivity of the PEDOT-PSS increases with increasing EDOT-to-PSS mole ratios and the specific electrical conductivity of ZSM-5 increases with decreasing Si/Al mole ratios. The electrical conductivity sensitivity of PEDOT-PSS_1:1/zeolite ZSM-5 composites towards CO negatively increases with decreasing Si/Al mole ratio of the ZSM-5 zeolite. PEDOT-PSS_1:1/ZSM-5(Si/Al = 23) has the highest electrical conductivity sensitivity response. The addition of ZSM-5 enhances the interaction between the PEDOT-PSS and CO gas, a desired characteristic of the zeolites. However, the composites produce irreversible responses; thus further work is required before it can be used as a CO sensing material. Heat treatment is one possible way to regenerate or to renew the sensing material, but the change in electrical conductivity of the PEDOT-PSS and the stability of the PEDOT-PSS should be taken into consideration.

Experimental part

Materials

As the monomer, 3,4-ethylenedioxythiophene, EDOT (AR grade, Aldrich), was used. Poly(styrene sulfonic acid), PSS, was used as the dopant. Sodium persulfate, $Na_2S_2O_8$ (AR grade, Aldrich), was used as the oxidant. Zeolite ZSM-5 samples (Si/Al: 23, 50, 80, and 280) in powder form were purchased from Zeolyst International and used in this experiment. Carbon monoxide gas (TIG, 1000 ppm) and nitrogen gas (TIG, 99 %purity)

were used to investigate the electrical conductivity sensitivity responses of the composites.

Polymerization of Poly(3,4-ethylenedioxythiophene)

PEDOT-PSS at various EDOT:PSS mole ratios in the range of 1:1 to 1:10 were prepared by mixing 3,4-ethylenedioxythiophene, the PSS solution, and $Na_2S_2O_8$ in water. After initial stirring at room temperature for 10 minutes, $Fe_2(SO_4)_3$ was added and the mixture was stirred vigorously for 24 hrs. The obtained dark, aqueous PEDOT-PSS mixture was purified by ion exchange with Lewatit M600 and Lewatit S100, resulting in dark blue, aqueous PEDOT-PSS solution. A transparent film of PEDOT-PSS was obtained by casting the aqueous PEDOT-PSS solution at 100°C for 24 hrs in a vacuum oven.

Composite Preparation

PEDOT-PSS powder was ground, sieved with a 38 μm sieve, and then dried prior to mechanically mixing with dried zeolite powders at a zeolite amount of 20 % (v/v). The mixtures were obtained by compressing with a hydraulic press machine at a pressure of 6 kN into a thin disc with a diameter of 10 mm and a nominal thickness of 1 mm.

Characterization

A Fourier transform infrared spectrometer (FTIR Nicolet, Nexus 670) with a resolution of 4 cm^{-1} and the number at scans of 32 was used to characterize the functional groups and the frequency changes before, during, and after CO exposure. The thermal stability of the PEDOT-PSS was investigated by using a thermogravimetric analyzer (Dupont, TGA 2950) with a heating rate of 10 °C/min under O_2 atmosphere. A scanning electron microscope (SEM JEOL, JSM 5200) was used to observe the morphology of the PEDOT-PSS, zeolites, and PEDOT-PSS/zeolite composites in powder form. An X-ray diffractometer (XRD Phillips, Rigaku) was used to examine the degree of crystallinity of the PEDOT-PSS and the crystal order of the zeolites. The surface area, pore width and pore volume of the ZSM-5 zeolite were measured using a surface area analyzer (Sorptomatic-1990). Temperature programmed desorption (Micromeritics, TPD/TPR 2900) was conducted and the HZSM-5 zeolite was pretreated at 500 °C. CO was adsorbed at room temperature and subsequently flushed with He. The TPD was started by increasing the temperature up to 600°C with 10°C /min ramp.

Electrical Conductivity Measurement and Gas Detection.

The electrical conductivity values of the PEDOT-PSS, ZSM-5 zeolites, and its composites under exposure to air, N_2, and, CO were measured in a special gas cell. It consisted of two stainless steel chambers connected in series. The first chamber and the second chamber were called mixing and measurement chambers, respectively. Temperature controllers connected to both chambers were used to monitor and control the temperature within the gas chambers. The second chamber contained two custom-built two-point probe meters connected to a voltage supply (Keithley, 6517A) for applying the constant voltage source (S/cm) values of σ and recording the resultant current. The specific conductivity of the pellets were obtained by measuring the bulk pellet resistance R (Ω). The relationship $\sigma = (1/Rt)(1/K) = (I/Vt)(1/K)$ was used to calculate specific conductivity, where t is the pellet thickness (cm), I is the resultant current (A), V is the applied voltage (V), and K is the geometric correction factor,

which is equal to the ratio w/l, where w and l are the probe width and the length, respectively. The geometrical correction factor (K) was determined by calibrating the custom-built two-point probe with semi-conducting silicon sheets of known resistivity values. Electrical conductivity values of several samples were first measured at various applied DC voltages to identify their linear Ohmic regimes. The electrical conductivity response and sensitivity of the composites were determined from following the equations: $\Delta\sigma = \sigma_{CO} - \sigma_{N_2\ initial}$ and $\Delta\sigma / \sigma_{N_2\ initial}$, respectively.

Acknowledgements: The authors are grateful for the financial support from the Conductive and Electroactive Polymers Research Unit of Chulalongkorn University, the Center of Petroleum Petrochemical and Advanced Materials, the Royal Thai Government (Budget of Fiscal Year 2552), and the Thailand Research Fund (PHD/0082/2550, and BRG).

References

[1] Adhikari, B.; Majumdar, S.; *Prog. Polym. Sci.* **2004**, 29, 699.
[2] Lange, U.; Roznyatovskaya, N.V.; Mirsky V.M.; *Anal. Chim. Acta.* **2008**, 614, 1.
[3] Bhambare, K.S.; Gupta, S.; Mench, M.M.; Ray, A.; *Sens. Actuator B-Chem.* 2008, **134**, 803.
[4] Fang, Y.K.; Lee, J.J.; *Thin Solid Films* **1989**, 169, 51.
[5] Dixit, V.; Misra, S.C.K.; Sharma, B.S.; *Sens. Actuator B-Chem.* **2005**, 104, 90.
[6] Mathur, S.C.K.; Mathur, P.; Srivastava, B.K.; *Sens. Actuator A-Phys.* **2004**,114, 30.
[7] Watcharaphalakorn, S.; Ruangchuay, L.; Chotpattananont, D.; Sirivat, A;, Schwank, J.; *Polym. Int.* **2005**, 54, 1126.
[8] Densakulprasert, N.; Wannatong, L.; Chotpattananont, D.; Hiamtup, P.; Sirivat, A.; Schwank, J.; *Mater. Sci. Eng. B* **2005**, 117, 276.
[9] Saxena, V.; Malhotra, B.D.; *Curr. Appl. Phys.* **2003**, 3, 293.
[10] Ram, M.K.; Yavuz, O.; Aldissi, M.; *Synth. Met.* **2005**, 151, 77.
[11] Ram, M.K.; Yavuz, O.; Lahsangah, V.; Aldissi, M.; *Sens. Actuator B-Chem.* **2005**, 106, 750.
[12] Guernion, N.; de Lacy Costello B.P.J.; Ratcliffe, N.M.; *Synth. Met.* **2002**, 128, 139.
[13] Bavastrelloa, V.; Erokhina, V.; Carraraa, S.; Sbranab, F.; Riccib, D.; Nicolini, C.; *Thin Solid Films* **2004**, 468, 17.
[14] Chen, Y.; Li, Y.; Wang, H.; Yang, M.; *Carbon* **2007**, 45, 357.
[15] Hosseini, S.H.; Entezami, A.A.; *J. Appl. Polym. Sci* .**2003**, 90, 49.
[16] Bai, H.; Shi, G.; *Sensors* **2007**, 7, 267.
[17] Prissanaroon, W.; Ruangchuay, L.; Sirivat, A.; Schwank, J.; *Synth. Met.* **2000**, 114, 65.
[18] Groenendaal, L.; Jonas, F.; Freitag, D.; Pielartzik, H.; Rynolds, J.R.; *Adv. Mat.* **2000**, 12, 482.
[19] Louwet, F.; Groenendaal, L.; Dhaen, J.; Manca, J. Van Luppen, J.; Verdonck, E.; Leenders, L.; *Synth. Met.* **2003**, 135-136, 115.
[20] Chuapradit, C.; Wannatong, L.R.; Chotpattananont, D.; Hiamtup, P.; Sirivat, A.; Schwank, J.; *Polymer* **2005**, 46, 947.
[21] Thuwachaowsoan, K.; Chotpattananont, D.; Sirivat, A.; Rujiravanit, R.; Schwank, J.W.; *Mater. Sci. Eng. B* **2007**, 140, 23.
[22] Soontornworajit, B.; Wannatong, L.; Hiamtup, P.; Niamlang, S.; Chotpattananont, D.; Sirivat, A.; Schwank, J.; *Mater. Sci. Eng. B* **2007**, 136, 78.

[23] Han, D.; Yang, G.; Song, J.; Niu, L.; Ivaska, A.; *J. Electroanal Chem.* **2007**, 602, 24.
[24] Garreau, S.; Louarn, G.; Buisson, J.P.; Froyer, G.; Lefrant, S.; *Macromolecules* **1999**, 32, 6807.
[25] Chun, L.; Imae, T.; *Macromolecules*, **2004**, 37, 2411.
[26] Martin, B.D.; Nikolov, N.; Pollack, S.K.; Saprigin, A.; Shashidhar, R. Zhang, F.; Heiney, P.A.; *Synth. Met.* **2004**, 142, 187.
[27] Kiebooms, R.; Aleshin, A.; Hutchison, K.; Wudl, F.; Heeger, A.; *Synth. Met.* **1999**, 101, 436.
[28] Wichiansee, W.; Sirivat, A.; *Mater. Sci. Eng. C* **2009**, 29, 78.
[29] Jönsson, S.K.M.; Birgerson, J.; Crispin, X.; Greczynski, G.; Osikowicz, W.; van der Gon A.W.D.; Salaneck, W.R.; Fahlman, M.; *Synth. Met.* **2003**, 139, 1.
[30] Vacca, P.; Petrosino, M.; Miscioscia, R.; Nenna, G.; Minarini, C.; Sala, D.D.; Rubino, A.; *Thin Solid Films* **2008**, 516, 4232.
[31] Álvaro, M.; Cabeza, J.F.; Fabuel, D.; García, H.; Guijarro, E.; de Juan, J.L.M.; *Chem. Mater.* **2006**, 18, 26.
[32] Kooser, A.; Gunter, R.L.; Delinger, W.D.; Porter, T.L; Eastman, M.P; *Sens. Actuator B-Chem.* **2004**, 99, 474.
[33] Yang, Y.; Jiang, Y.; Jianhua, X.; Junsheng, Y.; *Polymer* **2007**, 48, 4459.
[34] Auerbach, S.M.; Carrado, K.A.; Dutta, P.K. *Handbook of Zeoite Science and Technology*, Marcel Dekker Inc., New York, **2001**.
[35] Costa, C.; Dzikh, I.P.; Lopes, J.M.; Lemos, F.; *J. Mol. Catal. A-Chem.* **2000**, 154, 193.

ส่วนที่ 2

Physically cross-linked cellulosic gel via 1-butyl-3-methylimidazolium chloride ionic liquid and its electromechanical responses

Wissawin Kunchornsup [1], Anuvat Sirivat [1,#]

[1]The Petroleum and Petrochemical College, Chulalongkorn University, Bangkok 10330, Thailand

Abstract.

Cellulose shows promising piezoelectric properties widely used in electroactive papers (EAPaps), however its solubility still remains a challenging problem. 1-Butyl-3-methylimidazolium Chloride ($BMIM^+Cl^-$), a well-known room temperature ionic liquid (RTIL), is utilized here to dissolve a micro-crystalline cellulose. The $BMIM^+Cl^-$ - cellulose gels are prepared by the solvent casting method. The elctromechanical properties of the cellulose gels are investigated under the oscillatory shear mode at electric field strengths between 0 to 1kV/mm and as functions of temperature. The storage modulus (G′) increases linearly with temperature up to 333 K at 1 rad/s in the absence of electric field strength. The storage moduli (G′) also increase linearly with temperature up to 313 K at 1 rad/s in the presence of 1kV/mm of electric field strength and decreases above 313 K, consistent with the behavior of dielectric permittivity (ε′).

The elastic-plastic-viscous transition is observed in the presence of 1 kV/mm. It is shown that the conditions imposed by electric field strength and temperature alter the transition temperature, and lower the dielectric constant, the storage modulus, and the actuation performance. In the deflection experiments, under applied DC electric field, the deflection distances of the gels linearly increase with increasing electric field strength along with the dielectrophoresis forces above the electrical yield strength of 100 V/mm. The back and forth swinging occurs under the constant electric field strength between 525-550 V/mm due to the competition between the anion and cation movements within the ionic liquid. Electrostatic force microscope (EFM) is then employed to investigate the gel topology and the cationic channel and aggregation that control the actuation behavior. The Phy gel is shown here to be promising for actuator applications over other existing dielectric elastomers studied at a room temperature in terms of the electrical yield strength, the bending angle, the generated dielectrophoresis force, the energy density, the force density, the mechanical power, the power density, G′ at 1 rad/s at 0.25% strain, and the relatively high $\varepsilon'_{r,\ 20\ Hz}$.
Keywords: Electromechanical responses, Cellulose, 1-butyl-3-methylimidazolium chloride (BMIMCl), ionic liquid, Actuator
Corresponding author. Tel.: +66 2 218 4131; fax: +66 2 611 7221.
E-mail address: anuvat.s@chula.ac.th (A. Sirivat).

1. Introduction

An ionomeric polymer is one of the electroactive polymers that can be utilized as the electromechanical devices and sensors. The pioneers of this field are Kuhn *et al.* [1,2] and Katchalsky [3] since the late 1940s. Recently, Nafion ionomer transducers, a Teflon-like backbone chain with pendant side chains that are terminated with neutralized sulfonate exchanged sites have been studied as transducers, in particular via the ion-exchange process [4,5,6]. It can be bent under electric field through a conductive electrode coating and swollen in suitable diluents due to the mobile cations and the diluents within the polymer matrix [7,8]. The charge imbalance across the electrodes was studied in the quasi-static displacement under applied voltages. The limitation of these systems is the hydration dependence, even though evaporation barriers were employed under the operation condition [9,10].

One of well-known and challenging electrolytes is the ionic liquid or the ionic compounds that exist as liquids at a low temperature. The interesting properties are non-volatility, high stability, suitable polarity, high ionic conductivity, and easy recyclability. Nafion swollen in 1-ethyl-3-methylimidazolium bis(triflouromethylsulfonyl)imide (EMI-IM) was studied and shown that the actuation speed and the ionic conductivity increased with increasing counterion size and increasing content of the ionic liquid, due to the counterions of the polymer acting as the primary charge carriers [11]. The use of 1-ethyl-3-methylimidazoliumtrifluoromethanesulfonylimide ionic liquid was then demonstrated as a viable solvent for Nafion™ polymer actuators and sensors. Experimental results also indicated that the Nafion™ polymer actuators solvated with this ionic liquid possessed the improved stability when operated in air as compared to the same materials solvated with water; although the magnitude of the response decreased at high frequencies relative to that of the materials solvated with water [12].

One of the most advantages of ionic liquid utilization is the utilization with cellulose as a matrix [13]. Cellulose possesses piezoelectric properties that are required

for actuation. The bending displacement of the 1-butyl-3-methylimidazolium hexafluorophosphate (BMIPF6) dispersed in a cellulose actuator was shown to be enhanced by a factor of four as compared to that of the pristine cellulose. However, the $BMIPF_6$ dispersion resulted in an increase in the amorphous region and the lowering of the cellulose thermal stability [14].

In the present work, we are interested in investigating further the 1-butyl-3-methylimidazolium chloride ($BMIM^+Cl^-$)-cellulose gel as a suitable electroactive polymer. The effects of DC electric field strength, temperature, and relative dielectric permittivity on the electromechanical responses and the actuation performance are reported here.

2. Experimental

2.1 Materials

Cellulose microcrystalline powder (AR grade, Sigma-Aldrich), 1-butyl-3-methylimidazolium chloride (BMIMCl) (HPLC grade, Sigma-Aldrich), and N,Ndimethylacetamide (DMAc) were used as received without further purification.

2.2 Preparation of physically cross-linked cellulosic gel

BMIMCl and the dried cellulose were mixed at a composition of 87% w/w of BMIMCl (2.15 g) and 13% w/w of cellulose (0.323 g) , equivalent to a 6.19:1 molar ratio of BMIMCl: glucose [15] , as this molar ratio allows the maximum dissolution of cellulose in BMIMCl at 100 °C. The cellulose was dissolved in BMIMCl at 100°C for 15 minutes. The obtained viscous solution was filled with 1.5 ml of N, N-dimethylacetamide (DMAc) as a plasticizer and a co-solvent, and stirred for 60 minutes. The solution was degassed and casted into a mold having a diameter of 25mm and a thickness of 1 mm and kept under a vacuum for 12 hours. The physically cross-linked cellulosic gel (Phy gel) was obtained after curing at the ambient conditions for 24 hours [16]. The Phy gel was then characterized for the electromechanical, dielectric, and topological properties.

2.3 Characterization of prepared physically cross-linked cellulosic gel (Phy gel)

The relative dielectric permittivity values were measured by an LCR meter (HP, model 4284A) connected to a rheometer (Rheometric Scientific, ARES) with a 25-mm parallel plate fixture. The thickness of the specimens is typically 1mm and the diameter is about 25 mm. The top and bottom sides of the specimens were coated with a silver adhesive to improve the electrical contacts between the specimens and the electrodes. The measurements were carried at temperatures between 303 and 333 K. The AC voltage applied was varied between 1 and 10 V, depending on the materials. The dielectric permittivity at a frequency of 20Hz was divided by 8.85 pF/m of free space to obtain the relative dielectric permittivty (ε'_r) or the dielectric constant.

The electromechanical properties were measured by the rheometer (Rheometric Scientific, ARES), fitted with a custom-built copper parallel plate fixture (diameter 25 mm). DC voltage was applied with a DC power supply (Instek, GFG 8216A), which can deliver an electric field up to 4 kV. A digital multimeter (Tektronix, CDM 250) was used to monitor the voltage input. The samples were prepared in the configuration of Polyimide_Phy gel_Polyimide sandwich to prevent the shortening of the circuit. The

Polyimide (PI), ®Kapton TH-012 (12 micron) was produced by and obtained from ©2006 Saint Gobain Performance Plastic Corporation. The PI film represents an excellent insulator up to 7kV/mm for the breakdown voltage; a dielectric constant value of 3.3; volume resistivity > 10^{16} Ω-cm. In these experiments, an oscillatory shear strain was applied and the dynamic modulus (G') was measured as a function of frequency, electric field strength, and temperature. Strain sweep tests were first carried out to determine the suitable strains to measure G' in the linear viscoelastic regime. The appropriate strain was determined to be 0.25% for Phy gel studied. The temporal response experiments of Phy gels were carried out at 1 kV/mm at T = 303 and 333 K. Then, the frequency sweep tests were carried out to measure G' of each sample as a function of frequency, electric field strength and temperature. The deformation frequency was varied from 0.1 to 100 rad/s. In each measurement, each Phy gel was pre-sheared at a low frequency and then the electric field was applied for 30 min to ensure the steady state condition before the G' measurements. The effect of temperature on the dynamic modulus and dielectric constant was studied at various temperatures between 303 and 333 K.

Electrostatic force microscopy (EFM, XE-100, Park System) measurements were carried out simultaneously by monitoring the detector signal amplitude at 5V and using conductive layer coated silicon tips with a nominal radius of 40 nm, NSC36/Ti-Pt. Each sample line was scanned at two heights above the surface. In the first scan, the tips response was dominated by the short-range van der Waals force under the Tapping Mode and recorded the surface morphology of the membrane. The second scan was taken under the Interleave Mode at the height of 10 nm to detect the electric field force of the membrane.

The dielectrophoresis forces were determined by measuring the deflection distances of the gels in the vertical cantilever fixture under electric field. (The experimental setup is shown in Figures 9 and 10) The specimens were vertically immersed in the silicone oil (viscosity=100 cSt) between parallel copper electrode plates (68 mm of length, 40 mm of width, and 2 mm of thickness). The gap between the pair of electrodes was 30 mm. A DC voltage was applied with a DC power supply (Goldsun, GPS 3003B) connected to a high voltage power supply (Gamma High Voltage, model UC5-30P and UC5-30N) which can deliver an electric field up to 25 kV. The output voltage from the high voltage power supply was calibrated using a Fluke 40 kV High Voltage Probe. A CCD video camera was used to record the movement during the experiment. Still pictures were captured from the video and the deflection distances in x (d) and y axes (l) at the ends of the specimen were determined by using the Scion Image software (version 4.0.3). The electric field strength was varied between 0 and 550 V/mm at the room temperature of 303±1 K. Both the voltage and the current were monitored. The resisting elastic force of the specimens was calculated under electric field using the non-linear deflection theory of a cantilever [17-22], which can be obtained from the standard curve between ($F_e l_0^2$) / (EI) and d / l_0 (l_0 =_initial length of specimens) [21]; F_e is the elastic force, d is the deflection distance in the horizontal axis, l is the deflection distance in the vertical axis, E is the Young's modulus–which is equal to 2G′(1+ν), where G′ is the shear storage modulus taken to be G′(ω=1 rad/s) at various electric field strengths and, ν is the Poisson's ratio (0.5 for an incompressible sample)–and I is the moment of inertia $1/12t^3w$, where t is the thickness of the sample and w is the width of the sample. The dielectrophoresis force can be

calculated from the static horizontal force balance consisting of the elastic force and the corrective gravity force term (mgsinθ), as shown in equation (i):

$$F_d = F_e + mg\sin\theta \ (N), \quad \text{(i)}$$

where g = 9.8 ms^{-2}, m = the mass of the specimen, and θ is the deflection angle.

To investigate the materials as potential actuators, the energy density, the force density, the mechanical power, and the power density of the gels are important factors for comparisons. These factors were calculated using Equations (ii)-(v), respectively [17-27]:

$$Energy\ density = \frac{1}{2}E\theta^2(J), \quad \text{(ii)}$$

$$Force\ density = \frac{F_d}{volume}\ (Ncm^{-3}), \quad \text{(iii)}$$

$$Mechanical\ power = \frac{1}{4}F_d\frac{d}{\tau_i}(W), \quad \text{(iv)}$$

$$Power\ or\ work\ density = \frac{Mechanical\ power}{volume}\ (Wcm^{-3}), \quad \text{(v)}$$

where τ_i is the induction time.

3. Results and discussion

3.1 Time dependence of the electromechanical response

First, the temporal characteristics of the Phy gel at 303 and 333 K under the 1 kV/mm electric field strength are investigated. The temporal characteristic of each sample was recorded in the linear viscoelastic regime at a strain of 0.25%, and a frequency of 1 rad/s. Figure 1 shows the change in G' of the Phy gel at 303 and 333 K under the 1 kV/mm electric field strength during a time sweep test, in which an electric field is turned on and off alternately. At the temperature of 303 or 333 K, G' immediately increases and rapidly reaches a steady-state value. The storage modulus increment under the turned on voltage results from three dominating mechanisms: the $BMIM^+$-cation polarization (the ionic polarization) [28-30], the cellulosic hydroxyl group polarization (the dipolar polarization) [19,20], and the shear induced cellulose chain alignment [31]. Then, with the electric field off, G' decreases but does not recover its original value due to some residual polarizations and the chain alignment. Subsequent on and off on electric field produces steady state responses after a duration of about 1,800 s. The response of G' can be divided into two regimes: the initial regime in which G' rapidly overshoots to a large value on the first cycle followed by a irreversible decay with electric field off; and the steady state regime in which G' subsequently exhibits a reversible cyclic response.

The higher temperature (333 K) promotes the two induced polarizations and the cellulose chain alignment in the absence of 1 kV/mm of electric field strength. This is because temperature enhances the mobility of $BMIM^+$-cation, the dipole-dipole interaction, and the cellulose chain alignment, so G'_o at 333 K is higher than G'_o at 303 K: ~3.00×10^5Pa and ~2.25×10^5Pa, respectively. However, in the presence of 1 kV/mm of electric field strength a lower $G'_{1kV/mm}$ value at 333 K (~3.97×10^5Pa) than $G'_{1kV/mm}$

value at 303 K (~5.82×10^5Pa) is obtained instead. In addition, $\Delta G'_{ind,\,sat}$ and $\Delta G'_{rec,\,sat}$ at 333K are lower than $\Delta G'_{ind,\,sat}$ and $\Delta G'_{rec,\,sat}$ at 303K: 45620; 25860; 65710; 64060 Pa, respectively. This is presumably caused by the ionic association of ionic liquid [32], the premature transition temperature of $BMIM^+Cl^-$ (fusion temperature=341.94 K) [33]), and the chain relaxation due to the imposed high electric field strength and temperature. Eventhough the dipolar polarization from the cellulosic hydroxyl group is promoted with increasing temperature [34,35] still the lower $G'_{1kV/mm}$ value at 333 K than the $G'_{1kV/mm}$ value at 303 K is obtained due to the fact that the Phy gel properties primarily depend on ionic contributions.

The time required for G' to reach the steady-state value under applied field is called the induction time, $\tau_{ind,\,sat}$. As shown in Table 1, τ_{ind} decreases with increasing temperature; they are 218 and 42 s at the temperatures equal to 303 and 333 K, respectively. The time required for G' to decay towards its steady-state value when the electric field is turned off is called the recovery time, $\tau_{rec,\,sat}$. It decreases with increasing temperature; they are 290 and 13 s at the temperatures equal to 303 and 333 K, respectively, as shown in Table 1. The dependence of both τ_{ind} and τ_{rec} on the temperature suggests that the higher temperature promote the polarizations and the cellulose chain alignment which enhance the storage modulus increment within a shorter time scale.

As shown in Table 2, the temporal response properties of the Phy gel: G'_o,$G'_{1kV/mm}$, storage modulus response ($\Delta G'_{1kV/mm}$) , and storage modulus sensitivity ($\Delta G'_{1kV/mm} / G'_o$) exhibit the highest values when compared with those of other dielectric elastomers that have been investigated.

3.2 Relative dielectric permittivity

The relative dielectric permittivity or the dielectric constant of the Phy gel at T = 303, 308, 313, 318, 323,328, 333 K and the frequency of 20 Hz, are 31.36, 31.92, 33.01, 31.15, 30.04, 28.81 and 27.88, respectively. The relative dielectric permittivity vs. frequency curves of the Phy gel at T = 303, 308, 313, 318, 323,328, and 333 K are shown in Figure 2. From Figure 2, the relative dielectric permittivity of Phy gel can be seen to increase significantly with increasing frequency at all temperatures when $f > 10^3$ Hz. The increment of relative dielectric permittivity with increasing frequency can be attributed to the ionic contribution that comes from the displacement of charged ions with respect to other ions, the $BMIM^+$ transportation [40]. Although the dipolar polarization exists which tends to decrease the dielectric permittivity with increasing frequency, the ionic polarization is presumably the dominating contribution since the Phy gel is an ionic-rich gel. As shown in Figure 3, the relative dielectric permittivity of the Phy gel increases linearly with increasing temperature from 303 to 313 K. The increase in temperature or the thermal energy available leads to the increase in the mobility of molecules. The motion of molecules in turn induces the dipole moment [41,42] and the ionic polarization, leading to the increase in the relative dielectric permittivity. With a further increase in temperature from 313 to 333 K, the relative dielectric permittivity linearly decreases due to the ionic liquid association. Such a high temperature promotes the molecular mobility, through the co-solvent used, N, N-dimethylacetamide (DMAc) that enhances the ionic liquid association, leading to depression of the relative dielectric permittivity. In addition, the higher temperature also accelerates the water evaporation, which in turn accelerates the ionic association in the absence of water molecule [32]. Such water molecule exists in the Phy gel because of its

hydrophilicity [15]. The comparison of the relative dielectric permittivity of the Phy gel and the dielectric elastomers suggests that the Phy gel possesses a much higher relative dielectric permittivity than others at all temperatures, even though the relative dielectric permittivity of the dielectric elastomers tends to increase with increasing temperature due to the induced dipolar interaction. The outstanding feature of the Phy gel thus arises from the synergism between the ionic polarization of the ionic liquid and the dipolar polarization of cellulosic hydroxyl group.

3.3 Effects of electric field strength and temperature on electromechanical properties

Figure 4 shows the storage modulus (G′) vs. frequency of the Phy gel at the electric field strengths of 0, 0.2, 0.4, 0.6, 0.8, and1.0 kV/mm. G′(ω=1 rad/s) increases from ~1.73×10^5 Pa to 4.21×10^5 Pa as electric field strength is varied from 0 to 1 kV/mm. The higher electric field strength induces the greater ionic polarization and effective pressure, which resulted from the dipole moment interaction [43] and the volume difference [28].

Figure 5 shows the rheological properties of the Phy gel as measured at the electric field strengths of 0 and 1kV/mm within the temperature range of 303–333 K, and the frequency range of 0.1–100 rad/s. One sample was used for each of the G'_0 and $G'_{1kV/mm}$ measurements; the electric field strength was fixed and temperature was ramped up. Figure 5 shows the frequency sweep performed using the strain of 0.25% at various temperatures. Between 303 to 333 K, the storage modulus (G′) without applied electric field appears to increase with temperature but it is rather independent of frequency (ω= 0.1–100 rad/s); this can be referred to as the elastic or rubbery response regime. Under the applied electric field strength of 1 kV/mm, the responses can be divided into three regimes. At 303K, the storage modulus (G′) under the applied electric field strength of 1 kV/mm appears to be independent of frequency (ω= 0.1–100 rad/s); this can be referred to as the elastic rubbery-like response. At the temperature of 313 K, the measured modulus (G′) appears to increase non-linearly with frequency up to ω= 100 rad/s. The characteristics observed here is of the plastic response [44]. At the higher temperatures between 323 to 333 K, the modulus at low frequency decreases with increasing temperature. This behavior is the fusion transition regime of the ionic liquid [44] and can be related to the structure of $BMIM^+Cl^-$; it is in the fused state at these immediate temperatures which are close to the fusion temperature of 341.94 K. The change in the storage modulus ($G'_{1kV/mm}$) as a function of temperature of the Phy gel can be referred to as the rubbery-plastic-viscous transitions.

The change in the storage modulus with increasing temperature with and without applied electric field of the Phy gel are summarized and shown in Figure 6, at the frequency of 1 rad/s. In the figure, the storage modulus (G'_0) is compared to $G'_{1kV/mm}$, at the applied electric field strengths of 1 kV/mm. Electric field was first applied on each sample for a period of 30 min before $G'_{1kV/mm}$ was measured successively at each temperature. At a temperature below 317 K, $G'_{1kV/mm}$ is clearly higher than G'_o, above this temperature $G'_{1kV/mm}$ and G'_o are comparable in values which are quite independent with temperature. This is the main reason why the storage modulus response ($\Delta G'_{1kV/mm}$) and the storage modulus sensitivity ($\Delta G'_{1kV/mm}$ / $\Delta G'_o$) decrease with increasing temperature . The increase in G′ with temperature in the elastic regime of the Phy gel is consistent with the classical network theory [45]

$$G' = \nu_e k_B T \qquad \text{(vi)}$$

where k_B is Boltzmann's constant, T is the absolute temperature (K), and ν_e is number of effective strands per unit volume (cm^{-3}). Since the Phy gel has no covalent crosslinks, the linear dependence of G'_o on temperature stems from physical entanglements and of entropic in nature. The decrease of $G'_{1kV/mm}$ with T above 313 K can be related to the $BMIM^+Cl^-$ transition temperature where the free volume effect becomes dominant, in addition to the decline in the relative dielectric permittivity.

Figure 7 shows the effect of temperature on storage modulus sensitivity at various electric field strengths. The storage modulus sensitivity at all of various electric field strength decreses with increasing temperature as previously shown in Figure 6. Below 317 K, an electric field induces an increase on the storage modulus sensitivity, $G'_{1kV/mm}$ is higher than G'_o, because of the ionic polarization, the dipolar polarization, and the cellulose chain alignment. Above 317 K, the electric field induces a decline on the storage modulus sensitivity due to the transition temperature of $BMIM^+Cl^-$ making $G'_{1kV/mm}$ to decrease but G'_o to increase with temperature.

3.4 Effects of relative dielectric permittivity on electromechanical properties

The storage modulus response and sensitivity of the storage modulus of the Phy gel are investigated at the electric strengths of 0.2, 0.4, 0.6, 0.8, and 1.0 kV/mm vs. the dielectric constant at 20Hz and at the temperatures between 303 to 333 K as shown in Figure 8. There are essentially two regimes of the storage modulus response with respect to temperature or the dielectric constant. Within the lower temperature range between 303 and 313 K, the storage modulus response and sensitivity decrease slightly with increasing temperature or the relative dielectric permittivity. The latter decrease of the storage response is consistent with the fact that the dielectric constant increases with increasing temperature, thus obeying the electrostrictive theory [41]. The increase of the storage modulus response with increasing electric field within this temperature range is clearly due to the polarizations and the cellulose chain alignment. Within the high temperature range between 318 and 333 K, the storage modulus response and sensitivity decrease monotonically with increasing temperature or decreasing relative dielectric permittivity. This result is consistent with the result of Figure 3 where $\square'_r$ decreases with increasing temperature. It may be noted that the effect of electric field on the storage modulus response and sensitivity is less pronounced in the temperature range between 318 to 333 K relative to that of 303 to 313 K. The results obatined are in agreement with those of Pelrine *et al.*, 1998 [24] where they showed that the electromechanical reponses depends on various factors: the dielectric constant, the hardness, and the elastic properties of the materials [24].The present results also suggest that the fabricated Phy gel is a potential candidate for actuator applications near a room temperature.

3.5 Deflection measurement of Phy gel

The bending behavior Phy gel is investigated next under applied electric field. The samples are gripped between copper plates and immersed in a poly(dimethylsiloxane), as shown in Figures 9 and 10. A video recorder is used to record the displacement of the film. The deflection distance along x axis (d) and the deflection length (l) are measured through the analysis program. Under externally applied electric field strength, the free end samples bend toward to the positive side or the anode side via the ionic and electronic polarizations. First, the $BMIM^+$ cations move towards the neutral side due to the cation-anode repulsive force, as Cl^- counter ions are

immobilized and act as the physical crosslinks. Although the Cl^- anion could be a working mobilized ion as reported in the work of Mahadeva, 2009 [14,46], it only appears in the sample preparation of a relatively lower free volume or in the absence of DMAc co-solvent. In the absence of DMAc, the cation is restricted from movement because the lack of the co-solvent solvation to facilitate the cation mobility [14,46]. Thus it was not possible to create a bending via $BMIM^+$ volume difference, in the mode of side-by-side volume difference. This eventually results in Cl^- acting as dominating working mobilized ion. The migration of the cations towards the neutral electrode creates the ionic polarization, the side-by-side volume difference, and the blocking force leading the Phy gel to bend towards the anode electrode [28]. Secondly, the chemical structures of the micro-crystalline cellulose consist of many hydroxyl groups on the polymer chains. Under applied electric field, the hydroxyl groups can also pull electrons from the carbon atoms on the backbone. The polarities of the hydroxyl group thus become negative. This leads to the apparent deflection towards the anode (positive) side [47]. It is known that the actuation principle of EAPap is possibly a combination of the piezoelectric effect and the ion migration effect, and at the same time associated with the dipole moment of the cellulose ingredients. The effects of electric field strength on the deflection angle are investigated under the electric field strengths between 0 and 550 V/mm at the temperature of 300 ±1 K. (Still pictures of the experiments are shown in Figure 10 a to d: 0, 500, 525, and 550 V/mm .) Initially, the specimens are straight at the center of the testing fixture without electric field. After applying an electric field, the specimen starts to deflect towards the anode electrode. The back and forth swing is investigated under the electric field strength of 525-550 V/mm; this swinging is due to the competition between the anion and cation movements within the ionic liquid. Due to different effective sizes of the positive charges and negative charges (cations and anions may form clusters rather than bare ions in the processes of ion transport and storage), the back and forth swing generated by the positive and negative charges are different, causing the bending actuation as observed here [48]. Thus, it is clearly demonstrated here the periodic movement of the Phy gel unexpectedly occurs through the applied DC electric field.

3.6 Effect of electric field strength on deflection angle and dielectrophoresis force

The electrical yield strength—the electric field strength required for the materials to start to deflect—of Phy gel is 100 V/mm. This suggests that the Phy gel requires quite a low electrical energy to respond. The induction time—the period of time that the Phy gel required to deflect to the maximum distance after applying electric field—of Phy gel at E = 100, 200, 300, 400, and 500 V/mm is 1.34, 2.41, 3.35, 5.67, and7.13s, respectively. The recovery time—the period of time that the Phy gel required for deflect back to the starting position after turning off the electric field—of Phy gel at E= 100, 200, 300, 400, and 500 V/mm is 1.51, 2.59, 3.54, 5.84, and 7.43 s, as shown in Table3. Figure 11 shows the deflection angle and the dielectrophoresis force of the Phy gel versus electric field strength. The deflection angles generally become larger with increasing electric field strength. At E= 500 V/mm, the Phy gel shows the highest deflection angle, at 44° in the static deflection regime. At E=550 V/mm, the Phy gel shows the largest deflection angles, at -45° to 55° in the back and forth swinging regime. The present results can be related to the electrostriction theory [25]. As the electric field is applied, the dipole moments of molecules are generated from the ionic and electronic

polarization. The hydroxyl groups on the polymer chain and the $BMIM^+$ cations are polarized as the results of electric field. As the electric field strength increases, this leads to a further increase in the internal dipole moments. This leads to the increases in the degree of interaction with the electrodes, the deflection angle, $mg\sin\theta$, F_e, F_d, energy density, force density, and the corresponding mechanical strains. The effect of electric field strength on the dielectrophoresis force is shown in Figure 11. The dielectrophoresis forces of the present material systems are measurable above the electrical yield strengths in the *I-b* region; it is not measurable in the *I-a* region. The forces increase non-linearly with increasing electric field strength due to the increase in the internal dipole moments, the electric polarization, and the ionic polarization of the materials. The forces become saturated at a high electric field strength near the end of the *I-b* region. Further increasing electric field strength to be between 525 and 550 V/mm, the region *II*, the back and forth swinging deflection occurs. This region produces the highest dielectrophoresis force equal to ~7 to 17 mN through the back and forth swinging action.

Table 4 shows the comparison between the Phy gel with existing dielectric elastomers. In the actuator application, it is required for the actuation materials to possess the followings: the deformations (strains and bending angles), the dielectrophoresis force, the energy density, the force density, the power density, G′ at high or low frequencies, and the relative dielectric constant to be all high at a relatively low electric field strength. As shown in Table 4, the electrical yield strength of Phy gel is 0.10 kV/mm which is close to the values of existing dielectric elastomers (0.08 of AR71 and AR72). The bending angle of Phy gel is 43.6° that is a moderately promising angle. The actuation force at 303K in the terms of the generated dielectrophoresis force, the energy density, the force density, the mechanical power, the power density, G′ at 1 rad/s at 0.25% strain, and the relatively high $\varepsilon'_{r,\ 20\ Hz}$ are 4630 μN, 1.12E+09 J/m^3, 9.02E+04 N/m^3, 1.71 μW, 33.13 W/m^3, 4.21E+05 Pa, and 31.36, respectively. These values are relatively high when compared with existing dielectric elastomers. In conclusion, it can be said that the cellulose-ionic liquid gel is a promising material candidate for actuator applications over existing dielectric elastomers at a room temperature.

3.7 Topology and electrostatic interaction at the surface of Phy gel

Figure 12a shows the Phy gel topology through the EFM images. The surface is evidently not smooth in the nanoscale, whereas the macroscopic view is not clearly observable. Figure 12b shows that the hydrophilic ionic domains display bright regions in the EFM images that are connected through small hydrophilic ionic channels. The formed small channels connecting ionic domains can facilitate the proton and ionic transportation process inside the Phy gel consisting different degrees of hydrophilicity between the microcrystalline cellulose and the ionic liquid [49].

4. Conclusion

This work presents the electromechanical properties of the physically cross-linked cellulosic gel (Phy gel). The temporal responses, $\Delta G'_{ind,\ sat}$ and $\Delta G'_{rec,\ sat}$, decreases with increasing temperature, the decreases of $\tau_{ind,\ sat}$, $\tau_{rec,\ sat}$ occur at the high electric field strength and temperature, 1kV/mm and 333K, due to the premature transition temperature and the ionic association, inducing lower storage moduli. The relative dielectric permittivity increases with increasing frequency because of the ionic

polarization. The effect of temperature on relative dielectric permittivity is proportional at relatively low temperature, 303 to 313 K due to the temperature induced ion mobility and polarization. At relatively high temperature, 313 to 333 K, the effect of temperature on the relative permittivity is inversely proportional because of the ionic association. The electric field strength induces the internal dipole moment at a relatively low temperature, and the storage modulus increment. However, at a relatively high temperature above 313 K, the premature transition temperature and the decreases in the storage moduli and the relative dielectric permittivity can be observed. The deflection experiment shows the bendings towards the positive side or the anode side under electric field strength under above 100 V/mm, the electrical yield strength. The actuation is due to the ionic and electronic polarization via the $BMIM^+$ cation (observed by EFM image) and the cellulosic hydroxyl group, respectively. In addition, between 525 and 550 kV/mm, the back and forth swinging is observed due to the competition between the anion and cation movements within the Phy gel. The actuation performance in terms of the bending angle, the induction time, the recovery time, the resultant dielectrophoresis force, the energy density, the force density, the mechanical power, the power density, are superior over those of previously studied dielectric elastomers at a room temperature. The major limitation associated with the use of the ionic liquids as solvents for electro-active papers has been identified as the slow speed of response. However, the use of the ionic liquids to make effective actuators is demonstrated and the motivation for future work in this direction is established.

Acknowledgements

The authors would like to acknowledge the financial support from the following: the Conductive and Electroactive Polymers Research Unit Chulalongkorn University; the Thailand Research Fund, TRF-BRG; Nanotec; the Royal Thai Government Budget; Center for Petroleum, Petrochemicals, and Advanced Materials. The material support from Saint Gobain Sekurit Thailand Co. Ltd is also gratefully acknowledged.

References

[1] W. Kuhn, Reversible Dehnung und Kontraktion bei Anderung der Ionisation eines Netzwerks Polyvalenter Fadenmolekulionen, Experientia. 5 (1949) 318-9.

[2] W. Kuhn, B. Hargitay, A. Katchalsky, H. Eisenberg, Reversible dilation and contraction by changing the state of high-polymer acid networks, Nature. 165 (1950), 514-6.

[3] A. Katchalsky, Rapid swelling and deswelling of reversible gels of polymeric acids by ionization, Experientia. 5 (1949) 319-320.

[4] K. Sadeghipour, R. Salomon, S Neogi. Development of a novel electrochemically active membrane and 'smart' material based vibration sensor/damper, Smart Mater. Struct. 1 (1992) 172-9.

[5] K. Oguro. Actuator element.U.S.Patent 5,268,082 (1993).

[6] M. Shahinpoor, Y. Bar-Cohen, J. Simpson, J. Smith, Ionic polymer-metal composites (IPMCs) as biomimetic sensors, actuators and artificial muscles e a review, Smart Mater. Struct.7 (1998) R15-30.

[7] K. Mallavarapu, D.J. Leo, Feedback control of the bending response of ionic polymer actuators, J Intel Mat Syst Str. 12 (2001) 143-55.

[8] C.S. Kothera, D.J. Leo, Bandwidth characterization in the micropositioning of ionic polymer actuators, J Intel Mat Syst Str. 16 (2005) 3-13.

[9] Y. Bar-Cohen, S. Leary, M. Shahinpoor, J. Harrison, J. Smith, Flexible low-mass devices and mechanisms actuated by electroactive polymers. In: EAP actuators and devices, SPIE. 3669 (1999) 51-6.
[10] Y. Bar-Cohen, S. Leary, M. Shahinpoor, J.O. Harrison, J. Smith, Electroactive polymer (EAP) actuators for planetary applications. In: EAP actuators and devices, SPIE 3669 (1999) 57-63.
[11] M. D. Bennett, D. J. Leo, G. L. Wilkes, F. L. Beyer, T. W. Pechar, A model of charge transport and electromechanical transduction in ionic liquid-swollen Nafion membranes, Polymer. 47 (2006) 6782-6796.
[12] M. D. Bennett, D. J. Leo, Ionic liquids as stable solvents for ionic polymer transducers, Sensor Actuat A-Phys. 115 (2004) 79-90.
[13] M. D. Green, T. E. Long, Designing Imidazole-Based Ionic Liquids and Ionic Liquid Monomers for Emerging Technologies, Polymer Reviews. (2009) 49 291-314.
[14] S. K. Mahadeva, J. Kim, Electromechanical Behavior of Room Temperature Ionic Liquid Dispersed Cellulose, J. Phys. Chem. C. 113 (2009) 12523–12529.
[15] J. Kadokawa, M. Murakami, Y. Kaneko, A facile preparation of gel materials from a solution of cellulose in ionic liquid, Carbohydres Res. 343 (2008) 769–772.
[16] W. Kunchornsup, A. Sirivat, Effects of crosslinking ratio and aging time on properties of physical and chemical cellulose gels via 1-butyl-3-methylimidazolium chloride solvent, J Sol-Gel Sci Technol. 56 (2010) 19–26.
[17] S. Niamlang, A. Sirivat, Electromechanical responses of a crosslinked polydimethylsiloxane, Macromol. Symp. 264 (2007) 176-183.
[18] S. Niamlang, A. Sirivat, Dielectrophoresis force and deflection of electroactive poly(p-phenylene vinylene)/polydimethylsiloxane blends, Smart Mater. Struct. 17 (2008), art. no. 035036.
[19] J. Kim, K. Kang, S. Yun, Blocked force measurement of electro-active paper actuator by micro-balance, Sens. Actuators A-Phys. 133 (2007) 401-406.
[20] J. Kim, W. Jung, H. S. Kim, In-plane strain of electro-active paper under electric fields, Sensor Actuat A-Phys. 140 (2007) 225–231.
[21] S. P. Timoshenko, J.M. Gere, Mechanics of Materials, third ed., Chapman & Hall, New York, USA, 1990.
[22] T.S. Smith, R.M. Seugling, Sensor and actuator considerations for precision, small machines, Precis. Eng. 30 (2006) 245-264.
[23] Y. Jung, H. Park, N. Jo, H. Jeong, Fabrication and performance evaluation of diaphragm-type polymer actuators using segmented polyurethane according to chemical-hard-segment content, Sens. Actuators A-Phys. 136 (2007) 367-373.
[24] R.E. Pelrine, R.D. Kornbluh, J.D. Joseph, Electrostriction of polymer dielectrics with compliant electrodes as a means of actuation, Sens. Actuators A-Phys. 64 (1998) 77-85.
[25] I. Diaconu, D.O. Dorohoi, F. Topoliceanu, Electrostriction of a polyurethane elastomer-based polyester, IEEE Sensors J. 6 (2006) 876-880.
[26] M. Watanabe, T. Hirai, Space charge distribution in bending-electrostrictive polyurethane films doped with salts, J. Polym. Sci. Part B 42 (2004) 523-531.
[27] P. Hiamtup, A. Sirivat, A.M. Jamieson, Electromechanical response of a soft and flexible actuator based on polyaniline particles embedded in a cross-linked poly(dimethyl siloxane) network, Mater. Sci. Eng. Part C 28 (2007) 1044-1051.
[28] K. Mukai, K. Asaka, K. Kiyohara, T. Sugino, I. Takeuchi, T. Fukushima, T. Aida,

High performance fully plastic actuator based on ionic-liquid-based bucky gel, Electrochim Acta. 53 (2008) 5555–5562.
[29] N. Terasawa, I. Takeuchi, H. Matsumoto, Electrochemical properties and actuation mechanisms of actuators using carbon nanotube-ionic liquid gel, Sensor Actuat B-Chem. 139 (2009) 624–630.
[30] N. Terasawa, I. Takeuchi, H. Matsumoto, K. Mukai, K. Asaka, High performance polymer actuator based on carbon nanotube-ionic liquid gel: Effect of ionic liquid, Sensor Actuat B-Chem. 156 (2011) 539– 545.
[31] G. Y. Yun , H. S. Kim, J. Kim, K. Kim, C. Yang, Effect of aligned cellulose film to the performance of electro-active paper actuator, Sens. Actuators A-Phys. 141 (2008) 530–535.
[32] W. Liu, L. Cheng, Y. Zhang, H. Wang, M. Yu, The physical properties of aqueous solution of room-temperature ionic liquids based on imidazolium: Database and evaluation, J Mol Liq. 140 (2008) 68–72.
[33] U. Domańska, E. Bogel-Łukasik, Solid-liquid equilibria for systems containing 1-butyl-3-methylimidazolium chloride, Fluid Phase Equilibr. 218 (2004) 123-129.
[34] J. Kim, S. Yun, Z. Ounaies, Discovery of Cellulose as a Smart Material, Macromolecules. 39 (2006) 4202-4206.
[35] J. Kim, J. Ampofo, W. Craft, H. S. Kim, Modeling elastic, viscous and creep characteristics of cellulose Electro-Active Paper, Mech Mater. 40 (2008) 1001–1011.
[36] P. Ludeelerd, S. Niamlang, R. Kunaruksapong, A. Sirivat, Effect of elastomer matrix type on electromechanical response of conductive polypyrrole/elastomer blends, J Phys Chem solids. 71 (2010) 1243–1250.
[37] R. Kunanuruksapong, A. Sirivat, Poly(*p*-phenylene) and acrylic elastomer blends for electroactive application, Mat Sci Eng A-Struct. 454–455 (2007) 453–460.
[38] R. Kunanuruksapong, A. Sirivat, Electrical properties and electromechanical responses of acrylic elastomers and styrene copolymers: effect of temperature, Appl. Phys. A 92 (2008) 313–320.
[39] P. Thipdech, R. Kunanuruksapong, A. Sirivat, Electromechanical responses of poly(3-thiopheneacetic acid)/acrylonitrile-butadiene rubbers, eXPRESS Polymer Letters. 12 (2008) 2 866–877.
[40] C. Kittel, Introduction to Solid State Physics, eighth ed., John Wiley & Sons, Inc., 2005.
[41] G.G. Raju, Dielectrics in Electric Fields, Marcel Dekker, New York, 2003.
[42] A.J. Riad, M.T. Korayem, T.G. Abdul Malik, AC conductivity and dielectric measurements of metal-free phthalocyanine thin films dispersed in polycarbonate, Physica B. 270 (1999) 140.
[43] R. Kunanuruksapong, A. Sirivat, Effect of dielectric constant and electric field strength on dielectrophoresis force of acrylic elastomers and styrene copolymers, Current Applied Physics. 11 (2011) 393-401.
[44] T. Sato, H. Watanabe, and K. Osaki, Rheological and dielectric behavior of a styrene-isoprene-styrene triblock copolymer in n-tetradecane. 1. Rubbery-plastic-viscous transition, Macromolecules. 29 (1996) 6231-6239.
[45] M. Rubinstein, R.H. Colby, Polymer Physics, first ed., Oxford, 2003.
[46] S. K. Mahadeva, C. Yi, and J. Kim, Effect of Room Temperature Ionic Liquids Adsorption on Electromechanical Behavior of Cellulose Electro-Active Paper, Macromol Res. 17 (2009) 116-120.

[47] V.A. Bazhenow, Piezoelectric Properties of Wood, Consultants Bureau, 1961.
[48] Y. Liu, S. Liu, J. Lin, D. Wang, Vaibhav Jain, Reza Montazami, James R. Heflin, Jing Li,Louis Madsen, and Q. M. Zhang, Ion transport and storage of ionic liquids in ionic polymer conductor network composites, Appl Phys Lett. 96 (2010) 223503.
[49] S. Yi, F. Zhang, W. Li , Chi Huang, Haining Zhang, Mu Pan, Anhydrous elevated-temperature polymer electrolyte membranes based on ionic liquids, J Membrane Sci. 366 (2011) 349–355.

List of Tables

Table 1. Induction times and recovery times of Phy gels and the dielectric elastomers (AR70, AR71, NBR1, and SAR) under various temperatures

Sample	Temperature (K)	%strain (%)	Frequency (rad/s)	Electric field strength (kV/mm)	$\tau_{ind,\ 1st}$ (sec)	$\tau_{rec,\ 1st}$ (sec)	$\Delta G'_{ind,\ 1st}$ (Pa)	$\Delta G'_{rec,\ 1st}$ (Pa)	$\tau_{ind,\ sat}$ (sec)
Phy gel	303	0.25	1	1	130	223	349820	-87310	218
Phy gel	333	0.25	1	1	130	130	74280	-19980	42
AR70	300	1	1	1	-	-	-	-	424
AR71	300	0.1	1	1	451	97	2490	-256	120
AR70	300	1	1	2	418	256	28936	-8655	405
AR71	300	0.1	1	2	487	132	4795	-802	395
NBR1	300	0.1	1	1.2	-	-	-	-	1000
SAR	300	1	1	2	756	97	21905	-14013	440

Table 2. Rheological properties of Phy gel and the dielectric elastomers (AR70, AR71, AR72, SAR, and NBR)

Sample	G'_o (Pa)	Electric field strength (kV/mm)	$G'_{1kV/mm}$ or $G'_{2kV/mm}$ (Pa)	$\Delta G'_{1kV/mm}$ or $\Delta G'_{2kV/mm}$ (Pa)	$\Delta G'_{1kV/mm} / G'_o$ or $\Delta G'_{2kV/mm} / G'_o$	Frequency (rad/s)
Phy gel	173000	1	421000	248000	1.43	1
AR71	9959	2	16105	6146	0.617	1
AR70	19666	2	65418	45751	2.3264	1
AR72	12333	2	17025	4693	0.3805	1
SAR	38127	2	94869	56742	1.4882	1
SBR	21557	2	36429	14872	0.6899	1
SIS	50606	2	55668	5062	0.1000	1

Table 3. Electromechanical properties of Phy gel at various electric field strengths

Electric field strength (kV/mm)	θ (°)	mgsinθ (μN)	F_e (μN)	F_d (μN)	τ_i (s)	τ_r (s)	Energy density (J/m^3)	Force density (N/m^3)
0.1	2	12	94	106	1.34	1.51	1.91E+06	2.06E+03
0.2	15	79	780	858	2.41	2.59	1.36E+08	1.62E+04
0.3	30	153	1940	2100	3.35	3.54	4.72E+08	4.00E+04
0.4	40	202	3710	391	5.67	5.84	9.07E+08	7.50E+04
0.5	44	216	4410	4630	7.13	7.43	1.12E+09	9.02E+04

Table 4. Comparison of electromechanical properties of Phy gel and dielectric elastomers (AR70, AR71, AR72, SAR, SIS, SBR, SAR negative polarity, SIS negative polarity)

Sample	Electrical yield strength (kV/mm)	θ (°)	F_d (μN)	Energy density (J/m^3)	Force density (N/m^3)	Mechanical power (μW)	Power density (W/m^3)	$\varepsilon'_{r,\,20\ Hz}$	G′ at 1rad/s, 0.25%strain (Pa)	Temperature (K)	Reference
Phy gel	0.10	43.6	4630	1.12E+09	9.02E+04	1.71	33.13	31.36	4.21E+05	303	-
AR70	0.23	64.7	367	6.21E+04	2.47 E+04	0.067	5.38	6.21	3.25E+04	300	[43]
AR71	0.08	70.4	412	4.90 E+04	2.80 E+04	0.456	31.01	6.33	2.16 E+04	300	
AR72	0.08	57.2	318	1.59 E+04	1.70 E+04	0.179	9.48	4.14	1.06 E+04	300	
SAR	0.25	33.4	275	3.10 E+04	2.05 E+04	0.056	4.16	3.95	6.07 E+04	300	
SIS	0.4	11.0	71	1.43 E+03	3.39 E+03	0.004	0.10	2.74	2.58 E+04	300	
SBR	0.38	8.6	157	7.85 E+02	6.91 E+03	0.005	0.22	2.87	2.34 E+04	300	
SAR negative polarity	0.28	11.7	47	3.80 E+03	3.25 E+03	0.002	0.15	3.95	6.07 E+04	300	
SIS negative polarity	0.38	10.7	118	1.43 E+03	6.61 E+03	0.003	0.17	2.74	2.58 E+04	300	

List of Figure Captions

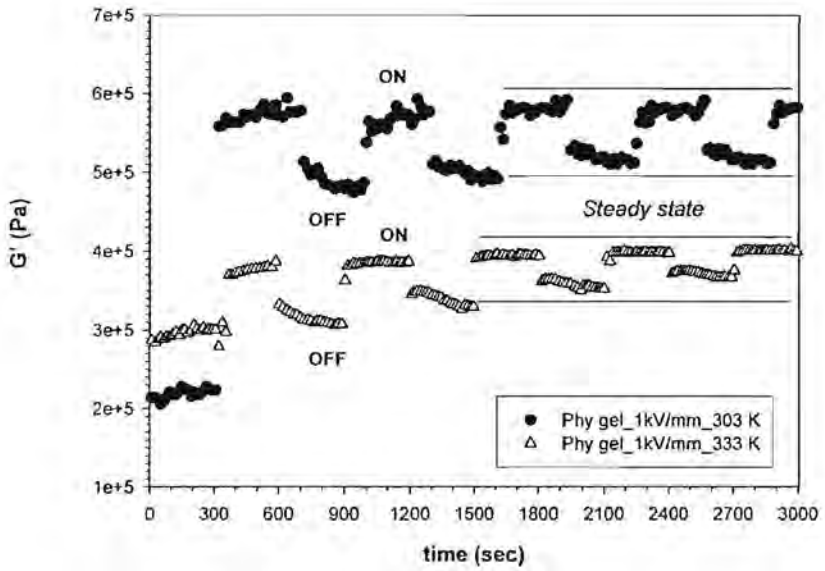

Figure 1. Temporal response of the storage modulus (G′) of the Phy gel under the electric field strength of 1kV/mm at 303 K and 333 K, a strain of 0.25%, and frequency of 1 rad/s.

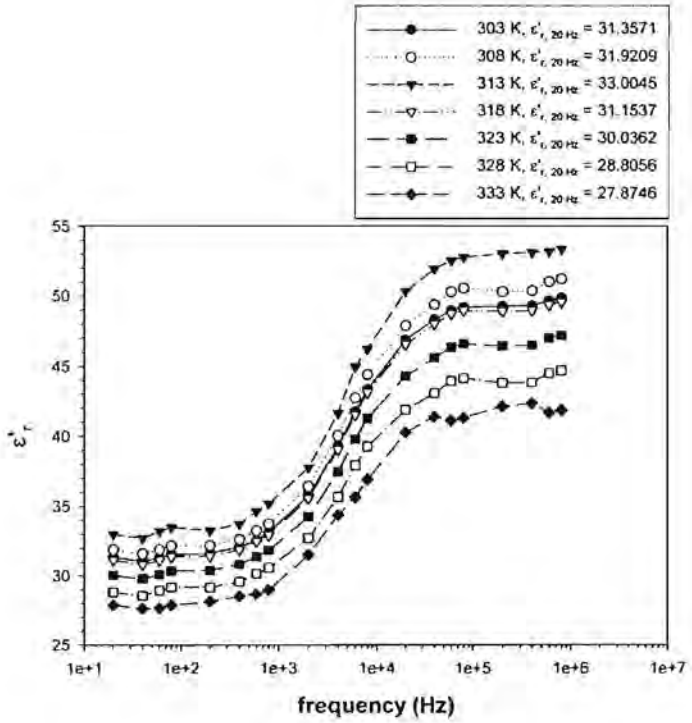

Figure 2. Dielectric permittivity vs. frequency of Phy gels at various temperatures (303 K to 333 K); thickness~1mm, applied voltage = 10V, with silver coating.

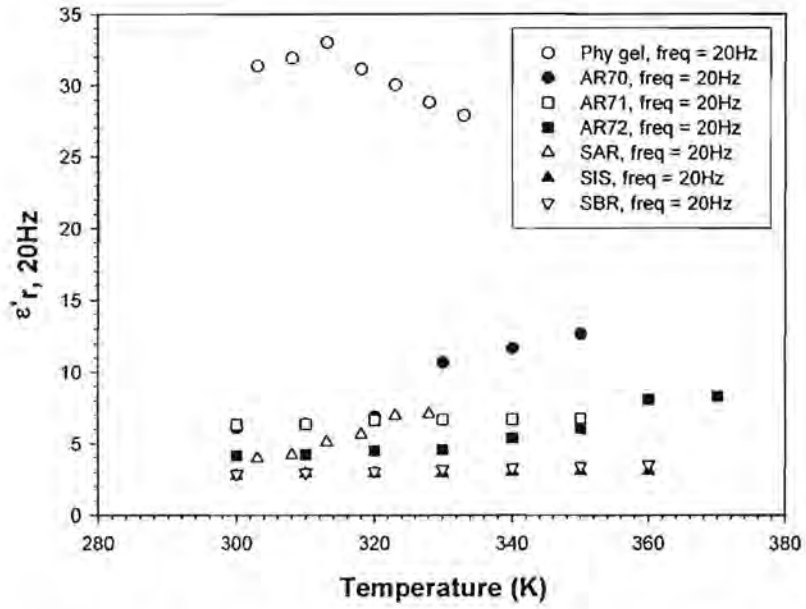

Figure 3. Relative permittivity of Phy gel and dielectric elastomers (AR70, AR71, AR72, SAR, SIS, and SBR) at 20Hz vs. temperature.

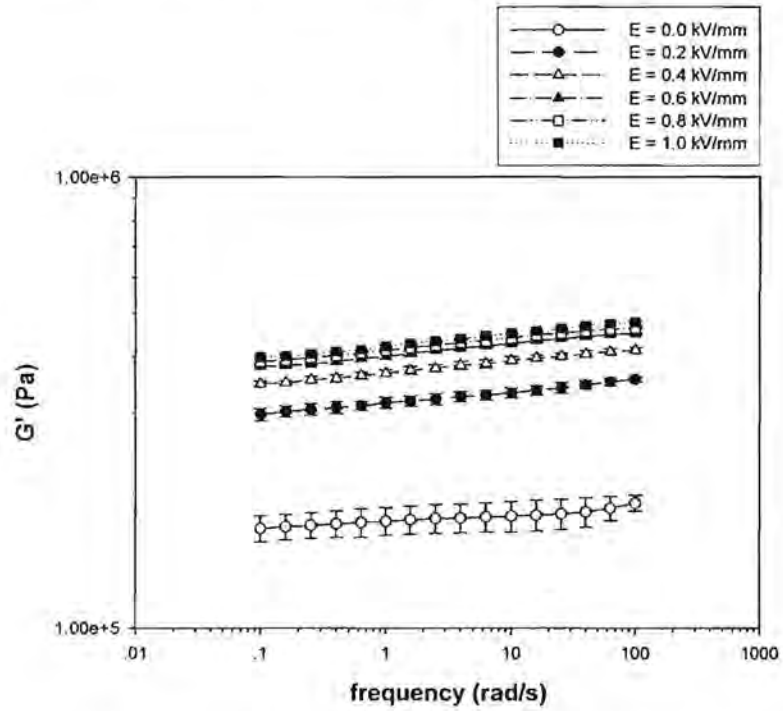

Figure 4. Storage modulus of Phy gels vs. frequency at various electric field strengths: 0.0, 0.2, 0.4, 0.6, 0.8, and 1.0 kV/mm and at 303K.

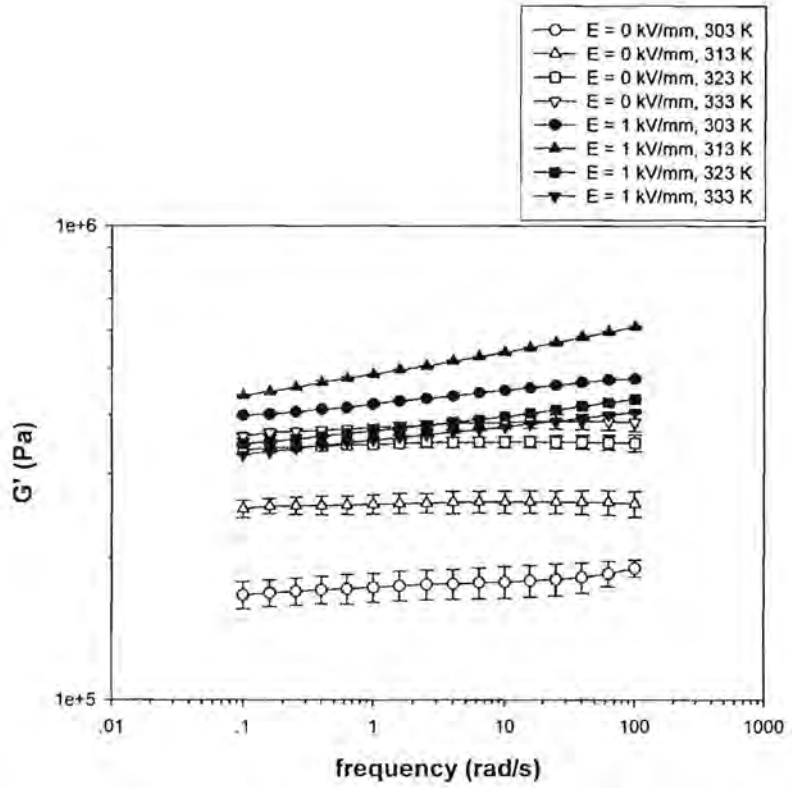

Figure 5. Storage modulus vs. frequency at various temperatures (303, 313, 323, and 333 K) under the electric field strengths of 0 and 1 kV/mm.

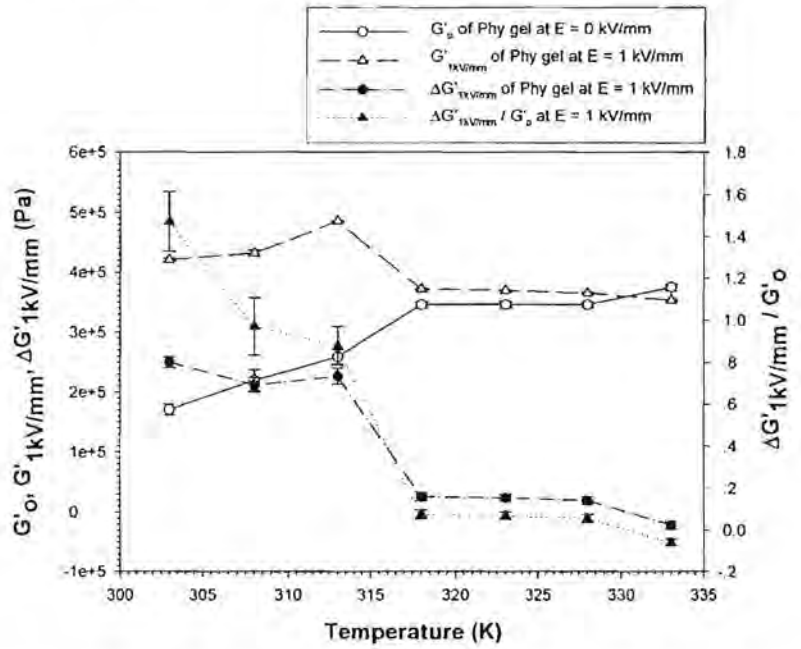

Figure 6. Storage modulus at E=0 kV/mm, storage modulus at E=1kV/mm, storage modulus response at E=1kV/mm, and sensitivity of storage modulus at E=1kV/mm at 1rad/s, and at strain = 0.25% vs. temperature of Phy gels.

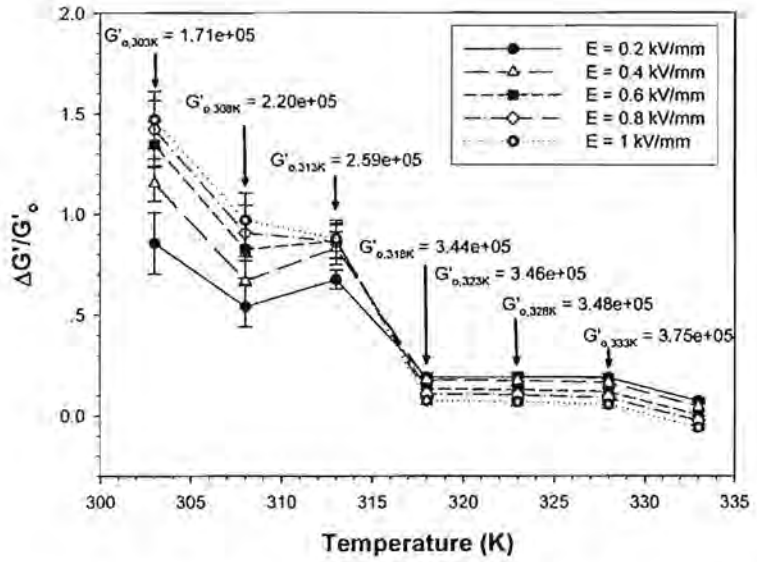

Figure 7. Sensitivity of storage modulus of Phys gels at various electric field strengths (0.2, 0.4, 0.6, 0.8, and 1.0kV/mm) at 1rad/s, and at strain = 0.25% vs. temperature (303, 308, 313, 318, 323, 328, and 333 K).

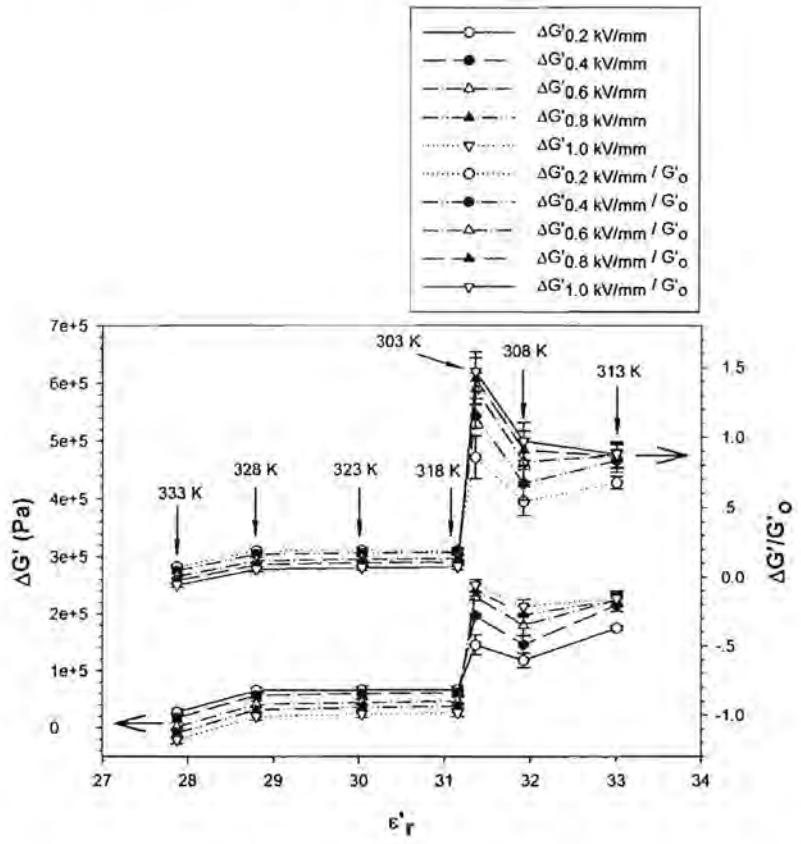

Figure 8. Storage modulus response and sensitivity at various electric field strengths (0.2, 0.4, 0.6, 0.8, and 1.0 kV/mm) vs dielectric permittivity at 20Hz of Phy gels.

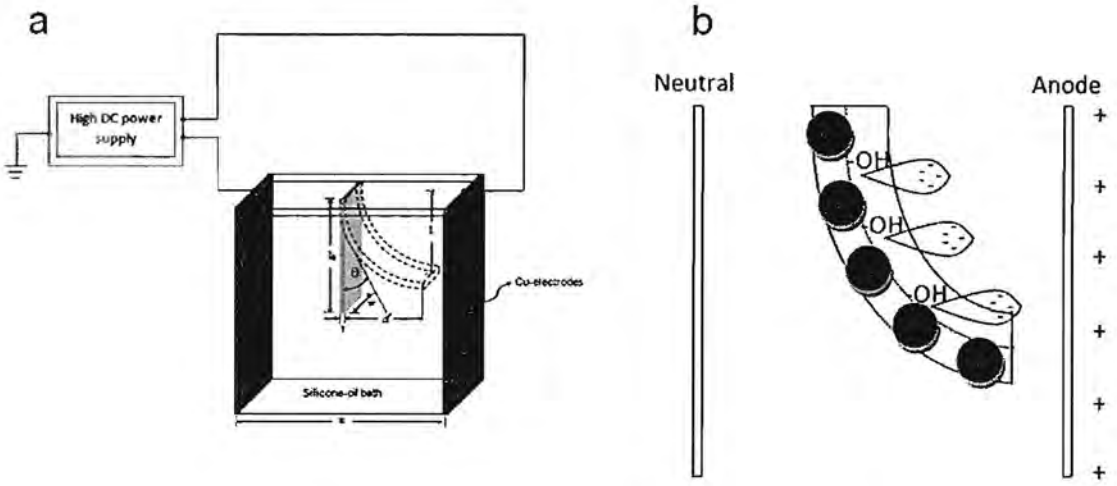

Figure 9. Schematics of: a) bending response measurement of Phy gel suspended vertically in a silicone-oil bath and sandwiched between copper electrodes (68mm of length, 40mm of width, and 2mm of thickness, with a distance of 30 mm between electrodes in a acrylic box). A DC electric field is applied horizontally at 30 ± 0.5 °C causing a deflection distance (a) of the gel from its original position to a new position (dashed line) b) Actuation mechanisms are from two dominating factors, i.e. the ionic polarization of $BMIM^+$ cation and the electronic polarization of cellulosic hydroxyl group.

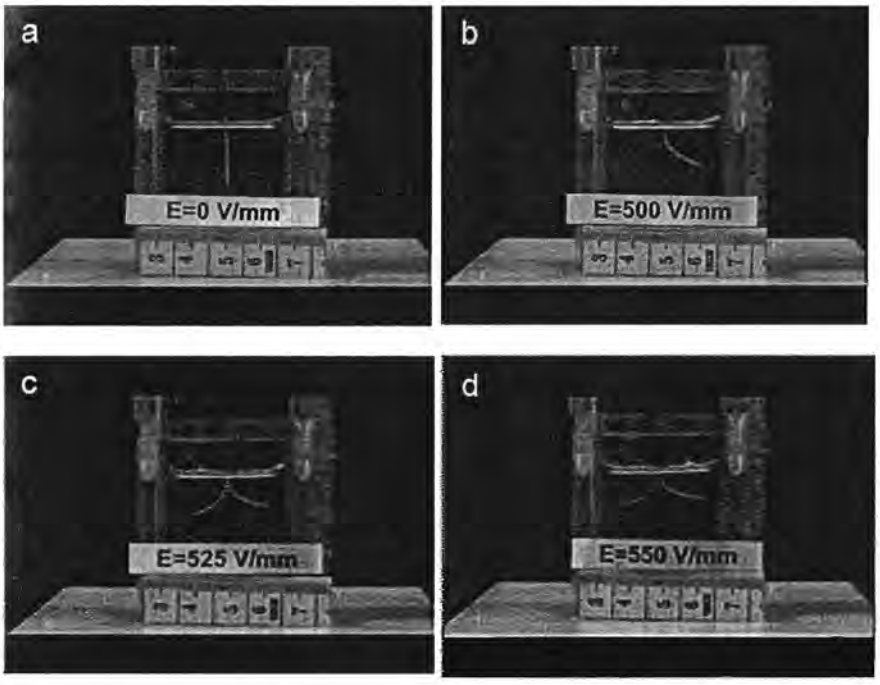

Figure 10. Deflection and back-forth swing images at 303 K under various applied voltages of the Phy gel: (a) E=0V/mm; (b) E=500V/mm; (c) E=525V/mm; and (d) E=550V/mm. Note: The polarity of the electrode on the left and right hand sides are always GND and positive, respectively. Size of the Phy gel sample:16.5 mm of length,1 mm of thickness, 3 mm of width, and 0.0309 g of weight.

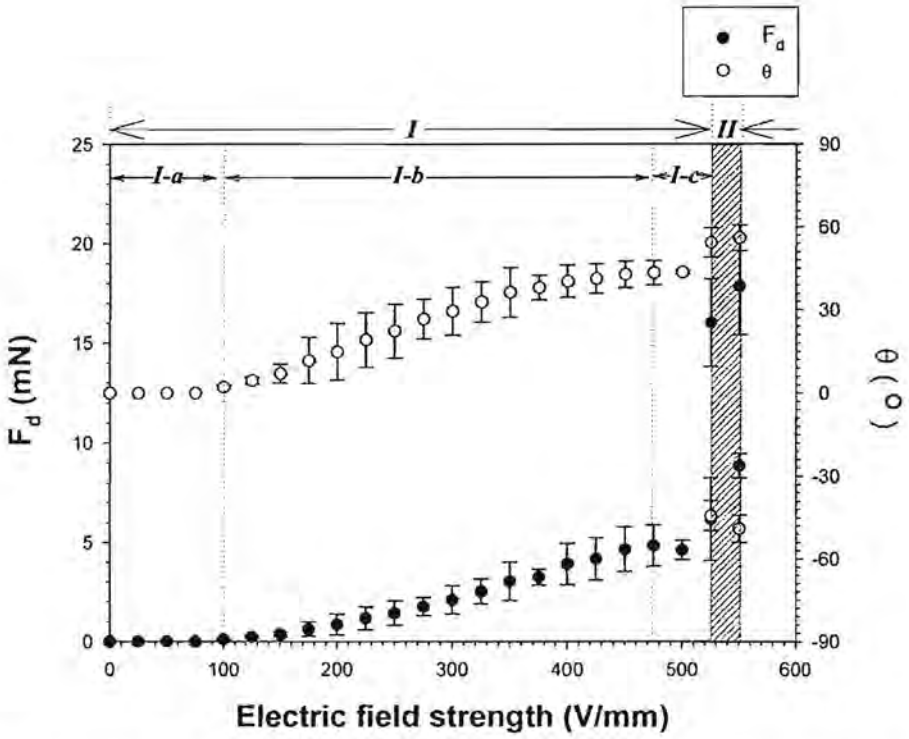

Figure 11. Dielectrophoresis force (F_d) and Bending angle (θ) vs. electric field strength (V/mm) at 303K; *I* and *I I* are the regions of the beam deflection and swing under direct current, respectively. Size of the Phy gel sample: 16.5 mm of length, 1 mm of thickness, 3 mm of width, and 0.0309 g of weight.

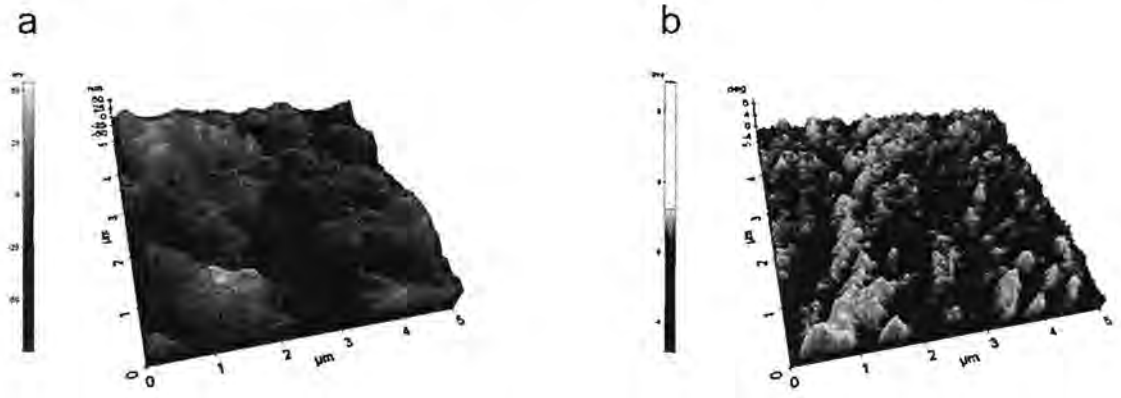

Figure 12. a)Topology image; b) EFM image under 5V of voltage bias of Phy gel at 303 K.

ส่วนที่ 3

Bio-Compatible Gelatins (Ala-Gly-Pro-Arg-Gly-Glu-4Hyp-Gly-Pro-) and Electromechanical Properties: Effects of Temperature and Electric Field

Thawatchai Tungkavet [1], Datchanee Pattavarakorn [2], and Anuvat Sirivat [1,*]

[1]The Petroleum and Petrochemical College, Chulalongkorn University, Bangkok 10330, Thailand.
[2]Department of Industrial Chemistry, Faculty of Science, Chiang Mai University, Chiangmai 50200, Thailand.

*Conductive and Electroactive Polymers Research Unit
The Petroleum and Petrochemical College
Chulalongkorn University
Soi Chula 12, Phyathai Rd.,
Bangkok 10330, Thailand
Tel: 662 218 4131, Fax: 662 611 7221
Email: anuvat.s@chula.ac.th
www.cepru.research.ac.th

Abstract

Gelatin (Ala-Gly-Pro-Arg-Gly-Glu-4Hyp-Gly-Pro-) is a protein produced by the partial hydrolysis of a collagen extracted from bones, connective tissues, organs, and some intestines of animals. In this work, gelatin films were prepared by the film casting method in an aqueous solvent. The electromechanical properties, thermal properties, and the degree of swelling were investigated as a function of gelatin crosslinking ratio or the gel strength, temperature, frequency, and electric field strength. The high, medium, low, and the 3 % crosslinked high-gel-strength gelatin films possess the storage modulus sensitivity values of 2.30, 2.16, 1.26, and 0.49, respectively; these values are much greater than those of other electroactive materials, suggesting the gelatins studied as a potential artificial muscle or actuator.

Keywords: Gelatin; gel strength; electromechanical properties; actuator; artificial muscle

1. Introduction

The exchange of electrical energy and mechanical energy has been of scientific and technological interest for many decades. Electromechanical energy conversion has been used in many applications, such as in muscle/insect-like actuators, robotics, etc. [1]. The development of electroactive materials for artificial muscle or actuators is sought after because of their many advantages. First, electroactive materials resemble natural living tissues more than any other classes of synthetic biomaterials because of their high water content, the soft consistency, and their high activation modes. Second, they are biocompatible, but not biodegradable. Third, their physical and chemical

properties vary with composition and can be tailored as desired. Fourth, they can take various shapes and are low-cost material.

Gelatin is a protein biopolymer derived from the partial hydrolysis of native collagens, which are the most abundant structural proteins found in the animal body: skin, tendons, cartilage, and bone [2]. Gelatin contains a large number of glycine (almost 1 in 3 residues, arranged every third residue), proline and 4-hydroxyproline residues. A typical structure is: Ala-Gly-Pro-Arg-Gly-Glu-4Hyp-Gly-Pro; it is unique in that it contains 14% hydroxyproline, 16 % proline and 26 % glycine. The only other animal product containing hydroxyproline is the elastin and then at a very much lower concentration, so hydroxyproline is used to determine the collagen or gelatin content of foods. It is a good film and particle forming material [3]. Due to a wealth of merits, such as biological origin, non-immunogenicity, biodegradability, biocompatibility, and commercial availability at relatively low cost, gelatin has been widely used in the pharmaceutical and medical fields as sealants for vascular prostheses, as carriers for drug delivery, as wound dressings, and as artificial muscle [4]. Nevertheless, gelatin exhibits poor mechanical properties, which limits its possible application as a biomaterial. The improvement of the mechanical properties of drawn gelatin has been related to the renaturation level of the protein, as evaluated through the differential scanning calorimetry [5]. The most interesting feature of gelatin is that it can be used for the production of practical biocompatible materials [6,7]. Several physical and chemical methods have been reported for crosslinking collagenous materials. Physical methods include the dehydrothermal treatment and the UV irradiation [8,9]; however, they are generally less efficient. Many chemicals–such as formaldehyde, glutaraldehyde, carbodiimide, and dextran dialdehyde– have been used to chemically modify the gelatin towards biomedical applications. Among them, glutaraldehyde (GTA) is by far the most widely used, due to its high efficiency in stabilizing the collagenous materials [10]. GTA–based crosslinking of collagenous materials significantly reduces biodegradation, making the materials biocompatible and nonthrombogenic, while preserving biological integrity, strength, and flexibility. GTA is also easily available, inexpensive, and capable of allowing the crosslinking in a relatively short time period.

In our work, we are interested in the development of gelatin as a candidate of an artificial muscle or actuator. The electromechanical properties, the thermal properties, and the degree of swelling were investigated and are reported here as functions of the gelatin strength, the crosslinking ratio, temperature, frequency, and electric field strength.

2. Experimental

2.1 Materials

Gelatin powder (high, medium, and low gel strengths; 250g bloom, 180g bloom, and 80g bloom, respectively) (AR grade, Fluka). The Bloom value is proportional to the storage modulus of the gelatin and it decreases with decreasing *Mn* [11]., and glutaraldehyde (50 % GTA solution) (AR grade, Sigma-Aldrich) were used as the starting materials for fabricating gelatin films. Table 1 shows data on characterization of our samples.

2.2 Preparation of gelatin films

Glutaraldehyde–gelatin crosslinked films (GTA–Ge) were prepared by adding an appropriate volume of GTA solution into a 10 vol% gelatin solution with GTA concentrations varying from 0.5 to 7 vol%. Non-crosslinked gelatin films (Ge) were prepared from an aqueous gelatin solution (10 %, v/v) at 50 °C and under a continuous stirring for 40 min. The GTA-Ge and Ge solutions were poured into plastic petri dishes (10 cm in diameter). Crosslinked films were obtained after allowing water evaporating at a room temperature for a period of four days. Figure 1 shows a schematic of the two proposed structures for gelatin – GA complexes and Pristine gelatin films (Ge) were prepared in a similar way, but without adding the crosslinking agent.

2.3 Characterization and testing of gelatin samples

2.3.1 Crosslinking density determination

In order to estimate the network crosslinking density, the number-average molecular weight of the chain segments between two crosslinking points, M_c, was calculated from equilibrium water uptake experiments performed at 20 °C, according to the Flory–Rehner equation [12]:

$$M_c = \frac{\rho V_1\left(\phi_g^{1/3} - 2\phi_g/f\right)}{\chi\phi_g^{\,2} + \ln\left(1-\phi_g\right) + \phi_g} \quad , \tag{1}$$

where ρ is the density of the dry gelatin determined by picnometry, V_1 is the molar volume of the solvent, χ is the polymer–solvent interaction parameter taken from the literature [12] ($\chi = 0.49 \pm 0.05$), and φ_g is the volume fraction of the swollen gelatin, which is estimated from the following relation:

$$\phi_g = \frac{W_0\rho_w}{W\rho_g - W_0\left(\rho - \rho_w\right)} \quad , \tag{2}$$

where W_0 is the initial weight of the sample, W is the weight of the swollen sample, ρ_w is the density of the water at room temperature, and ρ is the density of the dry and the uncrosslinked gelatin film.

2.3.2 Thermogravimetric analysis (TGA)

A thermal gravimetric analyzer (DuPont, model TGA 2950) was used to determine the amount of moisture content and the decomposition temperatures with a temperature scan from 30 to 600 °C with a heating rate of 5 °C/min, for the crosslinked films with % volumes of glutaraldehyde of 0.5,1, 3, 5, and 7, and the non-crosslinked gelatin films. The samples weighed from 5 to 10 mg were loaded into platinum pans and then heated under a nitrogen gas flow.

2.3.3 DSC analysis of gelatin films

The thermal properties of the pure gelatin at various gel strength were studied by DSC, (Instruments DSC METTLER 822), using 5 mg of various gel strength gelatin.

All measurements were performed under nitrogen atmosphere at a heating rate of 5 °C/min.

2.3.2 Electromechanical and thermal properties

The electrorheological properties of the crosslinked and uncrosslinked gelatins were investigated in terms of frequency, temperature, and electric field strength. A melt rheometer (Rheometric Scientific, ARES) was fitted with a parallel-plate fixture (diameter of 25 mm). A DC voltage was applied with a DC power supply (Instek, GFG8216A), which could deliver electric field strengths up to 1 kV/mm. A digital multimeter was used to monitor the voltage input. In these experiments, an oscillatory shear strain was applied and the dynamic moduli (G' and G") were measured as functions of frequency and electric field strength. Strain sweep tests were first carried out to determine the suitable strains to measure G' and G" in the linear viscoelastic regime. The appropriate strain was determined to be 0.2 % for the gelatin film samples. For the 3 % crosslinked high gel strength gelatin film sample, a strain of 0.14 % was used. Frequency sweep tests were carried out to measure the G' and G" of each sample as a function of frequency. The deformation frequency was varied from 0.1 to 100 rad/s. Prior to each measurement, the non-crosslinked gelatin and the 3 % high-gel-strength gelatin film samples were presheared at a low frequency (0.04 rad/s) under an electric field for 15 min to ensure the formation of equilibrium polarization before the G' and G" measurements. The experiments were carried out at a temperature of 27 °C and repeated at least two or three times. The effect of temperature was studied at various temperatures between 27 and 107 °C for the non-crosslinked gelatin film sample. The temporal response experiments were carried out at 1 kV/mm for the non-crosslinked gelatin and the 3 % crosslinking high-gel-strength gelatin film samples. Deflection of Gelatin films was carried out under various applied electric strengths. For each film, one end of the sample was fixed with a grip vertically in a transparent chamber containing two parallel electrodes. The input DC field was provided by a DC power supply (Gold Sun 3000, GPS 3003D) and a high voltage power supply (Gamma High Voltage, UC5-30P), which delivered various electric field strengths, from 25 to 600 V/mm. A digital video recorder (Sony handicam, HR1) was used to record the displacement of the films. The tip displacement was measured and calculated from a Scion Image (Beta 4.0.3) program.

We can calculate the static force balance, the deflecting force or the dielectrophoretic force (F_d) on the samples equals to the sum of the resisting elastic force (F_e) and the weight along the bending direction, where the film deflection distance at equilibrium is d. The dielectrophoretic force (N) is determined from the staic force balance equation as:

$$F_d = F_e + mg\sin\theta \quad , \qquad (3)$$

where m is the sample's mass (kg), g is the gravity (9.8 m/s^2), θ is the deflection angle, and F_e is the resisting elastic force (N). In our experiment, the film deflections with increasing electric field are linear. The linear deflection theory of one free-end film is, therefore, used where the elastic force can be calculated by the following equation [30, 31]:

$$F_e = \frac{dEI}{l^3} \quad , \qquad (4)$$

where E is the elastic modulus which is equal to $2G'(1+\nu)$ in which G' is the shear modulus and ν is the Poisson's ratio, which is equal to 1/2 for an incompressible material, I is the moment of inertia, equal to $t^3w/12$, where t is the sample thickness, w is the sample width, d is the deflection distance, and l is the sample length.

3. Results and Discussion

3.1 Determination of degree of swelling, weight loss of gelatin film, and molecular weight between crosslinks and Spectra of Gelatin

Crosslinked and un-crosslinked gelatin films were prepared under the same conditions, and they were kept in a desiccator at room temperature (27 °C) for a period of 2 days before testing to minimize any property changes during the experiments. Glutaraldehyde (GTA) is a fast-acting crosslinker for collageneous materials. The reaction of gelatin with different amounts of GTA was carried out at 50 °C in basic conditions [13]. All crosslinked films were stiffer than pure gelatin films, and they changed thier color to yellowish. Figure. 2 shows a pure gelatin film and a 3% crosslinked gelatin films. The 3% crosslinked film becomes more yellowish and slightly shrin. The color change is due to the formation of the aldimine linkages (CH=N) between the free amine groups of the protein and glutaraldehyde [14].

The FTIR spectra of the uncrosslink gelatins show peaks at 1630 cm^{-1}due to the C=O streching , 1550 cm^{-1} due to the N-H bending, and 2922 cm^{-1} due to the C-H stretching. In the spectrum of the 3%v/v crosslinked gelatin film, an additional peak appears at 1641 cm^{-1}. This peak is a characteristic of the aldimine stretching vibration which reveals the crosslinking of gelatin with glutaraldehyde [14]. For the uncrosslinked high gel strength gelatin, the uncrosslinked medium gel strength gelatin, and the uncrosslinked low gel strength gelatin, they are of the same of molecular structure

The GTA crosslinking induces a significant reduction in swelling. Swelling measurements at longer times were hindered by the solubility of the film, which began to dissolve in the solution. The calculated average molecular weight between two crosslinking points, *M*c, as a function of GTA concentration decreases drastically with GTA content, due to the formation of a denser network. Percentages of the crosslinking agent higher than 3 v/v.% (Molecular weight between crosslinked = 1920 ± 296 g/mol) did not induce further changes as no further reaction occurred.. Similar results were reported by Fraga and Williams [15], as caused by the termination of the reaction due to the vitrification in thermosetting systems. In addition, gelatin films with a percentage of crosslinking agent higher than 3 wt% do not possess any noticeable differences in the degree of swelling and the percentage of weight loss.

The thermal properties were obtained from the thermogravimetric analysis and the differential thermal analysis (TGA-DTA). The TGA data provide the thermal stability in the terms of onset degradation temperature and % weight residue of the gelatin samples of different Bloom indices and at various percentages of crosslinking ratios between 0%v/v (non-crosslinked gelatin) to 7%v/v (Crosslined gelatin). There are two transitions for the gelatin, namely: the first transition (45 to 100 °C), can be refered to the loss of water; and the second transition (240 to 360 °C), can be refered to the degradation of the gelatin backbone. The TGA thermograms of the non-crosslinked gelatin and the crosslinked gelatin show that the decomposition temperatures are not significantly different; the 7 %v/v GTA-Ge has highest percentage of weight residue.

DSC, a widely used thermoanalytical technique, was assess some of the physicochemical properties, such as endothermic or exothermic processes, characteristic of the Gelatin films at various gel strength. It shows typical thermograms recorded from the uncrosslinked gelatin films (High gel strength, Medium gel strength, Low gel strength, and 3%v/v Crosslinked high gel strength gelatin) which exhibit endothermic peak which can be refered to the melting temperatures [16]. For 3%v/v Crosslinking high gel strength gelatin, the melting temperature is higher than those of the uncrosslinked gelatin films so crosslinking can increases the thermal stability of gelatin films, as shown by the shift of the melting temperature to higher values [16]. The melting temperatures (T_m) of the main endothermic transition of uncrosslinked high gel strength gelatin, uncrosslinked medium gel strength gelatin, uncrosslinked low gel strength gelatin, and 3%v/v crosslinked high gel strength gelatin films were at 85.33, 81.41, 79.08, and 87.58C respectively.

3.2 Time dependence of the electrorheological response

We first show the temporal responses of the high, medium, low, and 3 % crosslinked high-gel-strength gelatin films by alternately switching on and off an electric field strength of E = 1000 V/mm. The temporal characteristics of each sample were recorded in the linear viscoelastic regime at a strain of 0.14 % at frequency of 100 rad/s. Figure. 3 shows the comparison in storage modulus, G′ of the high and 3% crosslinked high-gel-strength gelatin films, during the time sweep test. When the electric field is switched on, the G′ values of the high, medium, low, and 3 % crosslinked high-gel-strength gelatin films increase from 2 120 000 Pa to 4 570 000 Pa (1.15) in 2200 s, 835 000 Pa to 1 485 000 (0.79) in 5000 s, 1 260 000 Pa to 2 080 000 (0.65) in 2500 s, and 8 060 000 Pa to 10 900 000 Pa (0.35) in 2000 s, respectively. However, the G′ values of the gelatin films do not recover their original values when the electric field is switched off, possibly due to the interaction between the residue dipole moments remaining in the gelatin films [17].

3.3 Effect of electric field strength

The effect of electric field strength on the rheological properties of the high, medium, low and the 3 % crosslinked high-gel-strength gelatin films was investigated in a range of 0 to 1 kV/mm. Figure 4 shows the storage modulus response (ΔG′) of the high, medium, low and the 3 % crosslinked high gel strength gelatin films vs. electric field strength at a frequency of 100 rad/s, a strain of 0.14 %, and a temperature of 27 °C. The increases in ΔG′ with electric field strength are nonlinear within the range of 0.1 to 1 kV/mm. The storage modulus response values of these samples at an electric field strength of 1 kV/mm are 4 340 000, 2 820 000, 292 000, and 3 580 000 Pa for the high, medium, low, and the 3 % crosslinked high-gel-strength gelatin films, respectively. (The storage modulus sensitivity values of these samples at an electric field strength of 1 kV/mm are tabulated in Table 2; they are 2.30, 2.16, 1.26, and 0.49 for the high, medium, low, and 3 % crosslinked high-gel-strength gelatin films, respectively.)

When an electrical field is applied, induced dipole moments within the gelatin structure are generated, leading to intermolecular interactions. These intermolecular interactions induce the loss of free chain movements and thus a higher chain rigidity, as indicated by the higher G′ values [18,19]. The electric field is clearly shown here to enhance the rigidity of the gelatin films.. However, the storage modulus of the 3 % crosslinked gelatin improves to a lesser degree than those of the uncrosslinked gelatin

samples, due to its initially high rigidity in the absence of applied electric field. A higher electric field strength is expected to induce a higher dipole moment and to cause chain segment to pull themselves together in a tighter formation due to the greater electrostatic force, as evidenced by the dramatic increases in G′ with electric field strength [20]. Table 3 shows the storage modulus sensitivity characteristics of several electroactive polymers and dielectric elastomers. A sensitivity comparison of these materials can be made between Tables 2 and 3. At an identical electric field strength (1kV/mm), the styrene-isoprene-styrene triblock (D1114P) exhibits the highest sensitivity in its types, in which the storage modulus sensitivity is 0.122. However, when particles were added to the styrene-isoprene-styrene triblock and the silicone elastomer, the storage modulus sensitivities increased to 0.256 and 0.250, respectively. In our work, the gelatins possess superior responses, as shown in Table 2: the sensitivity values are 2.30, 2.16, 1.26, and 0.49 for the high, medium, low, and 3 % crosslinked high-gel-strength gelatin films, respectively. These sensitivity values are greater by nearly an order of magnitude than those of pure polymer matrices, triblock copolymers, or elastomers [21,22], operated at even higher electric field strengths or even with the additions of particles.

3.4 Effect of the operating temperature

The rheological properties under an electric field of the uncrosslinked and the crosslinked gelatin films were investigated at operating temperatures of 300 to 380 K. In order to exclude the effect of the gelatin samples, G'_o, $G'_{1Kv/mm}$ and $\Delta G' / G'$ are plotted versus temperature as shown in Figure 5. Here we used one sample each for the G'_o and $G'_{1Kv/mm}$ measurements. We can see that the storage moduli decrease linearly with increasing temperature; the deviations may originate from less of chain entanglements in certain temperature ranges. $G'_{1Kv/mm}$ is higher than that without electric field at any temperature investigated, as a result of the dipole–dipole interactions created by the electric field within the matrix. The storage modulus sensitivity of the gelatin sample increases significantly as temprature increases; this implies that temperature induce the free chain movement easier without electric field [30].

3.5 Deflection of gelatin films

The deflection of the gelatin films was studied by vertically suspending the films in a silicon oil bath; and a DC electric field was applied horizontally between two parallel flat copper electrodes, as shown in Figure 6. The amount of deflection at a specified electric field strength is defined by the geometrical parameters —d, l, and θ— which are illustrated in Figure 6. The tip displacement of the film was recorded by a digital video recorder (Sony Handicam, HR1). Figure 6 shows the bendings of the high-gel-strength and the low-gel-strength gelatin films immersed in silicone oil under an electric field strength of 600 V/mm. Upon applying an electric field, the free lower end of the film deflects towards the cathode side by an amount dependent on the field strength, indicating an attractive interaction between the cathode and the polarlized amine group, in which the gelatin structure possesses negative charges. (The deflection distance of the gelatin films under electric field is shown in Figure 7.) The low-gel-strength gelatin film shows a greater deflection value than the high-gel-strength gelatin. The films start to deflect at their critical electric field strengths (600 V/mm). Moreover, the high-gel-strength gelatin film has a lesser deflection response under the applied

electric field than the low-gel-strength film due to its initially higher rigidity, or its higher G′ value.

Figure 8 shows the dielectrophoretic force of the gelatin films under electric field. The dielectrophoretic forces of the low-gel-strength gelatin and the high-gel-strength gelatin films appear to increase monotonically with increasing electric field strength. (Table 4 shows the deflection responses achieved under an applied electric field on the gelatin films in terms of the deflection distance (d), the deflection angle (θ), the resisting elastic force (F_e), and the dielectrophoretic force (F_d). The resisting elastic force of the low-gel-strength gelatin film under an applied electric field is less than that of the high-gel-strength gelatin film. However, the low-gel-strength gelatin film exhibits a greater response in the bending mode than the others, suggesting its greater flexibility. In previous work, Thongsek *et al.*, [23] reported the dielectrophoresis force of Styrene-Isoprene-Styrene Triblock Copolymer (SIS D1114P), the maximum deflection distance and dielectrophoresis force at E = 600 V/mm is 2.86 mm and 36.4 μN, respectively. Alici *et al.*, [33] reported that the actuators based on polymer composites between polypyrrole and polyvinylidine fluorine could provide the output force equal to 0.6 mN at E = 1 V [26]. Dai *et al.*, [34] studied the bending force under applied electric field of ionic network membrane based on blends of water soluble poly (vinyl alcohol) (PVA) and highly ionic conductive poly 2-acrylamido-2-methyl-1-propanesulfonic acid (PAMPS). The bending force of PVA/PAMPS blend was equal to 4.9 mN at E = 40 V/mm [34]. Kunanuruksapong et al., [35] studied electromechanical response of acrylic elastromer (AR70). The maximum deflection distance and dielectrophoresis force at electrical strength (225 V/mm) is 12.41 mm and 0.367 mN, respectively. When comparing with our Gelatin films (low-gel-strength), the maximum deflection distance and dielectrophoresis force at E = 600 V/mm is 1.28 mm and 4.859 μN, respectively. Our materials give a lower dielectrophoresis force less than those of the polymer composites, the ionic network membrane, and the elastromers. However, the storage modulus sensitivity values of the gelatin are superior to those of the previous work.

4. Conclusions

In our work, the electromechanical properties of gelatin films were investigated as functions of electric field strength and operating temperature in terms the storage moduli under oscillatory shear mode. The storage modulus (G′) increases with increasing gel strength, as the applied electric field strength is equal to 1 kV/mm. ΔG′ and ΔG′/Go values of the gelatins increase with increasing temperature. At a temperature above 300 K, the storage moduli decrease linearly with increasing temperature. For the un-crosslinked gelatin films, the storage modulus response and the storage modulus sensitivity are higher than those of the crosslinked gelatin films. The storage modulus sensitivity of gelatin values are greater by nearly an order of magnitude than those of previously studied pure polymer matrices, triblock copolymers, or elastomers which were operated at even higher electric field strengths or even with the additions of particles. From the deflection measurement, the deflection distances of the low-gel-strength and the high-gel-strength gelatin films increase monotonically with increasing electric field strength. The low-gel-strength gelatin film shows the greatest deflection response.

5. Acknowledgements

The authors would like to acknowledge the financial support to A.S. from the Conductive and Electroactive Polymers Research Unit of Chulalongkorn University, the Center of Petroleum Petrochemical and Advanced Materials, the Thailand Research Fund (TRF-BRG), Nanotec and, the Thai Royal Government.

6. References

[1] S. Krause, K. Bohon. (2001) Electromechanical Response of Electrorheological Fluids and Poly(dimethylsiloxane) Networks. Macromolecules 34: 7179

[2] Y.Z. Zhang, J. Venugopal, Z.-M. Huang, C.T. Lim, S. Ramakrishna. (2006) Crosslinking of the electrospun gelatin nanofibers. Polymer 47: 2911-2917

[3] XJ. Yang, P.J. Zheng, Z.D. Cui, N.Q. Zhao, Y.F.Wang, K.D. Yao. (1997) Swelling behaviour and elastic properties of gelatin gels. Polym. Int 44: 448–452

[4] Y. Marois, N. Chakfe, X. Deng, M. Marois, T. How, M. King . (1995) Carbodiimide cross-linked gelatin, a new coating for polyester arterial prostheses. Biomaterials 16: 1131–1139

[5] A. Bigi, G. Cojazzi, S. Panzavolta, K. Rubini, N. Roveri. (2001) Mechanical and thermal properties of gelatin films at different degrees of glutaraldehyde crosslinking Biomaterial 22: 763-768

[6] E. Bottoms, C.W. Cater, S. Shuster. (1966) Effect of ultraviolet irradiation on skin collagen. Nature 211: 97–8

[7] J.P. Draye, B. Delaey, A. Van de Voorde, A. Van Den Bulcke, B. De Reu, E. Schacht. (1998) In vitro and in vivo biocompatibility of dextran dialdehyde cross-linked gelatin hydrogel films. Biomaterials 19: 1677–1687

[8] E. Schach, A.Van Den Bulcke, B. Bogdanov, J.P. Draye, B. Delaey. (1998) Gelatin-based hydrogel for wound dressing. Polym. Mater. Sci. Eng 79: 222–223

[9] E. Fujimori. (1965) Ultraviolet light-induced change in collagen macromolecules. Biopolymers 3: 115–9

[10] E. Khor. (1997) Methods for the Treatment of Collagenous Tissues for Bioprostheses. Biomaterials 18: 95–105

[11] C. Abrusci, A. Martin-Gonzalez, A.D. Amo, T. Corrales, F. Catalina. (2004) Biodegradation of type-B gelatin by bacteria isolated from cinematrographic films. A viscometric study. Polym Degrad Stabil 86: 283-291

[12] P.J. Flory, J.J. Rehner. (1943) Statistical Mechanics of Cross-Linked Polymer Networks II. Swelling. Chem. Phys 11: 521–526

[13] A.A. Apostolov, D. Boneva, E. Vassileva, J.E. Mark, S. Fakirov. (2000) Mechanical properties of native and crosslinked gelatins in a bending deformation. J. Appl. Polym. Sci 76: 2041–2048

[14] J.F. Martucci, R.A. Ruseckaite, A. Vazquez. (2006) Creep of glutaraldehyde-crosslinked gelatin films. Mat. Sci. Eng. A 435-436: 681-686

[15] A.N. Fraga, R.J.J. Williams. (1985) Thermal properties of gelatin films. Polymer 26: 113–118

[16] M. Li, Y.Guo, Y. Wei, A.G. Macdiamid, P.I. Lelkes. (2005) Electrospinning polyaniline-contained gelatin nanofibers for tissue engineering applications. Biomaterials 27: 2705-2715

[17] D. Chotpattananont, A. Sirivat, A.M. Jamieson. (2004) Electrorheological properties of perchloric acid-doped polythiophene suspensions. Colloid Polym. Sci 282: 357–365

[18] R.E. Perline, R.D. Kornbluh, J.P. Joseph. (1998) Electrostriction of polymer dielectrics with compliant electrodes as a means of actuation. Sensor Actuat.Phys. A 64: 77–85

[19] B. Liu, T.M. Shaw. (2001) Electrorheology of filled silicone elastomers. J. Rheol 45: 641–657

[20] T. Shiga. (1997) Deformation and Viscoelastic Behavior of Polymer gels in Electric fields. Advances in Polymer Science, vol. 134/20, Springer-Verlag, Berlin

[201] R. Pelrin, R. Kornbluh, J. Joseph, R. Heydt, Q. Pei, S. Chiba. (2000) High-field deformation of elastomeric dielectrics for actuators. Mat. Sci. Eng. C 11: 89-100

[22] R. Kunanuruksapong, A. Sirivat. (2007) Poly(*p*-phenylene) and acrylic elastomer blendsfor electroactive application. Mat. Sci. Eng. A 454-455: 453-460

[23] K. Thongsak, R. Kunanuruksapong, A. Sirivat, W. Lerdwijitjarud. (2010) Electroactive Styrene-Isoprene-Styrene Triblock Copolymer: Effects of Morphology and Electric Field. Mat. Sci. Eng. A 527: 2504-2509

[24] N. Tangboriboon, A. Sirivat, R. Kunanuruksapong, S. Wongkasemjit. (2009) Electrorheological properties of novel piezoelectric lead zirconate titanate Pb(Zr0.5,Ti0.5)O3-acrylic rubber composites. Mat. Sci. Eng. C 29: 1913-1918

[25] P. Hiamtup, A. Sirivat, A.M. Jamieson. (2008) Electromechanical response of a soft and flexible actuator based on polyaniline particles embedded in a cross-linked poly(dimethyl siloxane) network. Mat. Sci. Eng. C 28: 1044-1051

[26] W. Wichiansee, A. Sirivat. (2009) Electrorheological properties of poly(dimethylsiloxane) and poly(3,4-ethylenedioxy thiophene)/poly(stylene sulfonic acid)/ethylene glycol blends. Mat. Sci. Eng. C 29: 78-84

[27] T. Puvanatvattana, D. Chotpattananont, P. Hiamtup, S. Niamlang, A. Sirivat, A.M. Jamieson. (2006) Electric field induced stress moduli in polythiophene/polyisoprene elastomer blends. React. Funct. Polym 66: 1575-1588

[28] T. Shiga, A. Okada, T. Kurauchi. (1993) Electroviscoelastic Effect of Polymer Blends Consisting of Silicone Elastomer and Semiconducting Polymer Particles. Macromolecules 26: 6958-6963

[29] T. Shiga, A. Okada, T. Kurauchi. (1995) Electroviscoelastic effect of doped poly(3-hexylthiophene). J. Mater. Sci. Lett 14: 514-515

[30] T. Sato, H. Watanabe and K. Osaki. (1996) Rheological and Dielectric Behavior of a Styrene−Isoprene−Styrene Triblock Copolymer in *n*-Tetradecane. 1. Rubbery−Plastic−Viscous Transition. Macromolecules 29: 6231–6239

[31] S.P Timoshenko, J.N. Goodier. (1970) Theory of elasticity, 3rd ed. McGraw-Hill, Auckland

[32] J.M. Gere. (1972), Mechanics of Materials, 3rd ed. Chapman & Hall

[33] G. Alici, B. Mui, C. Cook. (2006) Bending modeling and its experimental verification for conducting polymer actuators dedicated to manipulation applications. Sensor Actuat.Phys. A 126: 396

[34] C.A. Dai, A. Kao, C. Chang, W. Tsai, W. Chen, W. Liu, W. Shih, C.C. Ma. (2009) Polymer Actuator Based on PVA/PAMPS Ionic Membrane: Optimization of Ionic Transport Properties. Sensor Actuat. A-Phy 155: 152-162

[35] R. Kunanuruksapong, A. Sirivat. (2010) Effect of dielectric constant and electric field strength on dielectrophoresis force of acrylic elastomers and styrene copolymers. Curr Appl Phys 1-10

List of Tables

Table 1 Data on Characterization of Gelatin

Sample	Non-crosslinked high gel strength gelatin	Non-crosslinked Medium gel strength gelatin	Non-crosslinked Low gel strength gelatin
Gel strength	250 g bloom*	180 g bloom*	80 g bloom*
pH	7.7	6.7	7.0
Calcium(%)	≤0.2	≤0.2	≤0.2
Chloride(%)	≤0.2	≤0.2	≤0.2
% Moisture	≤20	≤20	≤20
Molecular weight	75537	57909	41363

*Bloom is the weight in grams required to push a piston of a strictly defined shape 4 mm into a gelatin gel matured for 18 h at 10C.

*Molecular weight as measured by Ubblohde viscometer ($K = 1.66x10^{-5}$, $a = 0.855$).

Table 2 Comparison of the storage modulus sensitivities of gelatin films of various gel strengths

Material	Electric field (kv/mm)	Frequecy (rad/s)	Temp °C	Initial storage modulus (G_o) Pa	Storage modulus (G') Pa	Storage modulus sensitivity ($\Delta G'/Go$) Pa
Uncrosslinked High-gel-strength gelatin	1000	100	27	1 310 000	4 340 000	2.30
Uncrosslinked Medium-gel-strength gelatin	1000	100		892 000	2 820 000	2.16
Uncrosslinked Low-gel-strength gelatin	1000	100		129 000	292 000	1.26
3 % crosslinked high-gel-strength gelatin	1000	100		2 410 000	3 580 000	0.49

Table 3 Comparison of the storage modulus sensitivities of electroactive and dielectric elastomer materials

Materials	Electric field (kv/mm)	Frequecy (rad/s)	Temp (°C)	Storage modulus sensitivity (ΔG'/Go) Pa	Ref #
Acrylic elastomer 70	2000	100	27	0.439	[22]
Acrylic elastomer 71				0.586	
Acrylic elastomer 72				0.148	
Styrene-acrylic copolymers				1.195	
Styrene-isoprene-styrene triblock D1112P				0.746	
Acrylic elastomer 71 + PPP 10%(v/v)		1		0.306	
Acrylic elastomer 71 + PPP 30%(v/v)				0.971	
Styrene-isoprene-styrene triblock D1114P	1000	1		0.122	[23]
Styrene-isoprene-styrene triblock D1164P				0.102	
Styrene-isoprene-styrene triblock D1162P				0.050	
D114P + PDPA 5%(v/v)				0.040	
D114P + PDPA 10%(v/v)				0.256	
D114P + PDPA 30%(v/v)				0.095	
AR71/lead zirconate titanate Pb(Zr0.5Ti0.5)O3 (0.000019%v/v)	2000	1		0.149	[24]
AR71/lead zirconate titanate Pb(Zr0.5Ti0.5)O3 (0.038%v/v)				0.587	
poly (dimethyl siloxane) (PDMS)	2000	100		0.104	[25]
poly (dimethyl siloxane) (PDMS) + PANi 20% (v/v)				0.25	
poly (dimethyl siloxane) (PDMS) + PANi 2% (v/v)				0.111	
PDMS_5%PEDOT/PSS/EG	2000	100		0.077	[26]
PDMS_15%PEDOT/PSS/EG				0.333	
Crosslinked Polyisoprene 3% + Polythiopene 5% (v/v)	2000	100		0.523	[27]
Crosslinked Polyisoprene 3% + Polythiopene 10% (v/v)				0.33	
Crosslinked Polyisoprene 3% + Polythiopene 30% (v/v)				0.435	
Silicone gel	5000	60		not response	[28,29]
Silicone gel + PMACO 46%	1000			0.25	
Silicone gel + PMACO 46%	2000			0.75	
Silicone gel + PMACO 46%	3000			2	
Silicone gel + poly(p-phenylenes) 10%	1000	300		0.333	
Silicone gel + poly(p-phenylenes) 10%	3000	300		1.133	
Silicone gel + poly(p-phenylenes) 10%	5000	300		1.666	
poly(3-hexylthiophene) doped iodine (amorphous)	8.7	–		0.28	

Table 4 Electromechanical responses of the high-gel-strength gelatin and the low-gel-strength gelatin at various electric field strengths

Sample	E (V/mm)	d (mm)	l (mm)	θ (°)	F_e (μN)	F_d (μN)
Uncrosslinked High-gel- strength gelatin film	0	0	23.05	0	0	0
	100	0	23.05	0	0	0
	200	0	23.05	0	0	0
	300	0	23.05	0	0	0
	400	0	23.05	0	0	0
	475	0	23.05	0	0	0
	500	0.39	23.05	0.973	0.713	2.054
	525	0.52	23.05	1.305	1.137	2.933
	550	0.86	23.05	2.19	2.118	5.116
	575	0.87	23.05	2.21	2.180	5.217
	600	0.88	23.05	2.26	2.244	5.353
Uncrosslinked Low-gel- strength gelatin film	0	0	22.48	0	0	0
	100	0	22.48	0	0	0
	200	0	22.48	0	0	0
	300	0	22.48	0	0	0
	400	0	22.48	0	0	0
	475	0.38	22.48	0.952	0	0
	500	0.51	22.48	1.293	0.229	1.428
	525	0.88	22.48	2.247	0.317	1.940
	550	1.25	22.48	3.222	0.536	3.351
	575	1.26	22.48	3.25	0.776	4.807
	600	1.28	22.48	3.3	0.792	4.859
Uncrosslinked High-gel- strength gelatin film	0	0	23.05	0	0	0
	100	0	23.05	0	0	0
	200	0	23.05	0	0	0
	300	0	23.05	0	0	0
	400	0	23.05	0	0	0
	475	0	23.05	0	0	0
	500	0.39	23.05	0.973	0.713	2.054
	525	0.52	23.05	1.305	1.137	2.933
	550	0.86	23.05	2.19	2.118	5.116
	575	0.87	23.05	2.21	2.180	5.217
	600	0.88	23.05	2.26	2.244	5.353
Uncrosslinked Low-gel- strength gelatin film	0	0	22.48	0	0	0
	100	0	22.48	0	0	0
	200	0	22.48	0	0	0
	300	0	22.48	0	0	0
	400	0	22.48	0	0	0
	475	0.38	22.48	0.952	0	0
	500	0.51	22.48	1.293	0.229	1.428
	525	0.88	22.48	2.247	0.317	1.940
	550	1.25	22.48	3.222	0.536	3.351
	575	1.26	22.48	3.25	0.776	4.807
	600	1.28	22.48	3.3	0.792	4.859

Figure captions

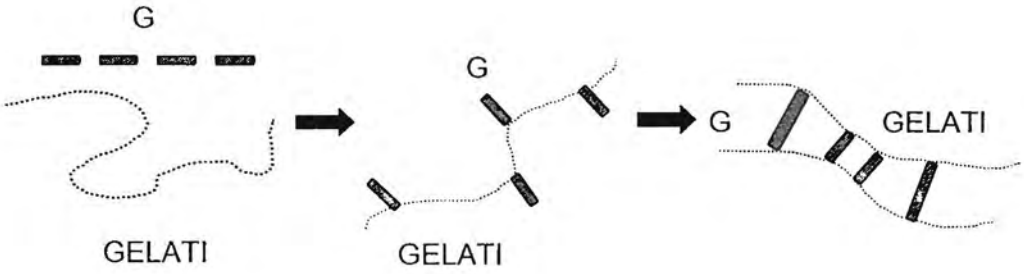

Fig. 1 Schematic of the two proposed structures for gelatin – GA complexes.

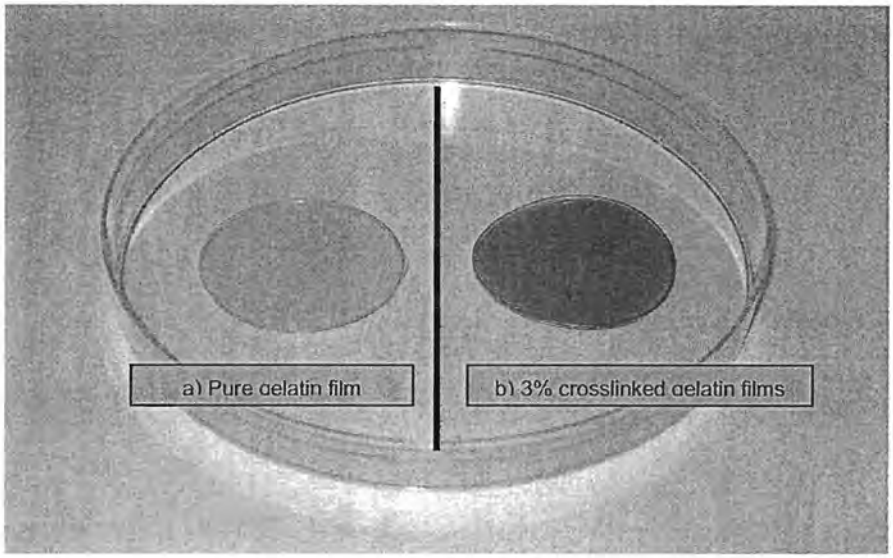

Fig. 2 The image of comparison appearance gelatin films

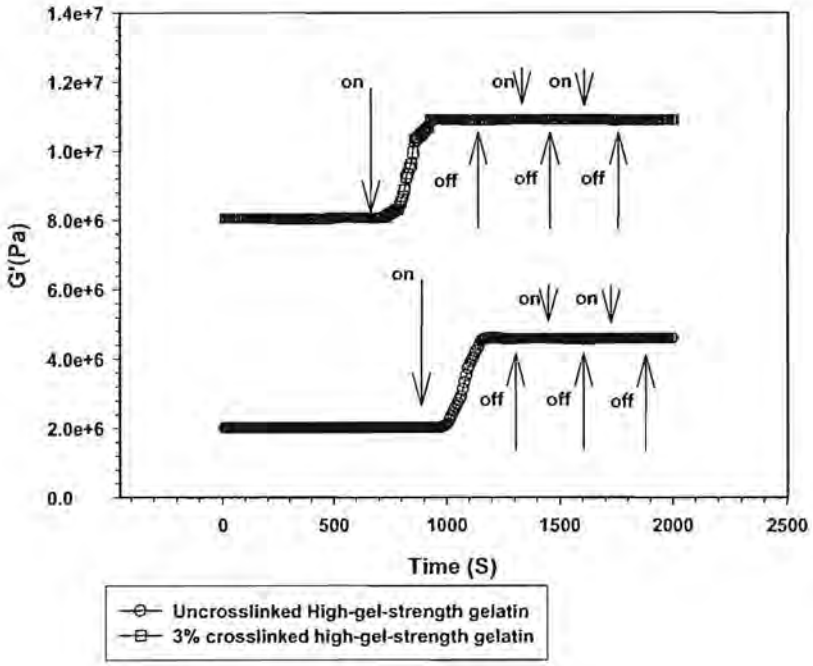

Fig. 3 Storage modulus (G') vs time of gelatin films of various gel strengths (100 rad/s, 1 kv/mm): ○) Uncrosslink High-gel-strength gelatin; and □) 3 % crosslinked high-gel-strength gelatin.

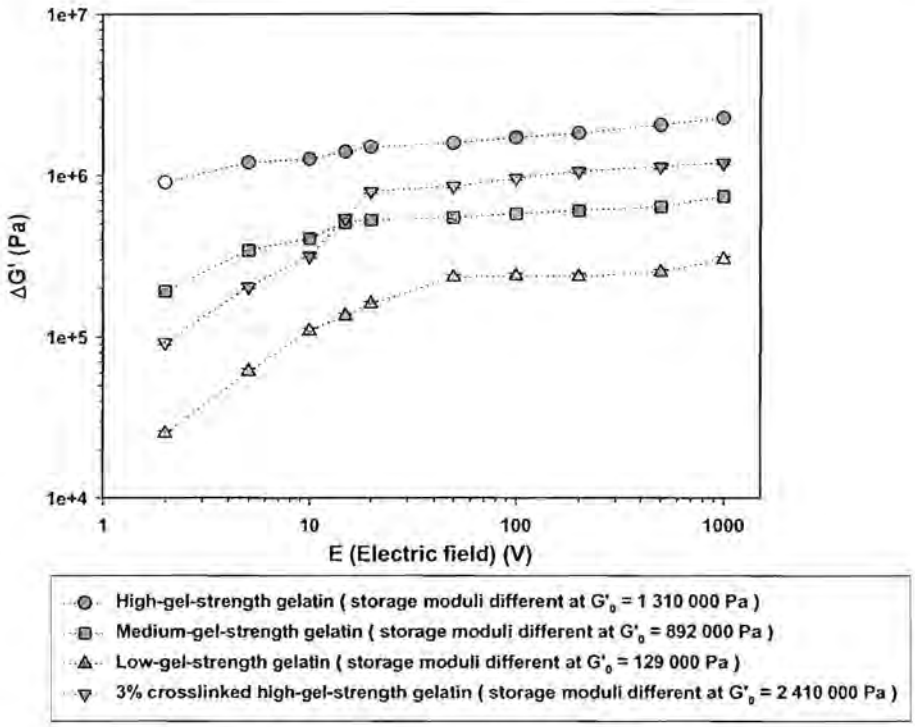

Fig. 4 Storage modulus different vs electric field strength of gelatin films at various gel strengths (100 rad/s, 0.14 %strain, 27 °C).

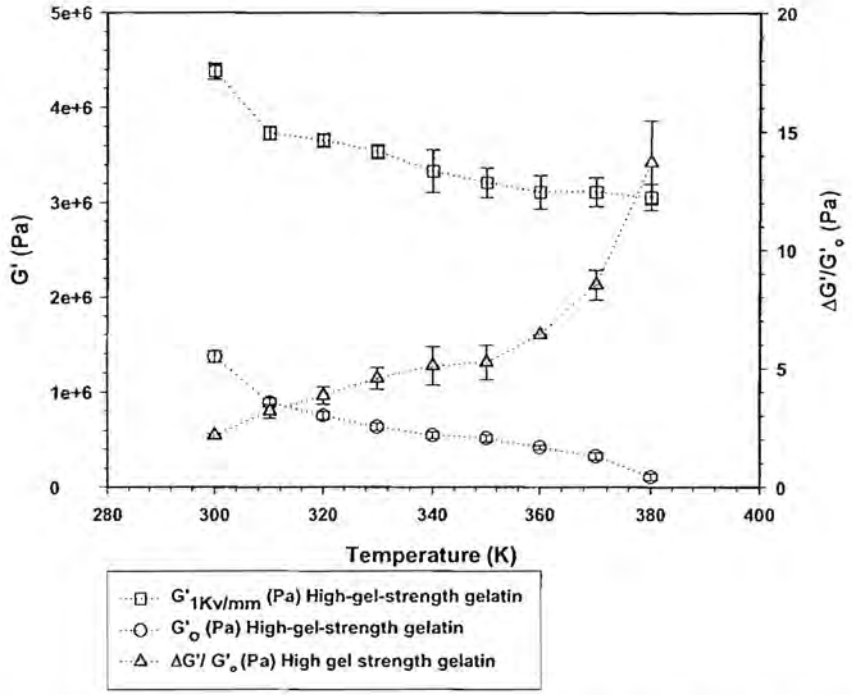

Fig. 5 Effect of temperature for Uncrosslink high-gel-strength gelatin films: Storage modulus (G') at various temperature for one sample at all temperature test (E = 0 and 1 Kv/mm, 100 rad/s, 0.14 %strain).

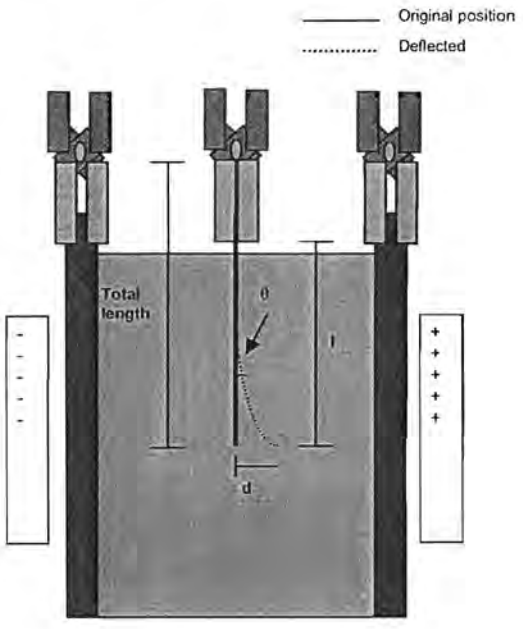

Fig. 6 Schematic of the apparatus used to observe the dielectrophoretics of the gelatin films.

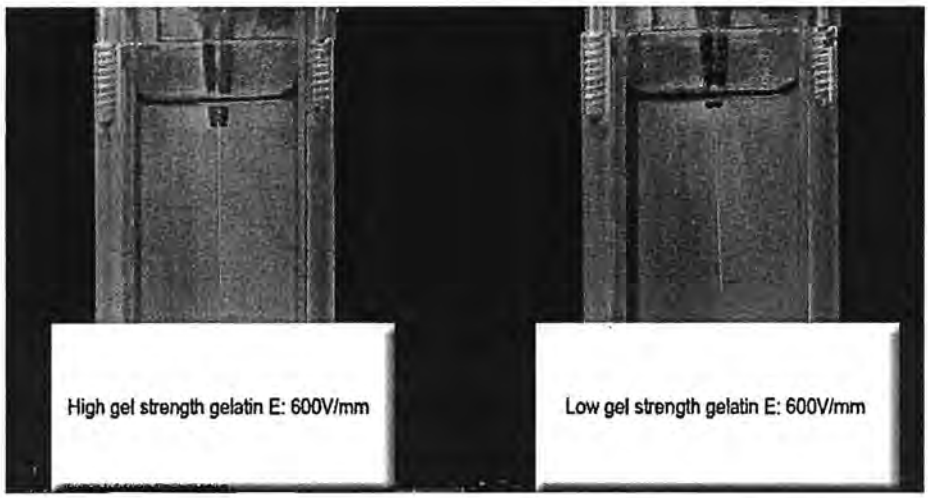

(a) (b)

Fig. 7 Deflection of the sample under electric field strength 600 V/mm: a) High-gel-strength gelatin; b) Low-gel-strength gelatin.

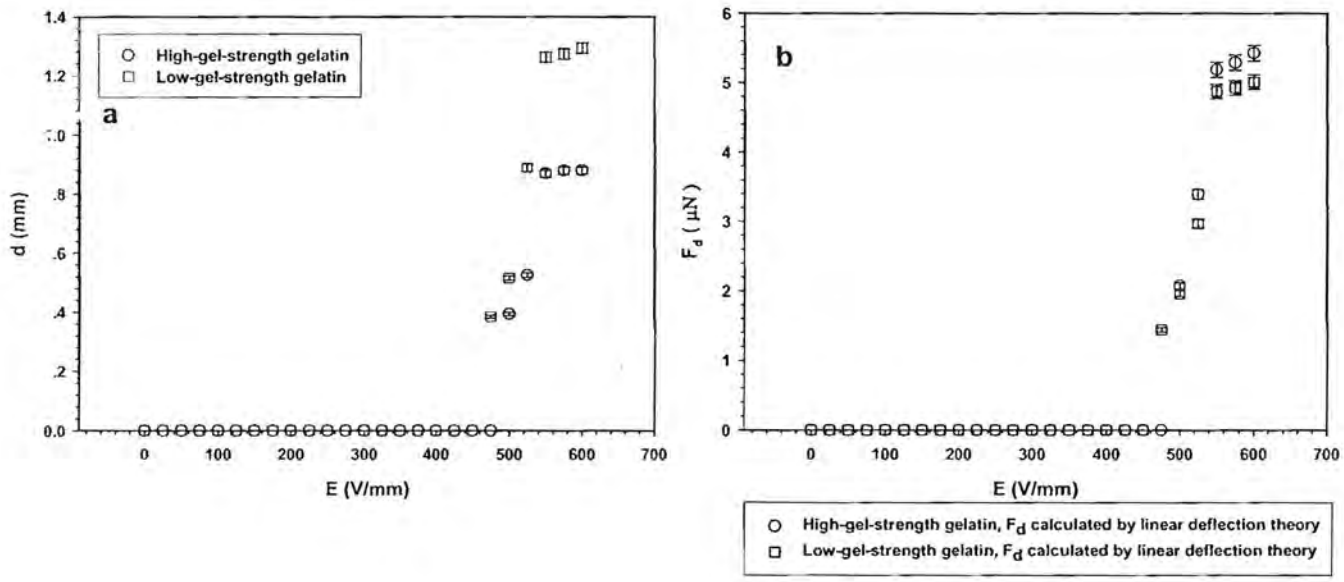

Fig. 8 a Deflection distances of high-gel-strength gelatin and low-gel-strength gelatin at various electric field strengths and b Dielectrophoretic force calculated through the Linear Deflection theory.

ส่วนที่ 4

Effects of Crosslinking Ratio, Model Drugs, and Electric Field Strength on Electrically Controlled Release for Alginate-based Hydrogel

Nophawan Paradee[a], Anuvat Sirivat[a*], Sumonman Niamlang[b], Walaiporn Prissanaroon-Ouajai [c]

[a] Conductive and Electroactive Polymers Research Unit, The Petroleum and Petrochemical College, Chulalongkorn University, Bangkok 10330, Thailand
[b] Department of Materials and Metallurgical Engineering, Faculty of Engineering, Rajamangala University of Technology Thanyaburi, Klong 6, Pathumthani, 12110, Thailand
[c] Department of Industrial Chemistry, Faculty of Applied Science, King Mongkut's University of Technology North Bangkok, Bangkok 10800, Thailand

Abstract

The drug release characteristics of calcium alginate hydrogels, (Ca-Alg), under an electric field assisted transdermal drug delivery system were systematically investigated. The Ca-Alg hydrogels were prepared by the solution-casting using $CaCl_2$ as a crosslinking agent. The diffusion coefficients and the release mechanism of the anionic model drugs, benzoic acid (BA) and tannic acid (TA), and a cationic model drug, folic acid (FA) on the Ca-Alg hydrogels were determined and investigated using a modified Franz-Diffusion cell in an MES buffer solution of pH 5.5, at a temperature of 37 °C, for 48 hours. The influences of the crosslinking ratio, —the mole of the crosslinking agent to the mole of the alginate monomer— mesh size, model drug size, drug charge , electric field strength, and electrode polarity were systematically studied. The drug diffusion coefficient decreased with an increasing crosslinking ratio and drug size for all of the model drugs. The drug diffusion coefficient is precisely controlled by an applied electric field and the electrode polarity depending on the drug charge, suitable for a tailor-made transdermal drug delivery system.

Keywords: Alginate hydrogel, Calcium alginate hydrogel, Diffusion coefficient, Electrically controlled drug release.
*Corresponding author, email: anuvat.s@chula.ac.th, Tel: 662 218 4131, Fax: 662 611 7221

1. Introduction

A Drug delivery system (DDS) is the process of introducing a drug into the body at a specific rate, at proper time intervals and with an appropriate amount of drug suitable for the treatment [1]. The transdermal drug delivery system (TDDs) has potential advantages for avoiding hepatic first pass metabolism, maintaining constant blood levels for longer periods of time, decreases side effects, decreases the gastrointestinal effect that occurs due to local contact with gastric mucosa, and the improved compliance [2]. The potential for many therapeutic agents being delivered by topical administration is limited by the ability of the drugs to permeate the skin, in particular the rate-limiting barrier [3]. Electrically driven TDDs are currently being

developed to provide a more controlled systemic delivery of drugs that are not easily delivered by other routes [4].

The use of an electric field as an external stimulus has been successfully employed to enhance and to control the precise amount of released drug [5]. Juntanon et al. [6] studied the release of sulfosalicylic acid as an anionic model drug of the poly(vinyl alcohol) (PVA)n hydrogel as a matrix under an applied electric field. They concluded that the diffusion coefficient of the drug increased with increasing electric field strength. For the effect of electrode polarity, the diffusion coefficient of a drug under a cathode was apparently higher than those not under a current and anode, respectively because of the greater repulsive force between the drug and the cathode [6].

Hydrogels can be fabricated as a matrix for controlled drug release. It is a hydrophilic three dimensional polymer network that consists of a crosslinked polymer and water in the interspaces of the network, but is insoluble in water. Some hydrogels change their volume in response to changing environmental conditions such as pH, temperature, solvent composition, and electrical stimuli [7, 8]. Alginate (Alg), an anionic polysaccharide extracted from brown algae, is one of many biopolymers that exist as a hydrogel due to its unique properties: biocompatibility, biodegradability, non-toxicity, and transparency. . It is composed of linear chains of α-L-guluronic acid (G) and the β-D-mannuronic acid (M) [9]. Alg can be formed into a hydrogel by using an ionic interaction bonding agent between the carboxylate group as located on the Alg backbone and a cation crosslinking agent. The crosslinking agent may consist of a divalent cation such as Ca^{2+} [10, 11, 12, 13], Zn^{2+} [11], or Ba^{2+} [12], or a trivalent cation, especially Al^{3+} [12, 13]. Normally, Calcium-alginate (Ca-Alg) hydrogels are widely used in gel form because they can easily be transformed into a GG block or the so called "egg-box" structure [11].

The objective of this work is to investigate the controlled release behavior of Ca-Alg hydrogels under the effects of a crosslinking-ratio, model drug, and applied electric field.

2. Materials and methodology

2.1. Materials

Alginic acid sodium salt (Na-Alg) from brown algae was purchased from Sigma-Aldrich. Calcium chloride dihydrate ($CaCl_2 \cdot 2H_2O$) was purchased from Ajax Finechem and used as a crosslinker. There are 3 model drugs: benzoic acid (BA) (A.C.S.reagent), anionic drug; tannic acid (TA) (A.C.S.reagent), anionic drug; and folic acid (FA), cationic drug; they were purchased from Sigma-Aldrich. 2-(N-Morpholino) ethanesulfonic Acid (MES) monohydrate was purchased from Sigma-Aldrich and used as a buffer solution pH 5.5.

2.2. Preparation of drug-loaded alginate hydrogel

A weighted amount of Na-Alg was dissolved in distilled water to prepare a Na-Alg solution at a fixed concentration of 0.4% w/v, then a weighted amount of model drug—BA, TA, or FA— was added at 0.13 wt% (based on the weight of Na-Alg) into the Na-Alg solution under constant stirring. In order to crosslink, $CaCl_2$ was used as a crosslinker at various crosslinking ratios (moles of crosslinker to moles of uronic acid monomer units): 0.3, 0.5, 0.7, 1.0, and 1.3 [14, 15]. Each of solutions was immediately mixed and then cast onto a mold at a nominal film thickness of 0.3 mm to produce drug loaded Ca-Alg hydrogels at various crosslinking ratios.

2.3. Morphology

The morphology of the Ca-Alg hydrogel was examined using Hitachi S4800, a scanning electron microscope (SEM). After the hydrogel was immersed in distilled water at 37 °C for 3 days, it was rapidly frozen in liquid nitrogen at -40 °C for 24 hr, and lyophilized at -50 °C for 24 hr in a freeze-dryer (LABCONCO, Freezone 2.5). The sample was scanned at a 120x magnification.

The Ca-Alg hydrogel swelling was studied to determine the degree of swelling and the weight loss of Ca-Alg hydrogel in a MES buffer solution at 37 °C for 24 hr, using the following Eq. (1) and (2) [16]:

$$\text{Degree of swelling (\%)} = \frac{M - M_d}{M_d} \times 100 \tag{1}$$

and

$$\text{Weight loss (\%)} = \frac{M_i - M_d}{M_i} \times 100 \tag{2}$$

where M is the weight of the sample after immersing in the buffer solution, M_d is the weight of the sample after immersing in the buffer solution in its dry state and M_i is the initial weight of the sample in its dry state.

In order to correlate the release behavior of the loaded model drug to the physical characteristics of the Ca-Alg hydrogels, experiments were carried out to determine the molecular weight between crosslinks ($\bar{M}_c$), the mesh size (ξ), and the crosslinking density (ρ_x). A sample of the Ca-Alg hydrogel was cut, then immediately placed in distilled water at 37 °C. For 5 days it was allowed to swell to equilibrium, and then weighed in air and heptane. Finally, the sample was dried at 25 °C in a vacuum oven for 5 days. Once again, it was weighed in air and heptane. These weights were used to calculate the polymer volume fraction [16].

The Flory-Rehner equation modified using Bray and Merrill equation as follows in Eq. (3) was used to determine the $\bar{M}_c$ [16, 17].

$$\frac{1}{\bar{M}_c} = \frac{2}{\bar{M}_n} - \frac{\left(\frac{\bar{v}}{V_1}\right)\left[\ln\left(1 - v_{2,s}\right) + v_{2,s} + \chi_1\left(v_{2,s}\right)^2\right]}{v_{2,r}\left[\left(v_{2,s}/v_{2,r}\right)^{1/3} - 0.5\left(v_{2,s}/v_{2,r}\right)\right]} \tag{3}$$

where $\bar{M}_n$ is the number averaged molecular weight of the polymer before crosslinking ($\bar{M}_n$ = 450000 g/mol), $\bar{v}$ is the specific volume of alginate ($\bar{v}$ = 0.60 cm^3/g of alginate) [17], V_1 is the molar volume of the water (V_1 = 18 mol/cm^3) [17], $v_{2,r}$ is the volume fraction of the polymer in a relaxed state, $v_{2,s}$ is the volume fraction of the polymer in a swollen state, and the Flory polymer-solvent interaction parameter (χ_1) for alginate is 0.473 [17].

The ξ was calculated by the following equation [18, 19].

$$\xi = v_{2,s}^{-1/3}\left[C_n\left(\frac{2\bar{M}_c}{M_r}\right)\right]^{1/2} l \tag{4}$$

where C_n is the Flory characteristic ratio (C_n = 27.33), l is the carbon-carbon bond length of the monomer unit (l = 5.15 Å), M_r is monomer molecular weight (M_r = 198 g/mol), and $\bar{M}_c$ is the molecular weight between crosslinks.

The crosslinking density of the hydrogel was calculated using Eq. (5) [20].

$$\rho_x = \frac{1}{v\bar{M}_c} \tag{5}$$

2.4. Drug release experiment

2.4.1. Preparation of MES Buffer

An MES buffer solution was chosen to simulate the human skin pH condition of 5.5. To prepare 200 ml of MES buffer solution, 0.1 M of MES pH 5.5.was poured into the receptor chamber of a modified Franz-Diffusion cell.

2.4.2. Spectrophotometric Analysis of Model Drug

A UV/Visible spectrophotometer (UV-TECAN infinite M200) was used to determine the spectra peaks of the model drugs. Each model drug, in an aqueous solution, was scanned for its maximum absorption wavelength. The absorbance value at the peak wavelength of the model drug can be correlated with the model drug concentration, thus the calibration curves with the various model drugs were generated.

2.4.3. Actual Drug Content

The actual amount of drug in the drug-loaded Ca-Alg film (circular disc about 1.8 mm in diameter, thickness 0.3 nm) was quantified by dissolving in 4 ml of dimethylsulfoxide (DMSO) and then 0.5 ml of the solution was added into 8 ml of the MES buffer solution. The amounts of the drugs in the solution were determined by the UV/Visible spectrum peaks at the wavelengths of 232 nm for BA, 280 nm for FA, and 276 nm for TA, and from the calibration curves for the actual drug content determination.

2.4.4. Transdermal Transport Studies

Diffusion was studied by using modified Franz-Diffusion cells. A diffusion cell consists of two compartments—a donor compartment, which was exposed to an ambient condition, and a receptor component which was filled with MES buffer solution pH 5.5 and maintained at 37 °C in a circulating water bath. The model drugs diffused through a nylon net (mesh size = 2.25 mm^2) which was placed on top the MES buffer solution. The area available for permeation was 2.51 cm^2. The nylon net was allowed to come into contact with the MES buffer in the receptor chamber; the buffer was magnetically stirred throughout the experiment period (48 hr) at a thermostatically maintained temperature (37±2 °C). For the study of the effect of crosslinking ratio, drug-loaded Ca-Alg hydrogels of various crosslinking ratios (0.3, 0.5, 0.7, 1.0, and 1.3) were placed on top of a similar nylon net above the receptor compartment. For the study of the effect of electric field strength on the release of the model drug from the Ca-Alg hydrogel, a cathode electrode (aluminum) was connected to a power supply (KETHLEY 1100 V Source Meter), which provided various electrical voltages (V = 0, 0.05, 0.5, 1.0, 3.0, and 5.0 V) across the hydrogel, nylon net, and buffer solution. The total duration of the constant applied electric field strength to the experiment setup was ~ 48 hr. The drugs diffused through a polymer matrix and the membrane into the solution. A sample of 0.1 ml was withdrawn at various time intervals and simultaneously replaced with an equal volume of the fresh buffer solution. The drug amount in the withdrawn solution sample was determined by UV/Visible spectrophotometer.

3. Results and discussion

3.1. Characterization

3.1.1. Swelling behavior of drug-loaded Ca-Alg hydrogel

The Ca-Alg hydrogels were prepared at the various crosslinking ratios (0.3, 0.5, 0.7, 1.0, and 1.3) in proportion to the amounts of $CaCl_2$ used. The effect of this variable on the swelling behavior, the $\bar{M}_c$, the ξ, and the drug diffusion ability were investigated.

Fig. 1 shows the degree of swelling and the weight loss of Ca-Alg hydrogels at various crosslinking ratios after the immersion in MES buffer solution pH 5.5 at 37 °C for 5 days. The results show that the degree of swelling and the weight loss decrease, with increasing crosslinking ratios or increasing $CaCl_2$ concentration, in the hydrogels because the lower crosslinked hydrogel has a longer alginate strand between crosslinks producing a looser network for easier diffusion. It can be swollen appreciably and the pore sizes are larger, as determined by the equilibrium swelling theory developed by Peppas [16] and shown in the SEM images of the Ca-Alg hydrogels after swelling (Fig. 2).

The swelling data are used to evaluate the crosslinked structure of these hydrogels. The $\bar{M}_c$, the ξ, and the ρ_x are parameters used in characterizing the porous structure of the hydrogel. These characteristic values of each hydrogel matrix were determined using the equilibrium swelling theory developed by Peppas and Bray and Merrill [16, 17]. Table 1 shows the $\bar{M}_c$, the ξ, and the ρ_x of each Ca-Alg hydrogel at various crosslinking ratios with and without electric field. The molecular weight between crosslinks and the mesh size value are larger at the lower crosslinking ratio. The mesh size of the hydrogels varies between 641 Å and 3313 Å under no current and between 1277 Å and 3887 Å under applied current. Thus, the comparison of mesh size values with electric field and without electric field clearly indicates that the electric field has an effect on the alginate structure through the generated electro-repulsive force between the negatively charged electrode and the negatively charged carboxylate group in the alginate structure.

Fig. 2 shows the morphologies of Ca-Alg of various crossinking ratios after swelling without an electric field. Fig. 2 (a-e) show the porous structures and the pore sizes which are larger at lower crosslinking ratios. Fig. 3 (a-c) shows that smaller pore sizes are visibly present without an electric field relative to those of the Ca-Alg under electric field.

3.2. Release kinetic of model drugs from Ca-Alg hydrogels

In order to investigate the three model drugs —BA, TA, and FA— transport mechanism from the Ca-Alg hydrogels, the actual amount of drug within the sample is reported as the percentage of the weight of the model drug loaded over the weight of Ca-Alg in the Ca-Alg solution. The actual amount of drug present in the sample was about 95.1±3.2% for BA, 92.1 ± 3.8% for TA, and 92.3±5.1% for FA.

The experimental data were analyzed by two diffusion models. The mechanism for the drug release is described by the Korsmeyer-Peppas model [21, 22], which describes the drug release from a polymeric system according to Eq. (6). The amount of drug released can be generally fitted to the Korsmeyer-Peppas model, a power law in time:

$$\frac{M_t}{M_\infty} = kt^n \tag{6}$$

where M_t/M_∞ is fraction of drug released at time t, k is the kinetic constant (with units of T^{-n}) and n is the diffusional exponent for drug release that is used to characterize different release mechanisms. In particular, the Higuchi's equation [22, 23] describes the fraction of drug release from a matrix which is proportional to the square root of time.

$$\frac{M_t}{M_\infty} = k_H t^{1/2} \tag{7}$$

where M_t and M_∞ are the masses of drug released when the time equals t and infinite time, respectively, and k_H is the Higuchi constant (with the unit of T^{-n}). The Higuchi equation (7) corresponds to a particular case of Eq. (6) when n is exactly equal to one half.

If the Higuchi model of drug release (i.e. Fickian diffusion) is obeyed, then a plot of M_t/M_α versus $t^{1/2}$ will be a straight line with a slope of k_H.

The diffusion coefficients of the model drugs from the Ca-Alg hydrogels are calculated from slopes of plots of drug accumulation versus the square root of time according to Higuchi's equation [23, 24]:

$$M_t = 2C_o A \left(\frac{Dt}{\pi}\right)^{1/2} \tag{8}$$

where M_t is the amount of drug released (g), A is the diffusion area (cm^2), C_o is the initial drug concentration in the hydrogel (g/cm^3), and D is the diffusion coefficient of the drug (cm^2/s).

3.2.1. Effect of crosslinking ratio and drug

The amounts of FA released from the drug-loaded Ca-Alg hydrogels of various crosslinking ratios (Alg_0.3, Alg_0.7, and Alg_1.3 as representatives) versus time t during 48 hours are shown in Fig- 4a. Evidently, there are two stages of release with the corresponding scaling exponents n_1 and n_2. For FA, n_1 is always greater than n_2, regardless of the polymer crosslinking density and whether with or without an electric field applied; the data are tabulated in Tables 2a and 2b, respectively. It is noted that n_1 increases with increasing crosslinking density with and without electric field applied; the exceptional case is BA without an applied electric field. On the other hand, n_2 also increases with increasing crosslinking density with and without electric field applied; the exceptional case is BA with an applied electric field.

The distinct n values of the Ca-Alg hydrogels clearly indicate two diffusion stages (n_1 and n_2) for the model drugs. The first stage is presumably an initial burst followed by drug diffusion. The second stage is governed by the swelling of the polymer via the inward diffusion of water during which the drug is dissolved and diffuses outward. Nevertheless, the matrix erosion can also affect the diffusion which can be attributed to polymer degradation [25]. The n_1 value of the first stage, without an electric field applied, of Alg_1.0 and Alg_1.3 with FA and TA as the model drugs varies between 0.5 and 1 which indicates the anomalous transport kinetic, meaning the

drug is released by the combined mechanisms of pure diffusion and matrix swelling. The remaining n values are less than 0.5, which indicate the Quasi Fickian diffusion meaning that the drug release mechanism from the Ca-Alg hydrogel is diffusion controlled [9, 22, 25]. The smaller value of the diffusion exponent may be attributed to the diffusion occurring partially through the matrix swelling with water filled pores [22, 26, 27]. It is noticed from Tables 2a and 2b that both scaling exponents n_1 and n_2 for a given drug and matrix become larger under the presence of applied electric field.

The amounts of FA released from all FA-loaded hydrogels increase very rapidly over the first 1 hr; after this period they increase gradually until reaching equilibrium. The results plotting of the amounts of FA released, as functions of square root of time, clearly show a linear relationship, as shown in Fig- 4b. The amount of drug released evidently increases with decreasing crosslinking ratio due to the larger pore size of the lesser crosslinked hydrogel.

Fig. 5 show the amounts of the model drugs released from the same alginate matrix (Alg_0.7) versus square root of time. At a given time, the amount of BA released is higher than those of FA and TA, respectively. The highest amount released belongs to BA due to its smallest size (5.58 Å). The lowest amount released belongs to TA because of its biggest size (36.84 Å). The intermediate amount released is FA; its size is 8.31 Å. The Ca-Alg hydrogel structure can create a negative charge on the carboxylate group in the alginate structure, therefore it is expected that the electrostatic force affects the release behavior. BA and TA are negatively charged drugs; they generate a repulsive force with the negatively charged carboxylate group in the alginate structure. For the case of FA, the positively charged amine group (NH_2^+) in the FA structure can presumably bind with the negatively charged carboxylate group in the alginate structure via the attractive electrostatic force as proposed and shown in Fig. 6. The size effect is thus diminished here relative to the electrostatic effect. That is the reason why the released amounts of FA and TA are not significantly different, even though their sizes are different by a factor of four [28].

The diffusion coefficient of each system is calculated from the slope of the plot M_t versus $t^{1/2}$ using the Higuchi's equation. Fig. 7a and 7b show the diffusion coefficients of BA and FA from the Ca-Alg hydrogels versus crosslinking ratio and mesh size at electric field strengths of 0 V and 1 V, respectively, and at 37° C. From Fig. 7a, the diffusion coefficient of BA increases with decreasing crosslinking ratio due to the larger pore size at the lower crosslinking ratio resulting in a bigger pathway for the drug to diffuse. When an electric field is applied, the diffusion coefficient of BA in the alginate matrix of a given mesh size increases due to the electrostatic force driving the charged drug; the negatively charged BA is driven towards to the oppositely charged electrode [6]. However, the diffusion coefficient of FA in the alginate matrix, of a given mesh size (see Fig. 7b), decreases with the applied electric field because FA is positively charged.

3 2.2. Effect of electric field strength

Fig. 8 shows amounts of FA (cationic) released from the Ca-Alg hydrogel or the Alg_0.7 hydrogel versus $t^{1/2}$ at various electric field strengths from the negatively charged electrode (cathode in the donor part). The amount of drug released and the diffusion coefficient of FA decrease with increasing electric field strength due to the electrostatic force generated between the negatively charged electrode and the positively charged drug, so the drug diffusion is clearly retarded. Fig. 9 shows the diffusion

coefficients of the drug loaded Ca-Alg hydrogels with a crosslinking ratio of 0.7 (Alg_0.7) versus electric field strength under the negatively charged electrode (cathode in donor). The diffusion coefficients of BA and TA increase with increasing electric field strength because both drugs are negatively charged; a higher electric field strength induces a higher electrostatic force that drives the negatively charged drugs through the polymer matrix [6].As expected, the diffusion coefficient of FA, a positively charged drug decreases with increasing electric field strength.

3.2.3. Effect of electrode polarity

Fig. 10 shows the amounts of BA (anionic) released from the Ca-Alg hydrogel or the Alg_0.7 hydrogel versus time$^{1/2}$ under the negatively charged electrode (cathode in the donor part), the positively charged electrode (anode in the donor part), and without an applied electric field. The amount of drug release and the corresponding diffusion coefficient under cathode are higher than those under no electric field and under anode, respectively for BA. This is a direct result of the electro-repulsive force driving the charged drug through the polymer matrix and membrane into the buffer solution. The force is generated between the negatively charged drug BA and the negatively charged electrode. On the other hand, the electro-attractive force, retarding the charged drug diffusion, is generated between the negatively charged drug BA and the positively charged electrode [6].

The log-log plot of the diffusion coefficient as function of the ratio of drug size over mesh size of the Ca-Alg hydrogel is shown in Fig. 11a, under electric field strengths of 0 and 1 V, at 37 °C. The scaling exponent, m, can be determined from the following equation;

$$D = D_0(a_d/\xi)^{-m} \qquad (9)$$

where D is the diffusion coefficient of the drug; D_0 is the diffusion coefficient at a very small drug size; a_d is the drug size; ξ is the mesh size of the hydrogel, and m is the scaling exponent [6]. The scaling exponent m values for the drug diffusion through the Ca-Alg matrix without an electric field for BA, FA, and TA are 1.06, 0.96, and 0.80, respectively. Corresponding D_o values are 2.01×10^{-7} cm^2/s, 6.37×10^{-7} cm^2/s, and 7.02×10^{-7} cm^2/s, respectively. Under an electric field of 1 V, the scaling exponent m values of BA, FA, and TA are 1.28, 1.27, and 0.72, respectively. The D_o values are 2.08×10^{-6} cm^2/s, 4.97×10^{-6} cm^2/s, and 2.90×10^{-6} cm^2/s, respectively. These results are obtained from the data of the drug size over the mesh size ratio between 0.001 to 0.01; the exception is the case of TA under an applied electric field in which the data extends beyond the ratio of 0.01.

It can be seen that, under no electric field, the D data of the three drugs (BA, FA, and TA) fall into a common curve, suggesting that the influence of the drug charges and the interactions with the Ca-Alg matrices are negligible. Under an electric field strength of 1 V, the D of BA and TA are evidently increased since both drugs are anionic. On the other hand, the D of FA is decreased as expected since it is a cationic drug.

Fig. 11b shows the comparison of the D of Polyacrylamide (PAAM) [29], Polyacrylic acid (PAA) [30], and Polyvinyl alcohol (PVA) [6] hydrogels. The D of PAAM is higher than the PAA and PVA hydrogels, respectively with and without electric field stimulation. The D of the PAAM hydrogel is highest because of the ionic interaction between the protonated PAAM and the anionic drug (salicylic acid) is

relatively small in comparison to the hydrogen bonding. The *D* of PAA is higher than PVA due to the hydrogen bonds between acid groups and the ionized carboxylic acid groups in the PAA structure which is broken creating the negative charges on the carboxylate groups at pH 5.5. This results in the repulsive force between the negative charges on the carboxylate groups and the negative charges of the drug (sulfosalicylic acid). For PVA, the positive charges can be created at pH 5.5 because of the protonation [31] inducing lower *D* of PVA. In comparing the data between the Ca-Alg hydrogel of the current work and in other studies, the diffusion coefficient of the Ca-Alg hydrogel is nearly the same or comparable to that of PAAM under no electric field stimulation; but it is less than that of PAAM under 0.1V electric field strength. This is because the driving force is the electrostatic force that pushes the negatively charged drug through the PAAM matrix [32, 33]. The second cause is the breaking of the hydrogen bonds between the ionized carboxylic groups and the negative charges on the carboxylate groups at pH 5.5. So, this creates the additional driving force between the negatively charges of the drug (salicylic acid) and of the carboxylate groups in the PAAM matrix [31]. However the diffusion coefficient of the Ca-Alg hydrogel is many orders of magnitude higher than those of PAA and PVA, either with or without electric field stimulation because of the existing hydrogen bond of the anionic drug with PAA and PVA are relatively stronger interaction [6, 30].

Table 3 shows the drug size, mesh size and, the *D* of the drugs on Ca-Alg, poly(vinyl alcohol) (PVA), Polyacrylic acid (PAA) and Polyacrylamide (PAAM) hydrogels at various conditions. The *D* of the drugs from the Ca-Alg hydrogels are greater at lower crosslinking ratios and with smaller drug sizes. However, the diffusion coefficient can be increased or decresed by electric field stimulation depending on the drug charge. Kikuchi et al. [34] studied the *D* of dextrans as a model drug of different molecular weights embedded in Ca-Alg beads. The diffusion coefficient of the dextrans decreased with increasing dextran molecular weight because of size exclusion. Stockwell et al. [28] studied the *D* of chlorpheniramine on a Ca-Alg hydrogel of various alginate contents. The *D* of chlorpheniramine decreased with increasing alginate content since the increase in the alginate content decreased the rate of water penetration into the gel leading to a more rigid gel which retarded the drug release. Juntanon et al. [6], Chansai et al. [30], and Niamlang et al. [29] studied the *D*s of anionic drugs as sulfosalicylic acid [6, 30] and salicylic acid [29] on PVA, PAA, and PAAM hydrogels, respectively. They investigated that the diffusion of the anionic drug occurred through the drug diffusing out of the matrix by the concentration gradient in the absence of current, and the electrophoresis of the anionic drug under applied current. Therefore, the Ca-Alg hydrogel is a good candidate for the TDDs application due to the high *D* values obtained. In addition, its biocompatibility and renewable resource are more promising as compared to other synthetic polymers.

Thus, the above results confirm that the *D* of the drug in the TDDs depends on and can be controlled by many factors: the chemical composition of the drug; the drug molecular weight; the drug size; the polymer matrix; the drug-matrix interaction; and the experimental set up [30].

4. Conclusions

Drug-loaded Ca-Alg hydrogels were prepared by varying the crosslinking ratio to study the release mechanism and the diffusion coefficient of the drugs through the Ca-Alg hydrogels with and without electric field. Each hydrogel was characterized by

its swelling ability and mesh size. The degree of swelling, the weight loss, and the mesh size of Ca-Alg hydrogels decreased with increasing crosslinking ratios. The diffusion coefficients were determined based on the effects of the crosslinking ratio, mesh size, drug size, drug charge, electric field strength, and electrode polarity. For the effect of crosslinking ratio, the diffusion coefficient of the drug on Ca-Alg hydrogel increases with decreasing crosslinking ratio due to a larger mesh size of the hydrogel. For the effect of drug size, the diffusion coefficient of the drug on the Ca-Alg hydrogel decreases with increasing drug size at the same crosslinking ratio. However, the charged drug also affects the diffusion coefficient of the drugs on the Ca-Alg hydrogel due to the interaction between the charged drugs and the negatively charged carboxylate group in the alginate structure. The diffusion coefficient of the cationic drug (FA) on Ca-Alg is lower than the anionic drugs (BA and TA) due to the interaction between the cationic drug and the negatively charge carboxylate group in the alginate structure. In the case of the negatively charged drugs (BA and TA), under electric field, the diffusion coefficients of the drugs increase with increasing electric field strength due to the higher electro-repulsive force driving the drugs through the matrix. However, with the positively charged drug (FA), the opposite result occurs. In regards to electrode polarity, the diffusion coefficient of the drug depends on the drug charge. The diffusion coefficient of the negatively charged drugs under cathode is much higher than that under no current and anode, respectively due to the electro-repulsive force between the negatively charged drugs and the negatively charged electrode generated; with the positively charged drug, the opposite result occured.

Acknowledgements

We wish to express our thanks for the financial support provided by the Thailand Research Fund (RGJ PHD/0285/2551, and BRG), the Conductive and Electroactive Polymer Research Unit of Chulalongkorn University, the Royal Thai Government, and the Petroleum Petrochemical and Advanced Materials Consortium.

References

1. Gupta P, Vermani K, Grarg S. Hydrogel: from controlled release to pH responsive drug delivery. Drug Discov Today 2002;7:569-579.
2. Kshirsagar NA. Drug delivery system. Indian J Pharmacol 2000;32:S54-S61.
3. Stott PW, Williams AC, Barry BW. Transdermal drug delivery for eutectic system: enhanced permeation of model drug, buprofen. J Control Release 1998;50:297-308.
4. Riviere JE, Papich MG, Potential and problems of developing transdermal patches for veterinary applications. Adv Drug Delivery Rev 2001;50:175–203.
5. Chien YW, Lelawong P, Siddiqui O, Sun Y, Shi WM. Facilitated transdermal delivery device. J Control Release 1990;13:263-278.
6. Juntanon K, Niamlang S, Rujriravanit R, Sirivat A. Electrically controlled release of sulfosalicylic acid from crosslinked poly(vinyl alcohol) hydrogel. Int J Pharm 2008;356:1-11.
7. Kim JS, Yoon GS, Lee MS, Lee HJ, Kim S. Characteristics of electrical responsive alginate/poly(diallydimethylammonium chloride) IPN hydrogel in HCl solutions. Sensor Actuator 2003; B96:1-5.
8. Qiu Y, Park K. Environment-sensitive hydrogels for drug delivery. Adv Drug Delivery Rev 2001; 53:321-339.

9 Pasparakis G, Bouropoulos N. Swelling studies and in vitro release of verapamil from calcium alginate and calcium alginate-chitosan beads. Int J Pharm 2006;3323:34-42.
10. Badwan AA, Abumalooh A, Sallam E, Abukalaf A, Jawan O. A Sustained release drug delivery system using calcium alginate beads. Drug Dev Ind Pharm 1985;11:239-256.
11. Aslani P, Kennedy AR. Studies on diffusion in alginate gels. I. Effect of cross-linking with calcium or zinc ions on diffusion of acetaminophene. J Control Release 1996;42:75-82.
12. Al-Musa S, Fara AD, Badwan AA. Evaluation of parameters involved in preparation and release of drug loaded in crosslinked matrices of alginate. J Control Release 1999;57:223-232.
13. Gonzalez-Rodriguez ML, Holgado MA, Sanchez-Lafuenete C, Rabasco AM, Fini A. Alginate/chitosan particulate systems for sodium diclofenac release. Int J Pharm 2002;232:225–234.
14. Mohan N, Nair PD. Novel porous, polysaccharide scaffolds for tissue engineering applications. *Trends Biomater. Artif. Organs* 2005;18.
15. Pathak TS, Kim JS, Lee SJ, Baek DJ, Paeng KJ. Preparation of alginic acid and metal alginate from algae and their comparative study. J Polym Environ 2008;16:198-204.
16. Peppas NA, Wright SL. Drug diffusion and biding in ionizable interpenetrating networks from poly(vinyl alcohol) and poly(acrylic acid). Eur J Pharm Biopharm 1998;46:15-29.
17. Wells LA, Sheardown H. Photosensitive controlled release with polyethylene glycol-anthracene modified alginate. Eur J Pharm Biopharm 2011.
18. Peppas NA, Canal T. Correlation between mesh size and equilibrium degree of swelling of polymeric networks. J Biomed Mater Res 1989; 23:1183-1193.
19. Chan AW, Neufeld RJ. Modeling the controlled able pH-responsive swelling and pore size of networked alginate based biomaterials. Biomaterials 2009;30:6119-6129.
20. Peppas NA, Wright SL. Solute diffusion in poly(vinyl alcohol)/poly(acrylic acid) interpenetrating networks. Macromolecules 1996;29:8798-8804.
21. Korsmeyer RW, Gurny R, Doelker E, Buri P, Peppas NA. Mechanisms of solute release from porous hydrophilic polymer. Int J Pharm 1983;15:25-35.
22. Pradhan R, Budhathoki U, Thapa P. Formulation of once a day controlled release tablet of indomethancin based on HPMC-Mannitol. KUSET 2008;1:55-67.
23. Higuchi T. Mechanism of sustained-action medication: Theoretical analysis of rater of release of solid drugs dispersed in solid matrices. J Pharm Sci 1963;2: 1145-1149.
24. Reichling J, Landvatter U, Wagner H, Kostka KH, Schaefer UF. In vitro studies on release and human skin permeation of Australian tea tree oil (TTO) from topical formulations. Eur J Pharm Biopharm 2006;64:222–228.
25. Mahmoodi M, Khosroshahi ME, Atyabi F. Laser Thrombolysis and in vitro study of tPA release encapsulated by chitosan coated PLGA nanoparticles for AMI. International Journal of Biology and Biomedical Engineering 2010;4:35-4
26. Prajapati R, Mahajan H, Surana S. PLGA based mucoadhesive microspheres for nasal delivery: In vitro/Ex Vivo studies. IJNDD 2011;3:9-16.
27. Basak SC, Kumar KS, Ramalingam M. Design and release characteristics of

sustained release tablet containing metformin HCl. Braz. J. Pharm. Sci 2008;44:477-483.
28. Stockwell AF, Davis SS, Walker SE. In vitro evaluation of alginate gel systems as sustained release drug delivery system. J Control Release 1986;3:167-175.
29. Niamlang S, Sirivat A. Electrically controlled release of salicylic acid from poly(p-phenylene vinylene)/polyacrylamide hydrogels. Int J Pharm 2009;371:126-133.
30. Chansai P, Sirivat A, Niamlang S, Chotpattananont D, Viravaidya-Pasuwat K. Controlled transdermal iontophoresis of sulfosalicylic acid from polypyrrole/poly(acrylic acid) hydrogel. Int J Pharm 2009;381:25-33.
31. Veronika K, Eugenia K, Marc LM, Svetlana AS. Poly(methacrylic acid) Hydrogel Films and Capsules: Response to pH and Ionic Strength, and Encapsulation of Macromolecules. Chem. Mater. 2006:18:328-336.
32. Shilpa K, Gareth DR, Jayne L. Gelatin-stabilised microemulsion-based organogels: rheology and application in iontophoretic transdermal drug delivery. J Control Release 1999:60:355-365.
33. Sudaxshina M. Electro-responsive drug delivery from hydrogels. J Control Release 2003:92:1-17.
34. Kikuchi A, Kawabuchi M, Watanabe A, Sugihara M, Sakurai Y, Okano T. Effect of Ca^{2+} -alginate gel dissolution on release of dextran with different molecular weights. J Control Release 1999;58:21-28.

List of Tables

Table 1 The molecular weight between crosslinks, the mesh size, and the crosslinking density of Ca-Alg hydrogels of various crosslinking ratios with and without an applied electric field

Sample	Crosslinking ratio, X	Number-average molecular weight between crosslinks, $\bar{M}_c$(g/mol)		Mesh size, ξ (Å))		Cross-linking density, ρ_x (mol/cm^3) × 10^6	
		E = 0 V	E = 1 V	E = 0 V	E = 1 V	E = 0 V	E = 1 V
Alg_0.3	0.3	$2.24\times10^5 \pm 0.02$	$2.26\times10^5 \pm 0.05$	3313 ± 637	3887 ± 91	11.2 ± 0.116	11.0 ± 0.012
Alg_0.5	0.5	$2.03\times10^5 \pm 0.12$	$2.15\times10^5 \pm 0.02$	2289 ± 277	2657 ± 99	12.3 ± 0.787	11.6 ± 0.153
Alg_0.7	0.7	$1.52\times10^5 \pm 0.21$	$2.05\times10^5 \pm 0.02$	1545 ± 236	2236 ± 71	16.5 ± 2.790	12.2 ± 0.158
Alg_1.0	1.0	$1.28\times10^5 \pm 0.17$	$1.77\times10^5 \pm 0.07$	1174 ± 121	1689 ± 108	19.7 ± 0.176	14.1 ± 0.538
Alg_1.3	1.3	$0.57\times10^5 \pm 0.10$	$1.30\times10^5 \pm 0.09$	641 ± 90	1277 ± 82	44.5 ± 8.370	19.2 ± 0.148

Table 2a Release kinetic parameters and the linear regression values obtained from fitting the drug release experimental data

Sample	Release Kinetics											
	Benzoic acid				Folic acid				Tannic acid			
	n_1[1]	n_2[2]	k_H (h^{-n})	r^2	n_1	n_2	k_H (h^{-n})	r^2	n_1	n_2	k_H (h^{-n})	r^2
Alg_0.3	0.493	0.0833	1.7314	0.9647	0.3825	0.0653	2.1751	0.9742	0.1503	0.0684	1.9842	0.9722
Alg_0.5	0.4750	0.0730	1.4376	0.9185	0.4069	0.0843	2.1259	0.9926	0.2403	0.0541	1.9811	0.9911
Alg_0.7	0.4320	0.1158	1.3887	0.9733	0.4510	0.1032	1.8929	0.9585	0.2902	0.0949	1.9474	0.9591
Alg_1.0	0.4070	0.1441	1.2479	0.9834	0.6531	0.1176	1.6886	0.9861	0.6122	0.2360	1.4300	0.9949
Alg_1.3	0.3680	0.1625	1.1412	0.9678	0.8988	0.1308	1.4085	0.9033	0.8140	0.4830	1.3148	0.9550

Table 2b Release kinetic parameters and the linear regression values obtained from fitting the drug release experimental data at an electric field strength of 1 V

Sample	Release Kinetics											
	Benzoic acid				Folic acid				Tannic acid			
	n_1	n_2	k_H (h^{-n})	r^2	n_1	n_2	k_H (h^{-n})	r^2	n_1	n_2	k_H (h^{-n})	r^2
Alg_0.3	0.1472	0.1241	1.7989	0.8838	0.2310	0.1472	1.5769	0.9178	0.1268	0.0917	2.0136	0.9754
Alg_0.5	0.1416	0.10250	1.6887	0.9436	0.3668	0.1376	1.2636	0.9625	0.1293	0.1132	1.9686	0.9444
Alg_0.7	0.188	0.112	1.5879	0.9546	0.402	0.1289	1.2720	0.9985	0.1413	0.1265	1.7559	0.9731
Alg_1.0	0.3319	0.1051	1.3265	0.9074	0.8265	0.1198	0.8807	0.7175	0.1742	0.2064	1.5997	0.9579
Alg_1.3	0.7095	0.1004	1.2027	0.9649	0.940	0.1076	0.5510	0.9665	0.1856	0.3387	1.6018	0.9711

[1] n_1 is 1st stage of release

[2] n_2 is 2nd stage of release

Table 3 The diffusion coefficient of the drug on Ca-Alg PVA, PAA and PAAM hydrogels at various conditions.

Solute	M_w	*Drug size (Å)*	*Mesh size, ξ,(Å)*	*D (cm^2/s)*	*T(°C)*	*pH*	*E(V)*	*Remarks*
Benzoic acid	122	5.58	3313	1.64×10^{-5}	37	5.5	-	Crosslink ratio = 0.3
			2289	8.63×10^{-6}	37	5.5	-	Crosslink ratio = 0.5
			1545	6.31×10^{-6}	37	5.5	-	Crosslink ratio = 0.7
			1174	3.72×10^{-6}	37	5.5	-	Crosslink ratio = 1.0
			641	3.01×10^{-6}	37	5.5	-	Crosslink ratio = 1.3
			3887	3.04×10^{-5}	37	5.5	1	Crosslink ratio = 0.3
			2657	2.44×10^{-5}	37	5.5	1	Crosslink ratio = 0.5
			2236	1.48×10^{-5}	37	5.5	1	Crosslink ratio = 0.7
			1689	1.19×10^{-5}	37	5.5	1	Crosslink ratio = 1.0
			1277	7.53×10^{-6}	37	5.5	1	Crosslink ratio = 1.3
Folic acid	441	8.31	3313	1.10×10^{-5}	37	5.5	-	Crosslink ratio = 0.3
			2289	6.57×10^{-6}	37	5.5	-	Crosslink ratio = 0.5
			1545	4.28×10^{-6}	37	5.5	-	Crosslink ratio = 0.7
			1174	3.08×10^{-6}	37	5.5	-	Crosslink ratio = 1.0
			641	2.40×10^{-6}	37	5.5	-	Crosslink ratio = 1.3
			3887	7.45×10^{-6}	37	5.5	1	Crosslink ratio = 0.3
			2657	5.87×10^{-6}	37	5.5	1	Crosslink ratio = 0.5
			2236	3.14×10^{-6}	37	5.5	1	Crosslink ratio = 0.7
			1689	2.51×10^{-6}	37	5.5	1	Crosslink ratio = 1.0
			1277	1.89×10^{-6}	37	5.5	1	Crosslink ratio = 1.3
Tannic acid	1701	36.84	3313	2.61×10^{-6}	37	5.5	-	Crosslink ratio = 0.3
			2289	2.25×10^{-6}	37	5.5	-	Crosslink ratio = 0.5
			1545	1.81×10^{-6}	37	5.5	-	Crosslink ratio = 0.7
			1174	1.25×10^{-6}	37	5.5	-	Crosslink ratio = 1.0
			641	7.64×10^{-7}	37	5.5	-	Crosslink ratio = 1.3
			3887	4.02×10^{-6}	37	5.5	1	Crosslink ratio = 0.3
			2657	3.13×10^{-6}	37	5.5	1	Crosslink ratio = 0.5
			2236	2.65×10^{-6}	37	5.5	1	Crosslink ratio = 0.7
			1689	2.29×10^{-6}	37	5.5	1	Crosslink ratio = 1.0
			1277	1.78×10^{-6}	37	5.5	1	Crosslink ratio = 1.3
FITC-Dextran [34]	9400	N/A	-	1.16×10^{-6}	37	7.4	-	Calcium alginate beads
	40,500		-	6.73×10^{-8}	37	7.4	-	Calcium alginate beads
	145,000		-	3.90×10^{-9}	37	7.4	-	Calcium alginate beads
Chlorphenirami ne [28]	454	8.10	-	5.17×10^{-7}	37	1.2	-	65.2 % alginate bead
			-	1.18×10^{-6}	37	1.2	-	32.6 % alginate bead
			-	4.01×10^{-6}	37	1.2	-	10.9 % alginate bead
Sulfosalicylic acid [6, 30]	254	9.25	232	2.08×10^{-9}	37	5.5	-	Uncrosslink of PVA
			143	1.08×10^{-9}	37	5.5	-	PVA_crosslink ratio = 0.5
			71	5.13×10^{-10}	37	5.5	-	PVA_crosslink ratio = 2.5
			36	2.76×10^{-10}	37	5.5	-	PVA_crosslink ratio = 5.0
			250	7.42×10^{-9}	37	5.5	1	Uncrosslink of PVA
			150	4.62×10^{-9}	37	5.5	1	PVA_crosslink ratio = 0.5
			85	2.90×10^{-9}	37	5.5	1	PVA_crosslink ratio = 2.5
			33	1.97×10^{-9}	37	5.5	1	PVA_crosslink ratio = 5.0
			478.90	2.02×10^{-8}	37	5.5	-	Uncrosslink of PAA
			395.05	1.41×10^{-8}	37	5.5	-	PAA_crosslink ratio = 3.64E-03
			276.8	1.21×10^{-8}	37	5.5	-	PAA_crosslink ratio = 7.27E-03
			137.85	8.47×10^{-9}	37	5.5	-	PAA_crosslink ratio = 1.45E-02
			490.73	4.92×10^{-8}	37	5.5	1	Uncrosslink of PAA
			410.87	1.86×10^{-8}	37	5.5	1	PAA_crosslink ratio = 3.64E-03
			308.45	1.51×10^{-8}	37	5.5	1	PAA_crosslink ratio = 7.27E-03
			140.02	1.18×10^{-8}	37	5.5	1	PAA_crosslink ratio = 1.45E-02
Salicylic acid [29]	138	5.61	252	8.46×10^{-5}	37	5.5	-	PAAM crosslink ratio = 2.0E-03
			158	5.85×10^{-5}	37	5.5	-	PAAM crosslink ratio = 5.0E-03
			128	3.70×10^{-5}	37	5.5	-	PAAM crosslink ratio = 1.0E-02
			85	2.00×10^{-5}	37	5.5	-	PAAM crosslink ratio = 1.6E-02

			57	3.52×10^{-6}	37	5.5	-	PAAM crosslink ratio = 2.4E-02
			348	9.04×10^{-5}	37	5.5	1	PAAM crosslink ratio = 2.0E-03
			304	6.93×10^{-5}	37	5.5	1	PAAM crosslink ratio = 5.0E-03
			227	6.67×10^{-5}	37	5.5	1	PAAM crosslink ratio = 1.0E-02
			177	1.95×10^{-5}	37	5.5	1	PAAM crosslink ratio = 1.6E-02
			119	3.63×10^{-6}	37	5.5	1	PAAM crosslink ratio = 2.4E-02

Figure captions

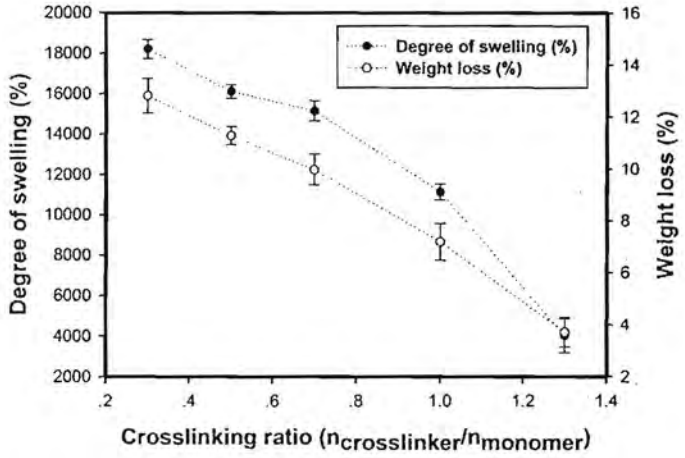

Fig. 1. The degree of swelling (%) and weight loss (%) of Ca-Alg hydrogels at various crosslinking ratios (Alg_0.3, Alg_0.5, Alg_0.7, Alg_1.0, and Alg_1.3 at 37° C after 5 days.

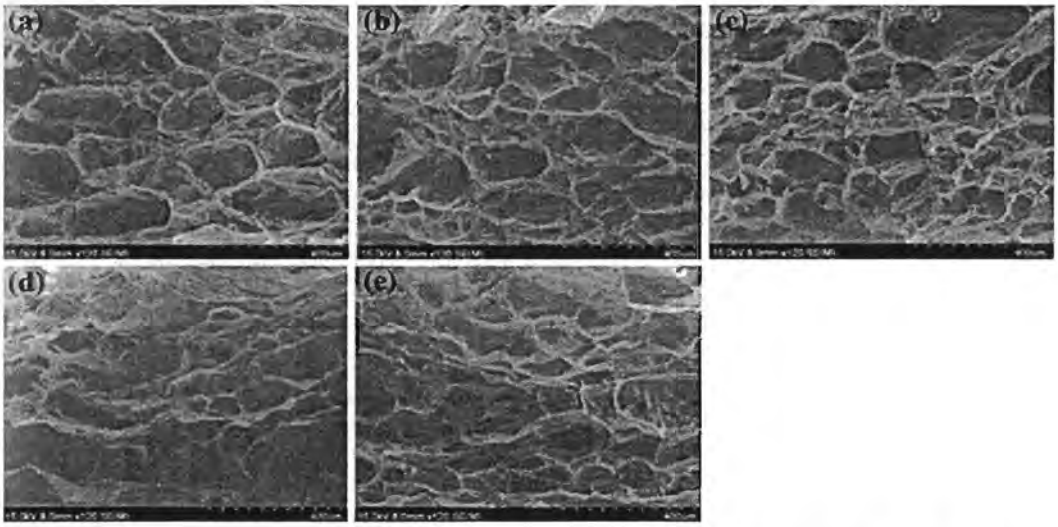

Fig. 2. The morphology of Ca-Alg after swelling: a) Alg_0.3; b) Alg_0.5; Alg_0.7; d) Alg_1.0; and e) Alg_1.3 at 120x magnification.

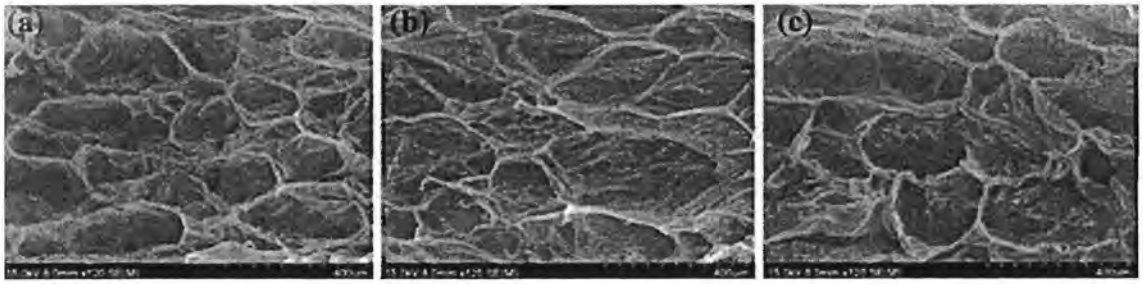

Fig. 3. The morphology of Ca-Alg (Alg_0.3) after swelling under electric field strengths of : a) 0 V; b) 1.0 V; and c) 5.0 V at 120x magnification.

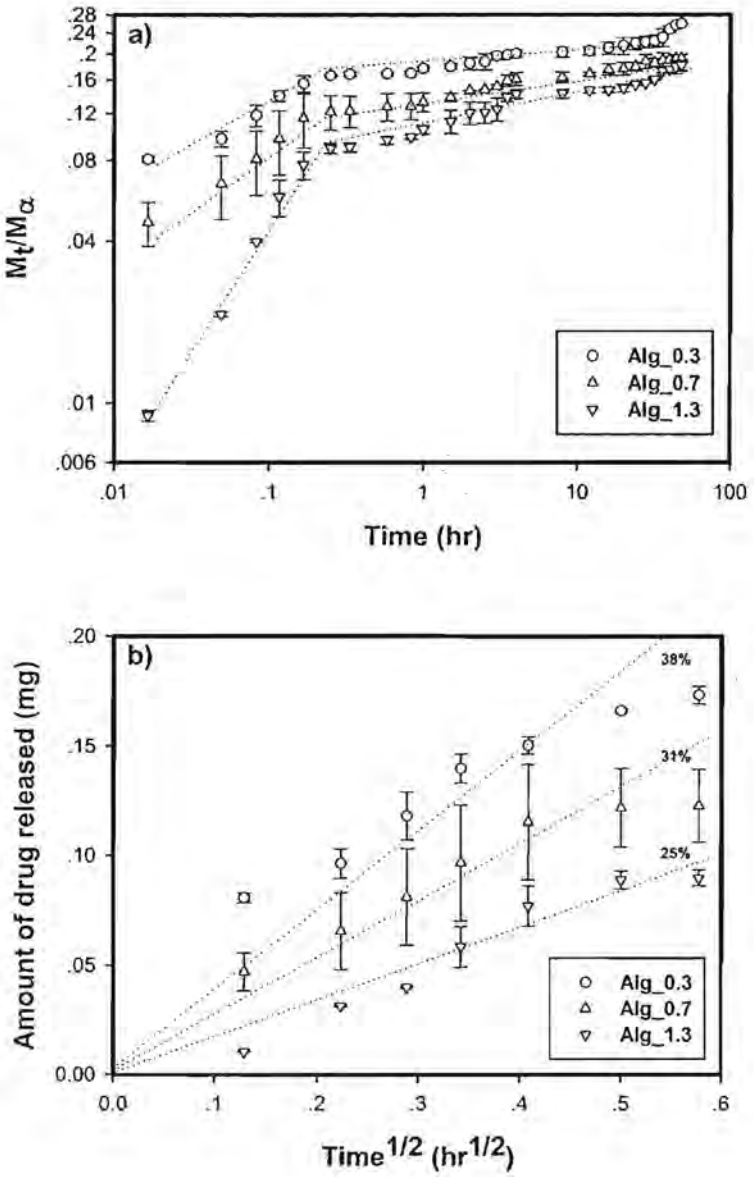

Fig. 4. Amount of folic acid released from Ca-Alg hydrogels of various cross-linking ratios versus: a) time and b) time$^{1/2}$.

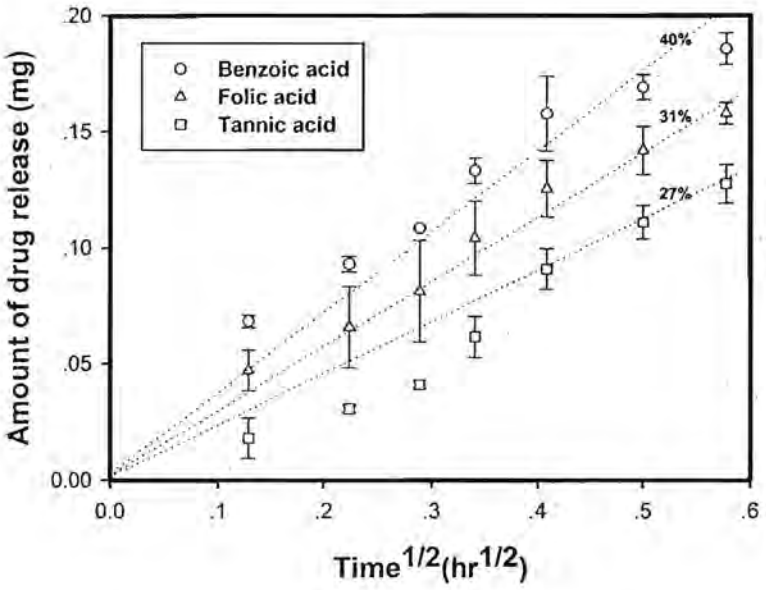

Fig. 5. Amounts of drug released from Alg_0.7 hydrogels of various drug sizes versus time$^{1/2}$.

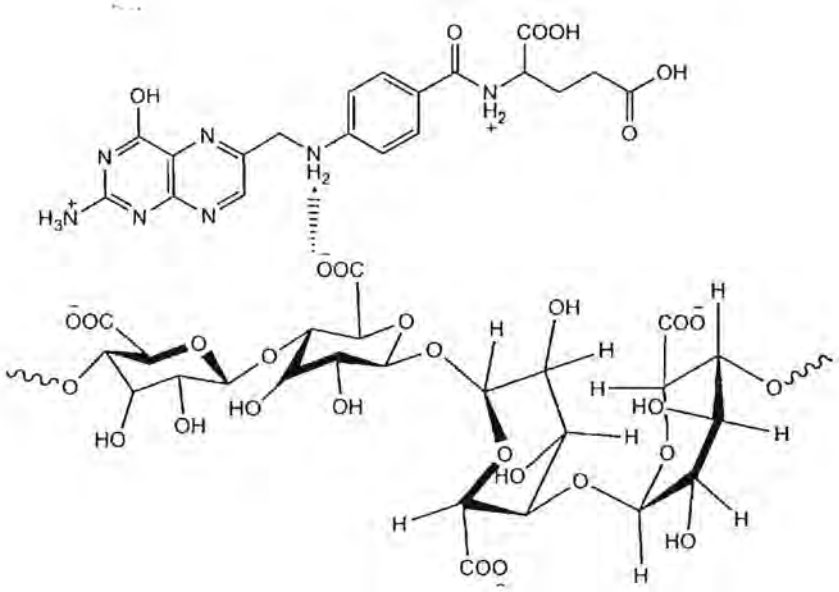

Fig. 6. The interaction between folic acid and alginate.

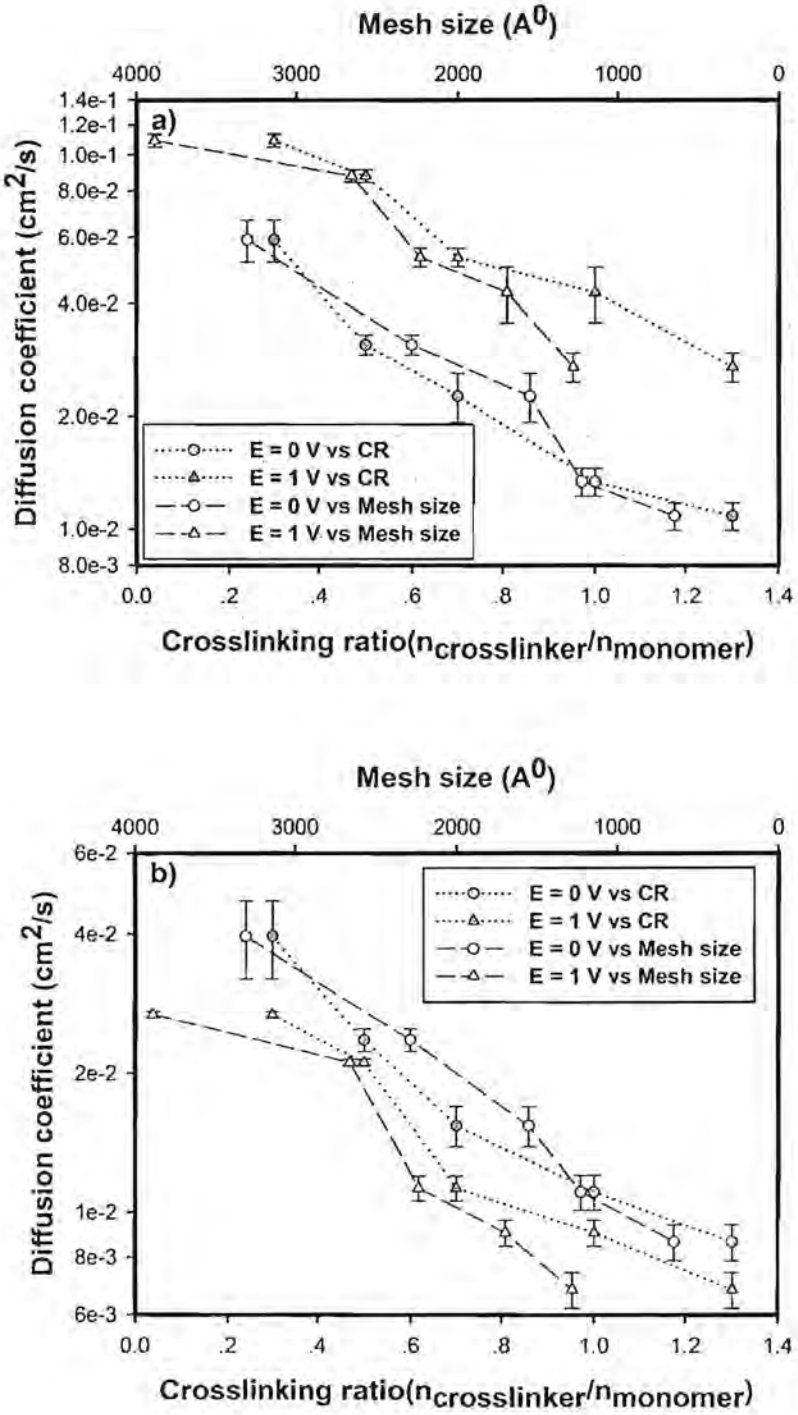

Fig. 7. The diffusion coefficients of drugs: a) benzoic acid and b) folic acid on Ca-Alg hydrogel versus crosslinking ratio and mesh size at electric field strengths of 0 and 1 V.

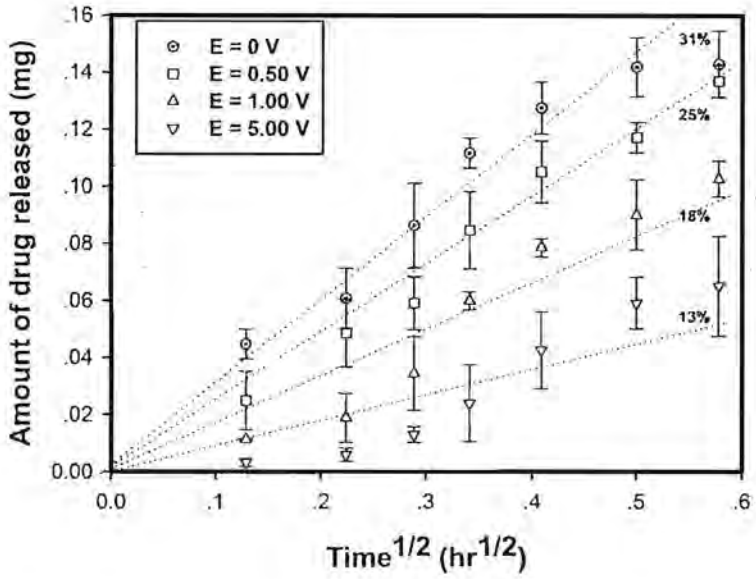

Fig. 8. Amount of folic acid released from Alg_0.7 hydrogels of various electric field strengths versus time$^{1/2}$.

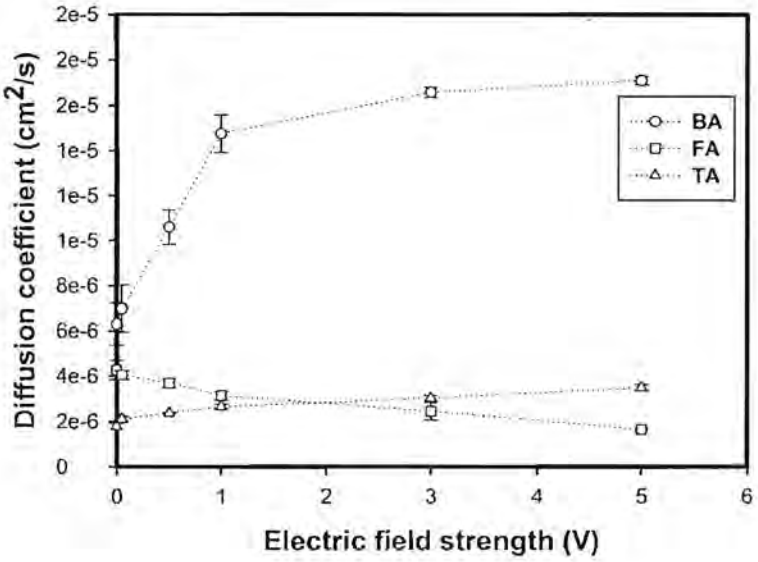

Fig. 9. The diffusion coefficients of drugs (BA, FA, and TA from Ca-Alg hydrogels versus electric field strengths of Alg_0.7 hydrogels.

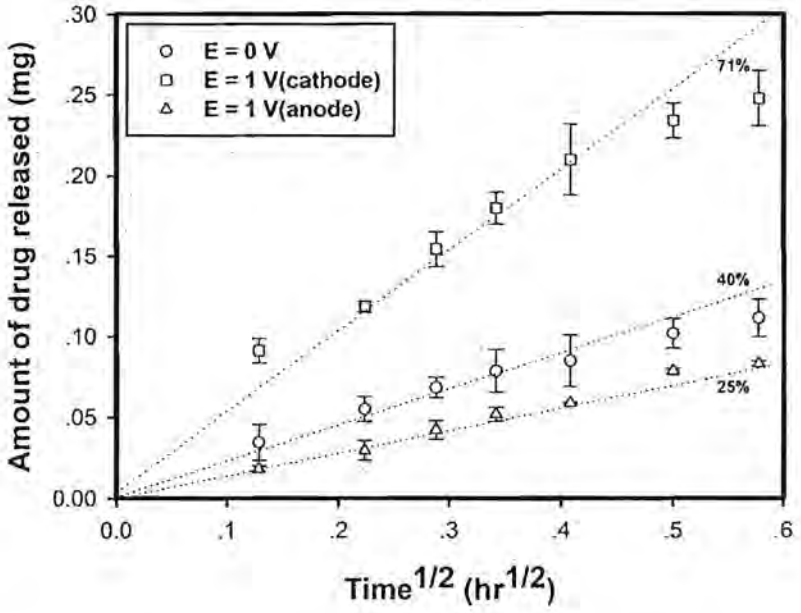

Fig. 10. Amount of benzoic acid released from Ca-Alg hydrogels versus time$^{1/2}$ with the hydrogel samples attached to the anode or cathode, Alg_0.7 hydrogels.

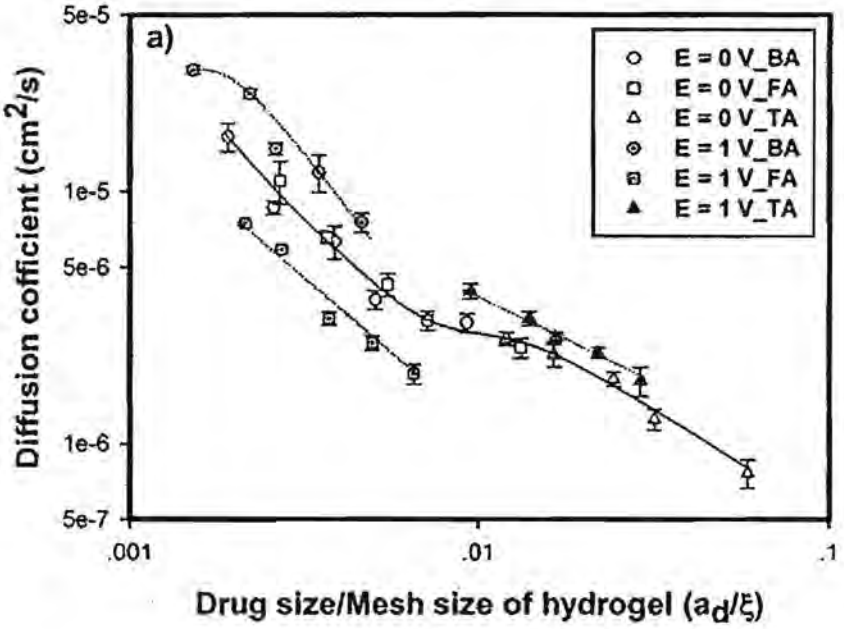

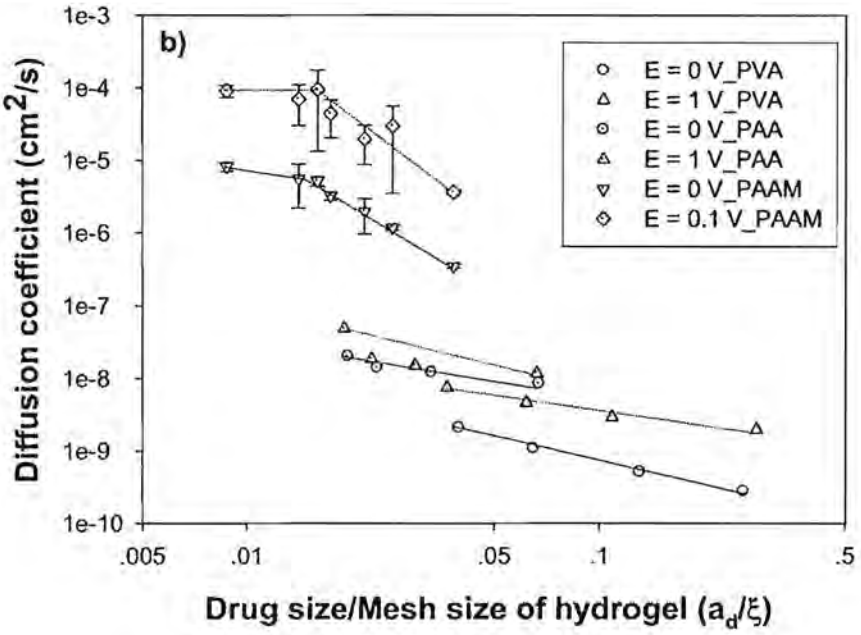

Fig. 11. a) The diffusion coefficients of drugs on Ca-Alg hydrogels versus drug size/mesh size of hydrogel at electric field strengths of 0 and 1 V. b) Comparison of diffusion coefficients of drug on PVA, PAA and PAAM hydrogel versus drug size/mesh size of the hydrogel at electric field strengths of 0 and 1 V.

ประวัตินักวิจัยและคณะ

หัวหน้าโครงการวิจัย

1. ชื่อ - สกุล (ภาษาไทย) นาย อนุวัฒน์ ศิริวัฒน์
   (ภาษาอังกฤษ) Mr. Anuvat Sirivat
2. รหัสประจำตัวนักวิจัยแห่งชาติ
3. ตำแหน่งปัจจุบัน ศาสตราจารย์ ระดับ 10
4. หน่วยงานที่อยู่ที่ติดต่อได้สะดวก พร้อมหมายเลขโทรศัพท์ โทรสาร และ E-mail: anuvat.s@chula.ac.th

   วิทยาลัยปิโตรเลียมและปิโตรเคมี จุฬาลงกรณ์มหาวิทยาลัย

   พญาไท ปทุมวัน กทม 10330

   โทรศัพท์ 02-218-4131, 01 480 0478 โทรสาร 02-611-7221

   E-mail: anuvat.s@chula.ac.th

5. ประวัติการศึกษา

ปริญญา	สาขาวิชา	มหาวิทยาลัย	ปี พ.ศ. ที่ได้รับ
B.S.	Mechanical Engineering	Cornell University	๒๕๒๐
M.E.	Mechanical Engineering	Cornell University	๒๕๒๑
Ph.D.	Mechanical Engineering	Cornell University	๒๕๒๖
Post Doctoral	Chemical Engineering	Johns Hopkins University	๒๕๒๘

6. สาขาวิชาการที่มีความชำนาญพิเศษ

   Conductive and Electroactive Polymers

   Stability Transition and Turbulence of Complex Fluids

   Light Scattering

7. ประสบการณ์ที่เกี่ยวข้องกับการบริหารงานวิจัยทั้งภายในและภายนอกประเทศ โดยระบุสถานภาพในการทำการวิจัยว่าเป็นผู้อำนวยการแผนงานวิจัย หัวหน้าโครงการวิจัย หรือผู้ร่วมวิจัยในแต่ละข้อเสนอการวิจัย เป็นต้น

ผลงานวิจัย (ย้อนหลัง 5 ปี)

7.1 International Refereed Publications

1) Soontornworajit, B., Wannatong, L., Hiamtup, P., Naimlang, S., Chotpattananont, D., Sirivat A., Schwank, J. (2007) Induced interaction between polypyrrole and SO_2 via molecular sieve 13X. Materials Science and Engineering B, 136, 78-86.

2) Suksamranchit, S., Sirivat, A. (2007) Influence of ionic strength on cationic surfactant and turbulent wall shear stress in aqueous solution. Chemical Engineering J., 128, 11-20.

3) Kunanuruksapong, R., Sirivat, A. (2007) Poly(p-phenylene) and acrylic elastomer blends for electroactive application. Mat. Sci. Engr. A, 454-455, 453-460.

4) Hlaing, N.D., Sirivat, A., Siemanond, K., Wilkes, J.O. (2007) Vertical two-phase flow regimes and pressure gradients: Effect of viscosity. Exp. Therm. Fluid Sci., 31, 567-577.

5) Chuangchote, S., Sirivat, A., Supaphol, P. (2007) Mechanical and electro-rheological properties of electrospun poly(vinyl alcohol) nanofibre mats filled with carbon black nonoparticles. Nanotechnology, 18, 145705.

6) Tanpaiboonkul, P., Lerdwijitjarud, W., Sirivat, A., Larson, R.G. (2007) Transient and steady state deformations and breakup of dispersed-phase droplets of immiscible polymer blends in steady shear flow. Polymer, 48, 3822-3835

7) Thuwachawsoan, K., Chotpattananont, D., Sirivat, A., Rujiravanit, R., Schwank, J. (2007) Electrical conductivity responses and interactions of poly(3-thiopheneacetic acid)/zeolites L, mordernite, beta and H_2. Materials Science and Engineering B, 140, 23-30.

8) Tangboriboon, N., Jamieson, A.M., Sirivat, A., Wongkasemjit, S. (2007) A novel route to perovskite lead zirconate from lead glycolate and sodium tris(glycozirconate) via the sol-gel process. Appl. Organometal. Chem., 21, 849-857.

9) Sukitpaneenit, P, Thanpicha, T., Sirivat, A., Weder, C., Rujiravanit, R. (2007) Electrical conductivity and mechanical properties of polyaniline/natural rubber composite fibers. J. Applied Polymer Science, 106, Issue 6, 4038-4046.

10) Tangboriboon, N., Sirivat, A., Wongkasemjit, S. (2008) Electrorheology and characterization of acrylic rubber and lead titanate composite materials. Applied Organometallic Chemistry, 22, 262-269.

11) Duangprasert, T., Sirivat, A., Siemanond, K., Wilkes, J.O. (2008) Vertical two-phase flow regimes and pressure gradients under the influence of SDS surfactant. Exp. Therm. Fluid Sci., 32, 808-817.

12) Puvanatvattana, T., Chotpattananont, D., Hiamtup, P., Naimlang, S., Kunanuruksapong, R., Sirivat, A., Jamieson, A.M. (2008) Electric field induced stress moduli of polythiophene/polyisoprene suspensions: effects of particle conductivity and concentration. Mat. Sci. Engr. C., 28, Issue 1, 119-128.

13) Tangboriboon, N., Jamieson, A.M., Sirivat, A., Wongkasemjit, S. (2008) A novel route to perovskite lead zirconate titanate from glycolate precursors via the sol-gel process. Applied Organometallic Chemistry 22, 104-113. (ISI Impact Factor: 1.270)

14) Juntanon, K., Niamlang, S., Rujiravanit, R., Sirivat, A. (2008) Electrically controlled release of sulfosalicylic acid from crosslinked poly(vinyl alcohol) hydrogel. Inter. J. Pharmaceutics, 356, 1-11.

15) Hiamtup, P., Sirivat, A., Jamieson, A.M. (2008) Electromechanical response of a soft and flexible actuator based on polyaniline particles embedded in a cross-linked poly(dimethyl siloxane) network. Mat. Sci. Engr. C, 28, Issue 7, 1044-1051.

16) Niamlang, S., Sirivat, A. (2008) Electromechanical responses of a crosslinked polydimethylsiloxane. Macromol. Symp. 264, 176-183.

17) Niamlang, S., Sirivat, A. (2008) Dielectrophoresis force and deflection of electroactive poly(p-phenylene vinylene)/ polydimethylsiloxane blends. Smart Mater. Struct. 17, 1-8.

18) Thanpitcha, T., Sirivat, A., Jamieson, A.M., Rujiravanit, R. (2008) Physical and electrical properties of chlorophyllin/carboxymethyl chitin and chlorophyllin/carboxymethyl chitosan blend films. Macromol. Symp. 264, 168-175.

19) Hiamtup, P., Sirivat, A., Jamieson, A.M. (2008) Hysteresis and strain hardening in the creep response of a polyaniline ER fluid. Journal of Colloid and Interface Science. 325, 122-129.

20) Kunanuruksapong, R., Sirivat, A. (2008) Electrical properties and electromechanical responses of acrylic elastomers and styrene copolymers: effect of temperature. Applied Physics A. 92, 313-320.

21) Hiamtup, P., Sirivat, A., Jamieson, A.M. (2008) Field strength dependence of the high-frequency viscoelastic relaxation process in polyaniline/silicone oil electrorheological suspensions. Express Polymer Letters. Vol.2, No.10, 688-694.

22) Pattamaprom, C, Larson, R.G., Sirivat, A. (2008) Determining polymer molecular weight distributions from rheological properties using the dual-constraint model. Rheol. Acta, 47, 689-700.

23) Wannatong, L., Sirivat, A. (2008) Polypyrrole and its composites with 3A zeolite and polyamide 6 as sensors for four chemicals in lacquer thinner. Reactive and Functional Polymers, 68, 1645-1649.

24) Thipdech, P., Kunanuruksapong, R., Sirivat, A. (2008) Electromechanical responses of poly(3-thiopheneacetic acid)/acrylonitrile-butadiene rubbers. Express Polymer Letters, Vol 2, 12, 866-877.

25) Thanpitcha, T., Sirivat, A., Jamieson, A.M., Rujiravanit, R. (2008) Synthesis of polyaniline nanofibrils using an in situ seeding technique. Synthetic Metals, 158, 695-703.

26) Thanpitcha, T., Sirivat, A., Jamieson, A.M., Rujiravanit, R. (2008) Dendritic polyaniline nanoparticles synthesized by carboxymethyl chitin templating. European Polymer Journal, 44, 3423-3429.

27) Prissanaroon, W., Pigram, P., Jones, R., Sirivat, A. (2008) A novel pH sensor based on hydroquinone monosulfonate-doped conducting polypyrrole. Sensors and Actuators B, 135, 366-374.

28) Wichiansee, W., Sirivat, A. (2008) Electrorheological properties of poly(dimethylsiloxane) and poly(3,4-ethylenedioxy thiophene)/poly(styrene sulfonic acid) blends. e-Polymers, 110.

29) Chotpattananont, D., Sirivat, A., Jamieson, A.M. (2008) Electric field induced gelation of poly(3-thiopheneacetic acid) polydi-methylsiloxane fluids. The Open Colloid Science Journal, 1, 1-9.

30) Hachawee, K., Lerdwijitjarud, W., Sittattrakul A., Sirivat, A. 2008 Structural effect of ferrocenecarboxymethylated polymers on their electrical behavior under the exposure to methanol and acetone vapors. Materials Science and Engineering B, 153, 10-20.

31) Wichiansee, W., Sirivat, A. (2009) Electrorheological properties of poly(dimethylsiloxane) and poly(3,4-ethylenedioxy thiophene)/poly(stylene sulfonic acid)/ethylene glycol blends. Materials Science and Engineering C, 29, 78-84.

32) Prissanaroon, W., Pigram, P., Jones, R., Sirivat, A. (2009) A sensitive and highly stable polypyrrole-based pH sensor with hydroquinone monosulfonate and oxalate co-doping. Sensors and Actuators B: 138, Issues2, 504-511.

33) Niamlang, S., Sirivat, A. (2009) Electrically controlled release of salicylic acid from poly(p-phenylene vinylene)/polyacrylamide hydrogels. International Journal of Pharmaceutics, 37, Issues 1-2, 126-133.

34) Tangboriboon, N., Sirivat, A., Kunanuruksapong, R., Wongkasemjit, S. (2009) Electrorheological properties of novel piezoelectric lead zirconate titanate $Pb(Zr_{0.5},Ti_{0.5})O_3$-acrylic rubber composites. Materials Science and Engineering C, 29, Issues 6, 1913-1918.

35) Thanpitcha, T., Sirivat, A., Jamieson, A.M., Rujiravanit, R. (2009) Polyaniline nanoparticles with controlled sizes using a cross-linked carboxymethyl chitin template. Journal of Nanoparticle Research, Volume 11, Issue 5, 1167-1177.

36) Chansai, P., Sirivat*, A., Niamlang, S., Chotpattananont, D., Viravaidya-Pasuwat, K. (2009) Controlled trandermal iontophoresis of sulfosalicylic acid from polypyrrole/poly(acrylic acid) hydrogel, International Journal of Pharmaceutics, 381, 25-33. (ISI Impact Factor: 3.350)

37) Phumman, P., Niamlang, S., Sirivat*, A. (2009) Fabrication of poly(p-phenylene)/zeolite composites and their responses towards ammonia. Sensors, 9, 8031-8046. (ISI Impact Factor: 1.739)

38) Janpaen, V., Niamlang S., Lerdwijitjarud, W., Sirivat*, A. (2009) Oscillatory shear induced droplet deformation and breakup in immiscible polymer blends.Physics of Fluids, 21, Issue 6, pp. 063102-063102-10. (ISI Impact Factor: 1.926)

39) Niamlang, S., Sirivat*, A. (2009) Electric field assisted transdermal

drug delivery from salicylic acid-loaded polyacrylamide hydrogels. Drug Delivery, 16, Issue 7, 378-388. (ISI Impact Factor: 1.456)

40) Thongchai, N., Kunanuruksapong, R., Niamlang, S., Wannatong, L., Sirivat*, A., Wongkasemjit, S. (2009) Interactions between CO and poly(*p*-phenylene vinylene) as induced by ion-exchanged Zeolites. Materials, *2*(4), 2259-2275. (ISI Impact Factor:1.677)

41) Hiamtup, P., Sirivat*, A., Jamieson A.M. (2010)Strain-hardening in the oscillatory shear deformation of a dedoped polyaniline electrorheological fluid. Journal of Materials Science, 45, 1972-1976 (ISI Impact Factor: 2.015)

42) Thongsak K., Kunanuruksapong R., Sirivat*, A., Lerdwijitjarud W. (2010) Electroactive styrene–isoprene–styrene triblock copolymer: Effects of morphology and electric field. Materials Science and Engineering A, Volume 527, Issues 10-11, 2504-2509 (ISI Impact Factor: 2.003)

43) Thanpitcha, T., Sirivat, A., Jamieson, A.M., Rujiravanit*, R. (2010) Fabrication and properties of solution-cast polyaniline/carboxymethylchitin blend films. Journal of Applied Polymer Science, Volume 116, Issue 3, 1626-1634. (ISI Impact Factor: 1.289)

44) Tangboriboon, N., Uttanawanit, N., Longtong, M., Wongpinthong, P., Sirivat*, A., Kunanuruksapong, R. (2010) Electrical and electrorheological properties of alumina/natural rubber (STR XL) composites. Materials, 3, 656-671. (ISI Impact Factor: 1.677)

45) Kamonsawas, J., Sirivat*, A., Niamlang S., Hormnirun, P., Prissanaroon, W. (2010) Electrical conductivity response of poly(Phenylene-vinylene)/ zeolite composites exposed to ammonium nitrate. *Sensors*, *10(*6), 5590-5603. (ISI Impact Factor: 1.739)

46) Changkhamchom, S., Sirivat*, A. (2010) Synthesis and properties of sulfonated poly(ether ketone ether sulfone) (S-PEKES) via bisphenol S: effect of sulfonation. Polymer Bulletin, Volume 65, 265-281. (ISI Impact Factor: 1.532)

47) Ludeelerd, P., Niamlang, S., Kunaruksapong, R., Sirivat*, A. (2010) Effect of elastomer matrix type on electromechanical response of conductive polypyrrole/elastomer blends. Journal of Physics and Chemistry of Solids, 71, Issue 9, 1243-1250. (ISI Impact Factor: 1.632)

48) Kunchornsup, W., Sirivat*, A. (2010) Effects of crosslinking ratio and aging time on properties of physical and chemical cellulose gels via1-butyl-3-methylimidazolium chloride solvent. Journal of Sol-Gel Science and Technology, Volume 56, 19-26. (ISI Impact Factor: 1.632)

49) Tangboriboon, N., Wongkasemjit, S., Kunanuruksapong, R., Sirivat*, A. (2011) An innovative synthesis of calcium zeolite type a catalysts from eggshells via the sol–gel process. Journal of Inorganic and Organometallic Polymers and Materials, 21, 50-60. (ISI Impact Factor: 1.452)

50) Tangboriboon, N., Khongnakhon, T., Kittikul, S., Kunanuruksapong, R., Sirivat*, A. (2011) An innovative $CaSiO_3$ dielectric material from eggshells by sol–gel process. Journal of Sol-Gel Science and Technology, Volume 58, Number 1, 33-41. (ISI Impact Factor: 1.632)

51) Kunanuruksapong, R., Sirivat*, A. (2011) Effect of dielectric constant and electric field strength on dielectrophoresis force of acrylic elastomers and styrene copolymers. Current Applied Physics, 11, 393-401. (ISI Impact Factor: 1.900)

52) Tangboriboon, N., Wongpinthong, P., Sirivat*, A., Kunanuruksapong, R. (2011) Electroactive alumina particles embedded in an acrylic elastomer. Polymer Composites, Volume 32, Issue 1, 44–51. (ISI Impact Factor: 1.231)

53) Thongsak, K., Kunanuruksapong, R., Sirivat*, A., Lerdwijitjarud, W. (2011) Electroactive polydiphenylamine/poly(styrene-block-isoprene-block-styrene) (SIS) blends: Effects of particle concentration and electric field. Materials Science and Engineering: C, Volume 31, Issue 2, 206-214. (ISI Impact Factor: 2.686)

54) Sirivat*, A., Patako, S., Niamlang, S., Lerdwijitjarud, W. (2011) Drop deformation and breakup in polystyrene/high-density polyethylene blends under oscillatory shear flow. Physics of Fluids, 23,1, 1-12. (ISI Impact Factor: 1.926)

55) Intanoo, P., Sirivat*, A., Kunanuruksapong, R., Lerdwijitjarud, W. (2011) Electromechanical properties of ethylene propylene diene elastomers: Effect of ethylene norbornene content. Materials Sciences and Applications, 2, 307-313. (ISI Impact Factor:)

56) Tangboriboon, N., Longtong, M., Sirivat*, A., Kunanuraksapong, R. (2011) Electrical and electromechanical properties of alumina/natural rubber STR 5L composites. Materials Technology, Volume 26, Issue 2, 100-106. (ISI Impact Factor: 0.591)

57) Yimlamai, I., Niamlang, S., Chanthaanont, P., Kunanuruksapong, P., Changkhamchom, S., Sirivat*, A. (2011) Electrical conductivity response and sensitivity of ZSM-5, Y, and mordenite zeolites towards ethanol vapor. Ionics, Volume 17, 607-615. (ISI Impact Factor: 1.288)

58) Thanpitcha, T., Li, Z.,Rujiravanit*, R., Sirivat, A.,Jamieson, A.M. (2011) Anomalous rheology of polypyrrole nanoparticle/alginate suspensions: effect of solids volume fraction, particle size, and electronic state. Rheologica Acta , Volume 50, 809-823. (ISI Impact Factor: 2.027)

59) Auimviriyavat, J., Changkhamchom, S., Sirivat*, A. (2011) Development of poly(ether ether ketone) (peek) with inorganic filler for direct methanol fuel Cells (DMFCS). Industrial and Engineering Chemistry Research, Volume 50, Issue 22, 12527-12533 (ISI Impact Factor: 2.206)

60) Tangboriboon, N., Phudkrachang, P., Kunanuruksapong, R. Sirivat*, A. (2011) Removing extractable protein in natural rubber latex by calcium chloride from chicken eggshells. Rubber Chemistry and Technology, Volume 84 Issue 4, 543-564(ISI Impact Factor: 0.438)

61) Tangboriboon, N., Phudkrachang, P., Kasemsumran, S., Kunanuruksapong, R., Sirivat*, A. (2012) An innovative measurement of extractable proteins from concentrated latex containing eggshell calcium oxide compounds by near-infrared spectroscopy. Spectroscopy Letter, Volume 45, 29-39. (ISI Impact Factor: 0.667)

62) Tangboriboon, N., Chaisakrenon, S., Banchong, A., Kunanuruksapong, R., Sirivat*, A. (2012) Mechanical and electrical properties of alumina/natural rubber composites. Journal of Elastomers & Plastics Volume 44 Issue 1, 21-41. (ISI Impact Factor: 0.623)

63) Chanthaanont, P., Sirivat*, A. (2012) Interaction of carbon monoxide with PEDOT-PSS/zeolite composite:effect of Si/Al ratio of ZSM-5 zeolite. e-Polymers, No. 010, 1-11. (ISI Impact Factor: 0.400)

64) Kunchornsup, W., Sirivat*, A. (2012) Physically cross-linked cellulosic gel via 1-butyl-3-methylimidazolium chloride ionic liquid and its electromechanical responses. Sensors & Actuators A, 175, 155-164. (ISI Impact Factor: 1.841)

65) Tungkavet, T., Sirivat*, A. (2012) Bio-compatible gelatins (Ala-Gly-Pro-Arg-Gly-Glu-4Hyp-Gly-Pro-) and electromechanical properties: effects of temperature and electric field. Journal of Polymer Research, Volume19, Issue 1, Article Number 9759, 1-9. (ISI Impact Factor: 2.019)

66) Tungkavet, T., Seetapan, N., Pattavarakorn D., Sirivat*, A. (2012) Improvements of electromechanical properties of gelatin hydrogels by blending with nanowire polypyrrole: effects of electric field and temperature. Polymer International, Volume 61 Issue 5, 825-833. (ISI Impact Factor: 2.125)

67) Petcharoen, K., Sirivat*, A. (2012) Synthesis and characterization of magnetite nanoparticles via the chemical co-precipitation method. Materials Science and Engineering B, Volume 177, Issue 5, 421-427. (ISI Impact Factor: 1.846)

68) Paradee, N., Sirivat*, A., Niamlang, S., Prissanaroon-Ouajai, W. (2012) Effects of crosslinking ratio, model drugs, and electric field strength on electrically controlled release for alginate-based hydrogel. Journal of Materials Science- Materials in Medicine, Volume 23, Issue 4, 999-1010. (ISI Impact Factor: 2.141)

69) Kunanuruksapong, R., Sirivat*, A. (2012) Dielectrophoresis force of poly(p-phenylene)/acrylic elastomer under ac electric field. Materials Research Innovations, Volume 16, Issue 2, 135-142. (ISI Impact Factor: 0.321)

70) Tangboriboon, N., Kunanuruksapong, R., Sirivat*, A. (2012) Meso-porosity and phase transformation of bird eggshells via pyrolysis. Journal of Ceramic Processing Research. Volume 13, 413-419. (ISI Impact Factor: 0.333)

71) Tangboriboon, N., Sirivat*, A., Kunanuruksapong, R. Wongkasemjit, S. (2012) Electroactive perovskite lead zirconate particles embedded in an acrylic elastomer. e-Polymers, No. 059, 1-18. (ISI Impact Factor: 0.400)

72) Sittiwong, J., Niamlang, S., Paradee, N., Sirivat*, A. (2012) Electric field-controlled benzoic acid and sulphanilamide delivery from poly(vinyl alcohol) hydrogel. AAPS

PharmSciTech, Volume 13, Issue 4, 1407-1415 (ISI Impact Factor: 1.584)

73) Intanoo, P., Sirivat*, A., Kunanuruksapong, R., Lerdwijitjarud, W., Kunchornsup, W. (2012) Electroactive polymer actuator from highly doped permethylpolyazine dispersed in ethylene propylene diene elastomer. Journal Polymer Research, Volume 19, Issue 10, Article Number 9981,1-10 (ISI Impact Factor: 2.019)

74) Permpol, T., Sirivat*, A., Supaphol, P., Wannatong, L.(2012) Polydiphenylamine-polyethylene oxide blends as methanol sensing materials. Polymer Technology, Volume 31, No.4, 401-413. (ISI Impact Factor: 1.096)

75) Macksasitorn, S., Changkhamchom, S., Sirivat*, A., Siemanond, K.(2012) Sulfonated poly(ether ether ketone) and sulfonated poly(1,4-phenylene ether ether sulfone membranes for vanadium redox flow batteries. High Performance Polymers, Volume 24, Issue 7, 603-608. (ISI Impact Factor: 0.850)

76) Kamonsawas, J., Sirivat*, A., Hormnirun, P. (2012) Poly(p-phenylene vilnylene)/zeolite Y composite as a ketone vapors sensor: effect of alkaline cation. Journal of Polymer Research, Volume 19, Issue 12, Article Number 20, 1-12. (ISI Impact Factor: 2.019)

77) Tangboriboon, N., Kunanuruksapong, R., Sirivat*, A. (2012) Preparation and properties of calcium oxide from eggshells via calcinations. Materials Science-Poland, Volume 30, Issue 4, 313-322. (ISI Impact Factor: 0.258)

78) Tangboriboon, N., Pakdeeniti, S., Kunanuruksapong, R., Sirivat*, A. (2012) Calcium silicate ($CaSiO_3$) as alternative ionic coagulant and solid lubricant for ceramic molds in natural rubber latex film preparation. Rubber Chemistry and Technology, Volume 85, No. 4, 645-660. (ISI Impact Factor: 0.438)

79) Changkhamchom, S., Sirivat*, A. (2013) Polymer electrolyte membrane based on sulfonated poly(ether ketone ether sulfone) (S-PEKES) with low methanol permeability for direct methanol fuel cell application. Polymer-Plastics Technology and Engineering, Volume 52, 70–79. (ISI Impact Factor: 1.481)

80) Tangboriboon, N., Chaisakrenon S., Banchong A., Kunanuruksapong, R., Sirivat*, A. (2013) Mechanical and electrical properties of alumina–natural rubber composites. Plastics Rubber and Composites, Volume 42, 26-33. (ISI Impact Factor: 0.631)

81) Tangboriboon, N, Datsanae, S., Onthong, A., Kunanuruksapong, R.,Sirivat*, A. (2013) Electromechanical responses of dielectric elastomer composite actuators based on natural rubber and alumina. Journal of Elastomers & Plastics, Volume 45, 143- 161. (ISI Impact Factor: 0.623)

82) Kunanuruksapong, R., Sirivat*, A. (2013) Highly electroresponsive polymer blends of polyaniline nanoparticles and chloroprene Rubbers. Advances in Polymer Technology, Volume 32, 556-571. (ISI Impact Factor: 1.096)

83) Tungkavet, T., Sirivat*, A., Seetapan, N., Pattavarakorn, D. (2013) Stress relaxation behavior of (Ala-Gly-Pro-Arg-Gly-Glu-4Hyp-Gly-Pro-) gelatin hydrogels under electric eld: Time-electric eld superposition. Polymer, Volume 54, 2414-2421. (ISI Impact Factor: 3.379)

84) Kamonsawas, J., Sirivat*, A., Hormnirun, P. (2013) Sensitive and selective responses of poly(para-phenylene vinylene)/zeolite Y-based sensors toward ketone vapors. International Journal of Polymeric Materials and Polymeric Biomaterials, Volum 62, Issue 11, 583-589. (ISI Impact Factor: 1.865)

85) Petcharoen, K., Sirivat*, A.(2013) Electrostrictive properties of thermoplastic polyurethane elastomer: Effects of urethane type and soft-hard segment composition. Current Applied Physics, Volume 13, Issue 6, 1119-1127. (ISI Impact Factor: 1.814)

86) Tangboriboon, N., Phudkrachang, P., Mulsow, L.-O., Kunchornsup, W., Sirivat*, A.(2013) Removal of water extractable proteins from concentrated natural rubber latex by eggshells.Journal of Elastomers and Plastics, Volume 45, Issue 3, 253-269. (ISI Impact Factor: 0.623)

87) Permpool, T., Sirivat*, A., Aussawasathien, D., Wannatong, L. (2013) Development of polydiphenylamine/zeolite Y composite by dealumination process as a sensing material for halogenated solvents. Polymer-Plastics Technology and Engineering, Volume 52, Issue 9, 907-920 (ISI Impact Factor: 1.481)

Conference Proceedings

1) Kunanuruksapong, R., Sirivat, A. (2007)
Effect of temperature on the electromechanical properties of elastomers. ICheaP-8, Ishia, Italy, 24-27 June 2007.

2) Hiamtup, P., Sirivat, A. (2007)
Creep and recovery behaviors of polyaniline/silicone oil suspension under electric field. ICheaP-8, Ishia, Italy, 24-27 June 2007.

3) Niamlang, S., Sirivat, A. (2007)
The electro-responsive drug delivery from salicylic acid- loaded polyacrylamide hydrogels. ICheaP-8, Ishia, Italy, 24-27 June 2007.

4) Hiamtup, P., Sirivat, A. (2007)
Creep and recovery behaviors of polyaniline/silicone oil suspension under electric field. ICAPP 2007, Bangkok, Thailand, 25-28 June 2007.

5) Niamlang, S., Sirivat, A. (2007)
The electric field assisted drug release from polyacrylamide hydrogels. ICAPP 2007, Bangkok, Thailand, 25-28 June 2007.

6) Niamlang, S., Sirivat, A. (2007)
Electromechanical response of a cross-linked silicone elastomer. ICAPP 2007, Bangkok, Thailand, 25-28 June 2007.

7) Kunanuruksapong, R., Sirivat, A. (2007)
The effect of temperature on the electrorheological properties of various types of elastomers. ICAPP 2007, Bangkok, Thailand, 25-28 June 2007.

8) Phumman, P., Sirivat, A. (2007)
Fabrication of poly(p-phenylene)/zeolite composite as ammonia sensor. The effect of temperature on the electrorheological properties of various types of elastomers. ICAPP 2007, Bangkok, Thailand, 25-28 June 2007.

9) Thipdech, P., Sirivat, A. (2007)
Development of polythiophene/acrylonitrile-butadiene rubbers for artificial muscle. ICAPP 2007, Bangkok, Thailand, 25-28 June 2007.

10) Juntanon, K., Sirivat, A. (2007)
Controlled release of sulfosalicylic acid from poly(vinyl alcohol) hydrogel by electrical stimulation. ICAPP 2007, Bangkok, Thailand, 25-28 June 2007.

11) Chootongchai, S., Sirivat, A. (2007)
Vertical two-phase flow regime and pressure gradient under the influence of pipe diameter sizes and benzalkonium chloride surfactants. ICAPP 2007, Bangkok, Thailand, 25-28 June 2007.

12) Thanpicha, T., Sirivat, A., Jamieson, AM., Rujiravanit, R. (2007)
Physical and electrical properties of chlorophyllin/carboxymethyl chitin and chlorophyllin/ carboxymethyl chitosan blend films.
ICAPP 2007, Bangkok, Thailand, 25-28 June 2007.

13) Sukitpaneenit, P., Thanpicha, P., Sirivat, A., Weder, C., Rujiravanit, R., (2007) Preparation and characterization of polyaniline/natural rubber composite films. ICAPP 2007, Bangkok, Thailand, 25-28 June 2007.

14) Phumman, P., Sirivat, A. (2007)
Electrical conductivity response of poly(p-phenylene)/ZSM-5 composite. Proceedings of 7th IEEE-Nano Conference, Hongkong, China, 2-5 August 2007.

15) Kunanuruksapong, R., Sirivat, A. (2007)
Effects of temperature and dielectric permittivity on electrorheological Properties of Elastomers. Proceedings of 7th IEEE-Nano Conference, Hongkong, China, 2-5 August 2007.

16) Thipdech, P., Sirivat, A. (2007)
Polythiophene/acrylonitrile-butadiene rubber as an artificial muscle. Proceedings of 7th IEEE-Nano Conference, Hongkong, China, 2-5 August 2007.

17) Naimlang, S., Sirivat, A. (2007)
The electric field assisted drug release from polyacrylamide hydrogels. Proceedings of 7th IEEE-Nano Conference, Hongkong, China, 2-5 August 2007.

18) Juntanon, K., Sirivat, A. (2007)
Electric field-induced release of sulfosalicylic acid from poly(vinyl alcohol) hydrogel. Proceedings of 7th IEEE-Nano Conference, Hongkong, China, 2-5 August 2007.

19) Kunanuruksapong, R., Sirivat, A. (2008)
Dielectrophoresis force and the electromechanical responses of elastomers. 3rd International Conference Smart Materials Structures Systems. Acireale, Sicily, Italy, 8-13 June 2008.

20) Changkhamchom, S., Sirivat, A. (2008)
Sulfonated poly(ether ether ketone) (S- PEEK) as derived from bisphenol-S for PEN 3rd International Conference Smart Materials Structures Systems. Acireale, Sicily, Italy, 8-13 June 2008.

21) Niamlang S., Sirivat, A., (2008)
Effect of electric field strength on the diffusion of salicylic acid through polyacrylamide hydrogels. 3rd International Conference Smart Materials

Structures Systems. Acireale, Sicily, Italy, 8-13 June 2008.

22) Chansai P., Sirivat, A., (2008)
Electrical field responsive polypyrole in poly(acrylic acid) hydrogel for transdermal drug delivery. 3rd International Conference Smart Materials Structures Systems. Acireale, Sicily,Italy, 8-13 June 2008

23) Kunanuruksapong, R., Sirivat, A. (2009)
A study of the dielectrophoresis force of elastomeric materials for artificial muscle applications. Proceedings of 16th SPIE, San Diego, USA, 8 – 12 March 2009.

24) Chanthananont, P., Sirivat, A. (2009)
Carbon monoxide detection by PEDOT-PSS/zeolite composites gas sensing materials. Proceedings of 16th SPIE, San Diego, USA, 8 – 12 March 2009.

25) Changkhamchom, S., Sirivat, A. (2009)
Development of proton exchange membrane from bisphonol S for using in direct methanol fuel cell. Proceedings of 16th SPIE, San Diego, USA, 8 – 12 March 2009.

26) Tangboriboon, N., Wongpinthong, P., Sirivat, A., Kunanuruksapong, R. (2009) An innovation of embedded alumina/acrylic rubber composite materials. Proceedings of 14th International Conference on NIR Spectroscopy, Bangkok, Thailand, 9-13 November 2009.

27) Kunchornsup, W., Sirivat, A. (2010)
Novel cellulosic gel preparation for using in electro-responsive applications. SPIE Smart Structures/NDE, San Diego, USA , 7 - 11 March 2010.

28) Aiumviriyavat, J., Sirivat, A. (2010)
Development of poly(ether ether ketone) with inorganic filer for direct methanol fuel cells (DMFCs). The 1st National Research Symposium on Petroleum, Petrochemicals, and Advanced Materials and The 16th PPC Symposium on Petroleum, Petrochemicals, and Polymers, Bangkok, Thailand, 22 April 2010.

29) Konkayan, S., Sirivat, A. (2010)
Development of polt(3-thiopheneacetic acid)/zeolite Y as a gas sensor for ammonia. The 1st National Research Symposium on Petroleum, Petrochemicals, and Advanced Materials and The 16th PPC Symposium on Petroleum, Petrochemicals, and Polymers, Bangkok, Thailand, 22 April 2010.

30) Tungkavet, T., Sirivat, A. (2010)
A study of electromechanical properties on gelatin at various gel strength as an actuator or an artificial muscle. The 1st National Research Symposium on Petroleum, Petrochemicals, and Advanced Materials and The 16th PPC Symposium on Petroleum, Petrochemicals, and Polymers, Bangkok, Thailand, 22 April 2010.

31) Intanoo, P., Sirivat, A. (2010)
Electromechanical properties of permethylpolyazine-ethylene propylene diene elestomer (EPDM) blends. The 1st National Research Symposium on Petroleum, Petrochemicals, and Advanced Materials and The 16th PPC Symposium on Petroleum, Petrochemicals, and Polymers, Bangkok, Thailand, 22 April 2010.

32) Permpool, T., Sirivat, A. (2010)
Electrospun polydiphenylamine-polyethylene oxide as a methanol sensor. The 1st National Research Symposium on Petroleum, Petrochemicals, and Advanced Materials and The 16th PPC Symposium on Petroleum, Petrochemicals, and Polymers, Bangkok, Thailand, 22 April 2010.

33) Kamonsawas, J., Sirivat, A., Hormnirun, P., Prissanaroon, W. (2010)
Poly(phenylene vinylene)/zeolite Y composites responses towards ammonium nitrate vapor.6th NCCC, Bangkok, Thailand, 26-27 August 2010.

34) Cheawchanpattanagone, L., Sirivat, A., Siemanond, K. (2011)
Processing of iron nuggets from low grade iron ore. The 17th PPC Symposium on Petroleum, Petrochemicals, and Polymers, Bangkok, Thailand, 26 April 2011.

35) Macksasitorn, S., Sirivat, A., Siemanond, K. (2011)
Properties comparison of sulfonated poly(ether ether ketone) and sulfonated poly(1,4-phenylene ether ether sulfone) membranes for vanadium redox flow battery. The 17th PPC Symposium on Petroleum, Petrochemicals, and Polymers, Bangkok, Thailand, 26 April 2011.

36) Taweekarn, N., Sirivat, A. (2011)
Synthesis and characterization of sulfonated poly(aromatic imide-co-aliphatic imide) (S-coPI) for direct methanol fuel cell. The 17th PPC Symposium on Petroleum, Petrochemicals, and Polymers, Bangkok, Thailand, 26 April 2011.

37) Mungkalodom, P., Sirivat, A. (2011)
Synthesis and characterization of poly(2,5-dimethoxyaniline) for use as electrochromic smart materials. The 17th PPC Symposium on Petroleum, Petrochemicals, and Polymers, Bangkok, Thailand, 26 April 2011.

38) Rattana, M., Sirivat, A. (2012)
Controlled release of salicylic acid from gelatin hydrogel. The 3rd Research Symposium on Petrochemical and Materials Technology and The 18th PPC Symposium on Petroleum, Petrochemicals, and Polymers, Bangkok, Thailand, 24 April 2012.

39) Suephatthima, B., Sirivat, A. (2012)
Physical and electrochromic properties of poly(2,5-dimethoxy aniline) synthesized in oxalic, nitric, and hydrochloric acids. The 3rd Research Symposium on Petrochemical and Materials Technology and The 18th PPC Symposium on Petroleum, Petrochemicals, and Polymers, Bangkok, Thailand, 24 April 2012.

40) Supattarasakda, K., Sirivat, A. (2012)
Synthesis and characterization of size-controlled hematite (α-Fe_2-O_3) nanoparticles via the chemical precipitation method. The 3rd Research Symposium on Petrochemical and Materials Technology and The 18th PPC Symposium on Petroleum, Petrochemicals, and Polymers, Bangkok, Thailand, 24 April 2012.

41) Umsarika, P., Suphapol, P., Sirivat, A. (2012)
Novel proton exchange sulfonated polyimide membrane for direct methanol fuel cell. The 3rd Research Symposium on Petrochemical and Materials Technology and The 18th PPC Symposium on Petroleum, Petrochemicals, and Polymers, Bangkok, Thailand, 24 April 2012

42) Rojanakatanyoo, S., Sirivat, A., Siemanont, K. (2012)
Processing of iron nuggets from low grade iron ore. The 3rd Research Symposium on Petrochemical and Materials Technology and The 18th PPC Symposium on Petroleum, Petrochemicals, and Polymers, Bangkok, Thailand, 24 April 2012.

43) Pinit, J., Sirivat, A. (2013)
Electrochromic properties of poly(o-toluidine) coated on indium tin oxide (ITO) plastic. PETROMAT and PPC SYM 2013, Bangkok, Thailand, 23 April 2013

44) Charoonrak, N., Sirivat, A. (2013)
Development of poly(p-phenylene)/crosslinked poly(ε-caprolactone) as electroactive shape memory composite. PETROMAT and PPC SYM 2013, Bangkok, Thailand, 23 April 2013

45) Kotaphan, P., Sirivat, A., Schwank, J. (2013)
Composite membrane of sulfonated poly(2,6-dimethyl-1,4-phenylene oxide) and zeolite for direct methanol fuel cell applications. PETROMAT and PPC SYM 2013, Bangkok, Thailand, 23 April 2013

46) Pairatwachapun S., Sirivat, A. (2013)
Electrically-controlled release of acetylsalicylic acid from carrageenan hydrogel. PETROMAT and PPC SYM 2013, Bangkok, Thailand, 23 April 2013

47) Srisawasdi, T., Sirivat, A., Jamieson A.M. (2013)
Silk fibroin/polycarbazole composite as artificial muscle. PETROMAT and PPC SYM 2013, Bangkok, Thailand, 23 April 2013

Oral Presentations

1) Kunanuruksapong, R., Sirivat, A. (2008)
The effect of elastomers type on the electromechanical responses and dielectrophoresis force.Thai-Japan joint Symposium on Advances in Materials Science and Environmental Technology, Bangkok Thailand, 19-20 August 2008.

2) Naimlang, S., Sirivat, A. (2008)
The release characteristic of salicylic acid from salicylic acid doped poly(p-phenylene vinylene)-looaded polyacrylamide hydrogel.
Thai-Japan Joint Symposium on Advances in Materials Science and Environmental Technology, Bangkok Thailand, 19-20 August 2008.

3) Changkhamchom, S., Sirivat, A. (2008)
Development sulfonated poly(ether ether ketone) for proton exchange membrane. ChemBio tech'08, Singapore, 19-20 December 2008.

4) Kunanuruksapong, R., Sirivat, A. (2009)
A study of the dielectrophoresis force of elastomeric materials for artificial muscle applications. RGJ Seminar Series LXII, Bangkok Thailand, 7 August 2009.

5) Chanthaanont, P., Sirivat, A. (2010)
Electrical conductivity response of PEDOT-PSS/zeolite to SO_2.
RGJ-Ph.D. Congress XI, Chonburi, Thailand, 1-3 April 2010.

6) Changkhamchom, S., Sirivat, A. (2010)
Electrical properties and methanol permeability of synthesized sulfonated poly(Ether ketone ether sulfone) (S-PEKES). RGJ-Ph.D. Congress XI, Chonburi, Thailand, 1-3 April 2010.

7) Sirivat, A. (2011)
Development of conductive polymers for sensor actuator and drug delivery applications. 37th Congress on Science and Technology of Thailand, Centara Grand Hotel, Bangkok Convention Center, 11 October 2011.

8) Sirivat, A. (2012)
Conductive and Electroactive Polymers: Actuation and Drug Controlled Release. การประชุมนักวิจัยรุ่นใหม่ พบ เมธีวิจัยอาวุโส สกว. ครั้งที่ 12, เพชรบุรี, 10-12 October 2012. [Invited Speaker]

9) Paradee, N., Sirivat, A. (2013)
Electrically-assisted transdermal delivery of drug from Ca-alginate hydrogel. CEAP 2013, Bangkok, Thailand, 22 April 2013

10) Kamonsawas, J., Sirivat, A., Hormnirun, P. (2013)
Sensitive and selective sensors based on poly(para-phenylene vinylene)/zeolite composites: Influece of alkaline cation. CEAP 2013, Bangkok, Thailand, 22 April 2013

11) Niamlang, S., Buranut, A., Niansiri, A., Sirivat, A. (2013)
Controlled aloin release from crosslinked polyacrylamide hydrogel: Effect of mesh size, electric field strength and conductive polymer. CEAP 2013, Bangkok, Thailand, 22 April 2013

12) Changkhamchom, S., Sirivat, A. (2013)
Sulfonated poly(ether ketone ether sulfone) (S-PEKES)/zeolite proton exchange membranes for direct methanol fuel cell. CEAP 2013, Bangkok, Thailand, 22 April 2013

13) Tungkavet, T., Seetapan, N., Pattavarakornt, D., Sirivat, A. (2013)
Effect of electric field and crosslinking ratios on stress relaxation of gelatin hydrogel. CEAP 2013, Bangkok, Thailand, 22 April 2013

Poster Presentations

1) Niamlang, S., Sirivat, A. (2007)
Electro-responsive drug delivery from salicylic-loaded polyacrylamide hydrogel. IMECE Annual Meeting 2007, Seattle, USA, 10-16 November 2007.

2) Niamlang, S., Sirivat, A. (2008)
Controlled release of salicylic acid from polyacrylamide hydrogel by electric field stimulation. Proceedings of 15th SPIE Conference, San Diego, CA, USA, 9 – 13 March 2008.

3) Niamlang, S., Sirivat, A. (2008)
Electric field sensitive poly(p-phenylene vinylene)/polydimethylsiloxane gel. Proceedings of 15th SPIE Conference, San Diego, CA, USA, 9 – 13 March 2008.

4) Kunanuruksapong, R., Sirivat, A. (2008)
The electrorheological responses and dielectropholysis force of elastomers at

various temperatures. Proceedings of 15th SPIE Conference, San Diego, CA, USA, 9 – 13 March 2008.

5) Niamlang, S., Sirivat, A. (2008)
Electric field enhanced diffusion of salicylic acid through polyacrylamide hydrogel. APS March Meeting 2008, New Orleans, Louisiana, USA, 10 – 14 March 2008.

6) Kamonsawas, J., Sirivat, A. (2008)
Induced interaction of NH4NO3 with poly(p-phenylene vinylene) by means of zeolite Y. APS March Meeting 2008, New Orleans, Louisiana, USA, 10 – 14 March 2008.

7) Thongsak, K., Sirivat, A. (2008)
Styrene – isoprene – styrene triblock copolymer (SIS)/polydiphenylamine blends for actuator application. APS March Meeting 2008, New Orleans, Louisiana, USA, 10 – 14

8) Chansai, P., Sirivat, A. (2008)
Controlled transdermal iontophoresis by polypyrrole/poly(acrylic acid) hydrogel. APS March Meeting 2008, New Orleans, Louisiana, USA, 10 – 14 March 2008.

9) Chanthaanont, P., Sirivat, A. (2008)
Development of PEDOT – PSS/zeolite composites as a gas sensor. APS March Meeting 2008, New Orleans, Louisiana, USA, 10 – 14 March 2008.

10) Changkhamchom, S., Sirivat, A. (2008)
Development of poly(ether ether ketone)(PEEK) derived from bisphenol-S for proton exchange membrane (PEM) in driect methanol fuel cell (DMFC). APS March Meeting 2008, New Orleans, Louisiana, USA, 10 – 14 March 2008.

11) Kunanuruksapong, R., Sirivat, A. (2008)
Effect of elastomers types to the dielectrophoresis force and electromechanical responses. APS March Meeting 2008, New Orleans, Louisiana, USA, 10 – 14 March 2008.

12) Kamonsawas, J., Sirivat, A. (2008)
Electrical conductivity response of Poly(p-phenylene vinylene) /zeolite Y composites response towards NH_4NO_3. SmartMat 2008, Chiang Mai, 22-25 April 2008.

13) Chansai, P., Sirivat, A. (2008)
Controlled trandermal iontophoresis of sulfosalicylic acid from polypyrrole/poly(acrylic acid) Hydrogel. SmartMat 2008, Chiang Mai, 22-25 April 2008.

14) Thongsak, K., Sirivat, A. (2008)
Styrene-isoprene-styrene triblock copolymer (SIS)/polydiphenylamine blends for actuator application. SmartMat 2008, Chiang Mai, 22-25 April 2008.

15) Chanthaanont, P., Sirivat, A. (2008)
Preparation of PEDOT-PSS/zeolite composite as a gas sensor. SmartMat 2008, Chiang Mai, 22-25 April 2008.

16) Changkhamchom, S., Sirivat, A. (2008)
Development of poly(ether ether ketone) (PEEK) derived from 4,4'-sulfonyl-diphenol for proton exchange membrane (PEM) in direct methanol fuel cells (DMFC). SmartMat 2008, Chiang Mai, 22-25 April 2008.

17) Niamlang, S., Sirivat, A. (2008)
Electric field sensitive of polyacrylamide hydrogels: drug delivery application. SmartMat 2008, Chiang Mai, 22-25 April 2008.

18) Kunanuruksapong, R., Sirivat, A. (2008)
The effect of electric field strength on the dielectrophoretic force of elastomers. SmartMat 2008, Chiang Mai, 22-25 April 2008.

19) Changkhamchom, S., Sirivat, A. (2008)
Synthesis of sulfonated poly(ether ether ketone) for proton exchange membrane. Thai-Japan Joint Symposium on Advances in Materials Science and Environmental Technology, Bangkok Thailand, 19-20 August 2008.

20) Chanthananont, P., Sirivat, A. (2008)
PEDOT-PSS/zeolite ZSM-5 composites as gas sensing materials. Thai-Japan Joint Symposium on Advances in Materials Science and Environmental Technology, Bangkok Thailand, 19-20 August 2008.

21) Sirivat, A. (2008)
Conductive polymers as sensors, actuators, and drug delivering devices. การประชุมนักวิจัยรุ่นใหม่ พบ เมธีวิจัยอาวุโส สกว. ครั้งที่ 8, จังหวัดเพชรบุรี, 16-18 ตุลาคม 2551
TRF Young Researchers Meet Maethee Researchers, Chaum, 16-18 October 2008.

22) Changkhamchom, S., Sirivat, A. (2008)
Sulfonated poly(etger ether ketone)(s-peek) for proton exchange membrane (PEM) Nanothailand Symposium 2008, Bangkok Thailand, 6-8 November 2008.

23) Chanthananont, P., Sirivat, A. (2008)
Gas sensing property of pedot–PSS-zeolite composites. Nanothailand Symposium 2008, Bangkok Thailand, 6-8 November 2008.

24) Kunanuruksapong, R., Sirivat, A. (2008)
Dielectrophoresis force and deflection angle of elastomeric materials: Effect of dielectric constant. ChemBio tech'08, Singapore, 19-20 December 2008.

25) Niamlang, S., Sirivat, A. (2008)
Controlled release of salicylic acid from from poly(p-phynylene vinylene)-loaded polyacrylamide hydrogels by electric field stimulation. ChemBio tech'08, Singapore, 19-20 December 2008.

26) Kunanuruksapong, R., Sirivat, A. (2009)
Dielectrophoresis Force and deflection behavior of dielectric elastomers under electric field: Effect of dielectric constants. Hybrid Materials 2009, Tours, France, 15-19 March 2009.

27) Niamlang, S., Sirivat, A. (2009)
Electric field assisted transdermal delivery of salicylic acid from poly(p-phynylene vinylene)- loaded polyacrylamide hydrogels. Hybrid Materials 2009, Tours, France, 15-19 March 2009

28) Niamlang, S., Sirivat, A. (2009)
Iontophoresis of salicylic acid from salicylic acid doped poly(p-phynylene vinylene)/polyacrylamide hydrogels. APS March Meeting, Pittsburgh PA, USA, 16 – 20 March 2009.

29) Chanthananont, P., Sirivat, A. (2009)
Sensitivity enhancement of PEDOT-PSS towards CO by zeolite ZSM-5 additive. APS March Meeting, Pittsburgh PA, USA, 16 – 20 March 2009.

30) Changkhamchom, S., Sirivat, A. (2009)
Development of polymer electrolyte membrane (PEM) from bisphonol S for direct methanol fuel cell (DMFC). APS March Meeting, Pittsburgh PA, USA, 16 – 20 March 2009.

31) Kunanuruksapong, R., Sirivat, A. (2009)
Dielectrophoresis force and actuation of acrylic elastomers and styrene copolymers for artificial muscle applications. Frontiers in Polymer Science 2009, Mainz, Germany,7-9 June 2009.

32) Niamlang, S., Sirivat, A. (2009)
Electric field enhanced diffusion of salicylic acid from salicylic acid doped poly(p-phynylene vinylene) polyacrylamide hydrogels. Frontiers in Polymer Science 2009, Mainz, Germany,7-9 June 2009.

33) Chanthaanont, P., Sirivat, A. (2009)
Electrical conductivity responses of PEDOT- PSS/zeolite composites towards CO. Frontiers in Polymer Science 2009, Mainz, Germany, 7-9 June 2009.

34) Changkhamchom, S., Sirivat, A. (2009)
Modification of poly(ether ether ketone)(PEEK) derived from bisphenol-S as proton exchange membrane (PEM). Frontiers in Polymer Science 2009, Mainz, Germany, 7-9 June 2009.

35) Chanthaanont, P., Sirivat, A. (2009)
PEDOT-PSS/zeolite ZSM-5 composites and electrical conductivity response towards CO.RGJ Seminar Series LXII, Bangkok Thailand, 7 August 2009.

36) Changkhamchom, S., Sirivat, A. (2009)
Synthesis of sulfonated poly(ether ketone ether sulfone) (S-PEKES) and the degree of sulfonation effect in its properties. RGJ Seminar Series LXII, Bangkok Thailand, 7 August 2009.

37) Kamonsawas, J., Sirivat, A. (2011)
Induced interaction of NH_4NO_3 with poly(P-phenylene vinylene) by mean of zeolite Y. SPIE Smart Structures/NDE, San Diego, California United States, 6-10 March 2011

38) Kunanuruksapong, R., Sirivat, A. (2011)
Development of dielectric elastomers for electro-responsive applications. E-NETT 2011, The 7th Conference on Energy Network of Thailand, Phuket, Thailand, 3-5 May 2011.

39) Changkhamchom, S., Sirivat, A. (2011)
Proton conductivity, methanol permeability, and thermal property of a novel sulfonated poly(arylene ether ketone sulfone) electrolyte membrane. E-NETT 2011, The 7th Conference on Energy Network of Thailand, Phuket, Thailand, 3-5 May 2011.

40) Chanthaanont, P., Sirivat, A. (2011)
Effect of univalent cation exchanged zeolites Y on electrical conductivity and response of PEDOT-PSS/zeolite Y Composites toward SO2. 2nd International Symposium Frontiers in Polymer Science, Centre de Congrès, Lyon, France, 29-31 May 2011.

41) Changkhamchom, S., Sirivat A. (2011)
Sulfonated poly(ether ketone ether sulfone) (S-PEKES): Effect of sulfonation degrees on proton conductivities and methanol permeabilities. 2nd International Symposium Frontiers in Polymer Science, Centre de Congrès, Lyon, France, 29-31 May 2011.

42) Paradee, N., Sirivat, A. (2011)
Perparation and characterization of alginate for controlled release application. Chiang Mai International Conference on Biometerials & Applications (CMICBA), The Empress Hotel, Chiang Mai, Thailand, 9-10 August 2011.

43) Kunchornsup, W., Sirivat, Anuvat. (2011)
Electromechanical responses of cellulosic gel prepared via 1-butyl-3-methylimidazolium chloride ionic liquid: Effects of electric field strength and temperature. 2nd Polymer Conference of Thailand (PCT-2), Chulabhorn Research Institute, Bangkok, Thailand, 20-21 October 2011.

44) Permpool, T., Aussawasathien, D., Wannatong, L., Sirivat, A. (2011)
Electrical conductivity responses of polydiphenylamine/zeolite Y composites to halogenated hydrocarbons, 2nd Polymer Conference of Thailand (PCT-2), Chulabhorn Research Institute, Bangkok, Thailand, 20-21 October 2011.

45) Petcharoen, K., Sirivat, A. (2011)
Electrical and magnetic properties of the size-controlled magnetite nanoparticles, 2nd Polymer Conference of Thailand (PCT-2), Chulabhorn Research Institute, Bangkok, Thailand, 20-21 October 2011.

46) Tungkavet, T., Seetapan, N., Pattavarakorn, D., Sirivat, A. (2011)
Electrical response of nanowire polypyrrole/gelatin as an actuator, 2nd Polymer Conference of Thailand (PCT-2), Chulabhorn Research Institute, Bangkok, Thailand, 20-21 October 2011.

47) Umsarika, P., Supaphol P., Sirivat, A. (2012)
Novel proton exchange membrane for direct methanol fuel cell. ACS 2012, San diego, USA, 25-29 March 2012.

48) Suephatthima, B., Sirivat, A. (2012)
Electrochromic properties of poly (2,5- dimethoxy aniline) synthesized in various acids. ACS 2012, San diego, USA, 25-29 March 2012.

49) Kunchornsup, W., Sirivat, A. (2012)
Electroactive 1-butyl-3-methylimidazolium chloride ionic liquid-microcrystalline Cellulose gel for actuator application. CIMTEC 2012, Tuscany, Italy, 10-14 June 2012.

50) Paradee, N., Sirivat, A. (2012)
Calcium-alginate hydrogel for electrically controlled drug release. CIMTEC 2012, Tuscany, Italy, 10-14 June 2012.

51) Kamonsawas J, Sirivat, A., Hormnirn, P., Prissanaroon-Ouajai, W. (2012)
Poly(para-phenylene vinylene)/zeolite Y composites and electrical conductivity response towards ketone vapors. CIMTEC 2012, Tuscany, Italy, 10-14 June 2012.

52) Changkhamchom, S., Sirivat A. (2012)
Novel sulfonated poly(arylene ether ketone sulfone) proton exchange

membrane for using in DMFC. CIMTEC 2012, Tuscany, Italy, 10-14 June 2012.

53) Chanthaanont, P., Sirivat, A. (2012)
Electrical conductivity and response for PEDOT-PSS/ion-exchanged zeolite Y composites toward SO2. CIMTEC 2012, Tuscany, Italy, 10-14 June 2012.

54) Tungkavet, T., Seetapan, N., Pattavarakorn, D., Sirivat, A. (2012)
Nanowire polypyrole and gelatin hydrogels blend for electroactive application. CIMTEC 2012, Tuscany, Italy, 10-14 June 2012.

55) Petcharoen, K., Sirivat, A. (2012)
The effect of reaction temperature and surface modification on magnetite nanoparticles. CIMTEC 2012, Tuscany, Italy, 10-14 June 2012.

56) Permpool, T, Assawasatien, D., Wannathong, L., Sirivat, A. (2012)
Fabrication of polydiphenylamine and zeolite Y composites as a sensing material. CIMTEC 2012, Tuscany, Italy, 10-14 June 2012.

57) Kunchornsup, W., Sirivat, A. (2013)
Polarizability investigation of 1-butyl-3-methylimidazolium cation in electroactive ionic liquid-cellulose gel actuator. SPIE 2013, San diego, USA, 10-14 March 2013.

58) Paradee, N., Sirivat, A. (2013)
Electrically controlled release of tannic acid from calcium-alginate hydrogel in transdermal drug delivery application. SPIE 2013, San diego, USA, 10-14 March 2013.

59) Macksasitorn, S., Changkhamchom, S., Sirivat, A., Siemanond, K. (2013)
Proton exchange membrane based on sulfonated poly(ether ether ketone and sulfonated poly(1,4-phenylene ether ether sulfone) for vanadium redox flow battery. SPIE 2013, San diego, USA, 10-14 March 2013.

60) Pinit, J., Sirivat, A. (2013)
Study of poly(0-toluidine) as electrochromic properties coated on indium tin oxide (ITO). CEAP 2013, Bangkok, Thailand, 22 April 2013.

61) Petcharoen, K., Sirivat, A. (2013)
Electrostrictive performance of thermoplastic elastomer polyurethanes under the influence of electric field. CEAP 2013, Bangkok, Thailand, 22 April 2013.

62) Charoonrak, N., Sirivat, A. (2013)
Development of poly(E-caprolactone)/poly(P-phenylene) as electroactive shape memory polymer blend. CEAP 2013, Bangkok, Thailand, 22 April 2013.

61) Kotaphan, P., Sirivat, A., Schwank, J. (2013)
Preparation and characterization of sulfonated poly(2,6-dimethyl-1,4-phenylene oxide) composite membrane for direct methanol fuel cell. CEAP 2013, Bangkok, Thailand, 22 April 2013.

62) Chanthaanont, P., Sirivat, A. (2013)
Sensitivity and response of PEDOT-PSS/ion-exchanged zeolite Y composite towards SO2. CEAP 2013, Bangkok, Thailand, 22 April 2013.

63) Pairatwachapun, S., Sirivat, A. (2013)
Controlled transdermal delivery of acetylsalicylic acid from carrageenan hydrogel. CEAP 2013, Bangkok, Thailand, 22 April 2013.

64) Srisawasdi, T., Sirivat, A., Jamieson, A.M. (2013)
Developments of polycarbazole/Silk fibroin hydrogel for artificial muscle. CEAP 2013, Bangkok, Thailand, 22 April 2013.

65) Permpool, T., Sirivat, A., Aussawasathien, D., Wannatong, L. (2013)
Dealuminated polydiphenylamine/zeolite Y composite as a sensine material for halogenated Solvents. CEAP 2013, Bangkok, Thailand, 22 April 2013.

66) Kunchornsup, W., Sirivat, A. (2013)
Electromechanical and dielectric properties of ionic liquid/cellulose gel.

CEAP 2013, Bangkok, Thailand, 22 April 2013.

67) Petcharoen, K., Sirivat, A. (2013)
Effect of electric field strength on the dielectrophoresis force and the electrostrictive strain of thermoplastic elastomer polyurethanes. Frontiers in Polymer Science 2013, Spain, 21-23 May 2013.

68) Pinit, J., Sirivat, A. (2013)
Synthesis and characterizations of poly(o-toluidine) as electrochromic material. Frontiers in Polymer Science 2013, Spain, 21-23 May 2013.

69) Pairatwachapun, S., Sirivat, A. (2013)
Polythiophene/carrageenan hydrogel as drug release matrix under electric field. Frontiers in Polymer Science 2013, Spain, 21-23 May 2013.

70) Kotaphan, P., Sirivat, A., Schwank, J. (2013)
Sulfonated poly(2,6-dimethyl-1,4-phenylene oxide) composite membranes filled by zeolite for direct methanoi fuel cell. Frontiers in Polymer Science 2013, Spain, 21-23 May 2013

71) Charoonrak N., Sirivat, A. (2013)
Development of poly(para-phenylene)/poly(ε-caprolactone) as electroactive shape memory composite. Frontiers in Polymer Science 2013, Spain, 21-23 May 2013.

72) Srisawasdi, T., Sirivat, A., Jamieson, A.M. (2013)
Silk fibroin/polycarbazole composite as artificial muscle. Frontiers in Polymer Science 2013, Spain, 21-23 May 2013.

73) Tharaporn P., Sirivat, A., Aussawasathien, D. (2013)
Development of polydiphenylamine/zeolite Y composites and electrical conductivity responses toward halogenated hydrocarbons. EuroEAP 2013, Duebendorf, Switzerland, 25-26 June 2013.

74) Tungkavet T., Seetapan, N., Pattavarakorn, D., Sirivat, A. (2013)
Electromechanical properties of biocompatible gelatin as actuator. EuroEAP 2013, Duebendorf, Switzerland, 25-26 June 2013.

สรุปผลงานการวิจัยเรื่อง

การพัฒนาพอลิเมอร์นำไฟฟ้าเพื่อประยุกต์เป็นเซนเซอร์ แอคชูเอเตอร์ และการปลดปล่อยยา

หน่วยงาน: วิทยาลัยปิโตรเลียมและปิโตรเคมี จุฬาลงกรณ์มหาวิทยาลัย

ระยะเวลา: 1 ตุลาคม 2555 – 30 กันยายน 2556

ผู้วิจัย: ศ. ดร. อนุวัฒน์ ศิริวัฒน์

บทความและผลงาน

Outputs

International Refereed Publications

1) Chanthaanont, P., Sirivat*, A. (2012)
Interaction of carbon monoxide with PEDOT-PSS/zeolite composite:effect of Si/Al ratio of ZSM-5 zeolite. e-Polymers, No. 010, 1-11.
(ISI Impact Factor: 0.515)

2) Kunchornsup, W., Sirivat*, A. (2012)
Physically cross-linked cellulosic gel via 1-butyl-3-methylimidazolium chloride ionic liquid and its electromechanical responses. Sensors & Actuators A, 175, 155-164. (ISI Impact Factor: 1.841)

3) Tungkavet, T., Sirivat*, A. (2012)
Bio-compatible gelatins (Ala-Gly-Pro-Arg-Gly-Glu-4Hyp-Gly-Pro-) and electromechanical properties: effects of temperature and electric field.
Journal of Polymer Research , Volume 19, Issue 1, Article Number 9759, 1-9.
(ISI Impact Factor: 2.019)

4) Paradee, N., Sirivat*, A., Niamlang, S., Prissanaroon-Ouajai, W. (2012)
Effects of crosslinking ratio, model drugs, and electric field strength on electrically controlled release for alginate-based hydrogel.
Journal of Materials Science- Materials in Medicine,
Volume 23, Issue 4, 999-1010. (ISI Impact Factor: 2.141)

Conference Proceedings

1) Pimit, J., Sirivat, A. (2013)
Electrochromic properties of poly(o-toluidine) coated on indium tin oxide (ITO) plastic. PETROMAT and PPC SYM 2013, Bangkok, Thailand, 23 April 2013

2) Charoonrak, N., Sirivat, A. (2013)
Development of poly(p-phenylene)/crosslinked poly(ε-caprolactone) as electroactive shape memory composite. PETROMAT and PPC SYM 2013, Bangkok, Thailand, 23 April 2013

3) Kotaphan, P., Sirivat, A., Schwank, J. (2013)
Composite membrane of sulfonated poly(2,6-dimethyl-1,4-phenylene oxide) and zeolite for direct methanol fuel cell applications. PETROMAT and PPC SYM 2013, Bangkok, Thailand, 23 April 2013

4) Pairatwachapun S., Sirivat, A. (2013)
Electrically-controlled release of acetylsalicylic acid from carrageenan hydrogel PETROMAT and PPC SYM 2013, Bangkok, Thailand, 23 April 2013

5) Srisawasdi, T., Sirivat, A., Jamieson A.M. (2013)
Silk fibroin/polycarbazole composite as artificial muscle.
PETROMAT and PPC SYM 2013, Bangkok, Thailand, 23 April 2013

Oral Presentations:

1) Sirivat, A. (2012)
Conductive and Electroactive Polymers: Actuation and Drug Controlled Release. การประชุมนักวิจัยรุ่นใหม่ พบ เมธีวิจัยอาวุโส สกว. ครั้งที่ 12, เพชรบุรี, 10-12 October 2012. [Invited Speaker]

2) Paradee, N., Sirivat, A. (2013)
Electrically-assisted transdermal delivery of drug from Ca-alginate hydrogel. CEAP 2013, Bangkok, Thailand, 22 April 2013

3) Kamonsawas, J., Sirivat, A., Hormnirun, P. (2013)
Sensitive and selective sensors based on poly(para-phenylene vinylene)/zeolite composites: Influece of alkaline cation. CEAP 2013, Bangkok, Thailand, 22 April 2013

4) Niamlang, S., Buranut, A., Niansiri, A., Sirivat, A. (2013)
Controlled aloin release from crosslinked polyacrylamide hydrogel: Effect of mesh size, electric field strength and conductive polymer. CEAP 2013, Bangkok, Thailand, 22 April 2013

5) Changkhamchom, S., Sirivat, A. (2013)
Sulfonated poly(ether ketone ether sulfone) (S-PEKES)/zeolite proton exchange membranes for direct methanol fuel cell. CEAP 2013, Bangkok, Thailand, 22 April 2013

6) Tungkavet, T., Seetapan, N., Pattavarakorn, D., Sirivat, A. (2013)
Effect of electric field and crosslinking ratios on stress relaxation of gelatin hydrogel. CEAP 2013, Bangkok, Thailand, 22 April 2013

Poster Presentations:

1) Kunchornsup, W., Sirivat, A. (2013)
Polarizability investigation of 1-butyl-3-methylimidazolium cation in electroactive ionic liquid-cellulose gel actuator. SPIE 2013, San diego, USA, 10-14 March 2013.

2) Paradee, N., Sirivat, A. (2013)
Electrically controlled release of tannic acid from calcium-alginate hydrogel in transdermal drug delivery application. SPIE 2013, San diego, USA, 10-14 March

2013.

3) Macksasitorn, S., Changkhamchom, S., Sirivat, A., Siemanond, K. (2013) Proton exchange membrane based on sulfonated poly(ether ether ketone and sulfonated poly(1,4-phenylene ether ether sulfone) for vanadium redox flow battery. SPIE 2013, San diego, USA, 10-14 March 2013.

4) Pinit, J., Sirivat, A. (2013) Study of poly(0-toluidine) as electrochromic properties coated on indium tin oxide (ITO). CEAP 2013, Bangkok, Thailand, 22 April 2013.

5) Petcharoen, K., Sirivat, A. (2013) Electrostrictive performance of thermoplastic elastomer polyurethanes under the influence of electric field. CEAP 2013, Bangkok, Thailand, 22 April 2013.

6) Charoonrak, N., Sirivat, A. (2013) Development of poly(E-caprolactone)/poly(P-phenylene) as electroactive shape memory polymer blend. CEAP 2013, Bangkok, Thailand, 22 April 2013.

7) Kotaphan, P., Sirivat, A., Schwank, J. (2013) Preparation and characterization of sulfonated poly(2,6-dimethyl-1,4-phenylene oxide) composite membrane for direct methanol fuel cell. CEAP 2013, Bangkok, Thailand, 22 April 2013.

8) Chanthaanont, P., Sirivat, A. (2013) Sensitivity and response of PEDOT-PSS/ion-exchanged zeolite Y composite towards SO2. CEAP 2013, Bangkok, Thailand, 22 April 2013.

9) Pairatwachapun, S., Sirivat, A. (2013) Controlled transdermal delivery of acetylsalicylic acid from carrageenan hydrogel. CEAP 2013, Bangkok, Thailand, 22 April 2013.

10) Srisawasdi, T., Sirivat, A., Jamieson, A.M. (2013) Developments of polycarbazole/Silk fibroin hydrogel for artificial muscle. CEAP 2013, Bangkok, Thailand, 22 April 2013.

11) Permpool, T., Sirivat, A., Aussawasathien, D., Wannatong, L. (2013) Dealuminated polydiphenylamine/zeolite Y composite as a sensine material for halogenated Solvents. CEAP 2013, Bangkok, Thailand, 22 April 2013.

12) Kunchornsup, W., Sirivat, A. (2013) Electromechanical and dielectric properties of ionic liquid/cellulose gel. CEAP 2013, Bangkok, Thailand, 22 April 2013.

13) Petcharoen, K., Sirivat, A. (2013) Effect of electric field strength on the dielectrophoresis force and the electrostrictive strain of thermoplastic elastomer polyurethanes. Frontiers in Polymer Science 2013, Spain, 21-23 May 2013.

14) Pinit, J., Sirivat, A. (2013)
Synthesis and characterizations of poly(o-toluidine) as electrochromic material. Frontiers in Polymer Science 2013, Spain, 21-23 May 2013.

15) Pairatwachapun, S., Sirivat, A. (2013)
Polythiophene/carrageenan hydrogel as drug release matrix under electric field. Frontiers in Polymer Science 2013, Spain, 21-23 May 2013.

16) Kotaphan, P., Sirivat, A., Schwank, J. (2013)
Sulfonated poly(2,6-dimethyl-1,4-phenylene oxide) composite membranes filled by zeolite for direct methanoi fuel cell. Frontiers in Polymer Science 2013, Spain, 21-23 May 2013

17) Charoonrak N., Sirivat, A. (2013)
Development of poly(para-phenylene)/poly(ε-caprolactone) as electroactive shape memory composite. Frontiers in Polymer Science 2013, Spain, 21-23 May 2013.

18) Srisawasdi, T., Sirivat, A., Jamieson, A.M. (2013)
Silk fibroin/polycarbazole composite as artificial muscle. Frontiers in Polymer Science 2013, Spain, 21-23 May 2013.

19) Tharaporn P., Sirivat, A., Aussawasathien, D. (2013)
Development of polydiphenylamine/zeolite Y composites and electrical conductivity responses toward halogenated hydrocarbons. EuroEAP 2013, Duebendorf, Switzerland, 25-26 June 2013.

20) Tungkavet T., Seetapan, N., Pattavarakorn. D., Sirivat, A. (2013)
Electromechanical properties of biocompatible gelatin as actuator. EuroEAP 2013, Duebendorf, Switzerland, 25-26 June 2013.

CEAP
Anuvat Sirivat, Ph.D.
Conductive and Electroactive Polymers Research Unit
Tel : 662 218 4131, 662 611 7221
Fax : 662 611 7221, 662 215 4459
Mobile : 661 480 0478 Email : anuvat.s@chula.ac.th

Anuvat Sirivat
The Petroleum and Petrochemical College
Chulalongkorn University
Phyathai Rd., Bangkok 10330
Tel: 662 218 4131; Fax: 662 611 7221
Mobile: 081 480 0478; Email: anuvat.s@chula.ac.th
www.cepru.research.ac.th